PhD degree in Systems Medicine (curriculum in Molecular Oncology)

European School of Molecular Medicine (SEMM),

University of Milan and University of Naples "Federico II"

Settore disciplinare med/04

Functional role of the histone demethylase UTX in B cell development and antibody responses *in vivo*

Martina Sormani

The FIRC Institute of Molecular Oncology, IFOM, Milan

Matricola n. R11129

Supervisor: Dr. Stefano Casola, MD, PhD,
IFOM, Milan

Academic year: 2017-2018

Table of contents

List of Abbreviations **7**

Figures index **11**

Tables index **14**

Abstract **16**

1. Introduction **19**

1.1. Chromatin organization 19

1.1.1. Epigenetics 19

1.1.2. Polycomb Group Proteins 20

1.1.2.1. Functions of PRC2 22

1.1.3. The COMPASS family of methyltransferases 23

1.1.3.1. Functions of MLL complexes 25

1.1.4. Lysine demethylases 26

1.1.4.1. Functions of Jumonji-type lysine demethylases (KDM) 27

1.1.5. KDM6 family of demethylases 29

1.1.6. Ubiquitously transcribed tetratricopeptide repeat, X chromosome (UTX) 31

1.1.6.1. UTX regulation of gene transcription 31

1.1.6.2. UTX function in early embryonic development 32

1.1.6.3. UTX contribution to cell differentiation 34

1.1.6.4. UTX contribution to somatic cell reprogramming 37

1.1.6.5. UTX deregulation in cancer 38

1.1.6.6. UTX as Kabuki syndrome gene 40

1.1.6.7. UTX contribution to hematopoiesis 41

1.1.6.7.1. UTX regulation of T cell and invariant Natural Killer T cell development 42

1.2. B cell development 44

1.2.1. Early B cell development 45

1.2.1.1. V(D)J recombination 46

1.2.1.2. Transcriptional control of early B cell development 47

1.2.2. Peripheral B cell development 49

1.2.2.1. Transitional B cells 49

1.2.2.2. Mature B cell subsets 50

1.2.2.3. Determinants of peripheral B cell development 51

1.2.3. B cell migration 56

1.2.4. B cell immunity 59

1.2.4.1. T cell-independent B-cell responses 59

1.2.4.2. T-cell-dependent B cell responses 59

1.2.4.1. Transcriptional regulation of germinal center B cells 62

1.2.4.2. B cells and intestinal immunity 66

1.2.5. Terminal B cell differentiation 67
1.2.5.1. Plasma cell development 67
1.2.5.1.1. Master regulators of plasma cell development 68
1.2.5.2. Memory B cell development 70
1.2.6. Epigenetic control of B cell development 71
1.3. Aim of the study 74
2. Materials and methods 77
2.1. Mice 77
2.1.1. Mouse strains 77
2.1.2. Genomic DNA extraction from mouse tail biopsies 77
2.1.3. Mouse genotyping 77
2.1.4. Mouse immunizations 79
2.1.5. *In vivo* BrdU incorporation assay 79
2.2. Cell culture techniques 79
2.2.1. Preparation of cell suspensions from lymphoid organs 79
2.2.2. Primary B cell purification 80
2.2.3. *In-vitro*-induced Germinal Center B cells (iGB) 81
2.2.4. *In-vitro* B cell stimulation 81
2.2.5. *In vitro* proliferation assay 81
2.3. Imaging techniques 82
2.3.1. Immunostaining for flow cytometric analyses and cell sorting 82
2.3.1.1. Intracellular flow cytometric immunostaining 82
2.3.1.2. Flow cytometric detection of apoptotic cells 85
2.3.2. Immunostaining of tissue sections 85
2.3.2.1. Immunofluorescence 85
2.3.2.2. Immunohistochemical staining of tissue sections 86
2.4. Biochemical techniques 87
2.4.1. Immunoblot analysis 87
2.4.2. Enzyme-Linked Immunosorbent Assay (ELISA) 88
2.4.3. Chromatin immunoprecipitation 90
2.5. Molecular biology techniques 93
2.5.1. RNA and DNA extraction 93
2.5.2. First strand cDNA synthesis 93
2.5.3. qPCR and qRT-PCR analysis 93
2.5.4. Immunoglobulin somatic mutation analysis 95
2.6. Next-generation sequencing (NGS) applications 97
2.6.1. ChIP-sequencing 97
2.6.2. RNA-sequencing 98
2.7. Bioinformatic analyses 98

2.7.1. Bioinformatic analysis of ChIP-sequencing data 98
2.7.2. Bioinformatic analysis of RNA-sequencing data 99
2.8. Statistical analyses 100
2.8.1. Student's T test 100
2.8.2. Mann-Whitney test 100
2.8.3. 2 Way-Anova test 100
3. Results 102
3.1. The *Utx* gene is expressed throughout B cell development 102
3.2. Conditional targeting of the *Utx* gene in B-lineage cells 103
3.2.1. UTY functional redundancy and genetic background of UTX conditional mutant mice . 105
3.3. Consequences of *Utx* inactivation on B cell development 106
3.3.1. Effects of *Utx* deficiency on early B cell lymphopoiesis 106
3.3.1.1. *Utx* deficiency alters the fraction and numbers of bone marrow B cell subsets 106
3.3.2. Peripheral B cell differentiation in the absence of UTX 110
3.3.2.1. B cells are strongly reduced in the blood of *Utx* mutant animals 110
3.3.2.2. *Utx* deficiency reduces overall B cell numbers in secondary lymphoid organs 111
3.3.2.3. Reduced numbers of immature B cells in the spleen of B-cell specific *Utx* mutants 113
3.3.2.4. *Utx* deficiency interferes with peripheral B cell differentiation 114
3.3.2.5. Peripheral B cell homeostasis in the absence of UTX 119
3.3.2.5.1. B cell turnover is altered in the absence of functional Utx 119
3.3.2.5.2. Sphingosine-1-phosphate receptor 1 expression is reduced in *Utx* deficient B cells.. 121
3.3.2.5.3. *Utx* deficient B cells express less BAFF-R and display blunted responses to BAFF *in vitro* 122
3.3.2.5.4. A subset of NF-κB target genes is deregulated in *Utx* mutant B cells 124
3.4. The role of UTX in T-cell dependent B cell responses 126
3.4.1. UTX limits the number of GC B cells and the size of GCs 126
3.4.2. UTX restricts the pool of germinal center centroblasts 129
3.4.3. *Utx* deficiency alters GC responses in gut associated lymphoid tissues 132
3.4.4. Immunoglobulin somatic hypermutation and clonal selection in *Utx* mutant GC B cells 135
3.4.5. Altered serum Ig titers in B cell specific *Utx* mutant mice 136
..... 137
3.4.6. Effect of *Utx* deficiency on the production of antigen-specific IgM and IgG1 antibodies and antibody-secreting cells 137
3.4.6.1. Primary antibody responses 137
3.4.6.2. Secondary antibody responses 139
3.4.6.3. Formation of antigen-specific plasma cells in vivo in Utx mutant animals 140
3.5. Effects of *Utx* inactivation on terminal B cell differentiation 141
3.5.1. *Utx* expression is rapidly downregulated in B cells undergoing terminal differentiation. 141

3.5.2. Transcripts for PC transcription factors *Prdm1* and *Irf4* are reduced in *Utx* mutant GC B cells 142
3.5.3. UTX is required for *Irf4* upregulation in activated B cells 143
3.5.4 *In vitro* plasma blast differentiation in the absence of *Utx* 144
3.5.5. *Prdm1* gene expression in *Utx* mutant B cells undergoing PC differentiation *in vitro* 147
3.6. The impact of *Utx* deficiency on immunoglobulin isotype switching 148
3.6.1. *Utx* deficiency affects fractions of isotype-switched cells upon *in vitro* stimulation 148
3.6.2. *Utx* mutant B cells show suboptimal activation upon stimulation with TLR agonists 149
3.6.3. Defective IgG3 isotype switching in *Utx* KO B cells is independent of cell proliferation abnormalities 151
3.6.4. The immunoglobulin heavy chain locus is accessible to AID in the absence of *Utx* 152
3.6.5. Isotype-switched *Utx* KO B cells die comparably to their control counterpart 154
3.7. *Utx* deficiency affects selective transcriptional networks in mature B cells 154
3.8. The chromatin landscape of UTX mutant B cells 159
3.8.1. Effects of *Utx* inactivation on global H3K27 and H3K4 trimethylation 159
3.8.2. *Utx* deficiency does not perturb H3K4me3 deposition at promoter regions both in resting and GC B cells 160
3.8.3. Effects of *Utx* inactivation on the expression of genes marked by H3K4me3 and/or H3K27me3 in resting and GC B cells 161
3.8.4. H3K27 acetylation is affected at promoter regions in *Utx* deficient resting and GC B cells 162
4. Discussion 166
4.1. UTX in early B cell development 167
4.2. UTX and peripheral B cell differentiation and maintenance 168
4.3. UTX and B cell migration 173
4.4. UTX and T-cell dependent immune responses 175
4.5. UTX and immunoglobulin isotype switching 178
4.6. UTX and plasma cell differentiation 181
4.7. The gene expression profile and chromatin landscape of mature B cells lacking *Utx* 183
4.8. UTX and B cell transformation 186
4.9. What did we learn from studying Utx function in B cells? 187
4.10. Future goals 188
5. Supplementary information 194
6. References 196
Appendix 225
Acknowledgements 227

List of Abbreviations

2-OG	2-Oxoglutarate
AID	Activation Induced Deaminase
ASH2	absent, small, or homeotic discs 2
Atm	ataxia telangiectasia mutated
Atr	ataxia telangiectasia and Rad3 related protein
Bach2	broad complex-tramtrack-bric a brac and Cap'n'collar homology 2
BAFF	B-cell activating factor
BAFF-R	BAFF receptor
Bcl2	B cell CLL/lymphoma 2
Bcl6	B cell CLL/lymphoma 6
BCR	B cell receptor
BER	base excision repair
Blimp-1	B lymphocyte induced maturation protein 1
BM	bone marrow
bp	base pair
BrdU	Bromodeoxyuridine
C-term	Carboxy terminus
Casp-glow	FITC-conjugated VAD-FMK, a general caspase inhibitor
CB	centroblast
CC	centrocyte
Ccng1	CyclinG1
Cdkn2a	cyclin dependent kinase inhibitor A
cDNA	complementary DNA
CDR3	Complementarity Determining Region 3
CFP1	CXXC finger protein 1
ChIP	chromatin immunoprecipitation
cKit	v-kit Hardy-Zuckerman 4 feline sarcoma viral oncogene homolog;
CLP	common lymphoid progenitor
COMPASS	Complex of Proteins Associated with Set1
CSR	Class Switch Recombination
DDR	DNA damage response
Dll-1	Delta-like 1
DMEM	Dulbecco's Modified Eagle Medium
DNA	Deoxyribonucleic acid
dNTP	deoxynucleoside triphosphate
DSB	Double Strand Break

E2a	E2a immunoglobulin enhancer binding factors E12/E47
E2f	E2f transcription factor
Ebf1	early B-cell factor 1
Eed	embryonic ectoderm development
ELISA	Enzyme-linked immunosorbent assay
ER	Endoplasmic reticulum
ESC	Embryonic Stem Cell
EYFP	Enhanced Yellow Fluorescent Protein
Ezh2	enhancer of zeste homolog 2 (Drosophila)
FA	Formaldehyde
FACS	Fluorescence Activated Cell Sorting
FAD	Flavin Adenine Dinucleotide
FDC	Follicular Dendritic Cell
Flt3	Fms-related tyrosine kinase 3
FO	Follicular
GALT	Gut-associated lymphoid tissue
GC	Germinal center
GLT	Germline transcript
H2AK119Ub	mono-ubiquitinated Histone H2A at Lysine 119
H3K27ac	acethylated Histone H3 at Lysine 27
H3K27me3	tri-methylated Histone H3 at Lysine 27
H3K4me3	tri-methylated Histone H3 at Lysine 4
H3K4me1	mono-methylated Histone H3 at Lysine 4
HEV	High endothelial venules
HCF1	Host cell factor 1
HOX	Homeobox
HSC	Hematopoietic Stem Cell
Ig	Immunoglobulin
IgV	Variable gene
IgH	Immunoglobulin heavy chain
IgK	Immunoglobulin kappa chain
Igλ	Immunoglobulin lambda chain
IL	Interleukin
ILF	Isolated lymphoid follicles
Ink4a	Inhibitor of cyclin-dependent kinase 4a
Irf	Interferon regulatory factor
JARID2	Jumonji AT Rich Interactive Domain 2

JmjC	Jumonji C
JMJD3	Jumonji domain-containing protein 3
KDM	Lysine (K) demethylase
LN	lymph node
loxP	locus of X-over of P1
LPS	lipopolysaccharide
LSD1	Lysine-specific histone demethylase 1
mAb	monoclonal antibody
MACS	Magnetic-activated cell sorting
Mb-1	CD79a molecule, immunoglobulin-associated alpha
MHC	Major Histocompatibility Complex
MITF	Microphthalmia-associated transcription factor
MLN	mesentheric lymph nodes
MLL	Mixed lineage leukemia
MMR	mismatch repair
MPP	multipotent progenitor
MRN	protein complex consisting of Mre11, Rad50 and Nbs1
mRNA	Messenger RNA
MZ	Marginal zone
NCOA60	Nuclear receptor coactivator 60
Nf-κB	nuclear factor kappa-light-chain-enhancer of activated B cell
NHEJ	non-homologous end joining
NP	Nitrophenyl
N-term	Amino-terminus
PA1	PTIP-aasociated 1
NP-CGG	Nitrophenyl coupled to chicken gamma globulin
Pax5	paired box 5
PBS	Phosphate buffered saline
PC	plasma cell
PcG	Polycomb group
PCGF	polycomb group ring finger
Pcl	Polycomblike
PCR	Polymerase Chain Reaction
PLZF	Promyelocytic zinc finger
PP	Peyer's Patches
PRC	Polycomb reppresive complex
Prdm1	PR domain containing 1, with ZNF domain (Blimp1)
PTIP	Pax transactivation domain-interacting protein

R26	Rosa26
RAG	Recombination activation genes
RBBP5	Retinoblastoma-binding protein 5
Ring1	Ring finger protein 1, Ring1a, R1a
RNA	Ribonucleic acid
RSS	Recombination Signal sequence
RT	room temperature
RT-PCR	Reverse Transcriptase PCR
RT-QPCR	quantitative real time-PCR
RYBP	Ring1 and Yy1 binding protein
Sca1	stem cell antigen-1; Ly-6A/E
SEM	Standard Error of the Mean
SET	Su(var)3-9, Enhancer-of-zeste, Trithorax
SHM	Somatic Hypermutation
S1pr1	Sphingosine-1-phosphate receptor 1
SPL	Spleen
SRBC	Sheep Red Blood Cell
ssDNA	single stranded DNA
Suz12	suppressor of zeste 12 homolog (Drosophila)
SWI/SNF	SWItch/Sucrose Non-Fermentable
TGF-β	Transforming growth factor beta
TF	transcription factor
T_{FH}	T follicular helper cell
TLR	Toll-like receptor
Tp53	Tumor protein 53
TPR	Tetratricopeptide repeat
Trx	Trithorax
TrxG	Trithorax group
Trr	Trithorax related
WT	Wild-type
WDR5	WD repeat-containing protein 5
WDR82	WD repeat-containing protein 82
Xbp1	X-box binding protein 1
Utx	Ubiquitously transcribed tetratricopeptide repeat, X chromosome

Figures index

Figure 1. Composition of Polycomb group protein complexes PRC1 and PRC2.. 21
Figure 2. Evolution and composition of COMPASS complexes. 23
Figure 3. JmjC family members, domain structures and histone targets. 27
Figure 4. Simplified structures of the main H3K27me3 demethylases. 30
Figure 5. Schematic representation of B cell development. 45
Figure 6. Schematic view of peripheral B cell development. 50
Figure 7. Schematic view of the GC reaction. 61
Figure 8. Schematic representation of gut-associated lymphoid tissues (GALT). 67
Figure 9 Opposing transcriptional networks in GC and PC development. 70
Figure 10 . Schematic view of B cell development 102
Figure 11. *Utx* is expressed throughout B cell development. 103
Figure 12. Structure of the $Utx^{frtbgeo}$ conditional allele before and after FLP- and Cre-mediated recombination 104
Figure 13. B cell-specific *Utx* inactivation *in vivo* 104
Figure 14. Lack of UTX protein in splenic $Utx^{fl/fl}$; Mb-$1^{+/cre}$ B cell. 105
Figure 15. Frequency and absolute numbers of $B220^{+}$ B cells in the bone marrow are largely unaffected in B-cell specific *Utx* mutant mice 106
Figure 16. Effects of *Utx* inaction on bone marrow B cell subset distribution 107
Figure 17. Status of the *Utx* wild-type allele in bone marrow B cell subsets of Utx control and mutant mice 107
Figure 18. *Utx* deficient mice show a modest increase in the fraction and absolute numbers of bone marrow progenitor B cells 108
Figure 19. Increased fraction of pre-B cells in *Utx* mutant mice. 109
Figure 20. Reduction in recirculating B cells in the bone marrow of Utx deficient mice 109
Figure 21. *Utx* inactivation delays the transition from progenitor to immature B cells in the bone marrow 110
Figure 22. *Utx* deficient mice show a decrease in the fraction of B cells circulating in the blood 111
Figure 23. Reduced representation of B cells in secondary lymphoid organs of *Utx* mutant mice 111
Figure 24. Quantification of B cell numbers in secondary lymphoid organs of *Utx* control and mutant mice. 112
Figure 25. Efficiency of Cre-mediated recombination of the *Utx* floxed allele in splenic B cells of *Utx* conditional mutant mice 113
Figure 26. Transitional B cells are reduced in the spleen of *Utx* conditional mutant mice 114
Figure 27. *Utx* deficiency affects the proportion of splenic follicular and marginal zone B cells 115
Figure 28. Numbers and frequencies of splenic mature B cell subsets are altered in Utx conditional mutant mice 115
Figure 29. Analysis of FO and MZ B cells using complementary surface markers in Utx control and mutant mice 116
Figure 30. Utx mutant B cells home to splenic primary follicles and reach the marginal zone 117
Figure 31. Measurement of the marginal zone area in Utx control and mutant mice 117

Figure 32. Frequencies and absolute number of B cells in peritoneal cavity lavages of Utx control and mutant mice 118
Figure 33. The B-1/B-2 B cell ratio is altered in Utx conditional mutant mice 118
Figure 34. Distribution of B cells among the B-1 and B-2 B cell subsets is altered in the peritoneum of Utx mutant animals 119
Figure 35. In vivo BrdU labelling: experimental plan. 119
Figure 36. *Utx* mutant follicular B cells express lower *S1pr1* transcripts 122
Figure 37. BAFF-R transcript and protein levels are reduced in Utx mutant mice 123
Figure 38. Utx mutant B cells survive less to in vitro BAFF stimulation 124
Figure 39. Transcripts for NF-κB transcription factors and effectors are reduced in Utx mutant FO B cells 124
Figure 40. Reduced expression of a subset of NF-κB induced genes in *Utx* mutant follicular B cells 125
Figure 41. Modest increase in the fraction of GC B cells upon *Utx* inactivation 126
Figure 42 Increased average size of splenic BCL6^{+} GCs in *Utx* mutant mice 127
Figure 43. Close-to-complete Cre-mediated recombination of the Utx floxed allele in GC B cells of *Utx$^{fl/fl}$; Mb-1$^{cre/+}$* mutant mice 128
Figure 44. Germinal center B-cell specific Utx inactivation 128
Figure 45. Increased GC B cell frequency in spleen and GALT of *Utx$^{fl/fl}$; Aicda^{cre}* immunized mice 129
Figure 46. *Utx* inactivation leads to an increase in the germinal center centroblast fraction 130
Figure 47. *Utx* mutant GC B cells express preferentially centroblast-associated genes 131
Figure 48. Higher average expression of BCL6 protein in *Utx* mutant GC B cells 131
Figure 49. *Utx* mutant GC B cells express lower levels of BCL6 repressed genes. 132
Figure 50. The frequency of GC B cells is increased in GALT of *Utx* mutant mice 133
Figure 51. *Utx* deficient mice have less IgA^{+} PCs in small intestine lamina propria 134
Figure 52. Reduced transcript levels for homing receptors and TACI in *Utx* mutant GC B cells 135
Figure 53. *Utx* KO mice exhibit altered serum antibody titers in resting conditions. 137
Figure 54. Sera collection scheme for the analysis or primary and secondary T-cell dependent antibody responses 138
Figure 55. Normal antigen-specific IgM and IgG1 antibody responses in *Utx* mutant mice after immunization with alum-precipitated NP-CGG 138
Figure 56. Recall antigen-specific IgM and IgG1 antibody responses are comparable between *Utx* control and mutant mice 139
Figure 57. Timeline for the analysis of antigen-specific plasma cells *in vivo* 140
Figure 58. Newly formed antigen-specific plasma cells are reduced in the spleen of Utx mutant mice after recall immunization with the T-cell dependent antigen NP-CGG. 141
Figure 59. *Utx* expression is downregulated upon B cell activation 142
Figure 60. Reduced *Irf4* and *Prdm1* transcript levels in *Utx* mutant GC B cells 143
Figure 61. Reduced IRF4 protein levels in *Utx* mutant in-*vitro* activated B cells 145
Figure 62. *Irf4* transcript levels are reduced in *Utx* mutant B cells after CD40/IL21 stimulation 146
Figure 63. *In vitro* plasmablast differentiation in the absence of *Utx* 146
Figure 64. *In vitro* BLIMP1 upregulation in bona fide activated B cells and plasma blasts is not affected by *Utx* loss 147
Figure 65. *In vitro* IgG3 and IgG1 isotype switching is impaired in *Utx* mutant B cells 149

Figure 66. Growth curves of *in vitro* stimulated *Utx* control and mutant B cells. 150
Figure 67. Delayed cell division of a subset of Utx mutant B cells stimulated *in vitro* with LPS 151
Figure 68. Impaired switching to IgG3 of *Utx* mutant B cells does not depend on defects in cell proliferation 152
Figure 69. Normal expression of Ig C_H germline transcripts in *Utx* mutant activated B cells 153
Figure 70. *Aicda* expression is comparable between *Utx* control and mutant B cells stimulated *in vitro* with LPS.....153
Figure 71. The fraction of apoptotic IgG3-switched B cells remains unaffected by *Utx* inactivation.....154
Figure 72. Genes controlled by UTX in follicular B cells.....158
Figure 73. Genes controlled by UTX in GC B cells 158
Figure 74. Global H3K27 trimethylation and H3K4 mono/thrimethylation are unaffected in *Utx* mutant B cells.....159
Figure 75. H3K4me3 distribution at promoter regions in *Utx* proficient and mutant B cells.....160
Figure 76. Expression of H3K4me3- and/or H3K27me3-marked genes in *Utx* proficient and deficient B cells.....162
Figure 77. H3K27ac distribution at promoter regions in *Utx* proficient and mutant B cells 163
Figure 78. H3K27ac distribution across differentially acetylated promoter regions in *Utx* mutant and control B and GC B cells.....163
Figure 79. Changes in H3K27ac levels at promoters of representative Utx-controlled genes, in Utx mutant B cells 165

Tables index

Table 1. List of primers used for genotyping, annealing temperatures and amplicon sizes.....78
Table 2. PCR master mix used for genotyping.....78
Table 3. Genotyping PCR conditions. 78
Table 4. List of antibodies used for B cells negative purification. 80
Table 5. Surface markers used for B cell subsets sorting/gating. 82
Table 6. Antibodies used for flow cytometry. 84
Table 7. Antibodies used for immunoblotting analysis 88
Table 8. ELISA reagents for total antibody titers detection of resting mice. 89
Table 9. ELISA reagents for antigen specific antibody titers detection of immunized mice. 90
Table 10. Antibodies used for ChIP experiments. 92
Table 11. Primers list for qPCR and qRT-PCR.....94
Table 12. Reagents for V_H186.2 semi-nested PCR amplification 95
Table 13. PCR conditions to amplify V_H186.2 gene.....96
Table 14. Reagents for polyA overhangs formation. 96
Table 15. TOPO-TA cloning reaction mix.....97
Table 16. $BrdU^+$ labelled recirculating B cells are increased in the BM of *Utx* mutant mice.....120
Table 17. Recently immigrated immature B cells are underrepresented in the spleen of *Utx* mutant animals.....120
Table 18. IgH SHM analysis and clonal selection in *Utx* control and mutant GC B cells.....136
Table 19. Genes differentially expressed between *Utx* control and mutant B cells 155
Table 20. List of NF-κB transcriptional target genes downregulated in *Utx* KO FO B cells 194

Abstract

In this study, I addressed the role of the histone H3 lysine-27 (H3K27) demethylase *Utx/Kdm6a* in B cell development and T-cell dependent antibody responses. This work stems from multiple evidences pointing to a critical role exerted by H3K27 trimethylation, catalyzed by the Polycomb protein EZH2, in the establishment and maintenance of developmental programs relevant for early B cell lymphopoiesis, B cell maturation and for their recruitment into T-cell dependent and -independent immune responses.

Constitutive *Utx* expression throughout B cell lymphopoiesis provided the rationale to inactivate its function starting from early progenitors. To this aim, mice carrying a conditional knock-out allele for *Utx* were crossed to the *Mb-1*$^{cre/+}$ strain, expressing Cre recombinase starting from pro-B cells. Analyses of the effects of *Utx* inhibition were restricted to female animals, given that *Utx* is an X-linked gene, and considering the existence of a *Utx* paralogue *Uty*, encoded on the Y-chromosome, which may substitute (at least part of) for UTX function.

Inactivation of *Utx* in B-lineage cells revealed distinct contributions of the demethylase in different stages of B cell development. Specifically, *Utx* deficiency significantly enlarged the pool of pre-B cells, interfering with their differentiation into immature B cells. UTX also contributed to the egress of immature B cells from the bone marrow, as revealed by the significant contraction of the pool of circulating B cells, as well as by the reduction in the subset of newly generated B cells residing in the spleen. *Utx* deficiency was compatible with the differentiation of the three major subsets of mature B cells, namely B-2 B cells, splenic marginal zone B cells and peritoneal cavity B-1 B cells. However, absolute numbers and relative proportions of these mature B cells subsets present in secondary lymphoid organs were affected by *Utx* deficiency. Specifically, whereas B-2 B cells were less represented in the spleen, peritoneal cavity, and in gut associated lymphoid tissues (GALT), splenic marginal zone B cells were increased in numbers in *Utx* conditional mutant mice. In *Utx* mutant mice, peritoneal cavity B-1 B cells were over-represented at the expense of B-2 B cells. These results highlight a contribution of UTX to the control of B cell homeostasis and to the distribution of these cells among secondary lymphoid organs. In support of this, we report that *Utx* mutant B-2 B cells expressed lower levels of the BAFF receptor leading to a sub-optimal response to the pro-survival factor BAFF *in vitro*. Inactivation of *Utx* exerted a remarkable contraction in the population of B cells in GALT, including mesenteric lymph nodes and Peyer's patches. This defect was associated to significantly lower serum titers of IgA and in a decrease in the fraction IgA-secreting plasma cells localized in the lamina propria of the small intestine. The reduced fraction of intestinal IgA-expressing PCs correlated to lower expression in *Utx* mutant B cells of: 1) the *Taci* receptor which mediates April-induced IgA class-switching, 2) the chemokine receptor *Ccr6* which is required for the migration of B cells in areas of the Peyer's patch where

IgA switching takes place in response to interactions with dendritic cells; 3) β7 Integrin (*Itgβ7*) which is required for the homing of B cells to GALT and of IgA-secreting plasma blasts to the intestinal lamina propria. Importantly, the defects in IgA-associated gut immunity seen in *Utx* mutant mice resemble those described in patients affected by the Kabuki Syndrome, a genetic disorder caused by mutations in either *UTX* or in the gene encoding the H3K4 methyltransferase *KMT2D*.

Upon immunization with T-cell dependent antigens, *Utx* mutant B cells were recruited into the germinal center (GC). However, distribution of mutant B cells between the centroblast and centrocyte fractions was significantly skewed towards the former. The altered distribution of *Utx* mutant B cells within the GC was associated with a significant defect in antigen-driven selection, with limited impact on the production of high-affinity antigen-specific antibodies. Transcriptomic profiling revealed lower expression in *Utx* mutant GC B cells of the transcription factor *Irf4*. This defect may contribute to the impaired immunoglobulin isotype switching and the defective *in vitro* activation of *Utx* mutant B cells upon LPS stimulation or CD40 ligation.

Chromatin immunoprecipitation studies coupled to ultra-deep sequencing performed on *Utx* mutant resting and germinal center B cells revealed minor changes in the deposition of H3K4 trimethylation at gene promoters. Instead, *Utx* deficiency reduced the extent of H3K27 acetylation at promoters, affecting significantly the expression of a subset of them.

In summary, UTX exerts multiple roles throughout B cell lymphopoiesis, controlling mature B cell subset differentiation, mature B cell survival, B cell distribution among primary and secondary lymphoid organs, Ig isotype switching and antigen-driven germinal center B cell clonal selection. As a result of these defects, B cell-specific *Utx* deficiency causes a humoral immunodeficiency resembling a common variable hyper-IgM immunodeficiency, affecting primarily intestinal IgA-linked immunity.

Wisdom is the recovery of innocence at the far end of experience.

(David Bentley Hart)

1. Introduction

1.1. Chromatin organization

In eukaryotic cells, genomic DNA is highly compacted in the nuclear compartment. Packaging of the DNA in such a restricted space is achieved thanks to the presence and activity of specific proteins, known as histones (H). They are a family of positively charged proteins that bind to the DNA and help its folding, forming a condensed structure known as chromatin. The fundamental unit of chromatin is the nucleosome. It consists of 147 bp of DNA wrapped around a histone core composed of two subunits each of Histones H2A, H2B, H3 and H4, that all together form a heptamer complex (Kornberg 1974). Nucleosomes interconnected by stretches of linker DNA form the so-called "beads-on-a-string" structure (or 11 nm fiber). Incorporation of Histone H1 leads to a higher degree of chromatin compaction, forming a structure known as the 30 nm fiber, or chromatosome (Luger 2003). Upon cell division, chromatin is further condensed and becomes visible at the microscope as chromosomes. The mechanisms involved in the establishment of the higher order structure of chromatin are not yet fully understood (Kornberg and Lorch 1999). Chromatin compaction is regulated in several ways, one of which is represented by post-translational modifications (PTMs) targeting the N-terminal regions of histones. Histone modifications include phosphorylation, acetylation, methylation, ubiquitination, sumoylation and glycosylation (Davie and Murphy 1990; Liebich, Gesele et al. 1993; Grunstein 1997; Zhang and Reinberg 2001; Nathan, Sterner et al. 2003; Nowak and Corces 2004). Such modifications usually affect specific residues in the N-terminus tail of core histones. They do not only affect these proteins' biochemical properties, but they have a critical influence on gene expression by modulating chromatin accessibility. The combination of these PTMs targeting histone core subunits constitutes the so-called "histone code", which is read by chromatin factors and transcription factors, ultimately influencing the transcriptional status of genes (Jenuwein and Allis 2001). The deposition of PTMs on histone tails is mediated by the highly dynamic activity of histone modifying enzymes that have been extensively studied over the past two decades (Strahl and Allis 2000).

1.1.1. Epigenetics

The complexity of multicellular organisms is determined by the differentiation and coordination of several cell types, with different and specialized functions. Two main levels of regulation control the appropriate development of different cell subtypes. The first one is the genetic regulation which depends on the activity of cell-type specific transcription factors, that establish defined gene expression profiles. These transcriptional programs are crucial in defining cellular specialization and maintaining cell identity. The second level of regulation is

strictly related to the accessibility of chromatin to TFs and to the transcriptional machinery, which is controlled by a series of dynamic changes and modulations known as epigenetics. The term epigenetics defines those mechanisms leading to changes in gene expression that are heritable, functionally relevant and not associated to changes in the DNA sequence. Epigenetic changes influence chromatin conformation, determining whether it is less compacted and transcriptionally active (euchromatin) or more tightly compacted and transcriptionally silent (heterochromatin). Furthermore, heterochromatin can be defined as constitutive when it is stably repressed, or facultative when it can be de-repressed in certain conditions.

Research carried out in the last two decades has highlighted the importance of the epigenetic regulation of gene expression. In mammals, it is commonly mediated by histones PTMs, DNA methylation and nucleosomal remodelling. Together, these mechanisms are critical to ensure cell identity through multiple cell divisions.

1.1.2. Polycomb Group Proteins

Methylation of different lysine residues on core histone tails has different transcriptional outcomes depending on the specific position of the residue and on the type of PTM. In general, methylation of Histone H3 on lysine 27 (K27) or on lysine 9 (K9) is present in regions of chromatin that are transcriptionally silent. Silenced genes that are subjected to modulation are often associated with H3K27me3 deposition around the transcriptional start site (TSS), whereas H3K9me3 defines stably repressed chromatin. These and other histones PTMs are catalyzed by proteins acting within macromolecular complexes. Transcriptional gene silencing, in particular, is promoted by Polycomb Group (PcG) complexes, although very recent evidence associated their function also to active transcription (Scelfo, Piunti et al. 2015). PcG proteins act as transcriptional repressors to regulate a variety of biological processes including cell cycle progression, senescence, apoptosis, tissue homeostasis and cell fate decisions (Sparmann and van Lohuizen 2006; Gieni and Hendzel 2009). Polycomb genes were discovered in Drosophila melanogaster more than 70 years ago (Lewis 1945) as repressors of Homeotic (*Hox*) genes, important determinants of early embryonic development (Lewis 1978). In mammals, Polycomb proteins act within two main macromolecular complexes, the Polycomb Repressive Complex 1 (PRC1) and the Polycomb Repressive Complex 2 (PRC2) (Levine, Weiss et al. 2002). This view has been greatly expanded in the last decade revealing that the PcG system is much more diverse in mammals than in Drosophila. Specifically, PRC2 core components include Embryonic ectoderm development (EED), Suppressor of zest homologue 12 (SUZ12) and the catalytic SET domain-containing histone methyltransferase Enhancer of zeste homologue 2

(EZH2).

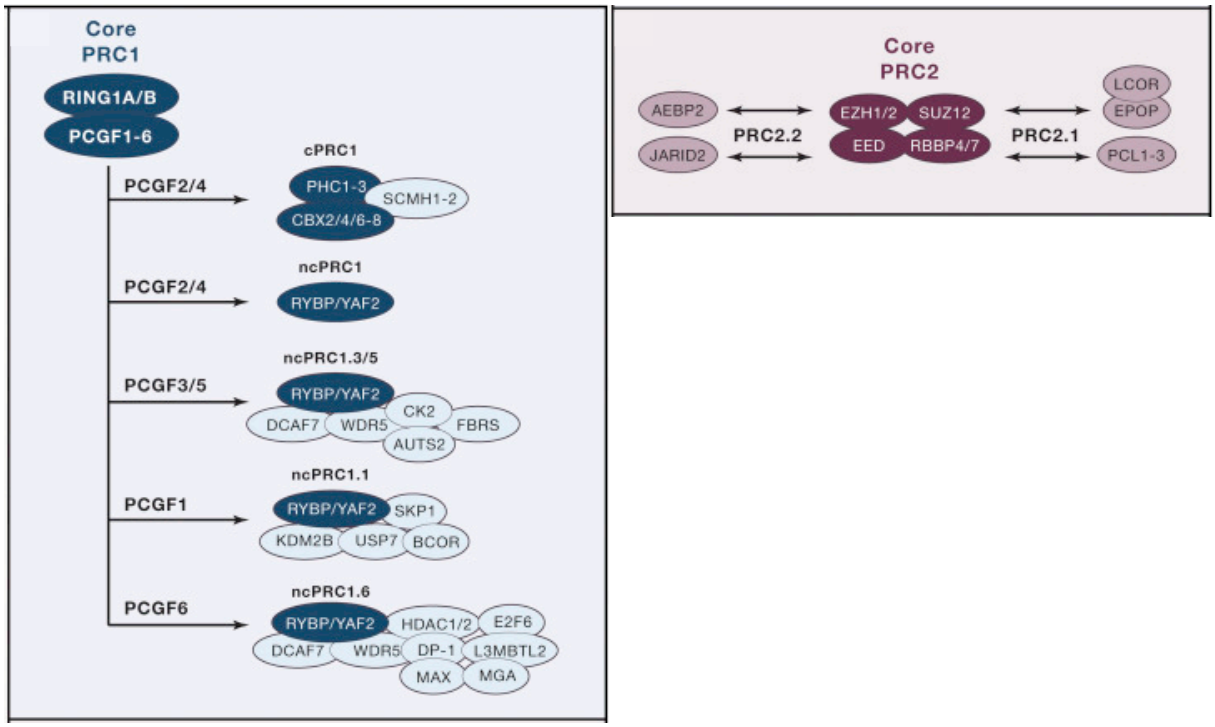


Figure 1. Composition of Polycomb group protein complexes PRC1 and PRC2. Composition of Polycomb group protein complexes PRC1 and PRC2. Left: the core of PRC1 complex, can associate with different PCGF proteins (PCGF1–PCGF6) defining canonical PRC1 complexes (cPRC1) and non-canonical (ncPRC1) PRC1 complexes. cPRC1 contains PHC and CBX proteins. Right: The core of the PRC2 complex associates with different accessory proteins to define the PRC2.1 and PRC2.2 complexes, respectively. (Adapted from Schuettengruber et al, 2017).

EZH2 catalyzes the di- and tri- methylation of lysine 27 on histone H3 (H3K27me2-H3K27me3). These modification can also be catalyzed by EZH2 paralog EZH1, that possesses a weaker activity (Margueron and Reinberg 2011). Additional PRC2 components include the zinc finger protein AE binding protein 2 (AEBP2), Jumonji AT-Rich Interactive Domain 1 (JARID2) and the retinoblastoma binding protein (RBBP 4/7) (Figure 1).

PRC2-dependent H3K27me3 can trigger the recruitment to target sites of PRC1, mediated by PRC1-specific Chromobox –domain (CBX) containing proteins. Recent studies revealed the existence of multiple forms of PRC1, which is subdivided into canonical and non-canonical complexes (Blackledge, Rose et al. 2015). All PRC1 complexes, however, share a conserved protein core composed of RING1 proteins RING1A and RING1B, which have E3 ubiquitin ligase activity, mediating ubiquitination of histone H2A on lysine 119 (H2AK119ub1). Concerted deposition of H3K27me3 and H2AK119ub1 histone marks contribute to target gene repression (Morey and Helin 2010). Core PRC1 components include also one of the six Polycomb group ring-finger domain proteins (PCGF1-6). Additionally, the canonical

complexes are specified by the presence of a CBX protein (CBX2/4, 6-8) that binds H3K27me3 and of a Polyhomeotic homologous protein (PHC1-3). Alternative, non-canonical complexes lack CBX proteins but possess different combinations of other subunits, like the zinc-finger domain and YY1 binding protein (RYBP), the subunit Bmi1 and the H3K36-specific histone demethylase KDM2B (Wilkinson, Pratt et al. 2010; Schuettengruber, Bourbon et al. 2017) (Figure 1). Recent studies have challenged the classical model of concerted PRC1 and PRC2 mediated gene repression (Cooper, Dienstbier et al. 2014; Blackledge, Rose et al. 2015). Indeed, it was shown that non-canonical PRC1 can be recruited to target sites by sequence-specific DNA binding proteins, independently of PRC2 and H3K27me3 recognition. (Gao, Zhang et al. 2012; Di Croce and Helin 2013).

1.1.2.1. Functions of PRC2

Studies on ES cells have highlighted the relevance of the Polycomb axis in the regulation of stem cells pluripotency and lineage commitment. Data obtained from Polycomb mutant mouse ES cells indicate that inactivation of PcG components is compatible with pluripotency of the stem cells but not with the induction of proper differentiation programs (Pasini, Bracken et al. 2007; Shen, Kim et al. 2009; Walker, Chang et al. 2010). Indeed, the induction of differentiation in Polycomb mutant ES cells causes concomitant activation of multiple lineage programs, resulting in aberrant differentiation (Chamberlain, Yee et al. 2008). Polycomb proteins are also crucial in regulating the balance of self-renewal versus differentiation of stem cells, in many different contexts, like during adipogenesis (Wang et al, 2010) or myogenic differentiation (Ezhkova et al, 2009).

Multiple evidences point to a critical role of PRC2 in the control of cell cycle progression, especially of G1-to-S transition. Indeed, expression of EZH2 contributes in promoting this transition through the repression of p16 (van den Heuvel and Dyson 2008) encoded by the *Cdkn2a* locus. Both PRC1 and PRC2 negatively regulate a more extended subset of cell cycle inhibitors, including p21 (*Cdkn1a*), p27 (*Cdkn1b*) and p57 (*Cdkn1c*) (Yang, Karuturi et al. 2009; Fan, Jiang et al. 2011). Moreover, Polycomb proteins have also been shown to contribute to the prevention of cellular senescence (Guo, Datta et al. 2007), particularly through active repression of the *Cdkn2a* locus (Chen, Gu et al. 2009).

Several studies have demonstrated a role for PcG proteins in the control of DNA damage response (DDR) (Chagraoui, Hébert et al. 2011; Ginjala, Nacerddine et al. 2011). In particular, the sequential recruitment of PRC2 and PRC1 at double strand breaks (DSBs) is important for the retention of DSBs repair proteins at the sites of damage (Ismail, Andrin et al. 2010; Ginjala, Nacerddine et al. 2011). EZH2 was also recently reported to trigger G1/S and G2/M cell cycle

arrest under conditions of genotoxic stress, eventually leading to DDR induction and protection from apoptosis (Wu, Lee et al. 2011)

1.1.3. The COMPASS family of methyltransferases

The first Trithorax Group (TrxG) gene, *Trithorax*, was isolated as a regulator of *Hox* gene expression in *Drosophila melanogaster*. Its mutation causes embryonic segments to be transformed into more anterior ones by antagonizing PcG proteins (Ingham and Whittle 1980; Ingham 1985; Struhl and Akam 1985). After TrxG additional genes were discovered to have mutant phenotypes counteracting PcG mutations and consistent with the loss of *Hox* functions, the overall group was defined as the Trithorax Group (TrxG) of proteins (Kennison and Tamkun 1988). Extensive research over the past decade has revealed that TrxG and PcG proteins act antagonistically to orchestrate the expression of many other key genes involved in cell differentiation and developmental processes, thus regulating a plethora of cellular functions (Schuettengruber, Bourbon et al. 2017).

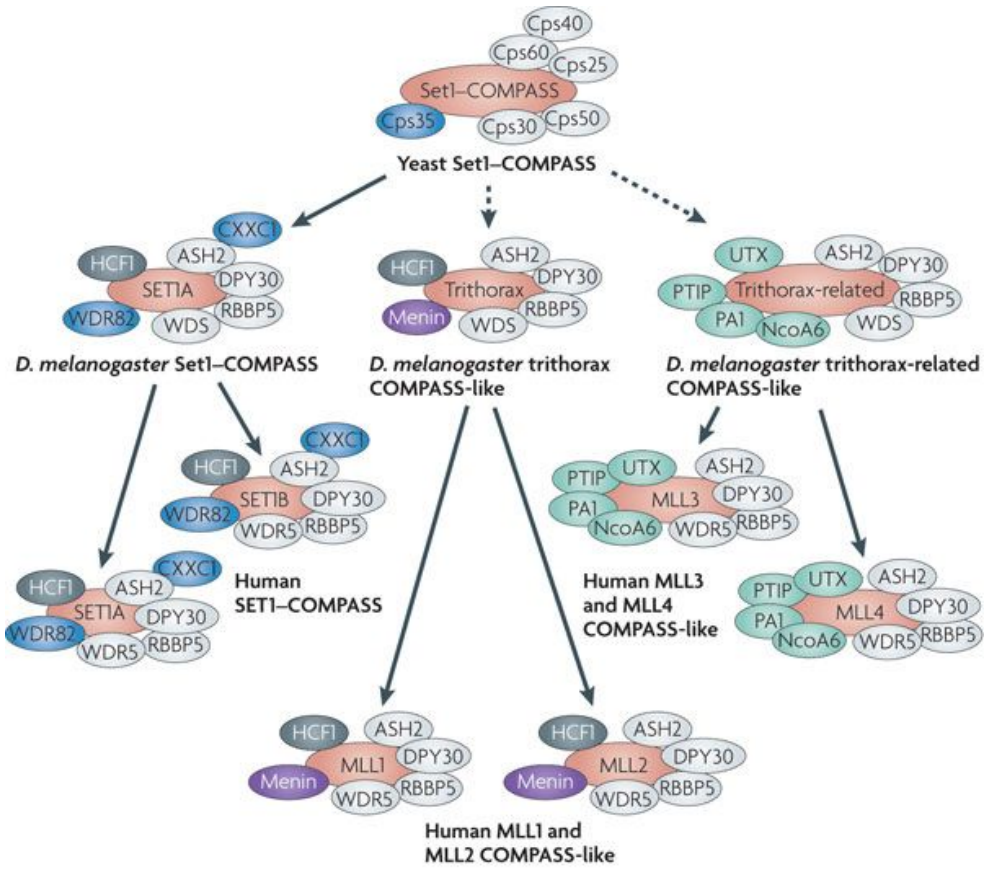


Figure 2. Evolution and composition of COMPASS complexes.

The founding member of the histone 3 lysine 4 (H3K4) methyltransferases, COMPASS, was identified in yeast. D. melanogaster Set1–COMPASS is the homologue of the yeast complex (shown by a solid arrow). There are two COMPASS-like complexes in D. melanogaster (shown by a dashed arrow): a trithorax-containing complex and

trithorax-related-containing complex. In humans, SET1 complexes (SET1A and SET1B) are homologues of yeast and D. melanogaster COMPASS. MLL1 and MLL2 are homologues of trithorax, and MLL3 and MLL4 are homologues of trithorax-related. The known common subunits shared between yeast, D. melanogaster and the human complexes are shown in grey. The common subunits in COMPASS from yeast to human are shown in blue. The shared subunits among the trithorax-related and MLL3 and MLL4 complexes are shown in green. (Adapted from Moha et al, 2010).

TrxG complexes are a very heterogeneous group that plays a widespread role in transcriptional activation. It comprises the switch/sucrose non-fermentable (SWI/SNF) complex and the Complex of Proteins Associated with SET1 (COMPASS) family. Here, I will focus my attention on the COMPASS family of epigenetic modifiers. This group of TrxG complexes is associated with histone PTMs, especially histone methylation, that counteract the repressive marks deposited by PcG proteins. In general, methylation of histone H3 on lysine 4 (K4), lysine 36 (K36), and lysine 79 (K79) is associated with transcription-competent chromatin. In addition, H3K4me3 is primarily found in close proximity to TSS, H3K4me1 is found both at TSS and in intergenic regions, frequently associated with regulatory enhancer sequences, whereas H3K36 preferentially marks gene bodies.

The histone methyltransferase complex SET1/COMPASS was first isolated in yeast and it is well conserved among multicellular organisms. Many COMPASS-like complexes evolved from this original complex and they all contain different SET-domain methyltransferases with unique functions (Piunti and Shilatifard 2016). All COMPASS complexes share a conserved protein core that includes the proteins WDR5, ASH2, RBBP5, and DPY30 (together abbreviated as WARD) (Figure 2). SET1/COMPASS additionally contains HCF1, WDR82 and the DNA-binding protein CFP1 and it mediates bulk H3K4me3. Mixed lineage leukemia 1 and 2 (MLL1/MLL2) COMPASS-like complex, the mammalian homolog of Drosophila Trithorax (Trx), additionally contains the proteins MLL1 or MLL2 in a mutually exclusive manner (Hu, Gao et al. 2013). MLL2 is responsible for H3K4me3 at bivalent promoters in mouse ESCs (Denissov, Hofemeister et al. 2014), whereas MLL1 is required for *Hox* genes expression, pointing to non-redundant functions of these two enzymes. Finally, MLL3/4 compass-like complex, the mammalian homolog of Drosophila Trithorax –related (Trr), includes the core subunits and nuclear receptor coactivator (NCOA60), the component Pax transactivation domain-interacting protein (PTIP), PTIP-associated 1 (PA1) and the histone demethylase Ubiquitously transcribed tetratricopeptide repeat, X-chromosome (UTX/KDM6A), which can specifically remove the PcG-mediated repressive H3K27me3 mark (Agger, Cloos et al. 2007; Piunti and Shilatifard 2016) (Figure 2).

1.1.3.1. Functions of MLL complexes

COMPASS or KMT2 complexes play important roles in transcriptional regulation. They are enriched at multiple transcriptional regulatory regions including gene promoters and enhancers (Shilatifard 2006; Schuettengruber, Martinez et al. 2011). Many results support a dynamic and context-dependent requirement of KMT2s for gene expression. They also suggest that H3K4 methylation may have inherent stability once set. In support of this view, individual deletions of KMT2s in differentiated cell, like MEFs, lead to surprisingly few changes in gene expression, when compared to deletions in mitotically active, progenitor cell types (Blobel, Kadauke et al. 2009; Wang, Lin et al. 2009). Indeed, large scale KMT2-dependent transcriptome changes are described during embryonic stem cells (ESCs) differentiation (Ang, Tsai et al. 2011) leukemic transformation (Cao, Townsend et al. 2014) or cellular response to external stimuli like LPS or retinoic acid (Austenaa, Barozzi et al. 2012; Guo, Chang et al. 2012).

Transgenic mice carrying mutant forms of KMT2 enzymes have defined a role for this family of enzymes in development. Homozygous deletion of all KMT2s leads to embryonic lethality at late stages of development. Specifically, *Kmt2g* and *Kmt2b* deleted embryos die at E10.5-11.5, *Kmt2d* mutants at E9.5, *Kmt2a* at day E12.5 and *Kmt2b* at 10.5 (Glaser, Schaft et al. 2006). Differently from other KMT2s, *Kmt2f* deletion leads to early embryonic lethality due to gastrulation failure at E5.5.

Many evidences support a direct involvement of KMT2s in transcriptional initiation and specifically in the binding of RNA Pol II at promoters and enhancers in various cells (Dou, Milne et al. 2005; Taverna, Li et al. 2007; Lee, Wang et al. 2013; Tang, Chen et al. 2013). Specifically, MLL3 and MLL4 (*Kmt2c* and *Kmt2d)* are the major histone methyltransferases responsible for H3K4me1 and activation of enhancers during cell differentiation, like adipogenesis (Yokoyama, Ficara et al. 2013). They function to prime these enhancers in coordination with lineage-specific transcription factors by maintaining open chromatin to facilitate RNA Pol II access (Lee, Wang et al. 2013). Another important function of this complex is coactivation of nuclear receptors signalling (Mo, Rao et al. 2006). Particularly, MLL4 is recruited to estrogen receptor (ER) α target genes by direct binding to ERα following estrogen stimulation (Mo, Rao et al. 2006; Lee, Kim et al. 2009).

Early studies identified MLL1 and MLL2 (*Kmt2a* and *Kmt2b)* as positive regulators of *Hox* gene expression (Yu, Hess et al. 1995). Deletion of both copies of MLL1 in mouse embryonic stem cells resulted in embryonic lethality, whereas MLL1 heterozygous mice demonstrated retarded growth, hematopoietic abnormalities and bidirectional homeotic transformations (Yu, Hess et al. 1995). Subsequent cellular studies also linked the role of MLL1 in regulating *Hox* gene expression to its involvement in leukemic pathogenesis (Ayton and Cleary 2003; Zeisig,

Milne et al. 2004). Despite the importance of MLL1 in these contexts, deletion of MLL1 in MEFs demonstrated that these methyltransferase is required only in 5% of the promoters carrying H3K4me3 mark (Wang, Lin et al. 2009). These included developmental regulators like *Hox* genes and resulted in decreased levels of Pol II, decreased expression and loss of H3K4 methylation at these genes. These findings point to limited functions restricted to specific genomic targets for MLL1-MLL2 COMPASS-like complexes.

In conclusion, dynamic functions of KMT2s family enzymes *in vivo* are ensured by a multi-level regulation of their activity in a spatiotemporal manner. Indeed, many of these proteins are subjected to regulatory proteolysis. It is reported that MLL1 remains associated to DNA during replication and mitosis to ensure perpetuation of transcriptional states (Blobel, Kadauke et al. 2009; Petruk, Sedkov et al. 2012). However, MLL1 level is also controlled by degradation, like at the G1/S and M/G1 transitions, by different E3 ubiquitin ligases (Wang, Muntean et al. 2012).

1.1.4. Lysine demethylases

Studies in the 1970s indicated that histone methyl groups had approximately the same half-life as that of the histone itself (Byvoet, Shepherd et al. 1972). Hence, histone methylation was considered as an irreversible modification, explaining thereby how epigenetic information was stored and inherited. Later studies revealed, however, a faster turnover of methylated histones which were constantly exchanged within nucleosomes during the cell-cycle (Annunziato, Eason et al. 1995). In addition to replication-dependent dilution of histone methylation during cell divisions, two possible mechanisms for erasing the methylation mark were suggested. For instance, the removal of histone methylation could be a result of either methylated histone replacement with unmethylated counterparts or methylated histone tail proteolytic removal. This phenomenon was explained with the isolation of the first lysine-specific demethylase LSD1/KDM1A, which confirmed the existence of an active process leading to the enzymatic removal of methyl-groups from histones (Shi, Lan et al. 2004). LSD1 actively removes methylation from Histone H3 on lysine 4 (H3K4) with a mechanism of action conserved in most eukaryotes. LSD1 acts as an amine oxidase that catalyzes oxidative demethylation of mono- and dimethylated lysine residues using Flavin Adenine Dinucleotide (FAD) as a cofactor (Shi, Lan et al. 2004). Shortly after the initial discovery of LSD1, biochemical studies led to identification of FBXL11/KDM2A/JARID2, that demethylates H3K36 via its deoxygenase Jumonji-C (JmjC) domain, which coordinates iron to mediate a 2-oxoglutarate (2-OG)-dependent demethylation reaction (Tsukada, Fang et al. 2006).

Hence, based on these observations, two classes of demethylases can be identified. The proteins of the KDM1 (Lysine-K-Demethylase 1) family are FAD-dependent amine oxidases, which can act only on mono and dimethylated lysine residues (Figure 3). The Jumonji C (JmjC)

domain is a signature motif for the other class of demethylases, which are Fe(II) and 2-OG-dependent enzymes. Based on sequence homology in the JmjC domain and on the overall architecture of associated motifs, JmjC domain-containing proteins have been classified into different groups, several of which have been found to possess histone demethylase activity (Figure 3).

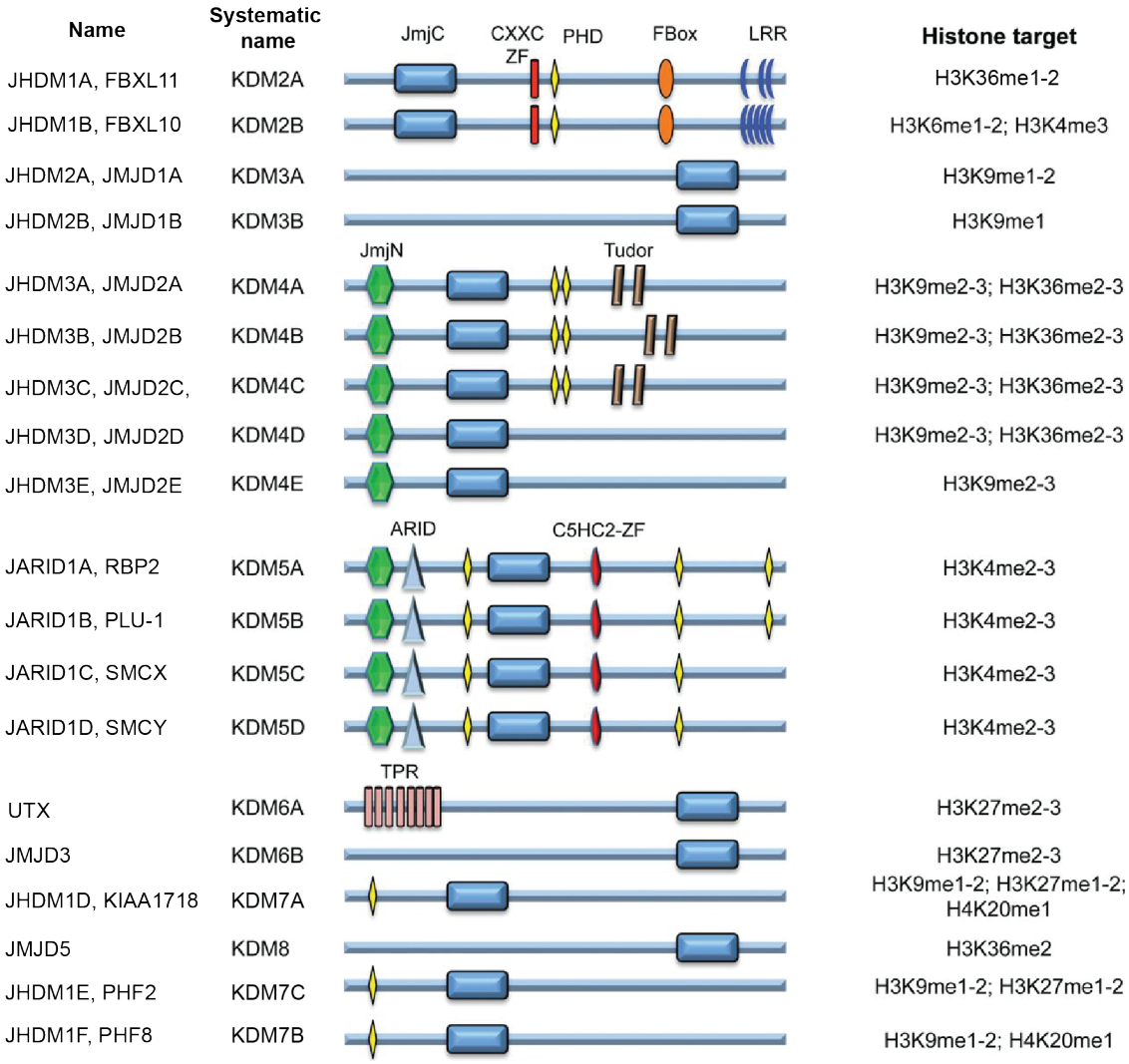


Figure 3. JmjC family members, domain structures and histone targets. Representation of main members of JmjC family, with official and systematic names, domain organization and histone modification targets. (ARID, AT-rich interactive domain; C5HC2-ZF, C5HC2 zinc finger domain; CXXC-ZF, CXXC zinc finger domain; FBox, F-box domain; JmjC, Jumonji C domain; JmjN, Jumonji N domain; LRR, leucine-rich repeat domain; TPR, tetratricopeptide domain; Tudor, Tudor domain) (Adapeted from Shmakova, et al, 2014).

1.1.4.1. Functions of Jumonji-type lysine demethylases (KDM)

The *Jmj* gene coding for the founding member of the Jumonji family, JARID2, was given the Japanese name jumonji, literally translated as "cruciform", based on the cross-like shape found during neural groove development of *Jmj* mutant mice (Takeuchi, Yamazaki et al. 1995;

Takeuchi, Watanabe et al. 2006). JmjC enzymes belong to a family of metalloproteins that display low sequence similarities but share few sequence motifs necessary for iron and 2-OG binding (Ng, Kavanagh et al. 2007). Paradoxically, JARID2 lacks essential residues necessary for catalytic activity, but has been shown to associate to PcG proteins in several cell types, including embryonic stem (ES) cells (Takeuchi, Watanabe et al. 2006; Pasini, Cloos et al. 2010). The initial studies highlight the fact that most, if not all, JmjC enzymes function as parts of transcriptional or chromatin protein complexes and in addition to their catalytic role, they exert the function of scaffold proteins.

The first enzymes characterized within the KDM2 family were KDM2A and KDM2B (or JHDM1A or FBXL10 and JHDM1B or FBXL11), catalyzing the demethylation of H3K36me2/1 histone marks. They play essential roles during development, as part of the OCT4-SOX2 regulatory axis and they can regulate reprogramming, pluripotency and stem cell properties (Wang, Chen et al. 2011; Wu, Johansen et al. 2013). KDM2B has been found in complex with PRC1 components and with corepressors like BCL6 corepressor (BCOR) and it has been shown to inhibit proliferation and prevent senescence through repression of the *Ink4b* locus (He, Shen et al. 2013). They also repress transcriptional activities of the NF-κB subunit RELA (Lu, Jackson et al. 2010) and of the transcription factor c-JUN (Koyama-Nasu, David et al. 2007). KDM2 members exert their critical roles both through demethylase dependent and independent scaffolding functions.

Two KDM3 family members exist in mammals: KDM3A (JMJD1A or JHDM2A) and KDM3B (JMJD1B or JHDM2B) and they possess specific H3K9me2/me1 demethylase activity. KDM3A is important for germ cell development and metabolism. *Kdm3a* KO mice display an adult obesity phenotype and in this context KDM3A has been implicated in the transcriptional control of metabolic genes in muscle and adipose tissues (Inagaki, Tachibana et al. 2009; Tateishi, Okada et al. 2009). In addition, KDM3A is linked to the expression of pluripotency-associated and hypoxia-inducible genes (Loh, Zhang et al. 2007; Krieg, Rankin et al. 2010). In contrast, functions of KDM3B require further studies.

KDM4 family comprises 4 members: KDM4A/JMJD2A/JHDM3A, KDM4B/JMJD2B/JHDM3B, KDM4C/JMJD2C/JHDM3C and KDM4D/JMJD2D/ JHDM3D. They catalyze the demethylation of H3K9me3/me2, a histone mark found in heterochromatin, and/or of H3K36me3/me2, although at a lower rate, with the substrate specificity varying between family members (Hillringhaus, Yue et al. 2011). The role of KDM4 demethylases in many types of tumors, like breast and prostate cancer (Cloos, Christensen et al. 2006) has been extensively investigated. However, little is known about the role of KDM4 family members in normal cells. KDM4A is involved in the specification of neural crest cells in the early mouse embryo (Strobl-Mazzulla, Sauka-Spengler et al. 2010). KDM4B regulates commitment of

mesenchymal stem cells to the osteogenic lineage by removing H3K9me3 mark from osteogenic lineage genes (Ye, Fan et al. 2012). It also controls pre-adipocytes proliferation and terminal differentiation (Guo, Li et al. 2012). Instead, KDM4D controls proliferation by interacting with p53 and it regulates cell-type specific enhancers in immune cells through H3K9me3 demethylation (Zhu, van Essen et al. 2012).

KDM5 proteins catalyze the demethylation of H3K4me3/me2. This family is constituted by KDM5A/JARID1A/RBP2, KDM5B/JARID1B/PLU-1, KDM5C/JARID1C/SMCX and KDM5D/JARID1D/SMCY. While studies in *C. elegans* and *Drosophila* show crucial developmental functions for H3K4me3 demethylases, *Kdm5a* knockout mice display only subtle phenotypes, including haematological abnormalities correlated with de-repression of cytokine genes (Klose, Yan et al. 2007). KDM5A has been linked to regulation of differentiation, cell cycle progression and mitochondrial function in different cell culture systems (Pasini, Hansen et al. 2008; Zeng, Ge et al. 2010; Váraljai, Islam et al. 2015). Of note, KDM5A, KDM5B and KDM5D have been reported to interact with PcG proteins, indicating a putative cooperation in transcriptional repression (Pasini, Hansen et al. 2008).

In conclusion, KDM7 family comprises three members, KDM7A/KIAA1718/JHDM1D, KDM7B/PHF8/JHDM1F, KDM7C/PHF2/JHDM1E. They have been shown to demethylate repressive histone marks such as H3K9me1/me2, H3K27me1/me2 or H4K20me1 (Fortschegger, de Graaf et al. 2010), thus mediating transcriptional co-activation, both RNA Pol II and Pol I-mediated (Horton, Upadhyay et al. 2010). Members of this group have been linked to neural functions and development (Huang, Xiang et al. 2010), regulation of pro-inflammatory responses (Stender, Pascual et al. 2012) and cancer (Sinha, Singh et al. 2008). Mutations described in PHF8 are also causative of an X-linked mental retardation often associated to developmental malformations. (Abidi, Miano et al. 2007)

1.1.5. KDM6 family of demethylases

Among the Jmj-type of lysine demethylases, only the KDM6 family exhibits histone H3K27-specific demethylase activity. It consists of three distinct members, namely Ubiquitously transcribed Tetratricopeptide repeat X chromosome (UTX/KDM6A), Jumonji domain-containing protein 3 (JMJD3 /KDM6B) and Ubiquitously transcribed Tetratricopeptide repeat Y chromosome (UTY/KDM6C). UTX and JMJD3, in particular, were discovered in 2007 (Agger, Cloos et al. 2007; Hong, Cho et al. 2007; Lan, Bayliss et al. 2007; Lee, Villa et al. 2007), when several studies described them as H3K27me3 specific demethylases both *in vitro* and *in vivo*, showing that they are conserved from *Caenorabditis elegans* to human (Hong, Cho et al. 2007).

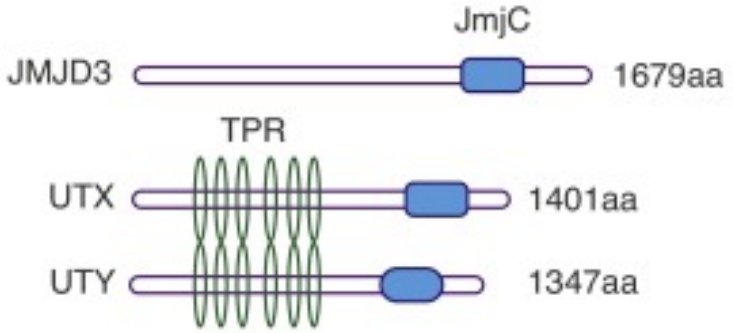


Figure 4. Simplified structures of the main H3K27me3 demethylases. UTX and JMJD3 are the two best-characterized H3K27me3 demethylases. The UTX paralog, UTY, has very weak, albeit detectable, demethylase activity due to a point mutation in the JmjC catalytic domain. JmjC: Jumonji C domain, TPR: tetratricopeptide repeats. aa: amino acids. (Adapted from Arcipowski et al, 2016).

All KDM6 members possess a JmjC catalytic domain followed by a GATA-like DNA-binding domain. UTX consists of 1401 aminoacids and like UTY, it contains a N-terminal located 6 proteins interaction-mediating tetratricopeptide repeat (TPR) domain (Kruidenier, Chung et al. 2012). JMJD3, instead, consists of 1679 aminoacids, but does not contain any characterized domains other than the JmjC domain. Of note, JMJD3 and UTX have 84% sequence similarity in the JmjC domain, whereas they share little if any homology outside of the catalytic domain (Figure 4). UTX and JMJD3 possess histone demethylase activity and they catalyze the removal of one methyl group from trimethyl or dimethyl H3K27, leaving as an end product the monomethyl form. Of note, the gene encoding JMJD3, *Kdm6b*, is on chromosome 17, while the gene encoding UTX, *Kdm6a*, is located on the X chromosome and, unlike most of the X-linked genes, is expressed biallelically in female cells (Greenfield, Carrel et al. 1998). Male cells, carrying only one UTX allele, express the Y-chromosome encoded paralog of UTX, UTY (*Kdm6c*), which has 88% sequence homology with the UTX protein. UTY was classically considered as catalytically inactive, although recent evidences demonstrated a residual demethylase activity due to a subtle sequence divergence in the JmjC catalytic domain (Walport, Hopkinson et al. 2014).

Among potential histone substrates, JMJD3 and UTX are highly specific for H3K27me3 and have little if any demethylase activity on other methylated lysines *in vitro* (Lee, Villa et al. 2007). Structural studies on UTX have shown that substrate specificity is mediated both by the JmjC domain, recognizing methylated K27, and by a novel zinc-binding motif located downstream of the catalytic domain and recognizing some residues of Histone H3 (Sengoku and Yokoyama 2011). Members of other classes of JmjC demethylases have little if any H3K27-specific demethylase activity, with the possible exception of KDM4 family (Labbé, Holowatyj et al. 2013). Apart from their catalytic activity, cumulative evidence supports the

importance of non-demethylase activities of both JMJD3 and UTX, in different cell contexts and developmental stages.

In the past years, many publications have emerged describing the roles of H3K27 demethylase enzymes in various biological contexts, such as development, inflammation and cancer. The following sections will be focused at describing the most relevant functions of the H3K27me3 demethylase UTX in different biological contexts.

1.1.6. Ubiquitously transcribed tetratricopeptide repeat, X chromosome (UTX)

1.1.6.1. UTX regulation of gene transcription

H3K27 methylation is a critical mediator of transcriptional gene repression and contributes to important biological processes including X inactivation, genomic imprinting, stem cell maintenance, animal body patterning and cancer (Lee, Villa et al. 2007; Herz, Madden et al. 2010; Van der Meulen, Speleman et al. 2014). Regulation of cellular H3K27me3 levels is mainly mediated by the antagonizing functions of the H3K27 methyltransferase EZH2 of the PRC2 complex and the H3K27me2/me3 demethylases UTX and JMJD3. Indeed, a decade ago UTX was identified co-purifying with MLL3/MLL4 complexes and functioning during retinoic acid signaling events (Lee, Villa et al. 2007). Since then UTX has been considered as part of the MLL 3/4 complexes responsible for H3K4 methylation, especially for the H3K4me1 mark, and many studies since then supported the view of a dynamic interplay between H3K27me2/me3 demethylation and H3K4 methylation during transcriptional gene activation. The composition of the MLL3/4 complex was confirmed in the Drosophila ortholog Trithorax related Trr (Mohan, Herz et al. 2011). Here, *dUTX* mutants show an increase in global H3K27me3 levels and a parallel reduction of global H3K4me1 levels, that however seems to be independent from direct *dUTX* demethylation capacity (Herz, Madden et al. 2010; Herz, Mohan et al. 2012). Notably, Trr and dUTX are enriched genome-wide near TSS, where they colocalize with RNA-Pol II, but also at active enhancers. These observations in Drosophila suggest that the UTX/MLL complex may play both a promoter-proximal and a promoter-distal role in transcriptional regulation (Herz, Mohan et al. 2012).

ATPase-dependent chromatin remodelling complexes, including the SWI/SNF family, contribute to regulation of chromatin accessibility, allowing transcriptional activation and repression. SWI/SNF family is mainly linked to transcriptional activation, whereby the ATPase complex members BRG1 and BRM interact with acetylated histone tails through their bromodomain (Wang, Allis et al. 2007). An interaction between the BRG1-containing SWI/

SNF remodeling complex and the histone H3K27me2/3 erasers UTX and JMJD3 was demonstrated resulting in general chromatin remodeling that was independent from their H3K27me2/3 demethylase potential. Furthermore, UTX and JMJD3 were shown to be functionally required for transcriptional activation of lineage-defining T-box transcription factors (including *T-bet*, *Eomes* and *Tbx5*) (Miller, Mohn et al. 2010), which represent essential transcriptional regulators in early cell-fate decisions, differentiation and organogenesis (Wilson and Conlon 2002). Furthermore, studies in Drosophila showed that Creb-binding protein (CBP) associates with dUTX and the ATP-ase BRM of the SWI/SNF complex, that resembles the mammalian BRM and BRG1 (Tie, Banerjee et al. 2012). CBP acts antagonistically to Polycomb at Polycomb target genes by catalyzing the deposition of the active chromatin mark H3K27ac (Tie, Banerjee et al. 2012). Genome-wide analyses showed that the three components co-occurred at Polycomb target genes enriched for H3K27ac, suggesting a collaborative effort in antagonizing Polycomb gene repression (Tie, Banerjee et al. 2012). Moreover, loss of *dUTX* or *Trr* results in a reduction of global H3K27ac levels in various tissues (Herz, Mohan et al. 2012). In agreement to these evidences in Drosophila, a recent study described an interesting epigenetic crosstalk at enhancer regions between UTX-MLL4 complex and the histone acetyltransferase p300. The authors demonstrated that UTX, in a demethylase-independent manner, facilitates the establishment of an "active (H3K4me1$^+$ H3K27ac$^+$) enhancer landscape" in ESCs by recruiting and coordinating the enzymatic functions of MLL4 and p300. Notably, loss of UTX leads to reduced levels of the H3K4me1 and H3K27ac histone marks and impaired transcription (Wang, Lee et al. 2012).

1.1.6.2. UTX function in early embryonic development

The mammalian embryo utilizes Histone PTMs to coordinate the drastic changes in gene expression programs and cellular specification that he undergoes throughout development. In particular, H3K27me3 is important in the early stages of embryonic development to maintain self-renewing embryonic stem cells (ESCs) and pluripotent cells and to repress tissue-specific developmental programs (Boyer, Plath et al. 2006). As differentiation progresses, H3K27me3 needs to be removed in order to re-activate lineage-specific patterns of developmental gene expression (Bernstein, Mikkelsen et al. 2006; Lee, Jenner et al. 2006). These rapid changes in early embryonic chromatin environment depend on H3K27 demethylases. Several groups found that UTX is needed for early embryonic development, whereas UTX and JMJD3 have been shown to be functionally redundant in promoting the development of the early oocyte to the blastocyst stage (Yang, Song et al. 2016). Indeed, several groups showed that complete loss of *Utx* in female mice leads to embryonic lethality between embryonic day (E) 10.5 and 12.5, whereas of *Utx*$^{+/+}$ heterozygous female mice are viable and fertile (Lee, Lee et al. 2012;

Shpargel, Sengoku et al. 2012; Thieme, Gyarfas et al. 2013). Indeed, *Utx*-deficient female embryos exhibit major defects in the formation of mesoderm-derived tissues, at mid-gestation, like defective posterior notochord formation, and die from impaired heart development. Furthermore, ChIP-sequencing analyses in *Utx*-null ESCs found increased H3K27me3 decoration at promoters, including gene encoding the critical transcriptional regulator of mesoderm differentiation *Brachiury* (Wang, Lee et al. 2012).

There was, however, a surprising evidence: these functions of UTX in early embryonic development did not require its demethylase activity. Indeed, $Utx^{A/Y}$ male mice are normal aroung E 9.5 without any defect in mesoderm formation. These mice have a diverse outcome due to abnormalities at later stages of development (E12, E13), but may survive until the end of embryonic development. Although some $Utx^{A/Y}$ male mice died around birth due to neural tube closure defect and inability to breathe, some of them (25%) live into adulthood. They are smaller and display a reduced lifespan, but they are fertile, suggesting that *Uty* may partially compensate the loss of *Utx* in hemizygous mutant males, rescuing the cardiac phenotype (Shpargel, Sengoku et al. 2012; Wang, Lee et al. 2012; Welstead, Creyghton et al. 2012). To further support these evidences, double $Utx^{A}Uty^{A}$ mutant mice are embryonic lethal and phenocopy $Utx^{A/A}$ female mice (Shpargel et al, 2012). Moreover, a demethylase-dead version of UTX rescued the early development of *Utx*-deficient embryos (Wang, Lee et al. 2012) Additional experiments excluded that this could have been caused by functional redundancy between UTX and JMJD3. Indeed, the development of *Utx* and *Jmjd3* double mutant male embryos proceeded through late gestation, similar to that of embryos lacking *Jmjd3* only (Shpargel, Starmer et al. 2014). Indeed, JMJD3 was shown to be dispensable for early B cell development, but it was crucial for post-natal development (Burgold, Voituron et al. 2012). Thus, the demethylase activity of UTX is dispensable for early embryonic development and apparently this enzyme does more than H3K27me3 demethylation.

Similar striking functions have been highlighted for UTX in the embryonic development of *Drosophila melanogaster* and *Caenorabditis elegans*. In *Drosophila,* homozygous mutants for the UTX ortholog *dUTX* are lethal and only 5% of animals survive the pupal stage, although not reaching adulthood (Herz, Madden et al. 2010). In accordance with these data, UTX-1 mutant worms die as late stage embryos or as malformed L1 larvae. In this context UTX-1 is critical for posterior and gonadal development in a demethylase-independent manner (Vandamme, Lettier et al. 2012). Interestingly, loss of UTX-1 complex members like SET-16 (MLL2/3), PIS-1 (PTIP) and WDR-5.1 (WDR5) gave rise to the same defects, further confirming that these genes are all acting in the same complex.

Studies in *Drosophila* first reported that dUTX was necessary for the controlled expression of 2 specific homeotic genes in very early fly development (Copur and Müller 2013). Furthermore, sex combs malformation, rough eyes, wrinkled wings and wing vein defects are observed in the *dUTX* mutants, which are reminiscent of *Trithorax* mutants and are in concordance with a putative effect of UTX protein on *Hox* gene regulation (Copur et al, 2003). *Hox* genes are highly conserved transcriptional regulators, especially controlling the development of the anterior-posterior axis (Lan, Bayliss et al. 2007). Aberrant expression of *Hox* genes leads to developmental defects and disease. (Shah and Sukumar 2010). Both Polycomb and Trithorax are implicated in the regulation of spatio-temporal expression of *Hox* genes, thus regulating body patterning and differentiation (Bracken, Dietrich et al. 2006). Evidence for involvement of UTX in regulation of *Hox* gene activity in mammals was demonstrated through UTX knock-down experiments in HEK293T cells in which loss of *Utx* resulted in transcriptional repression of *Hoxa* and *Hoxc* clusters and in an increase of H3K27me2/me3 levels at the promoter regions of *Hoxa13* and *Hoxc4*, but no changes in MLL or PRC2 occupancy were observed (Lee, Villa et al. 2007). Furthermore, ChIP for UTX showed a strong UTX binding at the TSS of many *Hox* genes in human fibroblasts, but not in mouse ESCs, where *Hox* genes are silences (Lan, Bayliss et al. 2007). In the same analyses, UTX direct targets were found enriched for genes belonging to a retinoblastoma gene network, associated to a gain in H3K27me3 upon UTX inactivation in the same cell type (Wang, Tsai et al. 2010).

Together, these evidences point to a crucial role of UTX in regulating early embryonic development by controlling transcription as well as levels of H3K27 methylation on *Hox* cluster genes.

1.1.6.3. UTX contribution to cell differentiation

During ESCs differentiation, there is a general reorganization of chromatin and redistribution of histone PTMs directly connected to the re-activation of developmental genes. Particularly, this process is associated to the loss of H3K27me3 (Boyer, Plath et al. 2006).

This event occurs mainly at the promoters of genes encoding for key developmental regulators, characterized by the concomitant presence of activating H3K4me3 and repressive H3K27me3 histone marks and consequently defined as bivalent genes (Bernstein, Mikkelsen et al. 2006; Mikkelsen, Ku et al. 2007). The resolution of this poised epigenetic configuration towards the activation state is mediated by the action of histone demethylases and it leads to transcriptional activation of lineage-specific genes. Hence, the activity of opposing PcG methyltransferases and demethylases targeting the same H3K27 histone residue is tightly regulated at the onset of differentiation. Moreover, H3K27me3 demethylases act in connection with MLL complexes H3K4me3 methyltransferases to oppose the activity of PcG proteins and induce expression of

developmental effectors (Cloos, Christensen et al. 2008). It has been proposed that once recruited at bivalent genes, H3K27me3 demethylases erase the H3K27me3 repressive marks while the MLL proteins catalyze H3K4 trimethylation to ultimately facilitate transcription of target genes (Agger, Cloos et al. 2007).

Through these finely balanced mechanisms, UTX has been shown to contribute to a variety of tissue-specific and developmental processes including cardiac development, hematopoiesis, myogenesis, adipogenesis, osteogenic differentiation, wound healing and aging. Indeed, loss of UTX seems to impact on the differentiation capacity of ESCs (Lee, Lee et al. 2012; Mansour, Gafni et al. 2012; Welstead, Creyghton et al. 2012; Morales Torres, Laugesen et al. 2013). This defect in inducing differentiation processes is reflected by loss of activation of a set of developmental genes, including endodermal markers (*Gata4, Gata6, Foxa2*) ectodermal markers (*Otx2, Sox1, Pax6*), and mesodermal markers (*Wnt3, Vegfr2, and Brachiury*) (Wang, Lee et al. 2012; Welstead, Creyghton et al. 2012; Jiang, Wang et al. 2013; Morales Torres, Laugesen et al. 2013), probably due to loss of UTX binding to the promoters of these genes. Notably, different contradicting evidences argued on whether UTX demethylase activity was required during ESCs differentiation. For example, UTX binds directly to the promoters of *Sox1* and *Brachiury*, without any change in H3K27me3 levels. On the contrary, the *Hoxb*1 gene exhibited a decrease in the levels of this mark upon differentiation of ESCs, suggesting that UTX still plays a demethylase-dependent role in the transcriptional regulation of *Hox* genes (Morales Torres, Laugesen et al. 2013)

UTX plays an important role in cardiac development. $Utx^{\Delta/Y}$ ESCs that differentiate *in vitro* into mature cardiac cells show absence of effective heart-like rhythmic contractions due to a failure in inducing cardiac-specific gene. Furthermore, $Utx^{\Delta/\Delta}$ female mice and $Utx^{\Delta}/Uty^{\Delta}$ male mice exhibited strong cardiac developmental defects (Lee, Lee et al. 2012). In this context, loss of UTX impairs the induction of cardiac-specific genes mediated by H3K27me3 demethylation, whereby cardiac transcription factors (GATA4, TBX5) recruit UTX to the promoter regions of cardiac-specific genes. Moreover, loss of UTX affects the interaction between the BRG1-containing SWI/SNF chromatin remodelling complex and the core cardiac transcription factor TBX5, an effect that is thought to be independent from the H3K27me2/3 demethylase activity of UTX (Lee, Lee et al. 2012).

Another crucial role of UTX has been reported during the activation and lineage progression of satellite cells during both myogenesis and muscle regeneration. Specifically, UTX demethylates muscle-genes in a two-step process: it gets recruited to the regulatory regions of muscle genes by a transactivator and it demethylates a region close to their TSS. Further demethylation in the gene body of muscle genes, however, requires the presence of RNA Pol II elongation (Seenundun, Rampalli et al. 2010). Through this double mechanism, UTX induces

the expression of *Myogenin* and *Creatin kinase* genes. Concomitantly, UTX was important for satellite cells-mediate muscle regeneration, since their differentiation potential in response to muscle injury was impaired by the conditional inactivation of UTX. Again, this defect was mediated by a failure to upregulate *myogenin*, which correlated to an accumulation of H3K27me3 at its promoter region (Faralli, Wang et al. 2016).

Histone demethylases UTX and JMJD3 were both shown to be important for osteogenic differentiation. A study reported that treatment of human mesenchymal stem cells (MSCs) with the double demethylase inhibitor GSK-J4, targeting both UTX and JMJD3, impaired cartilage discs formation, expression of chrondrogenic genes (*Sox9, Col2a1*) and collagen production. In this experimental setting, JMJD3 function was shown to be more relevant, since its expression, and not UTX one, was induced during chondrogenesis (Yapp, Carr et al. 2016). Two independent studies, however, reported a role for UTX in sustaining osteogenesis (Hemming, Cakouros et al. 2014; Wang, Lian et al. 2017). Particularly, UTX was shown to counteract glucocorticoid-induced inhibition of osteogenesis since its silencing in immortalized murine osteogenic progenitor cells skewed differentiation towards the adipogenic lineage. UTX sustained osteogenic-specific transcription programs and occupied *Osterix* and *Runx2* promoters. It also attenuated glucocorticoid-induced elevated levels of H3K27me3, especially at the promoters of glucocorticoid-induced genes, like *Dkk1* (Wang, Lian et al. 2017). Another work highlighted the importance of the epigenetic control of H3K27me3 in dictating MSCs lineage determination towards either osteogenic or adipogenic lineages. Enforced expression or knock-down of either EZH or UTX in these cells demonstrated their opposite functions in skewing differentiation to one lineage or the other, by controlling the expression of master regulatory genes respectively involved in adipogenesis or osteogenesis (Hemming, Cakouros et al. 2014). The function of UTX in controlling adipogenesis was further confirmed by a study where *Utx* inactivation was achieved both in murine ESCs and pre-adipocytes. Strikingly, whereas UTX-deficient ESCs exhibited reduced adipogenic potential, *Utx*-KO pre-adipocytes showed enhanced differentiation to adipocytes, suggesting that UTX functions as a positive or negative regulator, depending on the differentiation stage. Interestingly, the authors described *β-catenin/c-Myc* pathway as an important effector of UTX-mediated adipogenesis (Ota, Tong et al. 2017).

A further example of the importance of UTX in controlling differentiation events comes from neuronal development. Specifically, *Utx* inactivation in neuronal stem cells enhanced their proliferation by inhibiting cell-cycle exit and neuronal differentiation. *Utx* KO affected the expression of *Pten* and the protein levels of phospho- (p-) AKT and p-mTOR. Interestingly, UTX deficiency increased H3K27me3 levels at the promoter of *Pten,* thus affecting its expression. However, milder impairment in cortical development observed in males compared

to females suggest both demethylase –dependent and independent functions of UTX in neuronal development (Lei and Jiao 2018). In neural stem cells, a direct interaction between JMJD3 and p53 was described, whereby JMJD3 facilitated the nuclear localization of p53 (Sola, Xavier et al. 2011). In a more recent paper, it was proposed that p53 and JMJD3 are both upregulated upon DNA damage and that JMJD3 gets recruited to p53 targets to trigger apoptosis (Williams, Christensen et al. 2014).

1.1.6.4. UTX contribution to somatic cell reprogramming

Pluripotency is the unique characteristic of ESCs to induce the generation of the three germ layers endoderm, ectoderm and mesoderm, that are required to constitute all tissues of an adult organism (Rada-Iglesias, Bajpai et al. 2011). *In vitro* re-programming of somatic cells can be accomplished by ectopic expression of different transcription factors, classically OCT4, SOX2, KLF4 and MYC (OSKM) (Takahashi and Yamanaka 2006). Hence, pluripotency can be re-established by generating induced pluripotent stem cells (iPSCs) (Takahashi and Yamanaka 2006). This process is accompanied by genome-wide changes in the transcriptome and in the chromatin structure that are needed to achieve the switch to the pluripotent state (Rada-Iglesias, Bajpai et al. 2011). UTX has a critical role in efficient induction or re-establishment of pluripotency during the generation of iPSCs *in vitro*, but it is dispensable for maintenance of pluripotency (Mansour, Gafni et al. 2012). The need for UTX to ensure correct reprogramming is linked to its H3K27me3 demethylase activity. During iPSCs induction, UTX target genes are enriched with H3K4me3 in *Utx*- wild type MEFs, while aberrantly accumulating H3K27me3 in *Utx* mutant MEFs. These loci included the stem-cell maintenance genes *Sall1, Sall4* and *Utf1*, as well as validated *Klf4* and *Oct4* target genes. They all fail to reactivate during reprogramming due to loss of UTX. Hence, UTX important role during reprogramming is mediated by its H3K27me2/me3 demethylation activity and consists in the correct re-activation of essential pluripotency genes (Mansour, Gafni et al. 2012). On the contrary, JMJD3 plays an opposite role to UTX during somatic cell reprogramming, by upregulating the *Cdkn2a* locus, thus inhibiting this process (Zhao, Li et al. 2013). Moreover, UTX regulates the timely execution of H3K27me3 demethylation observed at E10.5-11 in primordial germ cells (PGCs), since UTX deficient PGCs show cell-autonomous aberrant epigenetic reprogramming dynamics during maturation *in vivo*. As a consequence, PGCs development is disrupted by day E12.5 and impairs germline transmission in mouse chimeras generated from *Utx*-mutant pluripotent cells. Notably, defects in germ-lineage development were not rescued by a catalytically dead version of UTX, suggesting that this phenotype depends from the absence of UTX demethylase activity (Mansour, Gafni et al. 2012).

1.1.6.5. UTX deregulation in cancer

Over the last years, deregulated histone methylation became a central topic in cancer biology research, especially the maintenance of the balance of H3K27 methylation. Indeed, deregulated expression of H3K27 methyltransferase *EZH2* is observed in a variety of solid cancers and hematopoietic tumors (Sauvageau and Sauvageau 2010; McCabe, Ott et al. 2012; Beguelin, Popovic et al. 2013). In 2009, a systematic screening of mutations of the histone methylation machinery in human cancer identified somatic loss-of-function mutations and deletions targeting the *UTX* gene in multiple cancer types (van Haaften, Dalgliesh et al. 2009). The highest prevalence, 10%, was observed in multiple myeloma, whereas 8% of esophageal squamous cell carcinomas and 1,4% of renal cell carcinomas carried inactivating *UTX* mutations. These results were further supported and integrated by subsequent identification of recurrent inactivating *UTX* mutations in several leukemia and solid tumors by whole exome- or genome-wide sequencing analyses. Intersection of these studies on primary cancers adjusted the frequencies of *UTX* mutations to 3,45% in multiple myeloma, 10-3% in leukemias and around 2% in renal and esophageal squamous cell carcinomas (Chapman, Lawrence et al. 2011; Gui, Guo et al. 2011; De Keersmaecker, Atak et al. 2012; Kandoth, McLellan et al. 2013; Van der Meulen, Speleman et al. 2014; Van der Meulen, Sanghvi et al. 2015). However, *UTX* lesions tend to be homozygous in females and to be accompanied by the loss of its paralog *UTY* in males, suggesting a tumor suppressor role (van Haaften, Dalgliesh et al. 2009; Robinson, Parker et al. 2012).

Among solid tumors, bladder cancer has one of the highest frequencies of *UTX* mutations (24%), typically affecting the JmjC catalytic domain. Interestingly, more than 50% bladder cancer patients harbor genetic aberrations in chromatin remodelers including acetyltransferases *CREBBP* and *EP300* and *MLL1* (Gui, Guo et al. 2011). The same mutation spectrum in histone modifiers was identified in medulloblastoma patients (Jones, Jager et al. 2012). Here, *UTX* mutations were found only in the two prognostically relevant subgroups with a higher male prevalence. In addition, more than 50% of *UTX* mutant male medulloblastoma patients had a deletion of the Y-chromosome (including *UTY*) compared to lower frequencies in *UTX* WT males.

UTX plays also a male-specific tumor suppressor role in T-cell acute lymphoblastic leukemia (T-ALL). Moreover, most mutations target the catalytic domain of UTX, suggesting that UTY cannot compensate for some demethyase-dependent activities of UTX. Knock-out of *Utx* in *Notch1*-driven mouse model leads to accelerated leukemia development and proliferation, together with accumulation of H3K27me3 at the promoters of putative tumor suppressor genes. *Utx*-null tumors were also more sensitive to EZH2 inhibition, emphasizing the clinical importance of the H3K27me3 balance (Van der Meulen, Sanghvi et al. 2015). Interestingly,

loss-of-function defects in UTX and EZH2 were found in chronic myelomonocytic leukemia (CMML) although occurring in a mutually exclusive manner (Jankowska, Makishima et al. 2011). In contrast to its tumor suppressor role in fibroblasts, where it activates the *Cdkn2a* locus, leading to cell cycle arrest under stress conditions (Bracken, Dietrich et al. 2006) and its downregulation in several cancer types, like lung and liver carcinomas, JMJD3 functions as an oncogene in T-ALL, where it is required for leukemia initiation and maintenance (Ntziachristos, Tsirigos et al. 2014).

A recent work by the Licht group characterized the role of UTX in an isogenic multiple myeloma (MM) cell system and reported that *UTX* loss accelerated cell growth and promoted clonogeneicity, adhesion and tumorigenicity of MM cells. Gene expression profiling revealed that the loss of *UTX* led to failure in activation of genes linked to cell growth and proliferation, cell adhesion and cell cycle. Most of these genes were identified as PRC2 targets, suggesting that the loss of *UTX* leads to abnormal PRC2 activity. Consistently with the latter observation, *UTX*-deficient cells showed increased *in vitro* and *in vivo* sensitivity to inhibition of EZH2. Such sensitivity was related to a decrease in the levels of *IRF4*, whose expression is a hallmark of MM, and of *c-MYC,* with a concomitant activation of *IRF4* repressors *BCL6*, *IRF1* and *BATF* (Ezponda, Dupere-Richer et al. 2017).

Moreover, an important function of UTX in supporting lymphomagenesis has just been suggested by a work where the effects of B-cell specific *Utx* inactivation were studied in an *Eμ-Myc* lymphoma model (Li, Zhang et al. 2018). The group demonstrated a dosage effect of UTX during tumorigenesis. Comparing to single copy deletion of *Utx,* deletion of both copies of *Utx* resulted in much faster rate of lymphomagenesis. Moreover, *Eμ-Myc; UTX*$^{-/y}$ mice developed lymphoma at a slower rate compared to female *Utx* KO animals, suggesting compensatory effects provided by UTY. Overall, UTX deficiency enhanced the aggressiveness of lymphomas, strongly promoting the disease progression and dissemination in different organs. Interestingly, *Utx*-KO tumors upregulated the proto-oncogene *Blk*, a signaling effector of pre-BCR that enhances proliferation of B progenitors *in vivo*. Another interesting gene was *Efnb1*, found highly overexpressed in *Utx*-KO lymphomas and involved in tumor invasion and angiogenesis. Its overexpression *in vivo* could recapitulate the phenotypes observed in UTX-deficient lymphomas. Moreover, UTX loss sensitizes tumor cells to treatment with the nucleoside analog cytarabine (Li, Zhang et al. 2018).

Finally, a Sleeping Beauty based insertional mutagenesis screen using a *Kras*-driven pancreatic mouse model identified genes involved in chromatin regulation among the candidate cancer driver genes, including *Utx*. This un-biased screening approach provides an independent confirmation of the potential role of UTX as a *bona fide* tumor suppressor gene in many different contexts in cancer biology (Mann, Ward et al. 2012).

However, recent evidences emerged pointing to a cell-context specific role of UTX in tumorigenesis, as overexpression of *Utx* in breast cancer has been reported to promote proliferation and invasion (Kim, Sharma et al. 2014). In agreement with this notion, UTX target genes seem to be very different among cell types, suggesting a more cell-specific role for this demethylase (Wang, Tsai et al. 2010; Kim, Sharma et al. 2014; Ntziachristos, Tsirigos et al. 2014).

1.1.6.6. UTX as Kabuki syndrome gene

Kabuki Syndrome (KS), or Niikawa-Kuroki Syndrome is a pediatric congenital autosomal dominant syndrome characterized by a stereotypical set of facial features, that include elongated palpebral fissures and prominent earlobes. It was first identified and described in 1981 by two Japanese groups, led by scientists Norio Niikawa and Yoshikazu Kuroki (Kuroki, Suzuki et al. 1981). It is named Kabuki syndrome because of the facial resemblance of affected individuals to stage makeup used in kabuki, a Japanese traditional theatrical form. Affected individuals display skeletal anomalies, dermatoglyphic abnormalities, severe cognitive disabilities and post-natal growth deficiency (Matsumoto and Niikawa 2003). Other frequently observed disorders can include several forms of congenital cardiac abnormalities, cleft palate, gastrointestinal malformations and ophthalmologic defects (Armstrong, Abd El Moneim et al. 2005; Schrander-Stumpel, Spruyt et al. 2005). KS results, in the majority of cases (60-70%) from autosomal dominant mutations in the histone methyltransferase *KMT2D* (*MLL4*). A smaller percentage of Kabuki patients (6-14%) carry mutations targeting the histone H3 lysine 27 demethylase *KDM6A*, *UTX*, suggesting that defects in histone-mediated gene expression drive the diverse pathology of this syndrome.

Kabuki-associated *UTX* mutations have been identified both in female and male patients and result from hypomorphic female heterozygous mutation and null male hemizygous mutation of *UTX* gene. Hence, a compensation by UTY in male patients could be hypothesized (Lederer, Grisart et al. 2012; Banka, Lederer et al. 2015), suggesting that UTX-mediated H3K27me3 demethylation may not be essential in craniofacial development. Consistently with this hypothesis, a recent work by the Magnuson laboratory has tried to characterize the genetic, molecular and genomic functions of UTX in the context of neural crest-based development. They specifically deleted *Utx* allele in neural crest cells and demonstrated that this model recapitulates many features of Kabuki syndrome, like cranio-facial dysmorphism, post-natal growth retardation, congenital heart defects and cleft palate (Shpargel, Starmer et al. 2017). Moreover, male *Utx* KO mice exhibited milder craniofacial features and growth retardation phenotypes compared to females, suggesting partial redundancy between UTX and UTY. Epigenomic and transcriptomic analyses of primary neural crest cells upon *Utx* inactivation

revealed that UTX regulates several factors and pathways that control neural crest cell biology and craniofacial development, like WNT and NOTCH pathway members. However, only a small subset of these targets experience UTX-mediated histone demethylation, while the majority of them display unaltered histone methylation. Interestingly, demethylase-dead *Utx* KI point mutant mice displayed almost normal facial features, suggesting that UTX can support craniofacial development through demethylase-independent mechanisms. Additionally, characterization of the spectrum of *UTX* mutations found in KS patients and of the effects that they have on demethylase activity demonstrated that the majority of them disrupted the catalytic function, while two of them maintained it (Shpargel, Starmer et al. 2017). Overall, this study provided the first evidences that KS can manifest through disruption of UTX functions different from its catalytic activity.

Immune dysfunction is a common feature of KS. Many patients manifest a common variable immunodeficiency (CVID), with recurrent otitis and infections being nearly a universal finding (Hoffman, Ciprero et al. 2005; Banka, Lederer et al. 2015; Lin, Lee et al. 2015). In addition, autoimmune diseases, especially immune thrombocytopenia, hemolytic anemia and vitiligo have been reported in patients with KS. To investigate the immune defects associated with KS, a study published in 2015 characterized the cellular and molecular B cell defects found in a cohort of 13 patients with KS. Apart from a not-fully penetrant decrease in $CD19^+$ B cells percentages observed in 4 patients, 90% of the patients displayed immunoglobulin A (IgA) deficiencies, whereas 40% of the patients carrying *KMT2D* mutations also displayed hypogammaglobulinemia. These patients also showed a significant reduction in antibody isotype-switched memory B cells. Consistently, they measured lower mutation rates, indicative of lower affinity for antigens, for IgG antibodies in *KMT2D* deficient patients. *In vitro* terminal differentiation experiments demonstrated impaired ability of *KMT2D* deficient B cells to upregulate *bona fide* markers of plasma cell differentiation (Lindsley, Saal et al. 2016). Hence, the authors postulate that all these phenotypes could be the result of disrupted epigenetic regulation of the *IgH* locus, specifically of KMT2-dependent diminished H3K4 methylation at specific sites important for immunoglobulin isotype switching and terminal differentiation. The lessons learned from the KS suggest potential roles for UTX in regulating adaptive immune responses, possibly supporting KMT2D functions, both in a demethylase-dependent or independent manner.

1.1.6.7. UTX contribution to hematopoiesis

Utx expression levels peak in hematopoietic stem and progenitor cells and drop during hematopoietic differentiation, especially towards the myeloid and erythroid lineages (Liu, Mercher et al. 2012). In $Utx^{\Delta/\Delta}$ female mice embryos, a lack of red blood cells was observed,

pointing to a role of UTX in hematopoiesis (Wang, Lee et al. 2012). Indeed, *Utx* knock-down experiments in the immortalized hematopoietic progenitor cell line EML and primary murine bone marrow (BM) cells impaired their colony forming ability. Moreover, the knock-down of *Utx* in primary murine BM cells affected the expression of key genes that regulate hematopoietic differentiation, such as *Mll1, Runx1* and *Scl*, which were shown to be direct targets of UTX. Specifically, UTX modulated their transcription by regulating H3K27me3 levels at respective promoter regions (Liu et al, 2012).

Female adult mice in which *Utx* was homozygously eliminated at 11-14 weeks of age showed an enlarged spleen, reduced hemoglobin levels, anemia, thrombocytopenia and mild leukocytopenia compared with normal controls. Additionally, *Utx* KO female mice displayed myelodysplasia with chromosomal instability and splenic erythropoiesis (Thieme, Gyarfas et al. 2013), together with the downregulation in their BM of the hematopoietic transcription factors *Tal1*, *Gata1, Ikaros,* and *Lyl1*. Notably, none of the phenotypes observed in *Utx* KO adult females was present in males, predictive of a demethylase-independent function of UTX in hematopoiesis.

In conclusion, an important function of UTX in regulating murine hematopoietic progenitor cells and zebrafish primordial germ cells migration was described, thus confirming migration screening assay results that identified this demethylase as a novel regulator of cell migration (Thieme, Gyarfas et al. 2013).

1.1.6.7.1. UTX regulation of T cell and invariant Natural Killer T cell development

Evidences in hematopoietic cells suggest that UTX could have potential functions also in more differentiated cells of the hematopoietic lineage. Different groups are now beginning to elucidate new emerging roles for the H3K27me3 demethylase UTX in immune cell differentiation and during immune responses.

Specifically, analysis of the differentiation of $CD4^+CD8^+$ thymocytes lacking both *Utx* and *Jmjd3* showed increased numbers of $CD4^+CD8^+$ thymocytes, contrasting with reduced numbers of peripheral and splenic T cells. This phenotype was cell intrinsic, as shown by BM chimera experiments. Gene expression analyses and reconstitution experiments revealed that this block was due to a complete failure to express the Sphingosine-1-phosphate receptor 1 (*S1pr1)*, the receptor required for thymic cell egress (Manna, Kim et al. 2015). Notably, disruption of either UTX or JMJD3 caused a less pronounced phenotype, suggesting substantial overlap between the activities of both enzymes in differentiating T cells. In resting thymocytes the authors did not observe any global genome-wide increase in H3K27me3 deposition at promoters that do

not normally harbor this mark. The double-demethylase inactivation preferentially targeted promoters that normally erase the mark during the transition from double positive to single $CD4^+$ cell, like the *S1pr1* gene. Thus, the two demethylases are required preferentially in the dynamics of differentiation-induced H3K27me3 removal rather than in its homeostasis. Moreover, the few genes whose expression was affected by the lack of UTX and JMJD3 were mostly less expressed in mutant cells compared to controls and exhibited increased H3K27me3 promoter decoration, suggesting that the demethylase activity is involved in UTX and JMJD3 control of gene expression in T cells. As a matter of fact, UTY failed to rescue *S1pr1* expression in thymocytes (Manna, Kim et al. 2015).

Together with a role in controlling T cell differentiation, UTX was also shown to support $CD4^+$ T follicular helper (T_{FH}) cells activation and responses that are essential for B cell antibody generation and the resolution of chronic viral infections. Specifically, mice with a T-cell specific *Utx* deletion had fewer $CD4^+$ T_{FH} cells, which also displayed reduced expression of multiple T_{FH}-related surface molecules involved in cellular interactions with B cells, like ICOS or SLMAF6, that sustain T_{FH} development and signaling for germinal center formation. As a consequence, GC B cells were decreased in T-cell specific *Utx* KO mice, together with impaired virus-specific immunoglobulin G (IgG1 and IgG2c) antibody production, resulting in unresolved chronic lymphocytic choriomeningitis virus infections. *Utx*-deficient T cells also showed decreased expression of interleukin 6 (IL6)-receptor-α and other T_{FH} related genes, like *Icos* and *Slamf6,* due to accumulation of H3K27me3 methylation. Additionally, Turner syndrome female patients, who lack part or all of X chromosome and are predisposed to chronic ear infections, had reduced *UTX* expression in immune cells and decreased circulating T_{FH} cells. Thus, it was clearly demonstrated a link between the role of UTX in T cells and immune responses to infections (Cook, Shpargel et al. 2015).

A recent work by the Winau group assessed the epigenetic mechanisms by which UTX controls invariant Natural Killer T (iNKT) cell development. The authors demonstrated that histone demethylases UTX and JMJD3 are required for iNKT cell development. Specifically, *Utx*-deficient iNKT cells exhibited a developmental block, although their functionality was not affected, whereas double inactivation of UTX and JMJD3 showed a phenotype similar to *Utx*-only KO, suggesting that deletion of *Jmjd3* had no additive effects. Moreover, inactivation of *Utx* resulted in the downregulation of genes encoding transcription factors and signalling molecules involved in the terminal maturation of iNKT cells, such as *T-bet* and *CD122*. Promoters of UTX-dependent iNKT signature genes accumulated H3K27me3 and harbored a lower abundance of H3K4me3 in the absence of UTX. In addition, UTX partnered with PLZF, an important transcription factor involved in INKT differentiation. Indeed, *Utx* deficient iNKT cells failed to activate its target genes, which carried more H3K27me3 around their promoters

in the absence of UTX (Beyaz, Kim et al. 2017). This result confirmed a previous report demonstrating that H3K27me3 levels at the bivalent PLZF gene promoter define a threshold enabling precise coupling of TCR specificity to lineage commitment (Dobenecker, Kim et al. 2015). Furthermore, gene promoters that exhibited UTX-dependent chromatin and transcriptional regulation were bound by the transcription factor JUNB, whose role in INKT cell development was newly identified by the authors (Beyaz, Kim et al. 2017). UTX was also required for the accessibility of super-enhancers of genes encoding factors that regulate the specification of the iNKT lineage. Thus, UTX engaged multiple gene-regulatory mechanisms to facilitate the lineage-specific gene expression and development of iNKT cells. Notably, lentiviral transduction of BM B cells with mutant *Utx* lacking the demethylase activity failed to rescue iNKT differentiation and signature-gene expression, suggesting that the demethylase function of UTX was essential for the proper generation of iNKT cells (Beyaz, Kim et al. 2017). JMJD3, on the contrary, was shown to be activated by the Janus Associated Kinase (JAK)-Signal Transducer and activator of transcription (STAT)-6 pathway during macrophage polarization, thus contributing to monocytes differentiation to M2 macrophages through H3K27 demethylation at promoters of M2-specific genes (Satoh, Takeuchi et al. 2010). In this context and in microglial cells, JMJD3 expression is also induced by the NF-κB pathway in response to inflammation stimuli (De Santa, Totaro et al. 2007).

Together, these results provide the first evidences that UTX is crucial for immune system cells development, especially for the fine regulation of the transitions of immune cells between multiple differentiation/activation states. These studies also suggest that UTX functions could be even more relevant during immune responses and support the need to further investigate its involvement in B cell development and immunity.

1.2. B cell development

B cell development is a tightly controlled process that occurs in the fetal liver during embryogenesis and in the BM after birth. Here, hematopoietic stem cells (HSCs) undergo controlled steps of proliferation and differentiation to ultimately generate functional, non-autoreactive cells (Figure 5). Studies carried out over the past two decades have greatly improved our knowledge on the mechanisms underlying B lymphopoiesis. This has been possible through the identification of the main molecular events associated with specific stages of B cell development, which now allows high-resolution investigations of the processes that instruct each differentiation step. Understanding the molecular mechanisms underlying the regulation of B cell lymphopoiesis has important implications especially in the fields of developmental and cancer biology.

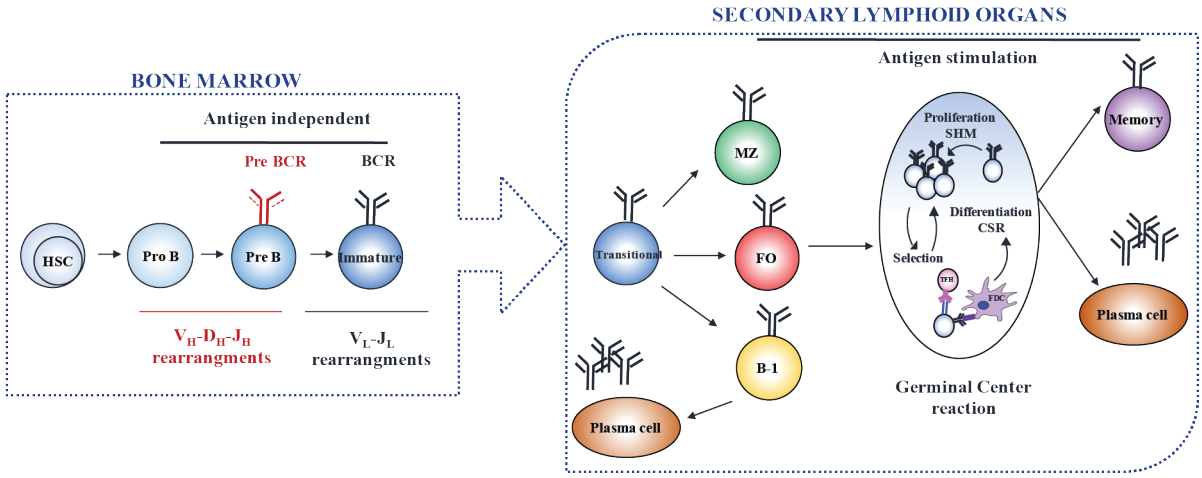


Figure 5. Schematic representation of B cell development. B cell development starts in the BM, where HSCs become committed to the lymphoid lineage and differentiate to pro-B cells. Upon expression of a functional surface Immunoglobulin (Ig) or B cell receptor (BCR), they leave the BM and migrate to secondary lymphoid organs, where they further differentiate to the three main mature B cell subsets, namely follicular (FO), marginal zone (MZ) and B-1 B cells. MZ and B-1 B cells are essentially involved in innate immune responses and in the production of low-affinity antibodies by differentiating into antibody-secreting plasma cells, following pathogen encounter. FO B cells are, instead, the main mediators of T-cell dependent immune responses. Following antigen encounter and supported by T cell help, they get recruited in the germinal center (GC) reaction, where B cells undergo cell proliferation, Ig somatic hyper-mutation, selection of high-affinity Ig mutants and become committed to terminal differentiation. The GC reaction aims at producing high-affinity Ig-expressing memory B and plasma cells secreting high-affinity antibodies specific for the cognate antigen. (Adapted from Rajewsky, 1996).

1.2.1. Early B cell development

In mice and humans, the early steps of B cell development start in fetal liver in prenatal life and continue in the BM after birth, as a lifelong process where HSCs progressively differentiate through a tightly regulated hierarchical process, where they gradually lose their multilineage potential. In order to give rise to lymphocytes, HSCs first differentiate into multipotent progenitors (MPP), which are characterized by loss of self-renewal ability. Together, the pool of HSCs and MPP is characterized by lack of lineage determinants, high expression of stem cell antigen-1 (Sca-1) and of the protein tyrosine-kinase receptor Kit and they are commonly known as the LSK subset (Ikuta and Weissman 1992; Li and Johnson 1995). Differentiation into B-lineage committed cells involves the expression of FMS-related tyrosine kinase 3 (FLT3), which is dependent on the Ikaros (IKZF1) and PU.1 transcription factors. FLT3 expression is associated to the first commitment of progenitors towards the lymphoid lineage, as its overexpression decreases the differentiation of MPP into megakaryocytes and erythrocytes (Adolfsson, Borge et al. 2001; Adolfsson, Mansson et al. 2005; Forsberg, Serwold et al. 2006; Yoshida, Ng et al. 2006). In response to FLT3 ligand and Interleukin-7 (IL7)

stimulation, MPPs start expressing early B cell factor 1 (*Ebf1*) and the transcription factor *E2a* (member of the E protein family), which mark the entry into the common lymphoid progenitor (CLP) stage (Medina, Pongubala et al. 2004; Nutt and Kee 2007). Further exposure of CLPs to IL7 results in the upregulation of Paired box protein 5 (*Pax5*), which marks the definitive commitment towards the B cell lineage (Lin and Grosschedl 1995; Sun 2004; Hagman and Lukin 2006).

1.2.1.1. V(D)J recombination

The protective function exerted by B and T lymphocytes relies on the expression of diversified immunoglobulin (Ig) molecules on their surface, namely the B and T cell receptor (TCR) respectively, mediating the recognition of foreign antigens. The BCR consists of two identical Ig heavy (H) and light (L) chains assembled together via disulfide bonds. Each Ig chain consists of a variable region responsible for the recognition of antigen and a constant region, which mediates the effector function of the BCR. The variable region of the receptor is generated via a gene rearrangement process known as VDJ recombination, whereby starting from hundreds of gene segments, a unique variable (V), diversity (D) and joining (J) gene segments are stochastically joined together (only V and J segments are joined to yield the IgL chain) (Tonegawa 1983). VDJ is catalyzed by the Recombination Activating Genes 1 and 2 (RAG1 and RAG2) (McBlane, van Gent et al. 1995; van Gent, McBlane et al. 1995; Melek, Gellert et al. 1998). RAG proteins bind to and cleave DNA at specific recombination signal sequences (RSSs) flanking each V, D and J gene segment (Eastman, Leu et al. 1996). Once cleaved, V, D and J gene segments are joined together by components of the classical non-homologous end joining (NHEJ) repair pathway (Li, Otevrel et al. 1995; Difilippantonio, Zhu et al. 2000).

VDJ recombination is a highly regulated process, which involves introduction of DNA DSBs and deletion of large genomic segments. Specifically, rearrangement of V_H genes precedes always that of V_L genes. Chromatin accessibility and regulation of RAG expression are central mechanisms that modulate VDJ recombination (Morshead, Ciccone et al. 2003; Johnson, Pflugh et al. 2004; Osipovich, Milley et al. 2004). IgH rearrangements occur in pro-B cells, defined on the basis of surface markers as $B220^{+}CD43^{+}c\text{-}Kit^{+}IgM^{-}$ cells. Once a functional/productive V_H gene is assembled, expression of an IgH chain leads to the transition of the cells to the pre-B cell stage. In pre-B cells, a pre-BCR complex is assembled on the cell surface, consisting of the newly rearranged IgH chain and of the surrogate IgL chains V-preB and l5. Signaling through the pre-BCR inhibits further rearrangements at the IgH locus, a process which is called allelic exclusion, while it stimulates clonal expansion of pre-B cells (Gorman and Alt 1998). This process is driven by IL7 and self-aggregation of the pre-BCR (Martensson and Ceredig 2000). Following clonal expansion, pre-B cells exit the cell cycle and

reactivate expression of RAG proteins to rearrange their IgL chain genes. Once a functional IgL chain is produced, successful pairing of IgH and IgL chains leads to the expression of a functional BCR on the cell surface. The latter event marks the transition from pre-B to $IgM^{hi}IgD^{-/lo}B220^{lo}$ immature B cells. Immature B cells in the BM undergo a stringent selection process aimed at eliminating the cells that express BCRs recognizing self- antigens with high affinity. Alternatively, auto-reactive immature B cells may undergo IgL chain receptor editing, a process whereby secondary V_L gene rearrangements are induced to replace the IgL chain to try to eliminate self-reactivity of the BCR (Edry and Melamed 2004; Nemazee 2006). Should these cells succeed to express a functional, non- autoreactive BCR, they are allowed to leave the BM and reach, through the blood stream, peripheral lymphoid organs to eventually complete their maturation (Allman, Ferguson et al. 1993; Rajewsky 1996).

1.2.1.2. Transcriptional control of early B cell development

Early B cell development is a tightly regulated process with numerous checkpoints for the quality control of cells generated at every stage. The first one occurs when the common lymphoid progenitors (CLP), commit to B lineage (Mansson, Hultquist et al. 2007). This step requires the simultaneous establishment of B cell-specific transcriptional programs and the suppression of alternative programs, orchestrated by a network of transcription factors, including E2a, EBF-1, PAX5 and Forkhead box (FOXO)-1. (O'Riordan and Grosschedl 1999; Sigvardsson, Clark et al. 2002; Cobaleda, Schebesta et al. 2007).

The transcription factor EBF1, in particular, plays a central role in committing B cells to the lineage-specific transcriptional developmental pathway, by activating B cell-genes. Its expression and function are regulated by the B cell master regulator E2a and by signaling via the IL7 receptor (Kikuchi, Lai et al. 2005; Kwon, Hutter et al. 2008). E2a and EBF1 induce the expression of *Pax5* and *Foxo1* in CLPs (Zandi, Mansson et al. 2008; Lin, Jhunjhunwala et al. 2010). In the classical view, E2a, EBF1 and FOXO1 establish a dynamic transcriptional network that sustains pro-B cell development. They bind to a large subset of genes involved in pre-B cell antigen receptor signaling and WNT pathway ((Lin, Jhunjhunwala et al. 2010)Lin et al, 2010), to coordinate cell growth and developmental progression. On the other hand, PAX5 sustains the activity of EBF1 and E2a, and controls the expression of B genes such as *CD19* and *Ig*α (Nutt, Heavey et al. 1999), preventing at the same time expression of lineage-inappropriate factors (Nutt, Heavey et al. 1999; Souabni, Cobaleda et al. 2002; Cobaleda, Schebesta et al. 2007; Revilla, Bilic et al. 2012), thus restricting the developmental options of lymphoid progenitors to the B-cell pathway (Nutt, Heavey et al. 1999).

Moreover, E2a and EBF1 activate *RAG1* and *2* genes to trigger VDJ recombination at the heavy chain locus, by also promoting the accessibility of the D_H-J_H region to the recombinases. PAX5, in addition, remodels the chromatin at the IgH locus in pro-B cells, to increase the proximity of more distal V_H genes to the rearranged D_H-J_H joint (locus contraction), a crucial process to allow RAG proteins to use these distal V_H genes for the recombination process. (Fuxa, Skok et al. 2004)

E2a also regulates Igκ rearrangements, as its ectopic expression together with RAG1 and RAG2 is sufficient to induce $V_κ$-$J_κ$ recombination in non- lymphoid cells (Romanow, Langerak et al. 2000). E2a conditional deficient mice carried a substantial impairment in the generation of BM pre-B cells and immature B cells, suggesting its crucial role in supporting these two developmental stages. Instead, whereas immature and mature splenic B cells were reduced in these mice, this effect was more attributable to a decreased production of B cells in the BM rather than to a functional dependency of mature B cells from E2a (Kwon, Thierry-Mieg et al. 2009) Further data confirmed that this transcription factor is dispensable for later stages of B differentiation.

Early commitment to the B cell lineage is also mediated by the BTB and CNC homology 1 basic leucine zipper transcription factor 2 (BACH2). Indeed, BACH2 functions with EBF1 in repressing myeloid transcriptional program in progenitor B cells (Itoh-Nakadai, Hikota et al. 2014). BACH2 is activated by PAX5 and it is required for the negative selection of pre-B cells that failed to rearrange their BCR heavy chain in a productive way (Swaminathan, Duy et al. 2014). In this action, it opposes the pro-survival function of B-cell lymphoma protein 6 (BCL6) that sustains pre-B cells at the pre-BCR checkpoint (Duy, Yu et al. 2010).

FOXO1 is a member of the FOXO family of Forkhead transcription factors, whose expression is induced in early B cell progenitors by EBF1. It has been particularly studied in lymphocytes early developmental stages using conditional Cre-loxP systems. Deletion of *Foxo1* gene in early B cell progenitors through $Mb\text{-}1^{cre/+}$ resulted in a developmental block at the pro-B cell stage, while its inactivation with $Cd19^{cre/+}$ caused a partial block at the pre-B cell stage (Dengler, Baracho et al. 2008). Particularly, in pre-B cells, it has been involved in the control of proliferation versus differentiation, by antagonizing PI3K signalling. Indeed, PI3K signalling induces expansion of pre-B cells thereby inhibiting transcription factors involved in the control of differentiation, like FOXO1. Downregulation of *Pi3k* and expression of *Foxo1* in pre- B cells (Herzog, Hug et al. 2008) arrested cells in G1 and induced the initiation of Ig rearrangements at the IgL locus. On the contrary, *Foxo1* deletion led to loss of *Il7ra, Rag1, Rag2* expression and defective VDJ rearrangements, together with compromised proliferation (Dengler, Baracho et al. 2008).

Important functions are exerted by Interferon regulatory factors (IRF) 4 and 8 in early B cell

development. They belong to the interferon regulatory factor superfamily of transcription factors. They exert their transcriptional control on target genes by forming homo- and hetero-dimers with other members of the family or with other transcription factors. These factors are expressed at the pre-B cell stage downstream of the pre-BCR signaling. Upon induction, they promote the expression of the transcription factors *Ikaros* and *Aiolos*, which, in turn, negatively regulate BCR signaling and cell cycle progression (Ma, Pathak et al. 2008). Moreover, IRF4 has also been shown to limit pre-B cell expansion by attenuating IL7 receptor signaling. Indeed, it controls expression of the chemokine receptor *Cxcr4* in pre-B cells, driving them away from IL7 secreting stromal cells.

1.2.2. Peripheral B cell development

1.2.2.1. Transitional B cells

Only a small fraction (less than 10%) of $B220^{+}IgM^{hi}IgD^{-}$ short-lived immature B cells produced daily, completes its development to become long-lived mature B cells (Rajewsky 1996). Once immature B cells reach the spleen as so-called transitional B cells (Allman, Ferguson et al. 1992; Allman, Ferguson et al. 1993), they express high levels of IgM while uniformly retaining expression of the early differentiation markers AA4.1/CD93 and of the Heat Stable Antigen (HSA)/CD24, combined with low levels of B220. Transitional B cells are divided into different subsets based on expression of additional surface molecules. Transitional T1 B cells represent the earliest immature B cells reaching the spleen and they are defined as $IgM^{hi}IgD^{-}CD23^{-}$. They develop into T2 B cells, the direct precursors of the long-lived mature B cells, acquiring expression of IgD and CD23 (Norvell and Monroe 1996; Loder, Mutschler et al. 1999) (Figure 6). An additional subset named T3, resembling T2 cells except for lower surface IgM expression, has been described, but its origin and function remain poorly understood (Allman, Lindsley et al. 2001). T1 and T2 cells reside in different splenic areas and they are also functionally distinct. T1 B cells retain sensitivity to negative selection and undergo apoptosis upon BCR engagement due to failure to upregulate pro-survival molecules and progress in the cell cycle (Norvell, Mandik et al. 1995; Chung, Sater et al. 2002). T2 B cells, on the contrary, respond to T helper cell-derived survival signals and to BCR engagement with proliferation and survival rather than with apoptosis (Chung, Sater et al. 2002) (Figure 6). *In vivo* bromodeoxyuridine (BrdU) labeling studies revealed rapid turnover of transitional B cells, as compared with the mature B pool. This evidence indicates a shorter lifespan of transitional B cells (1-4 days) in comparison with mature B cells (80-120 days) (Allman, Ferguson et al. 1993). At the molecular level, the B cell activating factor (BAFF/TNFSF13B/BLyS/TALL1) plays a major role in sustaining the differentiation from the transitional to the mature B cell

compartment. Indeed, B cell-specific deletion of BAFF or its receptor, BAFF-R, resulted in impaired development beyond the T1 stage (Schiemann, Gommerman et al. 2001; Sasaki, Casola et al. 2004).

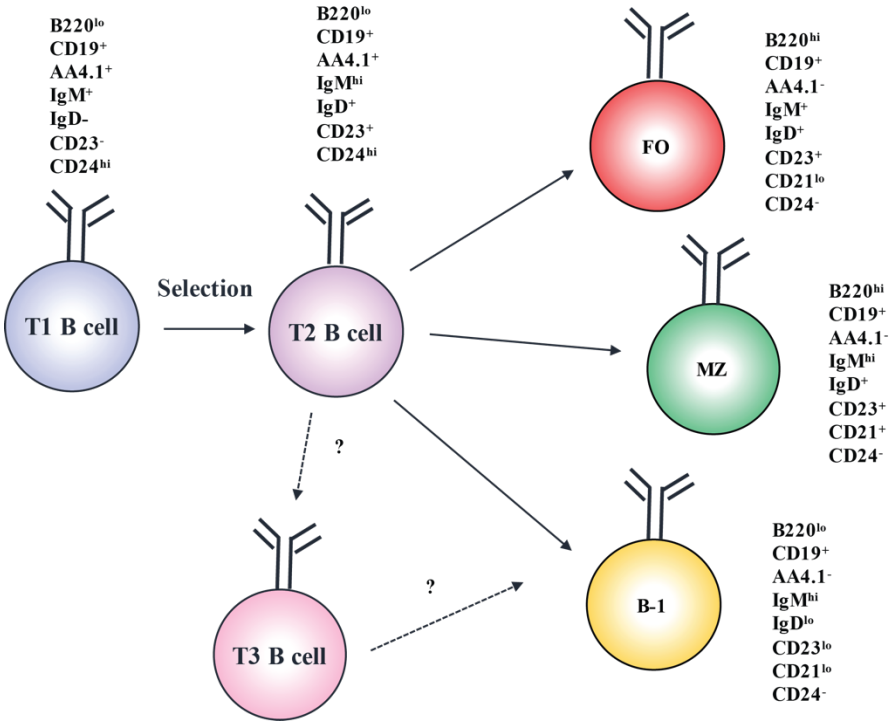


Figure 6. Schematic view of peripheral B cell development. Upon exit from the BM, newly formed T1 B cells undergo negative selection aimed at eliminating autoreactive B cells. Non-autoreactive T2 B cells are then driven towards the FO, MZ or B-1 fate depending on the expression of specific transcription factors and markers. Markers used for immunophenotypic characterization of each developmental stage are listed.

1.2.2.2. Mature B cell subsets

In the mouse, mature B cells are divided into three major phenotypically and functionally distinct subsets represented by Follicular (FO), Marginal Zone (MZ) and B-1 B cells (Casola 2007).

FO B cells

FO B cells, also called B-2 B cells, are the most abundant mature B cell subset present in secondary lymphoid organs. Identified as $IgM^{+}IgD^{+}CD21^{lo}CD23^{+}$, FO B cells are able to recirculate through B cell areas of the spleen, lymph nodes (LNs), BM and mucosa-associated lymphoid tissues (Pillai, Cariappa et al. 2004). They reside respectively within the white pulp of the spleen and in the cortical area of LNs, where they home to defined areas called follicles. FO B cells are the main mediators of T cell-dependent immune responses, although they can also take part to T cell-independent responses (Casola 2007). Upon T-cell dependent responses, they are recruited in the germinal center (GC) reaction. This step is strictly dependent from $CD4^{+}$ T cells, which recognize, via their TCR, processed antigen presented by antigen-specific

B cells through their Major Histocompatibility Complex (MHC)-class II molecules. As a result of the GC reaction, highly selected FO B cells terminally differentiate to become long-lived memory B cells or antibody-secreting plasma cells (PCs), although they can also directly differentiate to short-lived low affinity PCs upon recognition of T-independent antigens (Casola 2007).

MZ B cells

MZ B cells are identified as $IgM^{hi}IgD^{+}CD21^{+}CD23^{+}$ (Martin and Kearney, 2002). They consist of a self-replenishing subset residing in the spleen in close proximity to the marginal sinus. MZ B cells are recruited into both T-cell dependent and independent immune responses. They capture and transport antigens in the form of immune complexes to FO B cells residing in the nearby splenic follicle. MZ B cells get rapidly activated upon BCR-mediated recognition of blood-borne pathogens, proliferate and differentiate into PCs secreting low-affinity antibodies in a T-cell independent manner (Martin and Kearney 2002; Song and Cerny 2003; Cinamon, Zachariah et al. 2008).

B-1 B cells

This mature B cell subset, identified as $IgM^{hi}IgD^{lo}B220^{lo}CD19^{+}CD23^{lo}CD21^{lo}$, mainly resides in body cavity sierosa, including pleural and peritoneal cavities (Casola 2007). Based on surface expression of CD5, B-1 B cells can be further divided into the B-1a ($CD5^{+}$) and B-1b ($CD5^{-}$) B cell subsets (Stall, Adams et al. 1992). While B-1a B cells originate predominantly from fetal liver progenitors and they can be very poorly generated from bone marrow precursors in post-natal life, B-1b B cells derive also from HSCs residing in the BM, where they are also efficiently generated in adult mice (Montecino-Rodriguez, Leathers et al. 2006). B-1 B cells are capable of self-renewing and can auto-sustain their population throughout life. They express BCRs that recognize with low affinity self-antigens that cross-react with bacterial components. As a result of this interaction, they rapidly differentiate into short-lived PCs and start secreting the so-called natural IgM antibodies, that represent our first barrier against invading pathogens. (Fagarasan and Honjo 2003; Alugupalli, Leong et al. 2004; Haas, Poe et al. 2005; Hardy 2006). Upon recognition of T-cell dependent antigens, B-1 B cells can also function both as effectors and as regulators of adaptive immune responses (Baumgarth 2011).

1.2.2.3. Determinants of peripheral B cell development

Maturation of transitional B cells to become respectively FO, MZ and B-1 B cells and maintenance/survival of the mature B cell pool are mediated by a limited number of receptors, signalling pathways and transcription factors that are outlined below.

1.2.2.3.1. BAFF

B-cell activating factor BAFF is a member of the tumor necrosis factor family (TNF) that plays a crucial role in the generation and maintenance of mature B cells. BAFF binds to three different receptors: B cell maturation antigen (BCMA), transmembrane activator and calcium modulator and cyclophilin ligand interactor (TACI) and BAFF receptor (BAFF-R). BAFF-R is expressed on the surface of B lymphocytes (Bossen and Schneider 2006; Li, Su et al. 2008), activated T cells and regulatory T cells (Mackay and Leung 2006); TACI is expressed on B cells, monocytes (Chang, Arendt et al. 2006) and dendritic cells (Chang, Mihalcik et al. 2008). In humans, BAFF-R is expressed at low levels on the surface of B cells egressing from the BM and its expression increases with maturation (Sasaki, Casola et al. 2004; Darce, Arendt et al. 2007). BAFF-R is the main receptor that controls maturation and survival of late transitional and mature B cells. Indeed, mice lacking either BAFF or its receptor display a prominent block in the transition from the T1 to the T2 stage (Schiemann, Gommerman et al. 2001). Moreover, BAFF is required for survival of FO and MZ B cells, while it is dispensable for B-1 B cell maintenance (Crowley, Scholz et al. 2008; Scholz, Crowley et al. 2008). BAFF induces survival of B cells via activation of the Nuclear Factor Kappa-light-chain-enhancer of activated B cells (NF-κB) pathway (Sasaki, Derudder et al. 2006; Almaden, Tsui et al. 2014) and promotes cell growth, protein synthesis and glycolysis through activation of the protein kinase mammalian target of rapamycin (mTOR) pathway (Patke, Mecklenbrauker et al. 2006; Matsuzawa, Tseng et al. 2008; Vallabhapurapu, Matsuzawa et al. 2008; Woodland, Fox et al. 2008). Central to the pro-survival activity of BAFF is the induction of the expression of anti-apoptotic factors such as B cell lymphoma 2 (*Bcl-2*) and B-cell lymphoma-extra-large (*Bcl-xL*) and BCL-2 family member myeloid cell leukaemia sequence 1 (*Mcl1*) (Bouillet, Metcalf et al. 1999; Wang, Chao et al. 1999; Opferman, Letai et al. 2003; Cariappa, Boboila et al. 2007; Mills, Hippo et al. 2008). Importantly, recent work has shown intersections between BCR and BAFF-R signaling, with the tyrosine kinase SYK and the serine/threonine kinase AKT being the key signalling molecules connecting the two pathways (Schweighoffer, Vanes et al. 2013).

1.2.2.3.2. The BCR

Surface expression of a functional BCR is critical for survival of mature B cells. Indeed, acute ablation of the BCR signaling complex in resting B cells results in rapid disappearance of the cells (Lam, Kuhn et al. 1997; Kraus, Alimzhanov et al. 2004). Additionally, antigen specificity, BCR surface density and strength of intracellular signaling have all been implicated in transitional B cell fate decisions (Casola 2007). Specifically, immature B cells receiving strong signaling through the BCR are thought to differentiate towards the B-1 B cell compartment.

Weaker signaling coupled to additional cues will instead favour the development of FO and MZ B cells (Casola, Otipoby et al. 2004), with FO B cells requiring the lowest BCR signal among mature B lymphocytes. It remains to be demonstrated whether antigen plays a role in the selection of immature B cells, although a recent report excluded a major contribution of antigen in the selection of short-lived immature B cells (Kaplinsky, Li et al. 2014).

1.2.2.3.3. The NF-κB pathway

In mammals, the Nuclear Factor Kappa-light-chain-enhancer of activated B cells (NF-κB) family of transcription factors comprises 5 members: RELA, RELB, c-REL, NF-κB1 and NF-κB2, whose activation is initiated by two major pathways (Sasaki and Iwai 2016). The canonical pathway depends on the IκB kinase (IKK) complex, consisting of the structural component NF-κB essential modulator (NEMO) and the IκB kinases IKK1 and IKK2. This complex directs the degradation of a set of inhibitors of NF-κB and the induction of dimers containing RELA and/or c-REL together with processed NF-κB1 (p50). The stimulation of the alternative pathway, instead, is mediated by NF-κB inducing kinase NIK and IKK1 and it leads to the partial proteolysis of the inhibitory precursor NF-κB2 (or p100) and the activation of dimers containing RELB and/or the processed form of NF-κB2, known as p52. Numerous receptors activate the NF-κB signaling pathway in mature B cells, especially the BCR, which activates NF-κB canonical pathway and BAFF-R, that has been recently shown to activate both NF-κB pathways (Gardam and Brink 2014). On the other hand, BCR, CD40 and TLR receptors all individually engage NF-κB during B cell activation (Vallabhapurapu and Karin 2009) and the cross-talk among them is crucial in determining how NF-κB influences functional outcomes during B cell activation.

The NF-κB pathway largely contributes to the development of both mature B and T cells. The primary, although not exclusive, role of NF-κB in lymphocyte development is to assure B cell survival. Most of the insights about the role of NF-κB in B cell development have come from analyses of genetically engineered mice in which NF-κB components have been knocked-out or NF-κB activation has been constitutively induced. Particularly, B cell specific ablation of either NEMO or IKK2 resulted in a mild reduction of mature B cells numbers, although severely impairing transitional B cells. The ability of a BCL2 transgene to rescue mature B cells even if early B cell ablation of canonical NF-κB pathway leads to a severe block at the transitional B cell stage suggests that this pathway supports mature B cells maintenance thanks to its pro-survival activity (Derudder, Herzog et al. 2016). Consistently, the simultaneous deletion of RELA and c-REL in mature B cells led to a dramatic reduction in FO and MZ B cells, while also affecting in a transcription factor-specific manner GC formation (Milanovic,

Heise et al. 2017). B-lineage specific disruption of IKK1 impairs mature B cells lifespan and their capacity to proliferate. However, while this subunit seems to be dispensable for cytokine-induced activation of NF-κB by means of degradation of IκB, it is critical for the processing of p100 to p52 (Kaisho, Takeda et al. 2001). Similarly, interference with IKK2 activity or ablation of IKK2 in the B lineage impaired the generation of the three mature B cell subsets and of transitional B cells (Pasparakis, Schmidt-Supprian et al. 2002; Sasaki, Derudder et al. 2006; Derudder, Cadera et al. 2009; Sasaki and Iwai 2016). Notably, the most severe blocks at T1 to T2 transition occurred upon early B cell deletion of both IKK1 and IKK2 (Derudder, Cadera et al. 2009). In addition, compound deficiency of NF-κB1/ NF-κB2 arrested B cell development shortly after the transition from T1 to T2, leading to a complete absence of FO and MZ B cells; a milder reduction in FO B cells occurred with the concomitant inactivation of NF-κB1 and c-REL (Pohl, Gugasyan et al. 2002; Gerondakis, Grumont et al. 2006). In conclusion, although the strong impairments in B cell development observed in the NF-κB-deficient models presented were due to loss of survival, cells that managed to differentiate further upon ectopic expression of BCL2 remained unable to fully mature both phenotypically and functionally, suggesting that NF-κB is critical also for optimization of functions that accompany differentiation.

1.2.2.3.4. PAX5

The transcription factor PAX5 is a master regulator of B cell development and the major determinant of B cell identity. It is expressed starting from the pro-B cell stage, throughout B cell development (Fuxa and Busslinger 2007). In peripheral B cells, while preserving the B cell-specific gene expression program and cell identity, PAX5 promotes the survival of B lymphocytes. Indeed, conditional inactivation of PAX5 in mature B cells caused the transcriptional reprogramming of mutant cells that could commit to other cell types, like T cells and macrophages (Cobaleda et al. 2007; Delogu et al. 2006). PAX5 acts both as a transcriptional activator and repressor. It induces critical effectors of BCR signaling pathways while it represses genes expressed in in plasma cells, preventing premature onset of terminal differentiation (Delogu, Schebesta et al. 2006). PAX5 gets, indeed, silenced when B cells differentiate ultimately to antibody-secreting plasma cells.

1.2.2.3.5. NOTCH2

In mammals, the family of NOTCH receptors includes 4 members (NOTCH1-4), which recognize 5 ligands of the Jagged and Delta-like (DLL) families, respectively. NOTCH receptors get cleaved in response to ligand interaction and the intracellular cleaved receptor translocates to the nucleus where it regulates gene expression through the transcription factor RBP-jκ (Igκ-J region recombination-signal-binding protein 1) (Kopan and Ilagan 2009).

NOTCH signaling regulates important functions in the development of hematopoietic lineages (Maillard, Fang et al. 2005). Particularly, NOTCH2 is expressed on all mature B cells, and its natural ligand is Delta-like 1 (DLL1). B cell-specific deletion of *Notch2* impairs development of MZ B cells, while the FO B cell compartment remains untouched (Saito, Chiba et al. 2003). The role of NOTCH2 in MZ B cell development is further supported by the fact that animals carrying B cell-specific inactivation of the RBP-Jκ transcription factor, lack MZ B cells (Tanigaki, Han et al. 2002). Conversely, B cells lacking the NOTCH2 transcriptional repressor, MINT (MSH homeobox homologue 2 (MSX2)-interacting nuclear target), display preferential commitment towards the MZ B cell compartment, with a concomitant decrease in FO B cells (Kuroda, Han et al. 2003). Moreover, recent work has revealed that acute inactivation of *Notch2* in MZ B cells led to the rapid loss of B cells residing in the MZ, that did not undergo apoptosis but migrated away. Together, these observations indicate that NOTCH2 plays a pivotal role in MZ B cell development and maintenance (Simonetti, Carette et al. 2013).

1.2.2.3.6. IRF8/IRF4 axis

Recent reports suggest that both IRF8 and IRF4 regulate the cell fate decisions that control mature B cells differentiation towards either the FO or the MZ compartment. Indeed, IRF4 was recently found to restrict the MZ B cell population, since its deficiency led to retention of B cells in this compartment. Specifically, these defects were attributed elevated levels of the MZ regulator NOTCH2 in *Irf4*-mutant mature B cells (Simonetti, Carette et al. 2013). Additionally, *Irf4* inactivation resulted in overexpression of integrins and chemokine receptors known to mediate migration and retention of B cells in the MZ (Simonetti, Carette et al. 2013). Interestingly, also IRF8 was identified as a regulator of FO vs MZ differentiation (Feng, Wang et al. 2011). B cell-specific inactivation of *Irf8* resulted in accumulation of cells within the MZ together with a reduction in FO B cells (Feng, Wang et al. 2011). IRF8 was also shown to regulate B-1 B cell numbers in the peritoneal cavity in a B cell intrinsic manner, whereas New Zealand Black mice expressing low levels of *Irf4* show enhanced proliferation and survival of the B-1 B cell compartment and decreased ability to differentiate to plasma cells (Ma, Shukla et al. 2013).

1.2.2.3.7. FOXO1

Deletion of the transcription factor *Foxo1* in transitional B cells blocked class-switch recombination. Chen and colleagues have identified a specific role for FOXO1 in regulating B cell maturation (Chen et al, 2010). They identified a defect in FO B cells in mice where *Foxo1* was depleted starting from early B cell development. Concomitantly, these mice exhibit a higher percentage of MZ cells. Interestingly, in mice homozygous for the $Cd19^{cre}$ knock-in allele, which lack CD19 protein, MZ cells are absent, but this defect is reversed by the

concomitant deletion of FOXO1 (Chen, Jeon et al. 2010). This genetic analysis suggests the possibility that CD19 negatively regulates FOXO1 to promote MZ B cell development.

1.2.3. B cell migration

Lymphoid tissues possess the unique feature of strongly depending on cell migration for every aspect of their function. B lymphocytes, together with T cells, continuously enter secondary lymphoid organs from the blood and migrate within minutes to B cell follicles (or T cell zones). Spleen and lymphoid organs continuously sample antigen either from the blood or from the lymph or also from the intestinal lumen. B cells entering lymphoid organs migrate continually within their specific areas, surveying for antigens. Most naïve B cells entering a lymphoid organ fail to detect their specific antigen and after a period of 4-24 hours spent within the tissue they migrate out to return to circulation and go on to survey further lymphoid organs. If an antigen is encountered, responding B lymphocytes are retained within the tissue and they migrate from follicles to the T cell zone to interact with helper T cells. Upon an immune response, B cells stay within the antigen-positive tissue for days to become activated and undergo differentiation to become antibody-secreting plasma cells. Then, they migrate to the medulla of LNs and to the red pulp of spleen to exit from these organs. A small fraction of both naïve and antibody-secreting B cells also migrates back to the bone marrow (Cyster 2005; Arnon and Cyster 2014). Of the multiple molecules needed to direct B cell migration in and out from lymphoid organs, chemokines have the most prominent role. Lymphocyte entry to lymph nodes (LNs) and Peyer's patches (PPs) occurs from high endothelial venules (HEV) and involves a cascade of selectin- or integrin- supported rolling, chemokine-mediated integrin activation and integrin-mediated adhesion (von Andrian and Engelhardt 2003; Rosen 2004). Instead, entry to the spleen does not involve HEV, but lymphocytes are released into the organ from terminal arterioles that end in the marginal sinus or in the red pulp (Brelinska and Pilgrim 1982). Here, $\alpha L\beta 2$ and $\alpha 4$ integrins are involved in lymphocyte migration into the white pulp (Lo, Lu et al. 2003). Homing of B cells to lymphoid follicles depends on expression of CXCR5 and in minor part of CCR7 and EB12 (Forster, Emrich et al. 1994; Gatto, Wood et al. 2011) by B cells and of its ligand CXCL13 by radiation-resistant follicular stromal cells. Expression of this chemokine by stromal cells is strongly dependent on the cytokine lymphotoxin (LT)-$\alpha 1\beta 2$ signalling via LTβ receptor (Ngo, Korner et al. 1999). Interestingly, B cells provide a major source of LT-$\alpha 1\beta 2$ within the spleen (Forster, Mattis et al. 1996). In resting conditions, CXCR5 is expressed by all mature B cell subsets, including FO B cells, MZ B cells and B-1 B cells. Deficiency in CXCR5 strongly reduces B lymphocytes accumulation in the spleen and double inactivation of CXCR5 and CCR7, completely blocks B cell entry in this organ (Müller, Höpken et al. 2003). Among

splenic subsets, FO B cells are highly motile, whereas MZ B cells are non-circulatory and their homing to the MZ depends from αLβ2 and α4β1 integrin-mediated adhesion to ICAM1 and VCAM1, which are integrin ligands highly expressed in the MZ (Lu and Cyster 2002).

1.2.3.1. S1PR1

Lymphocyte exit from lymphoid organs is promoted by sphingosine-1-phosphate (S1P) acting via the G_i-coupled receptor, S1P-receptor-1 (S1PR1). It is expressed by the majority of B lymphocytes within spleen and lymph nodes and it is undetectable on the surface of cells circulating in the blood. Its ligand, S1P, is made by the action of two sphingosine kinases, SHPK1 and 2, present within most cell-types, and it is abundant in the blood and in the spleen (Christoffersen, Obinata et al. 2011). Thus, in lymph nodes, a gradient of difference in S1P concentration exists between the parenchyma and the blood, and cells are triggered to exit the organ by S1PR1 exposure to the higher S1P blood concentration. (Grigorova, Schwab et al. 2009). Notably, S1PR1 is strongly subjected to desensitization by its ligand (Cinamon, Zachariah et al. 2008). It was first indicated to be involved in lymphocyte circulation because of structural similarity with the immunosuppressant inhibitor FTY720, that gets phosphorylated by SHPK2 *in vivo*. Studies with this inhibitor showed a rapid loss of lymphocytes from the blood and the lymph and accumulation in the LNs and PPs (Suzuki, Enosawa et al. 1996; Chiba, Yanagawa et al. 1998), suggesting a defect in lymphocyte egress from lymphoid organs. S1PR1 is also involved in controlling B cell egress from the spleen. Direct support to this conclusion came from the observation that transferred S1PR1 deficient lymphocytes were found within the white pulp 2 days after transfer in similar frequencies as control cells, but they were completely absent from the blood (Matloubian, Lo et al. 2004). Moreover, in mice where blood S1P is intact but lymphatic S1P is depleted, lymphocyte numbers are low in the spleen compared to LNs and PPs, because they exit the spleen in response to circulatory S1P, but cannot return from other lymphoid organs through lymph. Further studies also report that S1PR1 is required for plasma cell egress from the spleen into blood (Cyster 2005; Kabashima, Haynes et al. 2006; Arnon and Cyster 2014).

S1PR1 expression is higher on MZ than on FO B cells and this could suggest a requirement for this receptor for the correct positioning of B cells within the MZ. Consistently, FTY720 treatment led to rapid displacement of B cells from the MZ (Cinamon, Matloubian et al. 2004) and the same observation was reported for S1PR1 conditional deletion in B cells (Allende, Tuymetova et al. 2010). A possible function of S1PR1 in MZ B cells could be to overcome the recruiting activity of CXCL13 to the follicle, since CXCR5 depleted mice MZ B cells were observed even in the absence of S1PR1 (Cinamon, Matloubian et al. 2004; Cyster 2005).

Two independent studies reported an important function for S1PR1 in controlling immature B

cells egress from the bone marrow to the blood (Pereira, Kelly et al. 2009; Allende, Tuymetova et al. 2010). The authors demonstrated that conditional S1PR1 deletion in early B cells progenitors did not impact on early B cell differentiation but it affected the egress of immature B cells from the BM to the blood, which also impaired mature and immature B cells fractions in the spleen. Indeed, immature B cells in contact with the BM vasculature displayed increased apoptosis as compared with control mice (Allende, Tuymetova et al. 2010). Consistent results were reported by others, although they also described an accumulation of immature B cells both in BM parenchyma and in the vasculature (Pereira, Kelly et al. 2009).

1.2.3.2. Mucosal B cell migration

Gut- associated lymphoid tissues (GALT) include PPs and isolated lymphoid follicles (ILFs), together with associated mesenteric lymph nodes (MLNs). As part of the mucosal surfaces, GALTs are continuously exposed to a variety of microbial organisms and they represent the first defense barrier against external pathogens. They also exert an important function in regulating the gut commensal flora. Their defensive ability depends on the daily massive release in the gut lumen of soluble IgA antibodies by IgA-producing PCs, which are mostly found in the intestinal lamina propria (Brandtzaeg, Halstensen et al. 1989). These protective functions all rely on the effective homing of both immune cells and antibody secreting cells to this compartment. The initial extravasation of naïve B cells from HEVs to GALTs is mediated in mice by the binding to glycosylated MadCAM-1 via CD62L (L-selectin), which B cells highly express on their surface. This initial event enables chemokine signaling-dependent adhesion of MadCAM-1 to the integrin $\alpha4\beta7$, which is required for correct homing to GALTs (Berg, McEvoy et al. 1993; Wagner, Lohler et al. 1996; Brandtzaeg and Johansen 2005). B cell migration to secondary lymphoid organs also depends on CXCR5 and CCR7. Homing to PPs, in particular, relies on the CXCR5-CXCL13 signaling axis, which supports extravasation of $CXCR5^+$ B cells into PPs via CXCL13-expressing HEVs (Okada, Ngo et al. 2002). In contrast to naïve B cells, activated/ antibody secreting plasma cells do not express CD62L, thus relying only on $\alpha4\beta7$- MadCAM-1 interactions for extravasation. Moreover, when B cells differentiate into PCs, a coordinated change in chemokine receptors expression occurs. CXCR5 and CCR7 are downregulated and CXCR4 is upregulated, causing PCs migration to the BM (Hauser, Debes et al. 2002). Additionally, CCR9 and its ligand CCL25 play a crucial role in intestinal tropism of effector B cells, since CCL25 is selectively expressed by the crypt epithelium of the small intestine (Bowman, Kuklin et al. 2002). Also, CCR10 is expressed on all IgA^+ PBs and its ligand CCL28, together with CCL25, enhances integrin $\alpha4$-dependent adhesion of IgA^+ PBs to Mad-CAM-1. CCR9 and CCR10 expression specifically enables IgA^+ PBs to migrate to all mucosal tissue, whereas their differential expression patterns compartmentalize their trafficking

to specific mucosal site, including the intestine (Kunkel, Kim et al. 2003). In conclusion, an important receptor involved in the recruitment and differentiation of memory B cells is CCR6, together with its ligand CCL20 (Kunkel, Kim et al. 2003). CCR6 was also recently shown to guide the migration of activated PPs B cells to the sub epithelial dome (SED), where interaction with dendritic cells is necessary to trigger IgA class witch recombination (Reboldi, Arnon et al. 2016).

1.2.4. B cell immunity

1.2.4.1. T cell-independent B-cell responses

In T-cell independent (TI) immune responses, B cells get activated and differentiate into short-lived PCs, without the help of T cells. All mature B cell subsets can potentially get recruited into TI immune responses. Given their proximity to the blood stream, MZ B cells represent the preferential subset that is activated in response to blood borne pathogens. During T-cell independent immune responses, B cells get activated as a result of the triggering of different receptors, depending on the type of antigen they interact with. There are two main types of TI antigens: Type I antigens and Type II antigens.

Type-1 antigens (TI-1) are able to trigger a polyclonal B cell response by stimulating receptors other than the BCR. An example of TI-1 antigen is lipopolysaccharide (LPS), a constituent of the cell wall of Gram-negative bacteria. In the presence of high levels of LPS, activation of B cells through Toll-like receptor-4 (TLR4) triggers a polyclonal unspecific antibody response. In case LPS levels are in the low range (not sufficient to activate cells only through the TLR4 receptor) only B cells recognizing the antigen through the BCR will get activated. In this case the antibody response with be antigen (LPS)-specific. Both immature and mature B cells can get recruited in TI-1 immune responses.

On the other hand, type-2 antigens (TI-2) share highly repetitive structures. Polysaccharides of encapsulated bacteria, including *S. pneumoniae*, represent typical examples of TI-2 antigens. Recognition of highly repetitive antigens in a BCR-dependent fashion leads to potent cross-linking of the BCRs, ultimately inducing terminal differentiation. B-1 B cells and MZ B cells represent the major B cell subsets recruited into TI-2 immune responses.

1.2.4.2. T-cell-dependent B cell responses

During T cell-dependent immune responses, antigens are presented to naïve FO B cells in the form of immune complexes often exposed on the surface of follicular dendritic cells (FDCs). Antigens are recognized and internalized by B cells via their BCR. Once internalized, protein antigens are cleaved and peptides loaded on MHC-class II (MHCII) molecules, eventually

exposed on the cell surface. Antigen-primed B cells migrate towards the edge of the follicular T cell zone, where they present the antigen to follicular helper T cells (T_{FH}). Concomitant MHCII/TCR pairing and co-stimulatory signals delivered following CD40/CD40L and CD80/CTLA4 interactions between B cells and T_{FH}, result in full B cell activation, inducing the GC response. GCs consist of a densely packed dark zone (DZ) where antigen-specific B cell centroblasts proliferate at high rate, and a light zone, where resting B cell centrocytes, T_{FH} cells, FDCs and macrophages reside in close proximity (Klein and Dalla-Favera 2008). Experimental confirmation of the features of these two populations came from work done by the Cyster laboratory, showing that the chemokine receptor CXCR4 is responsible for retaining a population of GC B cells in the DZ (Allen, Ansel et al. 2004). Some years later, *in situ* photoactivation was used to label LZ and DZ cell populations directly within the GC, by the Nussenzweig laboratory (Victora, Schwickert et al. 2010; Victora and Nussenzweig 2012). They report that although these two subpopulations were indistinguishable in terms of size or complexity, they could be clearly discriminated by flow cytometry by the two markers CD86 and CD83, when used in combination with CXCR4. Thus, LZ cells are $CXCR4^{lo}CD83^{hi}CD86^{hi}$ and DZ cells are $CXCR4^{hi}CD83^{lo}CD86^{lo}$ (Victora, Schwickert et al. 2010).

Within the DZ, centroblasts undergo clonal expansion and diversify their V genes through a process called Ig somatic hypermutation (SHM), which leads to single nucleotide substitutions/deletions preferentially within the portion of the V gene coding for the hypervariable regions (also called complementarity determining regions or CDRs) of the BCR. SHM depends on the activity of the Activation-Induced cytidine Deaminase (AID) enzyme, whose expression is induced in GC B cells (Muramatsu, Kinoshita et al. 2000). GC centroblasts upregulate a substantial number of genes associated with cell proliferation, while limiting the expression of negative regulators of the cell cycle. GC B cells also prevent full activation of the DDR pathway in order to undergo Ig SHM and class switch recombination (CSR) (Ranuncolo, Polo et al. 2007; Ranuncolo, Polo et al. 2008; Ranuncolo, Wang et al. 2008). Centroblasts are highly prone to undergo apoptosis as a result of the upregulation of pro-apoptotic factors, including CD95/FAS and of the downregulation of anti-apoptotic proteins, including members of the BCL2 protein family (Martinez-Valdez, Guret et al. 1996; Klein, Tu et al. 2003; Basso, Saito et al. 2010). The execution of programmed cell death is instrumental for the clearance of B cells displaying non-functional or low affinity BCRs as a result of Ig SHM (Figure 7) (Basso and Dalla-Favera 2010).

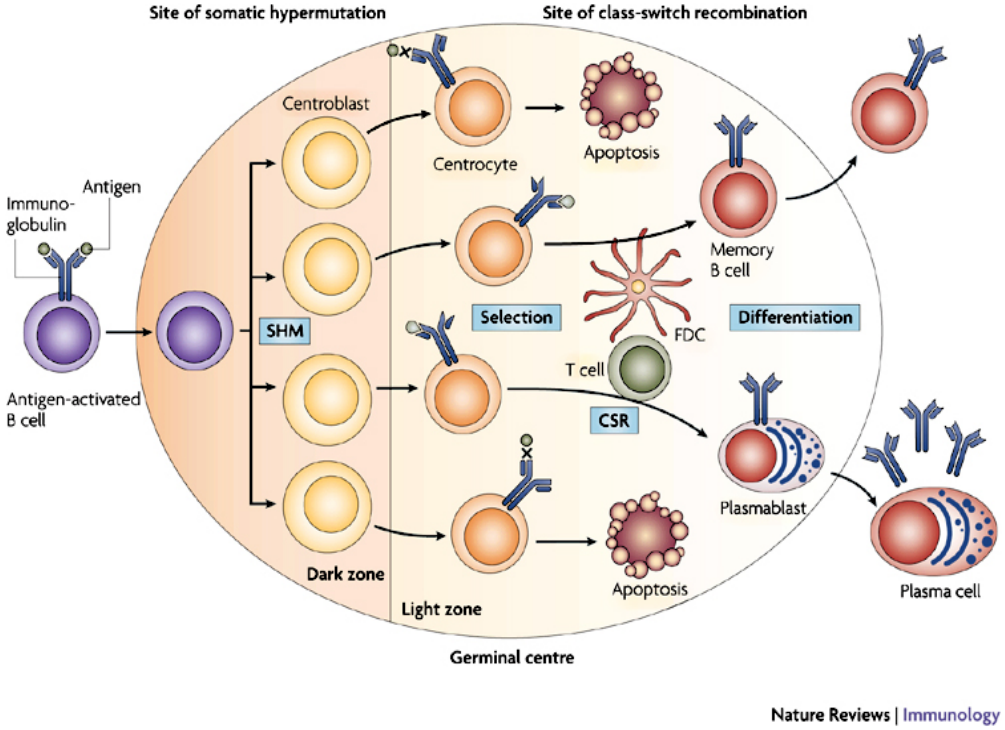


Figure 7. Schematic view of the GC reaction.

In T cell-dependent immune responses, following antigen encounter, FO B cells enter the GC reaction. The GC is characterized by the presence of a dark zone, where large centroblasts undergo massive proliferation and SHM of their Ig gene loci, and a light zone. In the light zone, smaller resting centrocytes are tested for specific antigen binding, undergo CSR and differentiate into high-affinity antibody-secreting plasma cells or memory B cells. (Adaptetd from Klein and Dalla Favera, 2008)

B cells expressing mutated BCRs migrate to the light zone of the GC, where they turn into resting centrocytes. In the light zone, centrocytes are selected on the basis of improved antigen binding via their BCR (Rajewsky 1996). Only B cells expressing BCRs with the highest affinity for the specific antigen will succeed in capturing the antigen presented on FDCs and will present it T_{FH} cells. Co-stimulatory signals provided by T_{FH} cells represent the key event for positive selection of GC B cells (Vinuesa, Tangye et al. 2005). This stringent selection process leads the majority of GC B cells to undergo apoptosis and to be rapidly cleared by local macrophages (Klein and Dalla-Favera 2008). T_{FH} cells residing in the GC also provide signals that promote Ig CSR, whereby B cells exchange their IgH constant region through a recombination process dependent on AID, to improve the effector function of their BCRs (Kawabe, Naka et al. 1994; Vinuesa, Tangye et al. 2005). *In vivo* imaging experiments have provided evidence that GC trafficking is not limited to a unidirectional movement of B cells from the DZ to the LZ, but is contributed by a substantial migration in the opposite direction. These observations support a model whereby B cells undergo iterative rounds of proliferation, Ig mutation and antigen-based selection, with the aim to express antibodies with increasing affinity for cognate antigen (Victora, Schwickert et al. 2010). Eventually, antigen-selected GC B cells activate

differentiation programs that lead to their exit from the GC as long-lived, terminally differentiated, antibody-secreting PCs or memory B cells.

1.2.4.1. Transcriptional regulation of germinal center B cells

1.2.4.1.1. BCL6

The transcription factor BCL6 is a master regulator of the GC response (Fukuda, Yoshida et al. 1997; Cattoretti, Pasqualucci et al. 2005). *Bcl6* encodes a zinc finger transcription factor, which acts primarily as a transcriptional repressor. BCL6 exerts its repressive function by interacting with co-repressors including BCOR, SMRT and NCOR (Dhordain, Lin et al. 1998; Huynh and Bardwell 1998; Wong and Privalsky 1998). Through these complexes, BCL6 is thought to silence genes involved in cell growth inhibition and apoptosis (Hatzi, Jiang et al. 2013), while it influences B cell development through the interaction with the Mi-2-NuRD (Nucleosome Remodeling Deacetylase) complex (Dent, Shaffer et al. 1997; Ye, Cattoretti et al. 1997; Fujita, Jaye et al. 2004; Parekh, Polo et al. 2007). BCL6 renders GC B cells tolerant to DNA damage through direct suppression of the DNA damage sensor ATR and other DDR factors such as Tp53 (Phan and Dalla-Favera 2004; Ranuncolo, Polo et al. 2008; Ranuncolo, Wang et al. 2008). On the other hand, excessive accumulation of DNA damage is prevented by a signaling pathway that promotes ATM-dependent phosphorylation and degradation of BCL6, in response to high levels of genotoxic stress (Phan, Saito et al. 2007; Ranuncolo, Polo et al. 2007). BCL6 supports GC B cell proliferation by inhibiting CDK inhibitors such as *Cdkn1a* and *Cdkn2a* (Klein, Tu et al. 2003; Basso, Saito et al. 2010). In GC B cells, BCL6 inhibits premature onset of the PC transcriptional program by directly repressing the *Prmd1/Blimp1* locus, required for PC development (Vasanwala, Kusam et al. 2002). Reduction of BCL6 expression is needed to allow the differentiation of GC B cells into antibody-secreting PCs. In centrocytes, *Bcl6* is transcriptionally silenced upon CD40 signaling (Niu, Ye et al. 1998; Polo, Ci et al. 2008). Moreover, BCR signaling leads to phosphorylation and hence degradation of BCL6 protein (Phan, Saito et al. 2007).

Interestingly, our lab showed that a substantial number of BCL6 targets were upregulated upon conditional inactivation of EZH2 in GC B cells (Caganova, Carrisi et al. 2013). This suggests that PRC2 and BCL6 may co-operate in silencing a subset of common targets (Velichutina, Shaknovich et al. 2010).

1.2.4.1.2. IRF8/IRF4 axis

In GCs IRF4 and IRF8 follow a reciprocal expression pattern. *Irf8* is highly expressed in centroblasts, which are negative for *Irf4*, whereas centrocytes differentiating to plasma blasts are positive for *Irf4* expression (Klein, Casola et al. 2006). However, recent studies reported

that *Irf8* deficiency in B cells does not affect the GC reaction, suggesting that IRF8 is not strictly required at this stage (Feng, Wang et al. 2011). On the contrary, IRF4 has been shown to be indispensable for GC biology. *Irf4* KO mice fail to form GCs due to insufficient induction of *Bcl6* and *Aicda*. A recent model has been proposed to describe the dynamic changes of *Irf4* levels in the GC reaction (Ochiai, Maienschein-Cline et al. 2013). Specifically, at low levels, IRF4 cooperates with ETS and AP-1 transcription factors to co-bind specific sequence motifs (EICE and AICE) to initiate GC program. At later stages its levels increase, leading to binding to other sequence motifs (ISRE) to induce GC reaction termination and PC differentiation program (Ochiai, Maienschein-Cline et al. 2013; Shukla and Lu 2014).

1.2.4.1.3. E2a

Several studies reported the crucial activity of E2a as a master regulator of B lineage specification. Interestingly, different evidences exist that support a role of E2a even in GC biology. *E2a* inactivation in the GC led to the loss of GC B cells, which was confirmed even by inactivation of this transcription factors in GC precursor B cells (Kwon, Hutter et al. 2008), suggesting that E2a is required for maintenance of GC B cells. Despite normal proliferation, survival and CSR, E2a deficient GC B cells showed higher expression of CD23 and CD38, normally downregulated upon GC entry (Kwon, Hutter et al. 2008). A later study demonstrated a cooperative role for E2a and another E protein, E2-2 in controlling essential functions of GC B cells and PCs. Moreover, both factors control the process of CSR, *in vitro* and *in vivo*. Interestingly, Iγ1 germline transcripts (GLTs) production and chromatin accessibility and active ($H3K27ac^+$) state of the Iγ1 promoter where not affected by the lack of E2a and E2-2. However, the abundance of H3K27ac and accessibility were lost at three distal enhancer elements of the IgH 3' regulatory region in *E2a/E2-2* double KO B cells, which are bound by Ea2, suggesting that these transcription factors control CSR process by controlling the activity of the 3' regulatory regions. Moreover, expression of *Aicda* was not induced in double KO cells (Wohner, Tagoh et al. 2016).

1.2.4.1.4. FOXO1

Studies where *Foxo1* was deleted in mature B cells show that it does not apparently interfere with GC development, but it prevents CSR both *in vitro* and *in vivo*, mainly because of reduced expression of *Aicda* (Dengler, Baracho et al. 2008). Two independent groups have recently shown that specific *Foxo1* deletion in GC B cells prevented the formation of DZ centroblasts, consistent with the fact that it was found highly expressed in this subset (Dominguez-Sola, Kung et al. 2015; Sander, Chu et al. 2015). It was also crucial for antibody affinity maturation as well as CSR, especially in the regulation of GLTs production. It was reported to act both as a transcriptional repressor and as an activator and to specifically bind genes differentially

expressed between centroblasts and centrocytes, like *Prdm1*/*Blimp1* (Dominguez-Sola, Kung et al. 2015). Additionally, a strong overlap was observed between FOXO1 and BCL6 transcriptional programs and bound loci, including genes involved in BCR signaling, B cell activation and PC differentiation. These evidences suggest a strong cooperation existing between these two transcriptional regulators. These findings were also confirmed by the Rajewsky group, which demonstrated a differential activation and expression of *Foxo1* and phosphatidil inositol 3 kinase (*Pi3k*) in GC centroblasts and centrocytes, that appears to be essential for regulating the sequence of events that a B cell undergoes upon recruitment in the GC (Sander, Chu et al. 2015). Moreover, FOXO1 was shown to control expression of *Batf* transcription factor in centrocytes, thus promoting GC B cells proliferation (Inoue, Shinnakasu et al. 2017).

1.2.4.1.5. BACH2

BACH2 plays a crucial role in GC formation upon antigen encounter. *Bach2* is transcriptionally regulated by PAX5, and expressed at every mature B cell stage (Muto, Hoshino et al. 1998). PAX5 turns on its expression together with *Aicda,* thus initiating the GC reaction. GC B cells are highly proliferating and thus undergo a high level of cellular stress and DNA damage, caused by physiological events linked to AID activity (Liu, Duke et al. 2008). In contrast to BCL6 action in allowing these processes, BACH2 triggers a program of oxidative-stress-induced cell death (Muto, Tashiro et al. 2002).

1.2.4.1.6. AID

Accumulation of somatic mutations at Ig V genes, known as SHM, is the pre-requisite for Ig affinity maturation, a process whereby GC B cells are selected on the basis of the affinity of their BCRs for cognate antigen (Berek, Berger et al. 1991; Jacob, Kelsoe et al. 1991). A rapid and effective response of GC B cells and their derivatives relies on the change of the isotype of the IgH chain constant region, the effector component of the Ig receptor, through Ig CSR. AID, identified by the Honjo group (Muramatsu, Kinoshita et al. 2000; Revy, Muto et al. 2000) (Petersen-Mahrt, Harris et al. 2002), initiates both SHM and CSR. AID catalyzes deamination of cytosine residues (Petersen, Casellas et al. 2001; Petersen-Mahrt, Harris et al. 2002). It was long thought to be expressed exclusively in activated B cells and predominantly in GC B cells. However, its expression was recently reported in several other tissues including germ cells and embryonic stem cells. Expression of AID-encoding gene, *Aicda,* in GC B cells is tightly regulated. The promoter of the *Aicda* gene contains binding sites for the transcription factor E2a. Moreover, PAX5 is thought to act with the E2a proteins to control *Aicda* transcription (Gonda, Sugai et al. 2003; Sayegh, Quong et al. 2003; Dedeoglu, Horwitz et al. 2004; Crouch, Li et al. 2007; Teng, Hakimpour et al. 2008; Xu, Schaffer et al. 2008).

AID is responsible for both SHM and CSR and it is part of a multi-protein complex (Ta, Nagaoka et al. 2003; Chaudhuri, Khuong et al. 2004; Basu, Chaudhuri et al. 2005; Pasqualucci, Kitaura et al. 2006; Vuong, Lee et al. 2009). Despite the increasing knowledge about AID, there is little understanding on its preferential targeting to Ig loci.

1.2.4.1.6.1. Ig SHM

SHM of Ig V genes occurs preferentially within the GC. It is a process where single nucleotide substitutions are introduced into a region of +150 bp to +2 kb from the promoters of rearranged Ig V genes. AID mediated cytosine to uridine deamination generates a U:G mismatch. Upon DNA replication, in the absence of mismatch repair, the product of AID activity results predominantly in C to T transitions. All other nucleotide substitutions observed at sites of SHM result from recognition of U:G lesions by proteins involved in either base excision (BER) or mismatch repair (MMR) pathways. The most common pathway to remove uridine from DNA is BER, based on UNG (Uracyl N-glycosylase), which excises uridine from the backbone resulting in an abasic site (Di Noia and Neuberger 2002; Di Noia and Neuberger 2007). The abasic site is then cleaved and low-fidelity DNA polymerases re-synthesize the DNA strand, introducing mutations and single strand DNA breaks. The U:G mismatch can be also recognized by the MMR proteins, MSH2 and MSH6 (Rada, Di Noia et al. 2004). Such recognition can trigger DNA synthesis in which additional mutations are introduced, leading preferentially to A:T substitutions. Moreover, error prone DNA polymerases have been implicated in the process of Ig SHM. (Jansen, Langerak et al. 2006) (Simpson and Sale 2003).

1.2.4.1.6.2. Ig CSR

CSR is an irreversible recombination process by which B cells replace the coding exons of Cμ and C∂ constant regions with that of a distinct Ig isotype. CSR is triggered upon transcription through CG-rich Ig switch (S) sequences located upstream of the exons coding for the different isotypes, generating the so-called germline transcripts (GLTs). Transcription through S regions generates long stretches of ssDNA, which become templates for AID action. Cytosine deamination is followed by the action of UNG and AP1, to induce DSBs in the S regions. The breaks are repaired in a process that requires several DDR proteins (Casellas, Nussenzweig et al. 1998; Manis, Gu et al. 1998; Shiloh 2003; Franco, Gostissa et al. 2006). DNA DSBs are initially recognized by the MRN complex (Petrini 1999) which recruits the ATM kinase to phosphorylate repair factors like 53BP1 and γH2AX, leading to cell cycle arrest and DNA repair (Shiloh 2003). CSR is completed by the joining of Sμ with one of the distal S regions, facilitated by the NHEJ pathway. CSR occurs in both T cell-dependent and T cell-independent responses. A combination of specific cytokines and co-stimulatory signals instructs the process of CSR by regulating the transcription of sterile promoters of Ig S regions (Schultz and Coffman

1991). During GC development, signals for CSR are transmitted to centrocytes by T_{FH} cells. Graded IRF4 expression plays a crucial role in CSR (Klein, Casola et al. 2006; Sciammas, Shaffer et al. 2006).

1.2.4.2. B cells and intestinal immunity

The defensive ability of GALTs strongly relies on the release of IgA. It constitutes the most abundant antibody class in our body, and it is mainly found in the intestine and in the serum. In the gut, IgA can be generated through multiple pathways. The highly organized follicular structures of the PPs, which develop in fetal life, constitute the most prominent IgA production site in the GALTS (Fagarasan, Kawamoto et al. 2010). Additional IgA production sites are the organized structures of the ILFs, which develop after birth in response to bacteria. Further IgA response occurs in the follicles of MLNs. The intestinal lamina propria, on the contrary, mostly functions as an IgA effector site, that supports differentiation and survival of IgA-secreting pcS (Fagarasan, Kawamoto et al. 2010) (Figure 8).

IgA production mostly occurs in PPs and MLNs via T cell-dependent responses, which involve the activation of resting FO B cells by T_{FH} and lead to the generation of IgA-secreting PCs that home to the intestinal lamina propria (Macpherson, McCoy et al. 2008). Specifically, in the presence of antigen-loaded follicular dendritic cells (FDCs), B cells undergo expansion, SHM, IgA CSR and affinity maturation in response to stimuli released by T_{FH} cells, like CD40L, interleukin-21 (IL21) and transforming growth factor β1 (TGF-β1). Interleukin 10 (IL10), retinoic acid (RA) and nitric oxide (NO) released from FDCs further contribute to enhance IgA production in the GC. Once exited from the GC, antibody-producing cells reach the lamina propria where they complete differentiation to become IgA secreting PCs (Gutzeit, Magri et al. 2014). Here, they can survive even for long times thanks to the release of proliferation inducing ligand APRIL (Fagarasan, Kawamoto et al. 2010; Pabst 2012) (Figure 8).

Mucosal T cell-independent IgA production also exists, and it occurs at both follicular and extra-follicular sites. Particularly, in ILFs and in the lamina propria, dendritic cells present luminal antigens to B cells while concomitantly releasing IgA and proliferation-inducing signals like BAFF, APRIL, TGF-β, IL10 and IL6, together with stromal cells. BAFF and APRIL, in particular, enhance both survival of IgA-secreting PCs and induction of IgA CSR in B cells (Tsuji, Suzuki et al. 2008; Fagarasan, Kawamoto et al. 2010; Suzuki, Maruya et al. 2010).

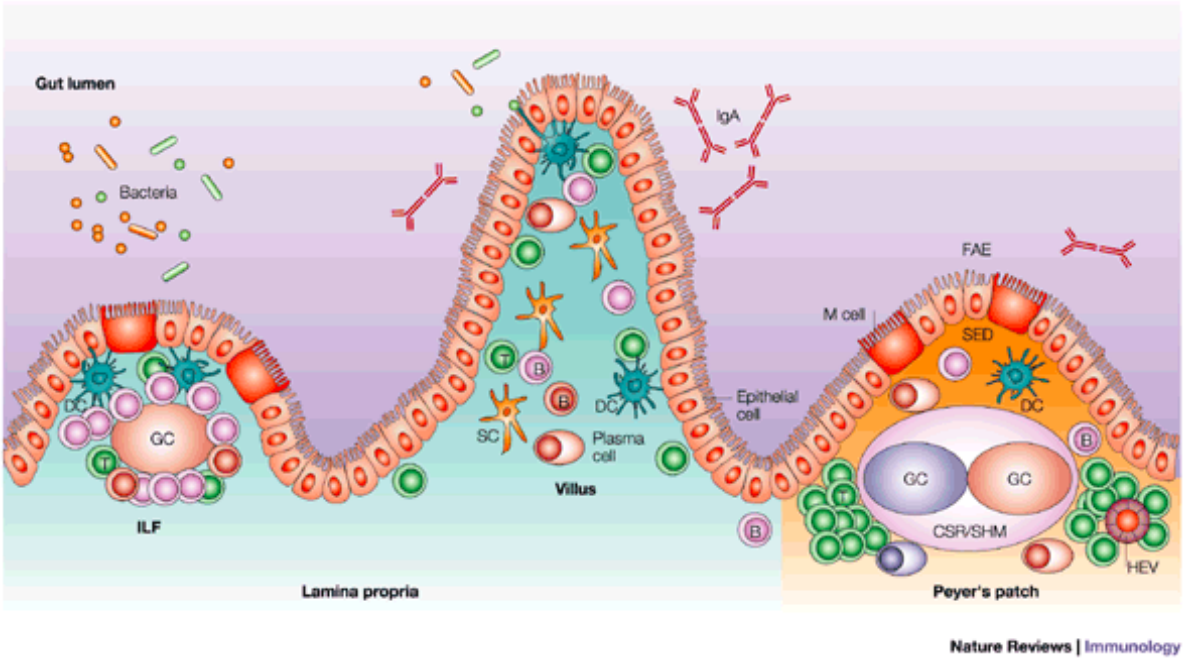


Figure 8. Schematic representation of gut-associated lymphoid tissues (GALT). Schematic representation of GALT, with organized lymphoid structures — Peyer's patches (PPs) and ILFs — and diffuse tissue of the epithelium and the lamina propria. PPs and ILFs are composed of a specialized follicle-associated epithelium (FAE) containing M cells, a subepithelial dome (SED) rich in dendritic cells (DCs), and B-cell follicle(s) that contain GCs, where B cells undergo CSR and SHM. Migration of B cells into the mucosa takes place through high endothelial venules (HEVs), located in the interfollicular regions of PPs. The diffuse tissues of the lamina propria contain a large number of immunoglobulin A (IgA) PCs, T and B cells, macrophages, DCs and stromal cells (SCs). Lamina-propria DCs take up antigens from the lumen and present them directly to T cells and B cells, which can induce IgA class-switching and differentiation *in situ*. Secreted IgA is transported across the epithelium. IgA^+ B cells and plasma cells are shown in red, IgG^+ cells in blue and IgM^+ cells in pink. (Adapted from Fagarasan and Honjo, 2010).

1.2.5. Terminal B cell differentiation

1.2.5.1. Plasma cell development

Following a T cell-dependent immune response, high-affinity B cells enter one of the two possible differentiation routes and either become terminally differentiated PCs or memory B cells. Differentiation into functional antibody-secreting PCs is a step-wise process that requires the combined expression of transcription factors *Blimp1*, *Irf4 a*nd X-box binding protein 1 (*Xbp1*) (Figure 9). The activation of BLIMP1 is critical in PC precursors to extinguish the GC and B cell transcriptional programs through the direct repression of *Pax5* and *Bcl6* (Lin, Angelin-Duclos et al. 2002; Shaffer, Lin et al. 2002). In line with this, PC differentiation is phenotypically characterized by loss of B-cell specific markers including CD19, CD23 and surface Ig, and by the acquisition of PC-specific ones such as CD138/Syndecan 1.

1.2.5.1.1. Master regulators of plasma cell development

1.2.5.1.1.1. BLIMP1

The transcription factor B lymphocyte induced maturation protein 1 (BLIMP1) is encoded by the *Prdm1* (Positive-regulatory-domain-containing 1) gene. BLIMP1 is required for the formation of both short-lived and long-lived PCs (Angelin-Duclos, Cattoretti et al. 2000; Shapiro-Shelef, Lin et al. 2003; Kallies, Hasbold et al. 2004). In GC B cells, *Prmd1* is repressed by the concerted actions of BCL6 and Metastasis-associated 1 family, member 3 (MTA3), which bind to intron 5 of the gene (Fujita, Jaye et al. 2004; Tunyaplin, Shaffer et al. 2004). In late GC B cells, induction of BLIMP1 depends on: 1) signaling through the IL21 receptor, which induces the activation of the transcription factor STAT3 and 2) CD40 signaling, leading to NF-κB dependent upregulation of IRF4 (Kwon, Thierry-Mieg et al. 2009). Together, STAT3 and IRF4 bind to an IL21 responsive element downstream the *Prmd1* gene and mediate its full expression (Kwon, Thierry-Mieg et al. 2009) (Figure 9). Recent evidence from our group has demonstrated a critical role for EZH2 in the modulation of IL21-dependent terminal differentiation. Indeed, we could show that EZH2 limits, through H3K27me3, the induction of *Blimp1* in response to IL21 stimulation, thereby contributing to the persistence of B cells within the GC (Caganova, Carrisi et al. 2013). To induce PC differentiation, BLIMP1 acts both as a transcriptional inducer and repressor. Specifically, BLIMP1: 1) inhibits cell proliferation induced by c-MYC and E2F1 (Lin, Wong et al. 1997; Shaffer, Lin et al. 2002)*;* 2) induces IRF4 expression (Shaffer, Lin et al. 2002; Sciammas and Davis 2004; Klein, Casola et al. 2006); 3) silences the (GC) B cell-specific transcriptional program via repression of *Pax5* and *Bcl6* (Lin, Angelin-Duclos et al. 2002; Shaffer, Lin et al. 2002) and 4) activates the transcription factor XBP1 to allow sustained secretion of Ig molecules (Reimold, Ponath et al. 1996; Shaffer, Lin et al. 2002) (Figure 9). Importantly, BLIMP1 appears also to be critical for the maintenance of long-lived BM PCs (Shapiro-Shelef, Lin et al. 2005).

1.2.5.1.1.2. IRF4

IRF4 is essential for PC development (Klein, Casola et al. 2006; Sciammas, Shaffer et al. 2006). *Irf4* levels rise in centrocytes as a result of CD40 signaling. In these cells, high levels of *Irf4* together with IL21 contribute to activate *Prdm1*/BLIMP1 expression, to promote CSR and hence to drive PC development. BLIMP1 can also induce *Irf4* expression (Sciammas, Shaffer et al. 2006) thereby generating a feed-forward positive loop that is needed to ensure repression of *Bcl6* (Sciammas and Davis 2004). Dynamic and progressive increase in the levels of IRF4 from the beginning to the termination of the GC reaction contribute to the progressive differentiation of B cells to towards the PC lineage and to the induction of the PC transcriptional program (Ochiai, Maienschein-Cline et al. 2013). IRF4 is also required to induce *Xbp1* and

thereby to sustain Ig secretion in PCs (Skalet, Isler et al. 2005; Sciammas, Shaffer et al. 2006) (Figure 9).

1.2.5.1.1.3. XBP1s and the unfolded protein response

The transcription factor XBP1 activates a transcriptional program that sustains the high rate of Ig synthesis of PCs (Reimold, Iwakoshi et al. 2001; Calfon, Zeng et al. 2002). Loss of XBP1 leads to impaired Ig secretion, ultimately resulting in failure to control infections (Reimold, Iwakoshi et al. 2001). In PCs, transcription of *Xbp1* is induced by BLIMP1 (Shaffer, Shapiro-Shelef et al. 2004), Activating Transcription Factor 6 (ATF6) and IL4 (Yoshida, Okada et al. 2000; Iwakoshi, Lee et al. 2003). *Xbp1* mRNA is then cleaved through the endoribonuclease function of the activated IRE1 dimers to yield a spliced form of the transcript (*Xbp1s)*. Spliced XBP1 displays the same DNA binding region as its precursor, but yields a more stable and more efficient transcriptional activator (Yoshida, Matsui et al. 2001; Calfon, Zeng et al. 2002; Lee, Tirasophon et al. 2002). XBP1 activates genes that elicit a PC-specific unfolded protein response (UPR) whereby, in contrast with stress-induced UPR, increase in size of the endoplasmic reticulum (ER) and enhanced protein synthesis co-exist and apoptosis is not induced (Gass, Gifford et al. 2002). XBP1 target genes encode factors that regulate organelle size (Shaffer, Shapiro-Shelef et al. 2004), protein targeting to the ER, protein folding, degradation of mis-folded proteins, protein glycosylation, trafficking between ER and Golgi and targeting of secretory vescicles to the plasma membrane.

1.2.5.1.1.4. BACH2

BACH2 is expressed in all mature B cells but PCs. *Bach2*-deficient mouse models revealed that BACH2 delays PC differentiation by directly inhibiting the PC master regulator BLIMP1 (Muto, Tashiro et al. 2004). In this context, the PAX5-BACH2-BCL6 axis delays PC differentiation and induces the production of high affinity antibodies by GC-terminated B cells upon immunization (Muto, Tashiro et al. 2004). This function of BACH2 is particularly relevant for antibody CSR, since it establishes a defined time-window for CSR to occur and concomitantly pauses terminal PC differentiation (Muto, Tashiro et al. 2004). Recently, it has been reported that antigen exposure lowers *Bach2* levels in Ig class-switched IgG1 memory B cells, thus facilitating their differentiation to PCs (Kometani, Nakagawa et al. 2013).

1.2.5.1.1.5. E2a/E2-2

Concomitant inactivation E2a and E2-2 in mature B cells resulted in a reduction of long-lived PCs residing in the BM, an effect that was prominently mediated by E2-2 (Wohner, Tagoh et al. 2016). Moreover, both *E2a* and *E2-2* KO mice also exhibited reduced antigen-specific PCs in the spleen. Further investigation on the role of these two proteins in the regulation of PCs differentiation led to the observation that *in vitro* stimulated double mutant B cells were arrested

in the activated B cell stage and failed to proceed through further differentiation. Therefore, loss of E2a and E2-2 arrested PC development at the pre-plasmablast stage (Wohner, Tagoh et al. 2016), suggesting a crucial role for these two transcription factors during plasma cell differentiation.

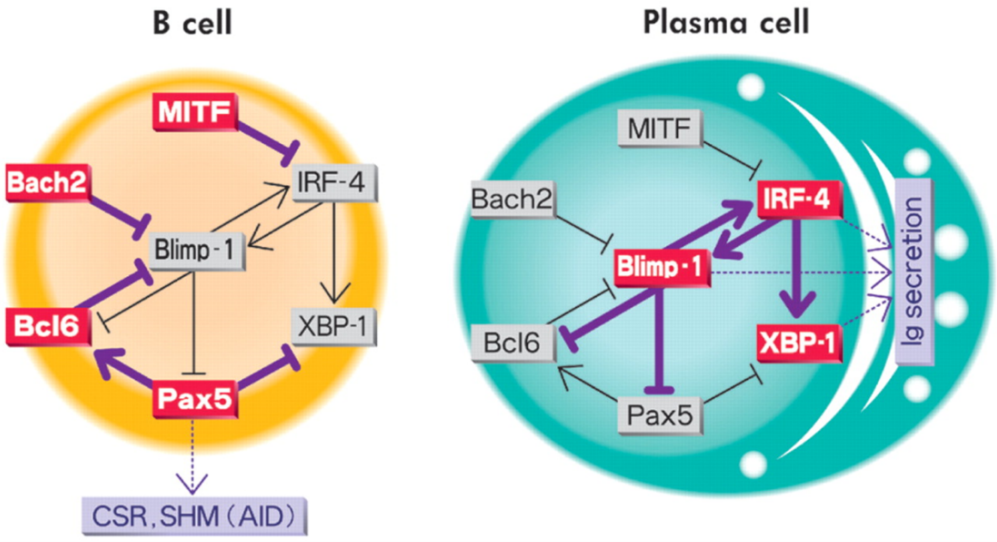


Figure 9 Opposing transcriptional networks in GC and PC development.

Transition of the transcription factor network from B cells to plasma cells. In B cells, BACH2, BCL6, MITF and PAX5 repress the plasmacytic transcription factors *Blimp1, Irf4*, and *Xbp1s* (left). In PCs BLIMP1, IRF4 and XBP1s promote PC differentiation (right), repressing B cell gene expression programs. The red boxes indicate the genes that are expressed. The grey boxes indicate the genes that are not expressed. The bold lines and arrows indicate effective repression and effective activation, respectively. The dashed arrows represent the biological outputs. (Adapted from Igarashi et al, 2007).

1.2.5.2. Memory B cell development

Memory B cells represent a subset of resting long-lived, antigen-experienced lymphocytes. Memory B cells are predominantly, but not exclusively, generated during the GC reaction and provide life-long protection against foreign antigens (Rajewsky 1996; Kaji, Ishige et al. 2012). Memory B cells can express either IgM or Ig-class switched antibodies. Recent work has assigned different functions to IgM and Ig-switched memory B cells. Whereas IgM^+ memory B cells are preferentially recruited into the GC during secondary immune responses, Ig-switched memory cells differentiate directly into PCs upon antigen re-encounter (Dogan, Bertocci et al. 2009). The different fate of IgM and IgG memory B cells may depend on the different signaling properties of the BCRs expressed by the two types of cells (Martin and Goodnow 2002; Kometani, Nakagawa et al. 2013; Pierce and Liu 2013). The mechanisms leading to B cell memory formation are still poorly understood. Activation of the transcription factor STAT5 as a result of cytokine stimulation of GC B cells has been proposed as a mechanism involved in memory B cell formation (Scheeren, Naspetti et al. 2005). Additionally,

sustained CD40 signaling during the GC response has been proposed to skew differentiation towards the memory B cell fate (Arpin, Dechanet et al. 1995). Finally, recent evidence suggested that differentiation into memory B cells expressing different Ig isotypes relies on divergent genetic programs activated by different transcriptional regulators (Wang, McHeyzer-Williams et al. 2012).

1.2.6. Epigenetic control of B cell development

B cell development is under the precise control of gene regulatory mechanisms that orchestrate maturation steps and promote the acquisition of B-specific functions. Indeed, step-wise and controlled expression of specific genes relies on the interplay between transcription factors, post-transcriptional control and epigenetic regulation. Particularly, epigenetic processes comprising histone PTMs, DNA methylation and non-coding RNAs (especially micro-RNAs) play a crucial role in the transcriptional control of B cell-related genes.

The early steps of B cell development require a series of epigenetic regulating events, which restrict B cell lineage (McManus, Ebert et al. 2011). The transcription factor PAX5, in particular, has been shown to control both active enhancers and promoters at B cell-specific target genes while simultaneously favoring the loss of active DNase I hypersensitive sites at repressed target genes. (McManus, Ebert et al. 2011). It exerts this double action by recruiting chromatin remodeling (BRG1- or HBRM-associated factors, BAF) and histone modifying (MLL, CREB-binding protein, CBP, Nuclear receptor co-repressor 1, NCoR1) complexes to target genes, thus maintaining B cell identity. In a similar fashion, the transcription factors E2a and E2-2 were shown to maintain chromatin accessibility at the promoters of their target genes, thus enabling their activation (Wohner, Tagoh et al. 2016).

Recent evidences are supporting the view that the same transcription factors may regulate different transcriptional networks at multiple stages of B cell development, potentially through the recruitment of different epigenetic modifiers, thereby controlling different aspects of B cell biology. In accordance with this view, the transcription factors E2a and E2-2 exert crucial functions also during CSR, by directly binding three regulatory enhancer regions at the IgH locus and inducing *Aicda* expression by controlling multiple associated enhancers. (Wohner, Tagoh et al. 2016), while PAX5 has been shown to regulate totally different sets of target genes in pro-B and mature B cells (Revilla-I-Domingo, Bilic et al. 2012). The same multi-step control of lymphopoiesis has been described for many other transcription factors, including the IRF4/IRF8 axis and it has also been recently proposed for FOXO1 (Dominguez-Sola, Kung et al. 2015; Sander, Chu et al. 2015).

The maintenance of B cell identity, exerted by PAX5 and other B-lineage transcription factors is absolutely essential through the entire maturation and activation processes of B lymphocytes.

However, upon terminal differentiation after T-dependent or independent immune responses, B cells have to silence their B-specific transcriptional program and upregulate PC genes. Hence, the master regulator of PC differentiation BLIMP1 acts mainly as a transcriptional repressor. In this context, it has been shown to recruit many chromatin remodeling and histone modifying complexes to regulate its target genes, like the demethylase LSD1 (Su, Ying et al. 2009) or histone deacetylases (Yu, Angelin-Duclos et al. 2000). A recent report identified for the first time BLIMP1 target genes in PBs and investigated its role in controlling PC differentiation. In particular, BLIMP1 was required to regulate transcription from the Ig_H locus. Moreover, BLIMP1 recruited several chromatin-modifying and remodeling complexes at its targets, as assessed by chromatin co-immunoprecipitation analyses. Among them, the PRC2, NuRD and BAF remodeling complexes (Minnich, Tagoh et al. 2016) have been identified.

Different groups are now beginning to unravel the contributions of chromatin modifiers to B cell development. In particular, two recent works reported similar and interesting findings in B lymphopoiesis in mice with *Kmt2d*/MLL4 inactivation. The Pasqualucci group demonstrated that conditional deletion of *Kmt2d*/MLL4 early during B cell development affected splenic and LNs mature B cell numbers, especially in the follicular B cells subset, together with the fraction of B cells recirculating in the bone marrow. However, these defects were absent or modest in unimmunized mice, whereas they were significant upon immunization, suggesting that they may reflect impaired homeostasis of mature B cells. Interestingly, the loss of *Kmt2d* early during B cell development led to abnormal GC B cell responses, while its inactivation after the GC reaction led to a milder phenotype, suggesting that *Kmt2d*-deficient precursor B cells have a higher propensity to enter the GC reaction. Moreover, the stage/timing of *Kmt2d* deletion influenced also the transcriptional changes occurring in GC population, even if the nature of these changes was highly similar (Zhang, Dominguez-Sola et al. 2015). Consistently with these findings, loss of *Kmt2d* provides substantial proliferative advantage to B cells upon *in vitro* stimulations with the cytokines CD40 and IL4. In accordance with the functions of KMT2D in normal activated B cells, *Kmt2d* deletion led to an increase in tumour incidence in mice overexpressing *Blc2*, which develop GC-derived lymphomas that resemble human follicular lymphomas (FL) (Zhang, Dominguez-Sola et al. 2015). Similar results were obtained by the Melnick group using a transplantation model with either wildtype or *Bcl2*- overexpressing hematopoietic progenitor cells (HPCs) transduced with *Kmt2d* short hairpin RNA (*shRNA*) (Ortega-Molina, Boss et al. 2015). In both studies, *Kmt2d* deficient mice also showed decreased levels of IgG1 antibodies after T-cell dependent immunizations, suggesting that the process of immunoglobulin isotype-switching could be affected in the absence of *Kmt2d*. This result was confirmed also by *in vitro* isotype-switching assays. In line with the latter observation, an earlier

report demonstrated that the MLL3/MLL4 complex component PTIP promotes specific chromatin changes that control the accessibility of the IgH locus, thus regulating transcription initiation and the onset of Ig isotype switching (Daniel, Santos et al. 2010). Interestingly, an independent group demonstrated that PTIP exerted its functions in transcription and CSR independently from MLL3/MLL4 but in association with the MLL component PA-I (Starnes, Su et al. 2016).

Recently, several studies assigned to PRC2 catalytic subunit EZH2 a critical role in the control of B cell lymphopoiesis. EZH2 expression is modulated during B cell differentiation, reaching the highest level in progenitor B cells. In accordance with this finding, conditional inactivation of *Ezh2* catalytic function starting in pro-B cells caused an early block in B cell development (Su, Basavaraj et al. 2003). As a result of this defect, conditional *Ezh2* mutant mice suffered from a severe B cell lymphopenia (Su, Basavaraj et al. 2003) (Su, Dobenecker et al. 2005) (Caganova and Casola, unpublished results). Mechanistically, *Ezh2* mutant progenitor B cells displayed impaired VDJ recombination, possibly resulting from defects in IgH locus contraction (Su, Basavaraj et al. 2003). In accordance with its low expression in resting B cells, conditional inactivation of *Ezh2* in the latter cells did not affect the three mature B cell subsets (Caganova, Carrisi et al. 2013). An increase in *Ezh2* expression is observed when resting B cells are recruited into the GC reaction during a T cell-dependent immune response (Beguelin, Popovic et al. 2013; Caganova, Carrisi et al. 2013). Specific ablation of *Ezh2* in GC B cells caused a significant reduction in the number of GCs. As a consequence of this impairment, mutant animals fail to generate high-affinity, long-lived, memory B cells and showed a substantial reduction in antigen-specific serum antibodies produced by PCs (Caganova, Carrisi et al. 2013). Furthermore, it was suggested that EZH2 promotes cell cycle progression through the silencing of the cell cycle regulators p16 and p19, encoded by the *Cdkn2a* locus. Surprisingly, the loss of *Cdkn2a* is not sufficient to rescue impaired GC responses of *Ezh2* mutants, demonstrating that the defects of *Ezh2* mutant GC B cells are independent of the regulation that EZH2 exerts on *Cdkn2a* locus (Caganova, Carrisi et al. 2013). Instead, a recent study demonstrated that deletion of the cell cycle regulator p21 (*Cdkn1a*) is able to rescue GC formation in *Ezh2* deficient mice, suggesting that EZH2 controls GC B cell proliferation by suppressing *Cdkn1a*, thus enabling G1-to-S cell cycle transition (Béguelin, Rivas et al. 2017). EZH2 is also critical to prevent B cell terminal differentiation. *Ezh2* deficient GC B cells upregulate the expression of PCs master regulators *Blimp1* and *Irf4*. According to these results, in GC B cells EZH2 directly modulates *Blimp-1* expression, thus preventing a premature exit from GC compartment to guarantee a protective adaptive immune response (Caganova, Carrisi et al. 2013). Additionally, a recent study showed that EZH2 function is crucial for PC differentiation also in T-independent immune responses, as inducible deletion of *Ezh2*

generated fewer antibody secreting cells due to dysregulated H3K27me3 and chromatin accessibility of B-cell genes that are normally repressed during PC differentiation (Guo, Price et al. 2017).

In conclusion, a recent study demonstrated a role for the acetyltransferase CREBBP in the transcriptional control of GC B cells and in the onset of PC differentiation. Specifically, *bona fide* CREBBP target genes were specifically enriched with signalling pathways associated to the GC LZ, where B cells receive specific cues to differentiate into either PCs or memory B cells. Indeed, CREBBP binding was also found at the regulatory sequences of master regulators of PC differentiation, including two well-known elements located upstream to the TSS of *Prdm1* and two putative regulatory regions of the *Irf4* promoter, supporting the involvement of CREBBP in the terminal differentiation of LZ B cells to PCs. Consistently with these findings, *Creebp*-deficient B cells showed enhanced response to activation stimuli and defective PC differentiation *in vivo* in the spleen and *in vitro* upon LPS and IL4 stimulation, accompanied by mildly reduced levels of serum IgG1 titers (Zhang, Vlasevska et al. 2017).

1.3. Aim of the study

Much progress has been made in the past decades in our understanding of the functions of UTX, since its discovery in 2007, in many different contexts, from early embryonic development to cell differentiation and somatic cell reprogramming (Mansour, Gafni et al. 2012), and from early hematopoiesis to immune cell development and functions. (Manna, Kim et al. 2015; Beyaz, Kim et al. 2017). Loss of *UTX* function is also commonly observed in various types of B cell-derived cancers, including B-ALL (van Haaften, Dalgliesh et al. 2009) and MM (van Haaften, Dalgliesh et al. 2009). Loss of function mutations in the X-linked *UTX* gene have also been associated to a human complex congenital disorder known as the Kabuki syndrome, where patients display a poorly characterized B-cell immune defect (Lindsley, Saal et al. 2016).

Despite all these evidences, how UTX contributes to B cell physiology and malignant transformation remains largely unknown. The aim of the present thesis is to challenge this question through the characterization of a conditional mouse model (Mansour, Gafni et al. 2012) where UTX demethylase is specifically inactivated in B cells using Cre/loxP technology. Our data highlight, for the first time, the involvement of UTX in the control of mature B cell subset differentiation. Loss of UTX had also an impact on B cell activation, highlighted by disturbed GC responses, and on B cell terminal differentiation. Chromatin analyses combined to transcriptomic profiling have started to unveil alterations in the epigenetic landscape and developmentally-relevant transcriptional networks which may contribute to step-wise B cell maturation and to the mounting of a protective antibody response. The results obtained in this

study aim to provide novel insights into the possible involvement of deregulated UTX function in the pathogenesis of immunological disorders, including B cell malignancies.

2. Materials and methods

2.1. Mice

Mice were maintained in the COGENTECH mouse husbandries at the IFOM-IEO Campus, in Milan, Italy. Animal handling and mouse experimentations were performed under the protocol # 438-2017, approved by the Italian Ministry of Health.

2.1.1. Mouse strains

Utx^{fl} conditional KO mice were previously described (Mansour, Gafni et al. 2012) and gently provided by Dr J. Hanna (Weizmann Institute, Israel). Mb-1^{cre} and *Aicda*^{cre} strains, both on the C57BL/6 genetic background, were previously described (Hobeika, Thiemann et al. 2006) (Kwon, Thierry-Mieg et al. 2009). *Utx*$^{fl/}$ mice were back-crossed to C57BL/6 mice for 12 generations. C57BL/6 mice were purchased from Charles River.

2.1.2. Genomic DNA extraction from mouse tail biopsies

Tail biopsies were incubated in 400 µl of lysis buffer (100 mM Tris-HCl pH 8.5; 5 mM EDTA; 200 mM NaCl; 0.2 % SDS) with Proteinase K (PK) (100 µg/mL) at 56°C, shaking at 750 rpm overnight. Lysed material was centrifuged at maximum speed for 1 minute, transferred into new 1.5 ml tubes and precipitated with 2.5 volumes of isopropanol. The DNA was pelleted by centrifugation, air-dried and dissolved in 400 µl of milli-Q water (Q-POD Element, Merck Millipore) by incubation at 56 °C for 20 minutes.

2.1.3. Mouse genotyping

Genotypes of mice were assessed by polymerase chain reaction (PCR) performed on genomic DNA extracted from tail biopsies. Primers used for PCR amplification, are listed in Table 1, PCR reagents are listed in Table 2 and PCR conditions are described in Table 3. PCRs were run on GeneAmp PCR System9700 (Applied Biosystems**)** thermocyclers.

Table 1. List of primers used for genotyping, annealing temperatures and amplicon sizes

Primers	Name	Sequence	Annealing	Amplicon	
Utx Frt-βgeo vs WT	Utx FRT del Fw3	ACGATACCACGATATCAACAAG	58° C	400 bp	
	Utx FRT del Rv2	CAAATATCCGCCTACTGCGAC			
Utx Flox vs WT	Utx geno_F2	AAAGCTGAAGGGAAAGTGGA	60°C	WT	410 bp
	Utx geno_R	GCAGGCAGCTTTTTAAATTTGT		Floxed	380 bp
Utx Cre deleted allele	Utx del Fw1	TCGGGAGGTCATAGGACAGT	60 °C	WT	1499 bp
	Utx geno_R	GCAGGCAGCTTTTTAAATTTGT		Deleted	700 bp
Mb-1$^{cre/+}$	Mb-1^{cre} Fw	CCCTGTGGATGCCACCTC	58° C	430 bp	
	Mb-1^{cre} Rv	GTCCTGGCATCTGTCAGAG			
Aicda^{cre}	Universal Cre Fw	ACGAACCAAGGTGACAGCAATG	60° C	Tg 350 bp	
	Universal Cre Rv	CTCGACCAGTTTAGTTACCC			

Table 2. PCR master mix used for genotyping.

PCR master mix	µl
5X Flexi Buffer	5
$MgCl_2$ 2.5mM	2
dNTPs 2.5mM	2
Primer Fw (50 M)	0.2
Primer Rv (50 M)	0.2
Go Taq Flexi	0.2
DNA	2
H_20	Up to 25

Table 3. Genotyping PCR conditions.

Temperature (°C)	Time (minutes)
94	2:30
95	0:30
TA 33-35X	0:30

72	0:30
72	5:00
4	hold

2.1.4. Mouse immunizations

Eight weeks to 10-months old mice were immunized by intraperitoneal injections of Alum (Imject ® Alum, aqueous solution of aluminium hydroxide (40 mg/ml) and magnesium hydroxide (40 mg/ml), Pierce)-precipitated NP_{27-28}-CGG (100µg per mouse, 4-Hydroxy-3-nitrophenylacetyl conjugated to chicken gamma globulin (Biosearch Technologies). Secondary immunizations were performed injecting animals intraperitoneally with 50 µg of alum-precipitated NP_{28}-CGG (in PBS 1X), 60 days after primary immunization. For FACS sorting of GC B cells, mice were immunized with 2 X 10^8 sheep red blood cells (SRBCs) (Thermo Scientific) and sacrificed 8 days later.

2.1.5. *In vivo* BrdU incorporation assay

Two to six months old mice were fed with 0.8 mg/ml of BrdU (Sigma-Aldrich) in the drinking water supplemented with 2% sucrose (Carlo Erba) for 7 days. The BrdU solution was replaced every other day. Mice were sacrificed on day 6 post-treatment and BrdU incorporation was assessed in B cells subpopulations retrieved from primary and secondary lymphoid organs respectively.

2.2. Cell culture techniques

2.2.1. Preparation of cell suspensions from lymphoid organs

Erythrocyte lysis buffer	
Solution A	0.17 M Tris HCl pH 7.65
Solution B	0.83 % NH_4Cl
Working solution	9 parts B: 1 part A

B cell medium	
DMEM	Lonza
10 % FBS	Life Technologies
2 mM glutamine	Euroclone
200 U/ml pen/strep	Euroclone
NEAA	Microtech
50 µM 2–mercaptoethanol	Life Technologies

1 mM Na Pyruvate	Microtech

Spleen (SPL), lymph nodes (LNs), tibias (# 2 per mouse) and Peyer's patches (PP, # 5 per mouse) were collected and processed to obtain single cell suspensions. Spleen, LNs and PPs samples were smashed between frosted slide glasses and subsequently filtered through 40 μm nylon meshes (Becton Dickinson, USA). Tibias were flushed with 1 ml of B cell medium. Lysis of erythrocytes from SPL and BM preparations was achieved incubating cell suspensions in 1 ml of Erythrocyte lysis buffer for three minutes at 4˚C. Lysis was stopped adding 10 volumes of B cell medium to the cell suspension. Cells were centrifuged at 1200 rpm for 5 minutes at 4˚C and resuspended in B cell medium before counting. Live cells were counted after staining the suspensions with the Erythrosin B dye (Sigma- Aldrich).

2.2.2. Primary B cell purification

MACS buffer
1X PBS
0,5% BSA
2 mM EDTA

Preparation of cell suspensions was achieved as described above. After counting, cell suspensions were labeled with a cocktail of biotin-conjugated antibodies against CD43, CD11b, CD11c, Ter-119, CD4, CD8, and CD3 (Table 4), followed by anti-Biotin magnetic MicroBeads (Miltenyi Biotec). B cells were purified after loading antibody-labelled cell suspension onto LS columns (Miltenyi Biotec) following the manufacturer's protocol (Miltenyi Biotec). This procedure allows the isolation of untouched resting B cells. Purity of B cells preparations was assessed by measuring the fraction of cells in the flow through expressing the pan-B cell markers B220 and CD19, and the non-B cell marker TCRβ. Cells were acquired on a FACSCalibur (BD Bioscience) instrument and analyzed with the FlowJo software (Tree Star).

Table 4. List of antibodies used for B cells negative purification.

Antibodies	Company	Dilution
Monoclonal rat anti mouse CD43 (S7) biotin	ebioscience	1/800
Monoclonal rat anti mouse CD11b (M1/171) biotin	ebioscience	1/800
Monoclonal Armenian hamster anti mouse CD11c (N418) biotin	ebioscience	1/800

Monoclonal rat anti mouse CD4 (GK1.5) biotin	ebioscience	1/400
Monoclonal rat anti mouse CD8 (53-6.7) biotin	ebioscience	1/400
Monoclonal Armenian hamster anti mouse CD3 (145-2C11) biotin	ebioscience	1/200

2.2.3. *In-vitro*-induced Germinal Center B cells (iGB)

Splenic B cells were purified as described above. The iGB protocol was applied as described in (Nojima, Haniuda et al. 2011). Briefly, primary B cells were seeded on previously irradiated (120 Gy for 1-hour), or Mitomycin C (10 μg/ ml; GlobalStem)-treated (3 hours at 37°C) BALB/c 3T3 fibroblasts expressing CD40L and BAFF (40 LB). B cells were seeded at a starting density of 1,25 x 10^4 cells/ mL in 30 ml of B cell medium supplemented with 1 ng/ml recombinant murine Interleukin 4 (IL-4; Peprotech). Cells were grown for three days at 37°C, in 5 % CO_2 after which medium was refreshed. At day 4 of the culture, cells were harvested and counted. To induce PC differentiation, iGB cells were seeded on a freshly irradiated 40LB feeder layer at a density of 1,25x10^4 cells/ml in 30 mL of B cell medium supplemented with 10 ng/ml of IL21 (Peprotech).

2.2.4. *In-vitro* B cell stimulation

Purified B cells were cultured in B cell medium and stimulated at a density of 0,5x10^6 /ml with 2.5 to 20 μg/ ml of Lipopolysaccharide (LPS; Sigma Aldrich), supplemented in some experiments with 5 ng/ml of IL4 (Peprotech). Alternatively, B cells were stimulated with 0,25 μg/ ml of functional-grade α-RP105 (eBioscience) antibody. For *in vitro* survival assays, primary B cells were seeded at a density of 0.5 - 1 x 10^6 cells/ml and cultured at 37°C, 5 % CO_2 for 8 days in the presence of recombinant human BAFF (6 ng/ ml, Peprotech).

2.2.5. *In vitro* proliferation assay

Primary splenic B cells purified through a MACS depletion protocol were labeled at 37°C for 20 minutes with 2.0- 2,5 μM Carboxyfluorescein diacetate succinimidyl ester (CFDA-SE, Abcam) diluted in pre-warmed 1X PBS, as previously described (Hasbold, Gett et al. 1999). The reaction was stopped diluting cells in pre-warmed B cell medium followed by two consecutive washes with 30 ml of pre-warmed B cell medium. Viable cells were counted using the Erythrosin B method and seeded according to the appropriate culture conditions. The extent of CFDA-SE labelling was assessed by flow cytometry prior to and 48 h, 72 h and 96 h after mitogenic stimulation. Cells were loaded on a FACSCalibur (BD Bioscience) and analyzed using the FlowJo software

2.3. Imaging techniques

2.3.1. Immunostaining for flow cytometric analyses and cell sorting

FACS buffer
1X PBS
1% BSA
0,05% NaN_3

For flow cytometric analyses, 1- $2x10^6$ cells were stained for 20 minutes on ice in 50 µl FACS buffer containing the appropriate mixture of fluorescently labeled antibodies and subsequently washed twice in 150 µl of FACS buffer. Cells were either freshly acquired on a FACSCalibur (BD Bioscience) or fixed with 1% formaldehyde in PBS for later acquisition. Data were analyzed with FlowJo software (Tree Star).

For FACS-assisted cell sorting, cells were resuspended in FACS buffer at a density of 10^8 cells/ml and stained for 15 minutes at 4˚C on rotation in FACS buffer. Cells were then washed twice in 10 volumes of FACS buffer, resuspendend in 1-3 ml of 1 X PBS/ 2% FBS and sorted using a FACSAria (BD Bioscience) instrument. Sorted cells were collected in 1 X PBS complemented with 33% FBS, centrifuged at 6000 rpm 4˚C for 5 minutes and resuspended in B cell lysis buffer RLT plus (Qiagen) for nucleic acids extraction.

The list of antibodies as well as working antibody dilutions used for flow cytometric analyses and FACS sorting are presented in Tables 5 and 6.

Table 5. Surface markers used for B cell subsets sorting/gating.

B cell subset	Surface markers staining
Pro-B	$B220^{lo}IgM^-CD43^+CD25^-$
Pre-B	$B220^{lo}IgM^-CD43^-CD25^+$
Follicular B	$CD19^+CD23^+CD21l^o$
Marginal zone B	$CD19^+CD23l^oCD21^{hi}$
Germinal center B	$CD19^+CD95^hiCD38^{lo}$
Plasma blasts	$B220^+CD19^+CD138^+$
Plasma cell	$B220^{lo}CD19^{lo}CD138^+$

2.3.1.1. Intracellular flow cytometric immunostaining

Cells were stained in 50 µl /$1x10^6$ of FACS buffer containing antibodies of choice (Table 6) for 20 min at 4°C in the dark and subsequently washed twice with 150 µl of FACS buffer. Surface

stained cells were fixed in BD Cytofix/Cytoperm™ buffer for 20 min RT, shaking, in U-bottom 96 well microplate, washed by Perm/Wash™ Buffer (P/W) and stained with the appropriate antibodies (Table 6) for 1 hour at RT, shaking. Cells were washed twice with P/W buffer and fixed in 1 % formaldehyde in PBS. Samples were acquired and analyzed using FACSCalibur (BD Bioscience) and FlowJo software. All centrifugation steps were performed at 1300 rpm for 3 minutes at 4°C.

Alternatively, surface stained cells were fixed with the True-Nuclear™ 1X Fix Concentrate (True nuclear transcription factor buffer set, Biolegend) for 30 min RT, shaking, in U-bottom 96 well microplate, washed twice by True-Nuclear™1X Perm Buffer and stained with the appropriate antibodies (Table 6) for 1 hour at RT, shaking. Cells were then washed twice with True-Nuclear™1X Perm Buffer and fixed in 1 % formaldehyde in PBS or resuspended in 1 X PBS for FACS acquisition.

Table 6. Antibodies used for flow cytometry.

Antibodies	Company	Dilution
Monoclonal rat anti-mouse IgM (R33.24.12) (Alexa 488)	Home-made	1/400
Monoclonal rat anti-mouse IgM (R33.24.12) (Alexa 647)	Home-made	1/800
Monoclonal rat anti-mouse CD19 (eBio1D3) (CY7PE)	eBiosciences	1/400
Monoclonal rat anti-mouse CD21/CD35 (eBioD89) (PE)	eBiosciences	1/1000
Monoclonal rat anti-mouse CD23 (B3B4) (FITC)	eBioscience	1/100
Monoclonal rat anti-mouse CD25 (PC61.5) (APC)	eBiosciences	1/100
Monoclonal rat anti-mouse CD38 (90) (APC)	eBiosciences	1/600
Monoclonal rat anti-mouse CD43 (eBioR2/60) (PE)	eBiosciences	1/100
Monoclonal rat anti-mouse IgD (PE)	eBiosciences	1/3000
Monoclonal rat anti-mouse Ig Kappa (R331.18) (Alexa 488)	Homemade	1/400
Anti-mouse Ig Lambda 1,2 (JC5-1) (APC)	Mylteni Biotec	1/50
Monoclonal rat anti-mouse IgG1 (A85-1) (biotin)	AbD Serotec	1/2000
Monoclonal rat anti-mouse IgG1(X56) (PE)	BD	1/20
Monoclonal rat anti-mouse IgG3 (R40-81) (biotin)	BD	1/500
Monoclonal rat-anti- mouse CD45R (B220) (RA3-6B2) (CY7PE)	eBiosciences	1/400
Monoclonal rat anti-mouse CD45R (B220) (RA3-6B2) (FITC)	eBiosciences	1/100
Monoclonal rat anti-mouse CD117 (c-Kit) (2B8) (APC)	eBiosciences	1/200
Monoclonal rat anti-mouse CD93 (AA4.1) (APC)	eBiosciences	1/400
Monoclonal rat-anti-mouse MHC II (M5/114.15.2) (PE)	eBiosciences	1/200
Monoclonal rat anti-mouse CXCR4 (2B11) (APC)	eBiosciences	1/200
Monoclonal hamster anti-mouse CD95 (Fas) (Jo2) (PE)	BD	1/170
Monoclonal rat anti-mouse CD86 (GL-1) (CY7PE)	eBiosciences	1/800
Monoclonal rat anti-mouse CD268 (BAFF-R) (7H22-E16) (APC)	BD	1/400
Monoclonal Rat anti-mouse CD5 (PE)	eBiosciences	1/200
Peanut Agglutinin (PNA) (FITC)	Vector laboratories	1/150
Streptavidin (APC)	eBiosciences	1/800
Streptavidin FITC	eBiosciences	1/400
Streptavidin (CY7PE)	eBiosciences	1/400
Monoclonal rat anti-mouse CD138 (281-2) (PE)	eBiosciences	1/200
Monoclonal rat anti-mouse IRF4 (3E4) (Alexa 647)	eBiosciences	1/800
Monoclonal rat anti-mouse IRF4 (3E4) (Alexa 488)	eBiosciences	1/800
Monoclonal rat anti-mouse BLIMP1 (5E7) (Alexa 647)	BD	1/200
Monoclonal rat anti-mouse BCL6 (K112-91) (Alexa 647)	BD	1/25
Monoclonal rat anti-mouse PAX5 (1H9) (PE)	BD	1/200

2.3.1.2. Flow cytometric detection of apoptotic cells

For detection of apoptotic cells, the CaspGLOW™ Fluorescein Active Caspase Staining kit (Thermofisher) was used according to the manufacturer's instructions, except for few steps of the protocol. Briefly, cells were incubated for 1 h at 37°C and 5 % CO_2 in 100 µl of B cell medium containing 0,5 µl of FITC-VAD-FMK (carbobenzoxy-valyl-alanyl-aspartyl-[O-methyl] fluoromethylketone), a cell-permeant active caspase inhibitor irreversibly binding to the catalytic site of all active caspases. Cells were collected by centrifugation (1300 g for 3 min) and washed with 200 µl of the CaspGLOW™ wash buffer (Thermofisher). If required, cells were also surface-stained as described above. Stained samples were acquired on a FACSCalibur (BD Bioscience) cytometer and data analyzed with the FlowJo software (Tree Star).

2.3.2. Immunostaining of tissue sections

Pre-incubation solution
1X PBS
0,005% FBS
0,001% BSA
0,05% Tween 20

2.3.2.1. Immunofluorescence

Immunofluorescence staining was performed on sections of spleens snap-frozen in liquid nitrogen. Frozen spleens were cut in 3-5 µm-thick slices, which were subsequently applied onto Superfrost ultra Plus® (Thermo Scientific) microscope slides. Samples were washed once in 1 X PBS, then fixed for 10 minutes at RT in an 80% ethanol solution. Tissue sections were washed 3 times for 5 minutes with 1 X PBS, incubated for 1 hour RT with pre-incubation solution (see above) and ultimately stained with antibodies of interest. Primary antibodies included monoclonal rat anti-human MOMA-1 (dilution 1:10 Abcam) and monoclonal rat-anti mouse CD45R (B220) conjugated with FITC (1:100 dilution; eBioscience). Incubation was performed at 4° C overnight in the dark. Slides were subsequently washed for 5 minutes with 1 X PBS followed by incubation for 1 hour at RT with streptavidin (dilution 1:200) coupled to Cy5 (Southern Biotech). Following 3 washes of 5 minutes each with 1X PBS, tissue sections were stained for 5 minutes with 4',6-diamidino-2-phenylindole (DAPI) in 1X PBS to label nuclei and finally rinsed in 1X PBS to eliminate excess staining solution. Slides were mounted using a 50% glycerol solution in H_2O and stored in the dark at + 4° C ready for acquisition. Images were acquired on a widefield BX61 microscope (Olympus) using the MetaMorph

(Molecular Devices) software. The surface of the marginal zone area was measured using ImageJ (NIH) subtracting the surface area of $B220^+$ B cells residing inside of the MOMA1-positive ring of metallophilic macrophages delimiting the follicle to the total surface area occupied in each follicle by $B220^+$ B cells. Normalization of the values was achieved taking into account the different sizes of the follicles by calculating its circumference.

2.3.2.2. Immunohistochemical staining of tissue sections

Na citrate buffer
10 mM Na citrate pH 6.0
0,05% Tween 20
1 L Distilled water

Immunohistochemical stainings were performed on sections of representative spleens and small intestines from control and *Utx* conditional mutant mice. Specifically, mice were sacrificed and small intestines collected and lumen flushed 3 times with 30 ml of 1 X PBS. Splenic sections were obtained from immunized mice. Biopsies of small intestine and spleen were fixed in formaldehyde 4 % /1 X PBS and embedded in paraffin. Tissue sections were cut at 3 to 5 µm of thickness. Sections were subjected to sequential washes in decreasing concentration of ethanol solutions (100%, 95%, 80%), for 3 minutes each, and finally re-hydrated for 5 minutes in water. For antigen unmasking, samples were incubated at 95°C for 45 minutes in sodium (Na) citrate buffer followed by cooling at RT for a 1 hour or more. Slides were incubated for 10 minutes at RT with peroxidase blocking solution (30% hydrogen peroxidase water solution, Sigma Aldrich), rinsed in PBS 1X 3 times for 5 minutes and incubated for 1-2 hours at RT in pre-incubation solution (see above). Sections were incubated overnight at +4°C with pre-incubation solution containing rabbit polyclonal anti-mouse BCL6 antibody (1:100 in pre-incubation solution; Cell Signaling, #4242) to score germinal center B cells. Slides were washed 3 times, 5' each, in 1 X PBS followed by staining with anti-rabbit IgG coupled to HRP (1:200, Vector Labs) for 45' at RT. Binding of the secondary antibody was revealed by staining tissue sections with the Vectastain Elite reagent (Vectastain Elite ABC-peroxidase Kit, Vector Lab), for 1 hour RT followed by incubation with the DAB peroxidase substrate solution (Vector Lab) for 1 minute. Slides were rinsed in water and de-hydrated in alcohol series (80%, 95%, 100%) for 10'' each. Slides were finally mounted in Eukitt (Sigma-Aldrich) and stored at RT until acquisition. Images were acquired on a Full Manual BX51 (Olympus) microscope. The area occupied by BCL6-expressing germinal center B cells was calculated using ImageJ software (NIH). $Bcl6^+$ GC foci were counted and divided by the number of follicles detected in each

splenic section. Lamina propria IgA^+ plasma cells were scored in a defined number of intestinal villi (25) for each sample. The average number of IgA^+ PCs per villus was finally calculated.

2.4. Biochemical techniques

2.4.1. Immunoblot analysis

Cells were harvested by centrifugation for 5 minutes at 6000 rpm and washed with ice-cold 1 X PBS. Whole cell protein extracts were obtained using either with RIPA (10 mM Tris-HCl, pH 8.0; 1 % Triton-X-100, 0.1 % SDS; 0.1 % Sodium Deoxycholate, 150 mM NaCl; 1 mM EDTA) or Laemmli (62.5 mM Tris-HCl, pH 6.8; 2 % SDS; 0.001 % Bromophenol Blue and 10 % glycerol) lysis buffer, supplemented with 1 mM DTT (Sigma), 1 mM PMSF (Sigma Aldrich) and protease inhibitors (EDTA-free cocktail Set III from Calbiochem,). Samples were incubated in lysis buffer from 30 minutes to 1 hour on ice. Sonication consisted of 10 cycles (high power), 30 seconds each (Bioruptor™ Next Gen, Diagenode). Lysates were centrifuged at maximum speed for 1 minute in a tabletop centrifuge to remove cell debris. Proteins were quantified with the DC™ protein assay (BioRad Laboratories) using bovine serum albumin (BSA) as standard to build a reference curve. Absorbance at 595 nm was measured using Wallac VICTOR^3 1420 Multilabel Counter (Perkin Elmer). 15-20 μg of proteins/sample or 0,5-1 x10^6 cells/sample in Laemmli loading buffer (62.5 mM Tris-HCl, pH 6.8; 2 % SDS; 0.001 % Bromophenol Blue and 10 % glycerol) together with 10 μl of NOVEX Sharp Pre-Stained protein standard (Life Technologies) were run onto 4-12 % polyacrylamide gradient gels or onto 10% polyacrylamide gels (Life Technologies). Gels were run in an XCell Surelock™ Mini-cell apparatus (Life Technologies) in NuPAGE 1 X MOPS or in 1 X MES SDS running buffers (Life Technologies) and transferred to nytrocellulose membranes (iBLOT gel transfer stack, Life Tecnologies) with the iBLOT dry blotting system (Life Tecnologies) for 6'30". After transfer, nitrocellulose membranes were stained with Ponceau S staining solution (0.1 % Ponceau S and 5 % acetic acid) to verify equal loading and appropriate transfer. Membranes were briefly washed in 1 X TBS-T (20 mM Tris-HCl, pH 7.4, 500 mM NaCl, 0.1 % Tween) and blocked for 1 hour at RT in blocking solution (5 % BSA or 5 % nonfat dry milk in 1 X TBS-T). Membranes were incubated with primary antibodies (listed in Table 7), diluted in blocking solution overnight at 4 °C. After 5 washes of 5 minutes each in 1X TBS-T, membranes were incubated with appropriate horseradish peroxidase (HRP)-conjugated secondary antibodies (see Table 7), diluted in blocking solution for 1.5 hours at RT. Membranes were washed 5 times for 5 minutes each in 1 X TBS-T and bound secondary antibody revealed with the SuperSignal™ West Pico Chemiluminescent Substrate (ThermoFisher Scientific). Membrane stripping was performed with Restore™ PLUS western blot stripping buffer (ThermoFisher Scientific). Immunoblotting images were acquired using the ChemiDoc system

(Bio-Rad). Protein quantification was performed using the ImageLab software tool.

Table 7. **Antibodies used for immunoblotting analysis**

Primary Antibodies	Company	Dilution
Rabbit anti- mouse UTX	Home-made	1/1000 (milk)
Rabbit anti- mouse H3K27me3 (C36B11)	Cell signalling	1/10000 (BSA)
Rabbit anti- mouse H3 total (ab1791)	Abcam	1/1000 (milk)
Rabbit anti- mouse H3K4me3 (ab8580)	Abcam	1/3000 (milk)
Rabbit anti- mouse H3K4me1 (ab8895)	Abcam	1/500 (milk)
Rat anti-mouse IRF4 (3E4)	Biolegend	1/50 (milk)
Secondary Antibodies	**Company**	**Dilution**
Goat anti-mouse Ig (7076S)	Cell signalling	1/2000
Goat anti-rabbit Ig (7074S)	Cell signalling	1/2000
Goat anti-rat Ig (7076S)	Cell signalling	1/2000

2.4.2. Enzyme-Linked Immunosorbent Assay (ELISA)

ELISA methods are immunoassay techniques that combine the specificity of immunological reaction with the sensitivity of enzyme assays and allow quantification of immunoglobulins or antigens. Coating of individual wells of flat bottom 384-well ELISA microplates (LUMITRAC high binding, Greiner Bio-one, Cat. no. 781074) was performed with 50 µl of capture antibody (listed in Table 8) or antigen (listed in Table 9), diluted in coating buffer (0.5 M Carbonate-bicarbonate buffer pH 9.6) O/N at 4°C. Coating solution was removed and plates washed 3 times/each with 450 µl of washing buffer (0.05 % Tween 20 in 1XPBS). Wells were blocked in blocking buffer (3 % BSA in 1XPBS) for 1 h at 37°C. 50 µl of mouse reference serum or reference antibody were diluted in Reagent Diluent (1 % BSA in PBS), added to the plate in each well and incubated for 1 hour at RT. The plate was washed 4 times with 450 µl of washing buffer. 50 µl of the detection antibody (Table 8 and Table 9) was added to each well and the plate was incubated for 1 hour at RT. The plate was washed again 5 times with 450 µl of washing buffer. 50 µl of Europium (Eu^{3+})-coupled streptavidin (Perkin Elmer, 1/10000 dilution in reagent diluent) was added in each well and the plate was incubated for 30 min at RT in the dark. Subsequently, the plate was washed 6 times with 450 µl of washing buffer. 50 µl of DELFIA enhancement solution (4001-0010 Perkin Elmer) was added to each well and plate incubated for 15 min at RT on a shaker (50- 100 rpm). Absorbance measurement was performed using the EnVision 2014 Multilabeled Plate Reader and Wallac EnVision Manager 1.12 Software (Perkin Elmer™).

Table 8. ELISA reagents for total antibody titers detection of resting mice.

capture antibodies	clone	Cat. No.	company	working conc.
Monoclonal rat anti-mouse IgM	LO-MM-3	MCA1293	AbD Serotec	2 µg/ml
Polyclonal goat anti-Mouse IgM	N/A	A90-201A	Bethyl	1 µg/ml
Monoclonal rat anti-mouse IgG1	LO-MG-13	MCA1289	AbD Serotec	1 µg/ml
Polyclonal goat anti-mouse IgG3	LO-MG3-13	A90-111A	Bethyl	1 µg/ml
Monoclonal goat anti-mouse Ig2a	LO-MG2a-9	MCA1588	AbD Serotec	0,5 µg/ml
Monoclonal goat anti-mouse Ig2b	LO-MG2b-1	MCA1589	BioRad	1 µg/ml
Polyclonal goat anti-mouse IgA	N/A	A90-130-A	Bethyl	1 µg/ml
standards				
mouse reference serum	N/A	RS10-101	Bethyl Laboratories	IgM 100 ng/ml
mouse reference serum	N/A	RS10-101	Bethyl Laboratories	IgM 10 ng/ml
mouse reference serum	N/A	RS10-101	Bethyl Laboratories	IgG1 10 ng/ml
mouse reference serum	N/A	RS10-101	Bethyl Laboratories	IgG3 1400 ng/ml
mouse reference serum	N/A	RS10-101	Bethyl Laboratories	IgG2a 100 ng/ml
mouse reference serum	N/A	RS10-101	Bethyl Laboratories	IgG2b 520 ng/ml
mouse reference serum	N/A	RS10-101	Bethyl Laboratories	IgA 220 ng/ml
Monoclonal mouse IgG2c	6.3	0122-01	Southern Biotech	100 ng/ml
Detection antibodies				
Monoclonal rat anti-mouse IgM (biotin)	R33.24.12	N/A	home made	125 ng/ml
Monoclonal rat anti-mouse IgG1 (biotin)	A85-1	550331	BD Pharmingen	250 ng/ml
Monoclonal rat anti-mouse IgG3 (biotin)	R40.81	553401	BD Pharmingen	1000 ng/ml
Monoclonal rat anti-mouse IgG2a (biotin)	LO-MG2a-7	MCA421	AbD Serotec	500 ng/ml
Monoclonal rat anti-mouse kappa chain (biotin)	R331.18	N/A	home made	500 ng/ml
Monoclonal goat anti-mouse IgA (biotin) pAb	N/A	A90-103B	Bethyl Laboratories	250 ng/ml

Table 9. ELISA reagents for antigen specific antibody titers detection of immunized mice.

antigens	cat#/clone	company	working conc.
NP (4)-BSA	N505010	Biosearch Technologies	2 μg/ml
NP (23)-BSA	N505010	Biosearch Technologies	2 μg/ml
BSA	N/A	N/A	2 μg/ml
standards			
Monoclonal rat anti-mouse NP specific IgM	B1-8	Homemade	10 ng/ml
Monoclonal rat anti-mouse low affinity NP-specific Ig	N1G9	Home made	100 ng/ml
Detection antibodies			
Polyclonal goat anti-mouse IgM (biotin)	A90-201B	Bethyl Laboratories	50 ng/ml
Monoclonal rat anti-mouse IgG1 (biotin)	A85-1	BD Pharmingen	125ng/ml

2.4.3. Chromatin immunoprecipitation

2.4.3.1. Cell fixation

Chromatin Immunoprecipitation (ChIP) was performed on pools of MACS-purified $CD19^+$ resting B cells and FACS-sorted $CD19^+CD95^{hi}CD38^{lo}$ germinal center B cells isolated from the spleen of $Utx^{+/+}$; $Mb\text{-}1^{cre/+}$ control and $Utx^{fl/fl}$; $Mb\text{-}1^{cre/+}$ mutant mice (129/SV X C57BL/6) 8 days after SRBC immunization. Sorted cells were washed twice with cold 1 X PBS and fixed (10^6 cells/ml for a total of 10^7 cells/sample) with freshly prepared 1 % formaldehyde in 1 X PBS for 10 minutes at RT, on rotation. Fixation was stopped by adding glycine to a final concentration of 0.125 M for 5 minutes at RT, on rotation. Cells were centrifuged at 1200 rpm at 4 °C for 10 minutes, washed with cold 1 X PBS and transferred to 1,5 ml tubes. After centrifugation at 4 °C, 6000 rpm for 5 minutes, cells were resuspended in SDS buffer (0,5 % SDS; 50 mM Tris HCl pH 8,1; 100 mM NaCl; 5 mM EDTA pH 8; 0,02 % NaN_3), (1 ml/ 10^7 cells), 1 mM PMSF (Sigma Aldrich) and protease inhibitor cocktail Set III (EDTA-free, Calbiochem,). Fixed cells were stored for least one O/N at -80°C.

2.4.3.2. Sonication

Frozen fixed cells were gradually defrosted in a water bath, centrifuged at 15°C, at 1500 g for 10 minutes and resuspended (260 μl/10^7 cells) in sonication buffer (1% SDS, 50 mM Tris HCl, 10 mM EDTA) containing 1 mM PMSF and 0.1% (vol/vol) protease inhibitor cocktail Set III (EDTA-free, Calbiochem,). Cells were transferred to 500 μl Diagenode tubes and sonicated first with Bioruptor™ (Diagenode), for 5 cycles, 30 seconds each (high power). Subsequently, up to 130 μL of the sonicated material was transferred to microTUBEs (Covaris) for a second

step of sonication performed in the S220 focused-ultrasonicator (Covaris). To obtain 200 bp fragments, the instrument parameters were set to a duty factor of 10 %, peak incidence power (W) of 175 and 100 cycles per burst according to manufacturer's guidelines. Each sonication round was performed for 6 minutes. Sonicated material was centrifuged at maximum speed (16100 g), at 4°C for 10 minutes and transferred to a new 1.5 ml tube to remove cellular debris. An aliquot (10 μl) of the sonicated chromatin was de-crosslinked to act as sonication control Up to 150 μL of a final solution of 1 % SDS, 0,1 M NaHCO3 300 mM NaCl, water and Proteinase K (0,5 μg/μl) was added to the aliquot of sonicated material and incubated overnight at 65 °C. The following day, 100 μl of water, 25 μl Na-Acetate 3 M pH 5,2 and 500 μl of 100% EtOH were added to the sonicated sample, followed by incubation for 1h at -80 °C. Chromatin was centrifuged at 13000 rpm, at 4°C for 20 minutes, washed with 75% EtOH and centrifuged at 13000 rpm, at 4°C for 10 minutes. DNA was resuspended in 30 μL of TE buffer (Tris HCl pH 8,1 10 mM; EDTA pH 8 5 mM) and quantified using Qubit double strand (ds) DNA high sensitivity (HS) assay (range: 0,2-100 ng) (ThermoFisher Scientific) with Qubit 2.0 Fluorometric quantitation (Life Technologies). Quality of DNA shearing was controlled using a high sensitivity DNA assay (concentration range: 100-10000 pg/ ml) (ThermoFisher Scientific) on a Bioanalyzer 2100 (Agilent Technologies).

2.4.3.3. Immunoprecipitation

Chromatin extracted from $CD19^+$ B cells was quantified using the Biorad DC™ protein assay or Nanodrop quantification of DNA, according to guidelines of DC protein assay instruction manual. BSA dissolved in IP buffer was used as standard protein reference, starting from a BSA concentration of 2 μg/μL, performing seven sequential two-fold dilutions. Fourty μg of chromatin was used for each immunoprecipitation assay and the final reaction volume was adjusted to 1 ml with IP buffer (Triton X-100 0.5%; Tris-HCl pH 8.1 50 Mm; NaCl 150 mM; EDTA pH 8 1 mM and water). An aliquot of chromatin (1 %) before immunoprecipitation (Input) was used as baseline for downstream analyses. Between 2,5- and 8 μg of primary antibodies (listed in Table 10) were used for each immunoprecipitation assay in an overnight reaction performed at 4 °C, on rotation. Next, 20 μl of superparamagnetic Protein G Dynabeads™ for each sample (Life Technologies) were equilibrated with 1ml of IP buffer, transferred to tubes containing the immunoprecipitation reaction and incubated for 4 hours at 4 °C on rotation. Subsequently, tubes containing immunoprecipitated material bound to beads were exposed to a magnetic field fitting them to an ice-cold magnet (Life Technologies) to wash off unbound chromatin and excess antibody. Beads washes included 3 steps with 1 ml ice-cold

150 mM Wash Buffer (1 % Triton-X 100; 150 mM NaCl; 50 mM Tris-HCl pH 8; 5 mM EDTA pH 8, water) and a final elution step with 1 ml of 1 X TE buffer.

2.4.3.4. Chromatin de-crosslinking

Up to 250 μL of a final solution of 1 % SDS, 0.1 M NaHCO3, 50 mM Tris HCl pH 8.1, 150 mM NaCl and water was added to the mixture of beads bound to antibodies and chromatin and to the input samples, and incubated for 5 minutes at 95 °C. Samples were fitted onto the magnet at RT to remove the beads. This step was repeated twice. Proteinase K (0,5 mg/ml) was added and samples incubated O/N at 65° C. The following day, DNA was precipitated adding to each sample 100 μl of water, 25 μl of 3 M Na-Acetate pH 5.2 and 500 μl 100% EtOH, followed by incubation for 1h at -80°. DNA was centrifuged at 13000 rpm 4° for 20 minutes, washed with 75% EtOH and centrifuged again 13000 rpm 4° for 10 minutes. DNA was resuspended in 30 μL of 1 X TE buffer and subjected to Qubit Fluorometric quantitation (ThermoFisher Scientific). 2-10 ng of input and immunoprecipitated material were employed for next generation sequencing.

Table 10. Antibodies used for ChIP experiments.

Primary Antibodies	Company	μg/ChIP
Monoclonal rabbit anti- H3K27me3 (C36B11)	Cell signalling	2,5-8 μg
Polyclonal rabbit anti- H3K27ac (ab4729)	Abcam	2,5- 5 μg
Polyclonal rabbit anti- H3K4me3 (ab8580)	Abcam	2,5- 5 μg
Polyclonal rabbit anti- H3K4me1 (ab8895)	Abcam	2,5- 5 μg

2.5. Molecular biology techniques

2.5.1. RNA and DNA extraction

Simultaneous purification of total RNA and genomic DNA was performed on purified B cells and sorted B cell subsets using the All Prep DNA/RNA mini kit (Qiagen) following the manufacturer's protocol. Purified DNA and RNA were quantified by a microvolume UV spectrophotometer (NanoDrop ND-100).

2.5.2. First strand cDNA synthesis

Total RNA was extracted from 0,3 - 3 x 10^6 B cells using the RNeasy mini kit (Qiagen), following the manufacturer's instructions. Possible DNA contamination was removed through a DNAse (Qiagen) digestion step, before RNA elution in 30 μl of RNase-free water. Total RNA was quantified by a microvolume UV spectrophotometer (NanoDrop ND-100). Complementary DNA (cDNA) was obtained by reverse transcription (RT) of total RNA (100 to 500 ng), using random primers (50 to 250 ng; Life Technologies), following the manufacturer's instructions. After an initial denaturation in the presence of random primers at 65°C for 5 minutes, RNA samples were transcribed in 1 X First Strand buffer (50 mM Tris-HCl (pH 8.3), 375 mM KCl, 3 mM $MgCl_2$,) 5 mM Dithiothreitol (DTT), 0.5 mM dNTPs, 40 units of RNase OUT and 200 units of Super Script II (Life Technologies) for 2 minutes at 25 °C followed by 50 minutes at 50 °C. A the end of this reaction, heat inactivation of the reverse transcriptase was achieved incubating samples for 15 minutes at 72 °C.

2.5.3. qPCR and qRT-PCR analysis

The efficiency of Cre-mediated recombination at the *Utx* locus was assessed by quantitative PCR (qPCR) using primers listed in Table 11, monitoring the remaining fraction of the intact allele. For gene expression analysis, Reverse Transcription quantitative PCR (RT-qPCR) was performed, as described below. 5 μl of primers mix (0,85 μM final concentration) and 10 μl of LightCycler® 480 SYBR Green I Master mix containing Hot-start polymerase (Roche), or of Takara Bio SYBR Premix Ex Taq II (Tli RNase H Plus) (Takara Bio) were added to DNA (5-15 ng) or first-strand cDNA in a final volume of 20 μl per reaction in 96-well plates (Roche). PCR conditions consisted of an initial denaturation step at 95 °C for 10 minutes, followed by 45 cycles of 95 °C for 10 seconds, 60 °C for 10 seconds and 72 °C for 10 seconds, followed by a final Taq polymerase elongation step of 10 minutes. Accumulation of fluorescent products was monitored using either the LightCycler® 480 version 1.5 or the LightCycler® 96 software, provided along with the LightCycler® 480 and LightCycler® 96 Real-Time PCR Systems

(Roche), respectively. Specificity of the PCR reactions was controlled through the assessment of the melting temperature profiles of the final PCR products (dissociation curve). Assessment of the *Utx* gene copy number was performed amplifying the gene with primers (listed in Table 11). annealing to exon-3 flanked by loxP sites. To normalize for DNA input, a segment of the *Gapdh* gene was amplified (Table 11).

Table 11. Primers list for qPCR and qRT-PCR.

Primers	Sequence	Target
Gapdh4d Fw	5'-AGCGCTGACCTTGAGGTCTCCTTG-3'	DNA
Gapdh4d Rv	5'-GTTGCCTACGCAGGTCTTGCTGAC-3'	DNA
Utx_exon 3_Fw	5'- CCTAGGCTGTTCGCTGCTAC-C3'	DNA
Utx_exon 3_Rv	5'- TGTACTGGCCCACAAAAATCT-C3'	DNA
Rplpo Fw	5'-TTCATTGTGGGAGCAGAC-3'	RNA
Rplpo RV	5'-CAGCAGTTTCTCCAGAGC-3'	RNA
Irf4 Fw	5'-CAATGTCCTGTGACGTTTGG-3'	RNA
Irf4 Rv	5'-GGCTTCAGCAGACCTTATGCT-3'	RNA
S1pr1 Fw	5'-CCTCTCGGACCTATTAGCAGGC-3'	RNA
S1pr1 Rv	5'-CGCAGAAACCACTGGGCAG-3'	RNA
Iγ1- Cγ1 Fw	5′-GGCCCTTCCAGATCTTTGAG-3′	RNA
Iγ1- Cγ1 Rv	5′-ATGGAGTTAGTTTGGGCAGCA-3′	RNA
Iγ3- Cγ3 Fw	5'-AACTACTGCTACCACCACCACCAG-3'	RNA
Iγ3- Cγ3 Rv	5'-ACCAAGGGATAGACAGATGGGG-3'	RNA
Iγ2b- Cγ2b Fw	5'-GATGGGGAGGAGTTGGCAGAT-3'	RNA
Iγ2b- Cγ2b Rv	5'-CGGAGGAACCAGTTGTATC-3'	RNA
Iε- Cε Fw	5'-ACTAGAGATTCACAACG-3'	RNA
Iε- Cε Rv	5'-ACTAGAGATTCACAACG-3'	RNA
Utx Fw	5'-GGCATGAACACAGTTCAACTATACA-3'	RNA
Utx Rv	5'-CAGAAGTTGTTATTTTCTTGATGACC-3'	RNA
Aicda Fw	5'-AGGACGAGTGACCTGAAGC-3'	RNA
Aicda Rv	5'-GCGTAGGAACAACAATTCCAC-3'	RNA

cDNA input was controlled amplifying by PCR a fragment of the housekeeping gene *Rplp0* with primers listed in Table 11 (Laborda 1991). Transcript fold-enrichment was calculated applying the ΔΔct method (Livak and Schmittgen 2001).

2.5.4. Immunoglobulin somatic mutation analysis

$CD19^{+}CD95^{hi}CD38^{lo}$ germinal center B cells from NP_{28}-CGG immunized *Mb-1*$^{cre/+}$ control and *Utx*$^{fl/fl}$*; Mb-1*$^{cre/+}$ mutant animals were purified by FACS-assisted cell sorting using a FACS Aria cell sorter (Becton Dickinson), as described in section 2.3.1.

2.5.4.1. Semi-nested PCR amplification

DNA extracted from the sorted B cells was subjected to a semi-nested PCR approach to amplify the V_H186.2 gene, as previously described (Jacob, Kelsoe et al. 1991). For the first round of PCR amplification, reagents listed in Table 12 and Primers VH186.2 Fw External and JH2 Rv were used (Table 12). PCR conditions are summarized in Table 13. For the second round of PCR amplification, reagents listed in Table 12 and primers VH186.2 Internal Fw and JH2 Rv were used (Table 12). PCR reactions were incubated for 30 min at -20°C to inactivate Taq polymerase. Subsequently, polyA tailing of PCR products was performed using reagents and conditions summarized in Table 14. Finally, PCR products were gel-purified (QIAquick Gel Extraction Kit (Qiagen), eluted in 30 µl of milliQ water, and cloned into the TOPO-TA vector as described below (Thermo Fisher Scientific).

Table 12. Reagents for V_H186.2 semi-nested PCR amplification

PCR master mix	**1st round**	**2nd round**
Reagents	µl	µl
H_20	34.7	34.7
10X Pfu buffer	5	5
dNTPs 10 mM	1	1
Primers VH186.2 Fw (50 µM): **External:** 5′-TCTTTACAGTTACTGAGCACACAGGAC-3′ **Internal:** 5′-CAGTAGCAGGCTTGAGGTCTGGAC-3′	 1 (External) -	 - 1 (Internal)
Primer JH2 Rv (50 µM): 5′-GGGTCTAGAGGTGTCCCTAGTCCTTCATGACC-3′	1	1
Pfu polymerase	1	1
DNA (5000 cells)	4.3-13.4	5 µl of first round PCR reaction
total	50	50

Table 13. PCR conditions to amplify V_H186.2 gene

Temperature (°C)	Time (minutes)	1st round	2nd round
95	2:30		
95	0:30	20X	30X
70	0:30		
72	1:30		
72	5:00		
4	hold		

Table 14. Reagents for polyA overhangs formation.

Tailing reaction	µl
Reagents	
Go Taq Flexi buffer 5X	10
$MgCl_2$ 25mM	4
dNTPs 2.5mM	4
Go Taq Flexi	1
2nd round PCR reaction	31
Temperature	Time (min)
72	30:00

2.5.6.2. Cloning of V_H186.2 gene rearrangements and plasmid DNA extraction

Ten to fifty nanograms of gel-purified PCR fragments were ligated to the TOPO-TA Vector (Thermo Fisher Scientific) using reagents listed in Table 15 and incubated for 10 minutes at RT. JM109 bacteria were thawed on ice. 3 µl of the ligation mixture was transfomed into JM109 competent cells according to the manufacturer's instructions. Briefly, 100 µl of JM109 bacteria were mixed with 3 µl of the ligation reaction for 20 min on ice. Cells were heat-shocked for 30 seconds at 42°C and immediately returned to ice for 2 min. 900 µl of warm SOC medium (0.5% Yeast Extract, 2% Tryptone, 10 mM NaCl, 2.5 mM KCl, 10 mM $MgCl_2$, 10 mM $MgSO_4$, 20 mM Glucose) was added and cells incubated for 60 min at 37°C shaking at 250 rpm. Cells were centrifuged for 1 min at 4000 rpm and 900 µl of supernatant was aspirated. Cell were resuspended in the remaining 100 µl of SOC medium, plated on ampicillin (50 µg/ml)-containing agar plates soaked with solutions of X-gal (20 mg /ml) and IPTG (1 mM) and incubated overnight at 37°C. White colonies (containing cloned PCR fragment disrupting the LacZ gene) were picked and allowed to expand overnight at 37°C in 3 ml of LB medium

containing ampicillin (50 μg /ml) in a shaker. The next morning, cells were centrifuged for 5 min at 4000 rpm and plasmid DNA was extracted following the protocol of Wizard® Plus Minipreps DNA Purification System (Promega). Plasmid DNA was eluted in 30 μl of milliQ water.

2.5.6.3. DNA Sanger sequencing and Immunoglobulin somatic mutation assessment

One microgram of plasmid DNA extracted from independent bacterial colonies was subjected to Sanger sequencing using the M13-21 universal forward primer (TGTAAAACGACGGCCAGT) which anneals in proximity of the multicloning site of the TA-TOPO vector. Unique V_H rearrangements containing the V_H186.2 V gene were identified analysing the CDR3 region with the open access IgBLAST software tool (https://www.ncbi.nlm.nih.gov/igblast/). Number of GC B clones was assessed by counting the numbers of sequences carrying a unique CDR3 region. To measure the mutation frequency, unique mutations scored in V_H186.2-bearing rearrangements (excluding the CDR3 region) were counted and divided over the total number of nucleotides sequenced for the same rearrangements. The frequency of B cells carrying the TGG -to-TTG substitution at codon 33 of the V_H186.2 gene conferring a ten-fold increase in the affinity for NP, was measured dividing the number of unique V_H186.2 rearrangements carrying the high-affinity mutation over the total number of unique V_H186.2 rearrangements.

Table 15. TOPO-TA cloning reaction mix.

TOPO-TA cloning	μl
Reagents	
SALT SOLUTION	1
TOPO-TA vector	1
Gel purified DNA fragment	3 (10-50 ng)
H_2O	1
total	6

2.6. Next-generation sequencing (NGS) applications

2.6.1. ChIP-sequencing

To determine the genome wide distribution of H3K27me3, H3K4me3 and H3K27ac 2 to 10 ng of sonicated DNA, including both immunoprecipitation material and input were used for construction of NGS libraries using the Ion Torrent library preparation kit (KAPA Biosystem) in collaboration with the IFOM Genomic Unit. Quantification of libraries was performed using

the Qubit dsDNA high sensitivity assay kit (ThermoFisher Scientific). Size distribution of ChIP-seq libraries was assessed using the Bioanalyzer 2100 (Agilent Technologies) instrument. NGS reactions were performed on an Ion Proton^{TM} instrument (Ion Torrent, Thermo fisher scientific) with the support of the IFOM Genomic Unit.

2.6.2. RNA-sequencing

To perform transcriptome analysis of follicular and germinal center B cells, total RNA purified from these cells was quantified by a microvolume UV spectrophotometer (NanoDrop ND-100). RNA quality was assessed using the RNA 6000 Nano kit (Agilent Technologies) on a Bioanalyzer 2100 (Agilent Technologies) instrument. 100 ng/sample of total RNA was used for NGS library construction. Briefly, total RNA was processed using the Dynabeads mRNA direct micro kit (ThermoFisher Scientific) to isolate polyadenylated (polyA) mRNA. Purified mRNAs were used to prepare cDNA libraries for strand-specific RNA sequencing which was performed on an Ion Proton^{TM} instrument with the Ion Total RNA Seq kit v2 (ThermoFisher Scientific), with the support of the IFOM Genomic Unit, in Milan.

2.7. Bioinformatic analyses

2.7.1. Bioinformatic analysis of ChIP-sequencing data

A range of $20x10^6$ to $35x10^6$ total reads was obtained from ChIP-sequencing experiments performed on $CD19^+$ B cells and GC B cells purified from *Mb-1*$^{cre/+}$ control and *Utx*$^{fl/fl}$*; Mb-1*$^{cre/+}$ mutant mice. 74 to 96% of total reads for each sample were correctly aligned, -end-to-end, to the mm10 genome using Bowtie 2 version 2.2.9 (Langmead and Salzberg 2012). ChIP-seq provided an average of $30x10^6$ of uniquely mapped reads for each profiled sample (both input and antibody-specific immunoprecipitated samples). To identify genomic regions enriched for H3K27me3, H3K4me3 and H3K27ac (peaks) in immunoprecipitated samples relative to the input samples, we used MACS2 (version 2.1.1) (Zhang, Liu et al. 2008) with default parameters. The MACS2 broad option was added in order to call broad peaks for H3K27me3 histone modification. Peaks were assigned to genes by assessing, for each RefSeq, whether a peak laid within a +/−5 Kb region around the transcription start site (TSS) for H3K27me3 and within a +/−1.5 Kb region around the TSS for H3K4me3 and H3K27ac. Graphs displaying the reads distribution around the TSS were generated starting from the bedGraph files, generated by MACS2, using the computeMatrix and the plotHeatmap tools of deepTools2 version 3.0.1 (Ramírez, Ryan et al. 2016) on the corresponding bigWig files. Venn diagrams showing the overlap among different list of genes were generated with the R/Bioconductor package VennDiagram (Chen and Boutros 2011) (https://CRAN.R-

project.org/package=VennDiagram). ChIP-enrichment analyses and pathways analyses were performed using the EnrichR (Chen, Tan et al. 2013; Kuleshov, Jones et al. 2016) (http://amp.pharm.mssm.edu/Enrichr/) web-based software. Gene lists provided by EnrichR were ranked based on the p-value.

2.7.2. Bioinformatic analysis of RNA-sequencing data

A range of $7x10^6$ to $55x10^6$ total reads was obtained for each FO and GC RNA sample purified from *Mb-1*$^{cre/+}$ control and *Utx*$^{fl/fl}$*; Mb-1*$^{cre/+}$ mutant mice. 60 to 80% of total reads for each sample were correctly aligned to the mouse mm9 transcriptome using TopHat version 2.1.1 (Trapnell, Pachter et al. 2009). Differentially expressed genes (DEGs) were called with DESeq2 (Love, Huber et al. 2014) using the read counts per transcripts calculated by HTSeq (Anders, Pyl et al. 2015). Genes with a False Discovery Rate (FDR) < 0.05 and a fold change > 1.2, 1.5, 1.8, 2, 2.5 and 3 or < -1.2, -1.5, -1.8, -2, -2.5, and -3 were defined as DEGs.

ChIP-enrichment analyses and pathways analyses were performed using the EnrichR software (Chen, Tan et al. 2013; Kuleshov, Jones et al. 2016).

Boxplots were generated with R starting from the read counts generated by HTSeq. Unsupervised hierarchical clustering and heatmaps were made with the R/Bioconductor package pheatmap (Pretty Heatmaps), R package version 1.0.1. (https://CRAN.R-project.org/package=pheatmap).

2.7.2.1. Evaluation of the centroblast vs centrocyte signature

Microarray data of murine centroblasts and centrocytes were retrieved from Gene Expression Omnibus (GSE23925). To identify DEGs between centrobasts and centrocytes, raw data were normalized with the RMA algorithm and DEGs were called using the makeContrasts function of the limma R/Bioconductor package (Ritchie, Phipson et al. 2015). The signature was defined considering genes with p value < 0.05 and fold change > 2 or < -2. The pheatmap library of R was used to perform the unsupervised hierarchical clustering of 3 independent *Utx*$^{+/+}$*: Mb-1*$^{cre/+}$ control and 3 *Utx*$^{fl/fl}$*: Mb-1*$^{cre/+}$ mutant mice and to generate a heatmap according to the level of expression of genes deregulated in centroblasts vs centrocytes.

2.7.2.2. Evaluation of the NF-κB signature

Two lists of genes transcriptionally down-regulated upon KO of specific subunits of both the canonical and the alternative NF-κB pathway in murine B cells from published datasets (De Silva, Silva et al. 2016), GEO GSE77374, (Heise, De Silva et al. 2014), GEO GSE58983, were

merged in order to generate a comprehensive list of NF-κB targets. The unsupervised hierarchical clustering and heatmaps according to the expression of NF-κB target genes was performed as described above.

2.7.2.3. Evaluation of the BCL6 signature

To evaluate whether down-regulated genes identified in the comparison between GC B cells sorted from *Utx*$^{+/+}$*; Mb-1*$^{cre/+}$ control and *Utx*$^{fl/fl}$*; Mb-1*$^{cre/+}$ mutant mice were enriched for BCL6 target genes, BCL6 targets identified in human GC B cells were retrieved from a published dataset (Basso, Saito et al. 2010). The mouse orthologs of the human BCL6 target genes with ChIP FDR < 0.01 (n=6164) were intersected with the list of genes down-regulated in UTX KO GC B cells when compared to the wild type GC B cells. A Chi-square with Yates correction was applied to evaluate the enrichment for BCL6 targets among the downregulated genes.

2.8. Statistical analyses

2.8.1. Student's T test

Statistical analysis of normally distributed values (Gaussian) was performed by two- tailed unpaired Student's t-test. Differences were considered significant at p-value<0.05.

2.8.2. Mann-Whitney test

The Mann-Whitney unpaired test was used as an alternative to the t-test when the population data does not follow a normal distribution. Differences were considered significant at p-value<0.05.

2.8.3. 2 Way-Anova test

Statistical analysis to compare two independent variables in grouped samples was performed using 2-way ANOVA test. Differences were considered significant at p- value<0.05.

3. Results

3.1. The *Utx* gene is expressed throughout B cell development

To establish the pattern of *Utx* gene expression throughout B cell lymphopoiesis (Figure 10), bone marrow pro-B and pre-B cells, as well as splenic mature B cells representing respectively follicular/B-2 (FO) and marginal zone (MZ) B cells were purified by cell sorting from wildtype C57/BL6 mice and subjected to quantitative RT-PCR (qRT-PCR) analysis. The analysis included also germinal center (GC) B cells isolated from the spleen of C57BL/6 mice immunized 8 days earlier with sheep red blood cells (SRBCs), as well as short-lived plasma blasts (PBs) and terminally differentiated plasma cells (PCs) retrieved from the spleen of SRBC-immunized mice. The list of markers employed for the purification of the B cell subsets is provided in the materials and methods section 2.3.1 (Table 5).

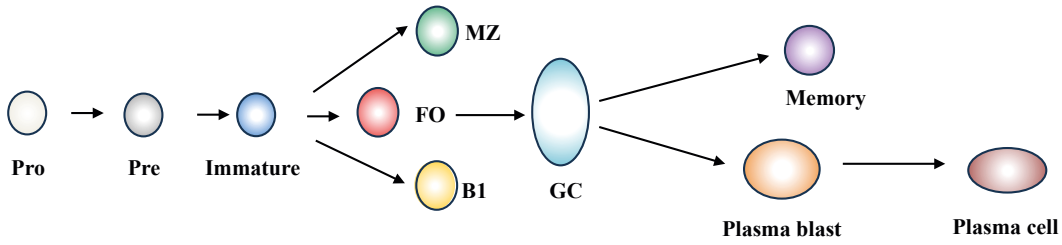


Figure 10 . Schematic view of B cell development

Utx transcripts were detected throughout B cell development, with higher levels measured in progenitors (Figure 11) when compared to their mature B cell counterparts. Among mature B cells, *Utx* was expressed at higher levels in FO B cells when compared to MZ B cells and to B lymphocytes recruited into the GC reaction. Upon induction of terminal differentiation, *Utx* mRNA levels increased transiently in short-lived plasma blasts (PBs), dropping again in cell-cycle arrested, terminally differentiated, PCs (Figure 11). These results are compatible with a role of UTX at multiple stages of B cell differentiation and activation.

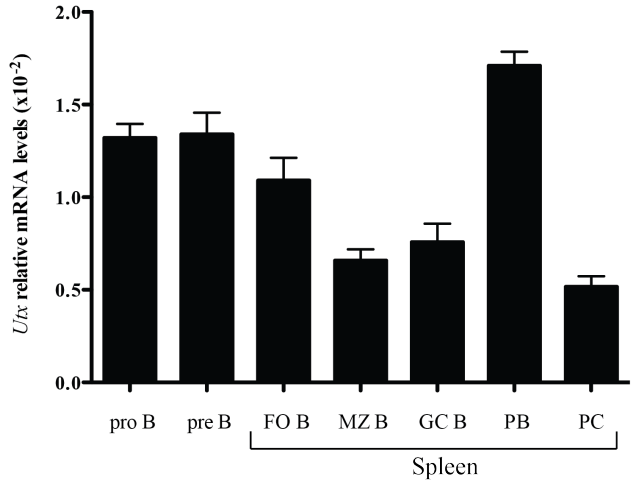


Figure 11. *Utx* is expressed throughout B cell development.

Quantitative RT-PCR analysis of *Utx* transcript in the indicated B cell subsets sorted from C57BL/6J wild-type mice. mRNA levels are relative to those of the housekeeping gene *Ribosomal protein large p0* (*Rplp0)*. pro B= pro-B cells; pre-B= pre-B cells; FO B= follicular B cells; MZ B= marginal zone B cells; GC B= germinal center B cells; PB= plasma blasts; PC= plasma cells.

3.2. Conditional targeting of the *Utx* gene in B-lineage cells

To specifically address the role of UTX in B cell development, we took advantage of *Utx* conditional knockout mice (Mansour, Gafni et al. 2012) obtained from the laboratory of Dr. J. Hanna (Weizmann Institute, Israel). These mice were generated by targeted disruption of the X-linked *Utx* locus via homologous recombination in mouse embryonic stem (ES) cells. The targeting strategy (Figure 12) was based on the introduction of two *loxP* sites flanking exon 3 of the *Utx* gene (Testa, Schaft et al. 2004). The same locus carried also an *frt*-flanked β−galactosidase reporter gene, preceded by a splicing acceptor site, to monitor *Utx* transcriptional activity.

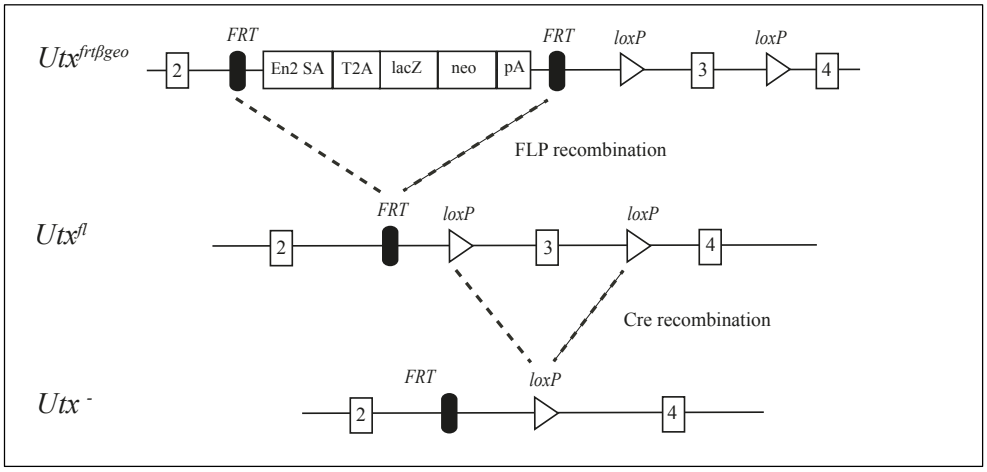


Figure 12. Structure of the *Utx*^{frtbgeo} conditional allele before and after FLP- and Cre-mediated recombination

The *Utx*^{frbgeo} conditional allele consists of an frt-flanked promoterless cassette carrying a splice acceptor (SA), a self-cleaving 2A peptide, the LacZ reporter gene, a neomycin resistance and a polyadenylation (pA) site inserted into the second intron of the *Utx* allele. Downstream of the gene trap, two loxP sites flank exon 3. Generation of a conditional *Utx*$^{fl/+}$ allele was obtained after removal of the trapping cassette via FLP mediated recombination; the *Utx*-KO allele was obtained after Cre- mediated recombination.

The resulting *Utx*$^{frtbgeo/+}$ mouse strain was bred to the FLPe-deleter strain (Rodriguez, Buchholz et al. 2000) to delete through the germline the *frt*-flanked βgeo cassette and hence generate *Utx*$^{fl/+}$ conditional mice (Figure 11). *FLPe*-mediated recombination leading to the successful removal of the reporter cassette was confirmed by PCR using genomic DNA extracted from the tail of F1 mice born from the cross between *Utx*$^{frtbgeo/+}$ and *FLPe* mice (data not shown).
Given the ubiquitous expression of *Utx* throughout B cell lymphopoiesis, we decided to inactivate its function starting from progenitor B cells. To this aim, *Utx*$^{fl/+}$ conditional mice were crossed to *Mb-1*$^{cre/+}$ knock-in animals (Hobeika, Thiemann et al. 2006) (Figure 13).

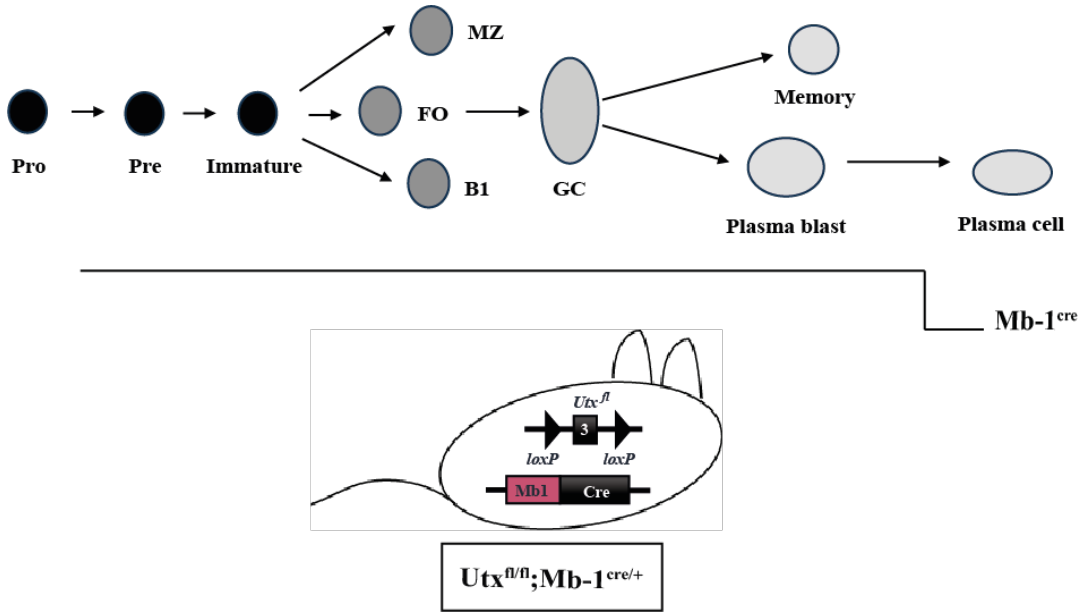


Figure 13. B cell-specific Utx inactivation *in vivo*

Onset of Cre-mediated recombination exerted by the Mb1-cre transgene in *Utx*$^{fl/fl}$; *Mb-1*$^{Cre/+}$ compound mutants

In *Mb-1*$^{cre/+}$ mice, the Cre transgene is under the control of the *Cd79a* (Mb-1/Igα) regulatory regions, leading to its expression starting from the pro-B cell stage. Cre-mediated deletion of *Utx* exon 3 leads to an out-of-frame mutation resulting in the loss the UTX protein expression. To test the efficiency of B-cell specific *Utx* deletion, CD19^{+} B cells were purified from the spleen of *Utx*$^{fl/fl}$; *Mb-1*$^{cre/+}$ experimental animals and from *Mb-1*$^{cre/+}$ controls. Protein extracts from the sorted populations were subjected to immunoblotting analysis to measure UTX protein

levels. To this aim, we produced a polyclonal rabbit anti-mouse UTX-specific antibody (Petrocelli and Casola, data not shown). Whereas control B cells expressed the UTX protein at measurable levels, they were below the limit of detection in the corresponding cells isolated from *Utx* conditional mutant mice. This result establishes extinction of *Utx* expression in splenic mature B cells of $Utx^{fl/fl}$; $Mb\text{-}1^{cre/+}$ compound mutant mice (Figure 14).

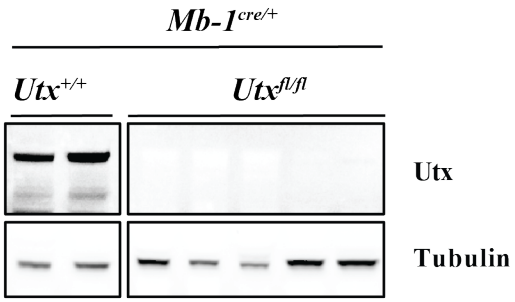


Figure 14. Lack of UTX protein in splenic $Utx^{fl/fl}$; $Mb\text{-}1^{+/cre}$ B cells
Immunoblotting assessment of UTX protein levels in purified $CD19^+$ splenic B cells of representative $Mb\text{-}1^{cre/+}$ control ($Utx^{+/+}$; *n=2*) and $Utx^{fl/fl}$; $Mb\text{-}1^{cre/+}$ ($Utx^{fl/fl}$; *n= 5*) mutant mice. Tubulin detection was included to control for protein input. Data are representative of 7 independent experiments.

3.2.1. UTY functional redundancy and genetic background of UTX conditional mutant mice

A number of recent studies have postulated partial functional redundancy between UTX and its Y-chromosome encoded paralogue UTY (Lee, Lee et al. 2012; Shpargel, Sengoku et al. 2012; Wang, Lee et al. 2012; Welstead, Creyghton et al. 2012; Thieme, Gyarfas et al. 2013). To exclude possible compensatory effects exerted by UTY under conditions of *Utx* deficiency, I have restricted the study of $Utx^{fl/fl}$; $Mb\text{-}1^{cre/+}$ compound mutants to females homozygous for the Utx^{fl} allele in most of the experiments.

Moreover, during the first stages of my studies, I focused my attention on the analysis of $Utx^{fl/fl}$ mice on a 129/SV x C57BL/6 mixed genetic background. Since the genetic background can influence the penetrance of a given genetic mutation (especially when disrupting an epigenetic determinant as UTX), I also backcrossed for twelve generations $Utx^{fl/+}$ mice to C57BL/6J mice to obtain the mutant strain on a close-to-pure C57BL/6J genetic background. Therefore, the initial observations made on $Utx^{fl/fl}$; $Mb\text{-}1^{cre/+}$ compound mutants on a mixed genetic background have been subsequently validated for at least the most relevant experiments on the corresponding strain on the pure C57BL/6J genetic background.

3.3. Consequences of *Utx* inactivation on B cell development

3.3.1. Effects of *Utx* deficiency on early B cell lymphopoiesis

3.3.1.1. *Utx* deficiency alters the fraction and numbers of bone marrow B cell subsets

To address the role of UTX in early B cell lymphopoiesis, we analyzed by flow cytometry B cells present in the bone marrow of *Mb-1*$^{cre/+}$ controls and *Utx*$^{fl/fl}$*; Mb-1*$^{cre/+}$ compound mutants. Both the fraction and absolute numbers of B220^{+} B cells were comparable between *Utx*$^{fl/fl}$*; Mb-1*$^{cre/+}$ mutant *(Utx*$^{-/-}$*)* and *Utx*$^{+/+}$*; Mb-1*$^{cre/+}$ control *(Utx*$^{+/+}$*)* mice (Figure 15).

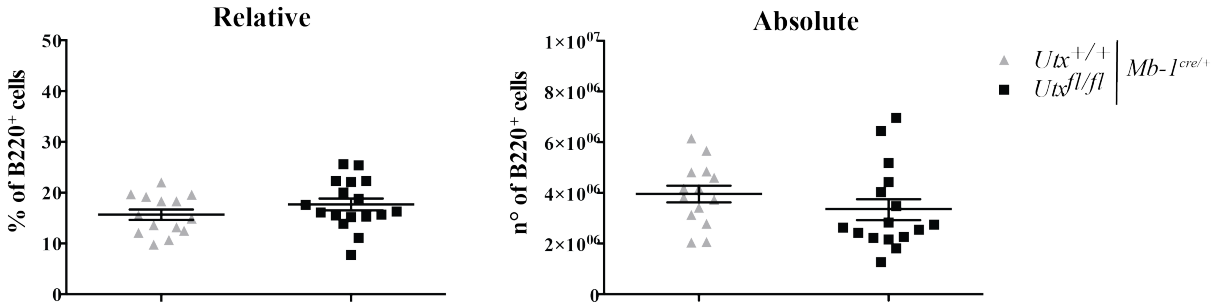


Figure 15. Frequency and absolute numbers of B220^{+} B cells in the bone marrow are largely unaffected in B-cell specific *Utx* mutant mice

Percentage (left) and absolute numbers (right) of B220^{+} B cells in the bone marrow of *Utx*$^{+/+}$ control (n=14), and *Utx*$^{fl/fl}$ mutant (n=16) mice, assessed by flow cytometric analysis. Each dot corresponds to a mouse. Lines represent the mean value ± SEM.

Flow cytometric analysis revealed that in *Utx* conditional mutant mice the transition of B cells from the B220^{lo}IgM^{-} progenitor stage (Hardy Fraction A-to-D) to the B220^{lo}IgM^{+} immature (Hardy Fraction E) and B220^{+}IgM^{+} (Hardy Fraction F) mature B cell stages respectively, was unperturbed (Figure 16) (Hardy, Carmack et al. 1991).

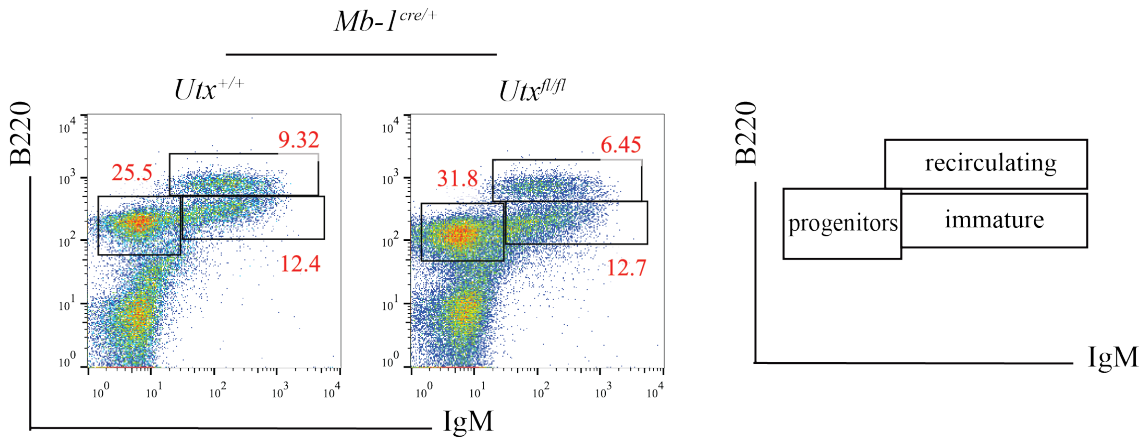


Figure 16. Effects of *Utx* inaction on bone marrow B cell subset distribution

Flow cytometric analysis of *Utx* control (left) and mutant (right) BM cell suspensions. Numbers within boxes indicate frequencies of the corresponding B cell subsets, classified as indicated on the right scheme. Data are representative of 10 independent experiments.

To measure the onset and the efficiency of Cre-mediated recombination, different B cell subsets were sorted from the bone marrow *of* $Utx^{fl/fl}$*;* $Mb\text{-}1^{cre/+}$ compound mutants and from $Mb\text{-}1^{cre/+}$ controls and subjected to quantitative genomic PCR to assess the status of *Utx* exon 3. After normalization for genomic DNA input, I found that around 70% of *Utx* alleles had undergone Cre-mediated recombination in pro-B cells. Cre-mediated recombination improved throughout lymphopoiesis with mature recirculating B cells reaching an efficiency of over 90% (Figure 17). This result establishes that in $Utx^{fl/fl}$*;* $Mb\text{-}1^{cre/+}$ mice, *Utx* gene inactivation starts in pro-B cells and reaches close-to completion by the stage of mature B cells. The results are in accordance with the observation that splenic B cells from compound mutants lack *Utx* protein, hence, excluding the existence of Cre-escape variants among the pool of peripheral B cells.

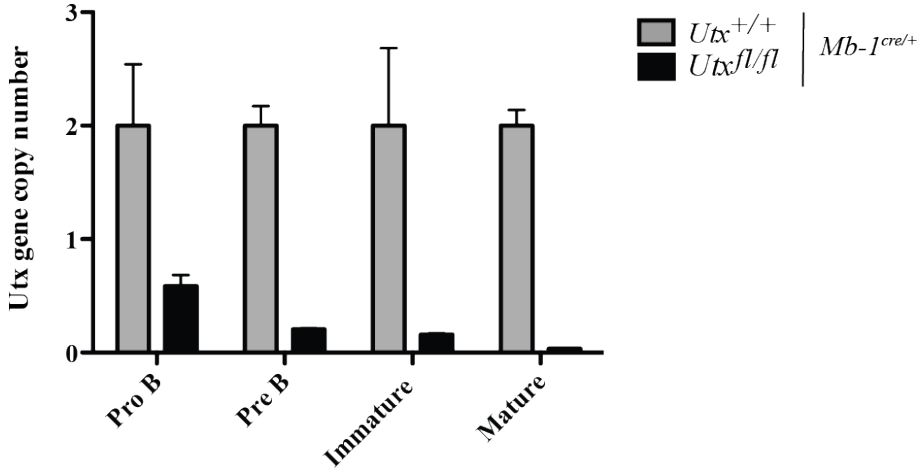


Figure 17. Status of the *Utx* wild-type allele in bone marrow B cell subsets of *Utx* control and mutant mice

Genomic qPCR analysis to determine the copy number of the intact *Utx* allele in the indicated BM B cell subsets purified from *Utx* control ($Utx^{+/+}$) and conditional mutant ($Utx^{fl/fl}$) mice. *Utx* copy number is normalized to that of the unrelated *Gapdh* gene and to that measured in the corresponding subset in *Utx* control animals. Error bars represent SD of triplicates.

To determine whether specific B cell subsets were affected by the inactivation of *Utx*, we performed flow cytometric analyses on BM single cell suspensions. Despite a certain degree of variability seen among animals belonging to the same experimental group, both the frequency and absolute numbers of $B220^{lo}$ IgM^- progenitor B cells were slightly but significantly increased in $Utx^{-/-}$ mutant mice when compared to controls (Figure 18).

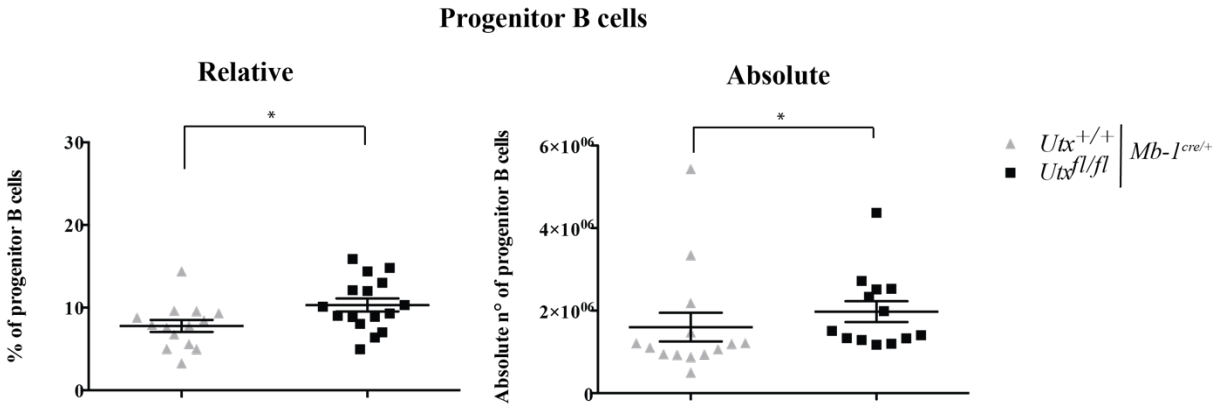


Figure 18. *Utx* deficient mice show a modest increase in the fraction and absolute numbers of bone marrow progenitor B cells

Frequency (left) and absolute number (right) of gated $B220^+IgM^-$ progenitor B cells in *Utx* control ($Utx^{+/+}$; $Mb\text{-}1^{Cre/+}$; *n*=14), and mutant ($Utx^{fl/fl}$; $Mb\text{-}1^{Cre/+}$; n=13/16) mice. Each dot represents a mouse. Lines represent the mean value ± SEM (non-parametric Mann Whitney test; * p< 0.05).

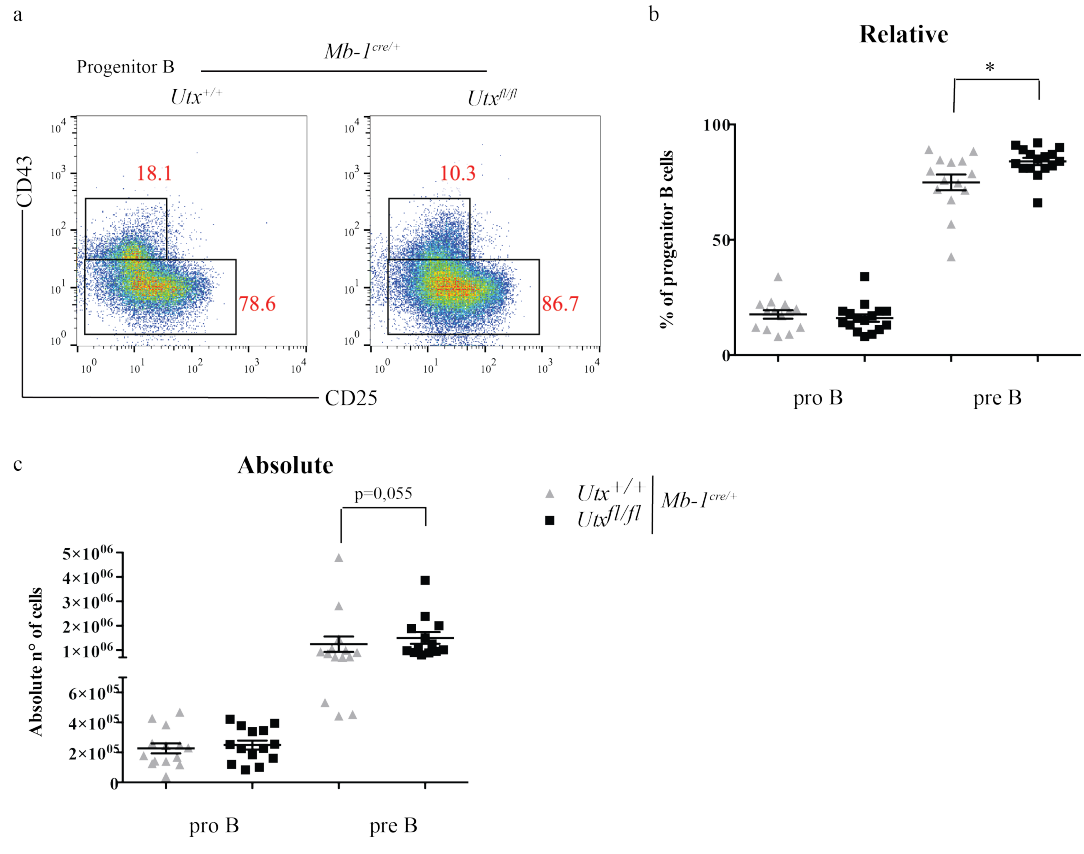


Figure 19. Increased fraction of pre-B cells in *Utx* mutant mice

a. Representative flow cytometric analysis of pre-gated $B220^{+}IgM^{-}$ progenitor B cells in the bone marrow of *Utx* control (left) and mutant (right) mice. Numbers within dot plots indicate frequencies of boxed pro-B ($CD43^{+}CD25^{-}$) and pre-B ($CD43^{-}CD25^{-}$) cells, respectively. Plots are representative of 10 independent experiments. Frequency (b) and absolute number (c) of $B220^{+}IgM^{-}$ proB ($CD43^{+}CD25^{-}$) and pre-B ($CD43^{-}CD25^{+}$) cells in mice with the indicated genotype. Lines refer to mean values ± SEM. Each dot represents a mouse. (Non-parametric Mann Whitney test; * $p< 0.05$).

Taking advantage of the CD25 and CD43 markers to further distinguish pro-B ($B220^{lo}IgM^{-}CD43^{+}CD25^{-}$) and pre-B cells ($B220^{lo}IgM^{-}CD43^{-}CD25^{+}$), I observed a modest, yet statistically significant, increase in the fraction of *Utx* mutant pre-B cells when compared to controls, contributing to an increase in the overall number of this B subset in *Utx* conditional deficient mice (Figure 19). In contrast, consistently with a yet partial inactivation of the *Utx* gene in pro-B cells, the fraction of these cells was unaffected in $Utx^{fl/fl}$; $Mb\text{-}1^{cre/+}$ mice when compared to controls (Figure 10).

The increased pre-B cell compartment in *Utx* conditional mutant mice was associated with a slight increase (11%) in the absolute numbers of immature B cells and with a significant reduction in the fraction of recirculating $B220^{hi}IgM^{+}$ B cell. The absolute number of these cells was also reduced by 30% when compared to those of controls (Figure 20).

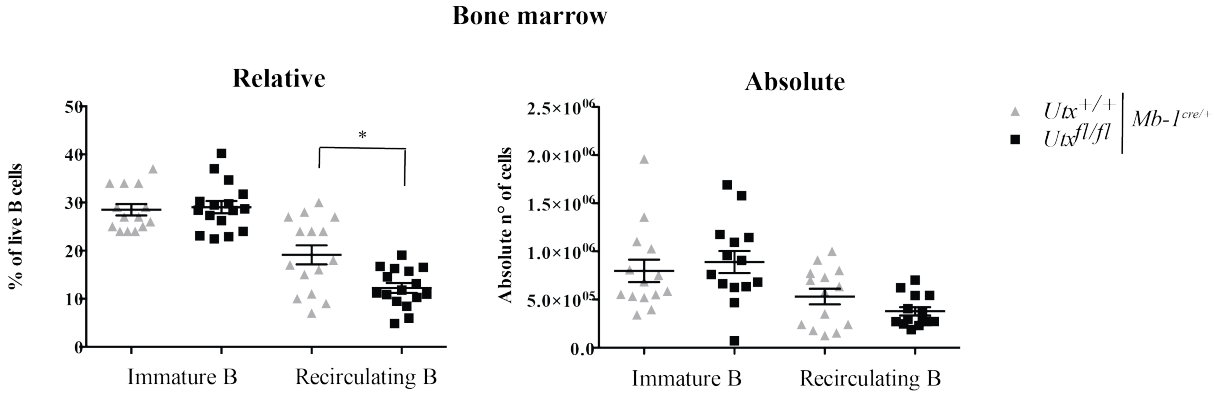


Figure 20. Reduction in recirculating B cells in the bone marrow of *Utx* deficient mice

Frequency (left) and absolute number (right) of gated $B220^{lo}IgM^{+}$ immature and $B220^{+}IgM^{+}$ recirculating B cells in the bone marrow of $Utx^{+/+}$control $Utx^{fl/fl}$ mutant mice. Each dot represents a mouse. Lines indicate the mean values ± SEM. (Non-parametric Mann Whitney test; * $p< 0.05$).

Taken together, these results indicate that inactivation of *Utx* in pro B cells leads to a modest yet consistent increase in the numbers of progenitor B cells, while reducing the number of mature B cells returning to the bone marrow. These data are compatible with a scenario in

which UTX optimizes the differentiation of progenitor B cells into IgM-expressing B cells and possibly regulates B cell homeostasis, favouring recirculation of mature B cells into the bone marrow. Consistently with this hypothesis, the ratio of progenitors/immature B cells is increased in *Utx* mutant mice compared to controls, pointing to a defect in this transition in the absence of *Utx* (Figure 21).

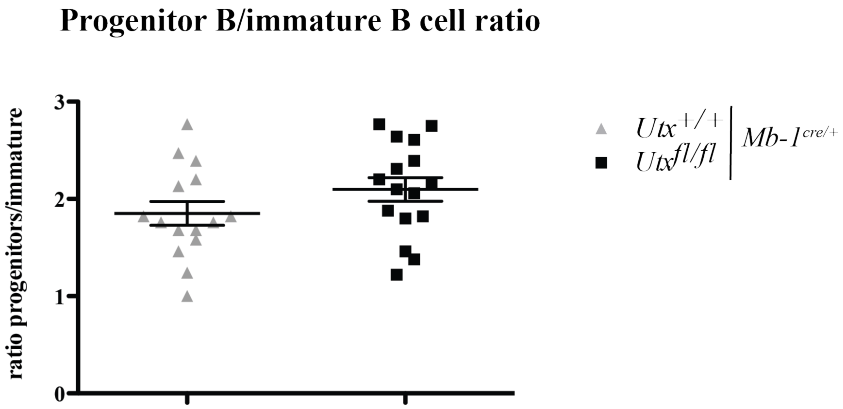


Figure 21. *Utx* inactivation delays the transition from progenitor to immature B cells in the bone marrow

Ratio of gated IgM$^-$B220$^+$ progenitor and B220^{lo}IgM$^+$ immature B cells in the bone marrow of *Utx* control and mutant mice. Lines refer to mean values ± SEM. Each dot represents the ratio measured in one animal.

3.3.2. Peripheral B cell differentiation in the absence of UTX

3.3.2.1. B cells are strongly reduced in the blood of *Utx* mutant animals

Considering the reduction in the numbers of recirculating B cells that we observed in the bone marrow of *Utx* mutant mice, we next asked whether this decrease was also present in the blood, suggesting a possible contribution of UTX to B cell egress and recirculation among different lymphoid organs. Analysis of peripheral blood cells of mutant and control mice displayed a strongly reduced pool of B220$^+$ B cells in response to *Utx* inactivation (Figure 22). This result, combined with fewer mature B cells measured in the bone marrow of *Utx* mutant mice supports a possible role for UTX in the control of B cell recirculation.

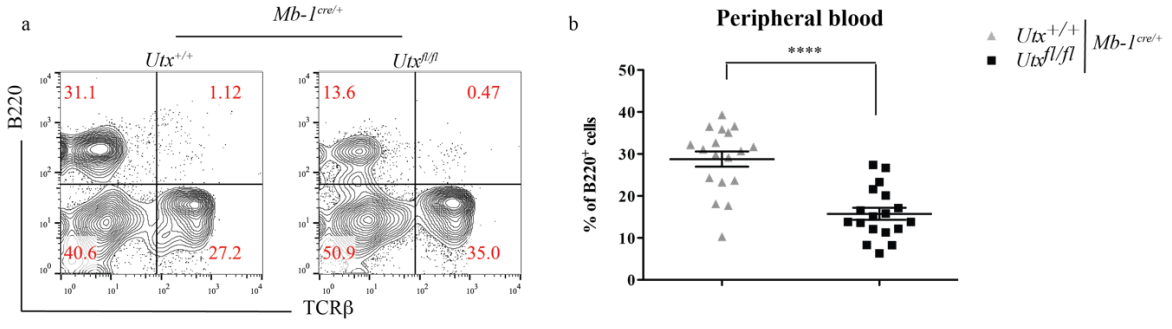


Figure 22. *Utx* deficient mice show a decrease in the fraction of B cells circulating in the blood

a. Representative flow cytometric analysis of peripheral blood mononuclear cells retrieved from representative *Utx* control (left) mutant (right) mice. Numbers within dot plot indicate frequencies of cells in the corresponding quadrants. Data are representative of 9 independent experiments. b. Fraction of gated $B220^+$ B cells in the blood of *Utx* control (triangles; *n*=18) and mutant (squares; *n*=18) mice. Each dot corresponds to a mouse. Lines represent mean values ± SEM. (parametric t test; **** p< 0,001).

3.3.2.2. *Utx* deficiency reduces overall B cell numbers in secondary lymphoid organs

To address the contribution of UTX to peripheral B cell development, we performed a comprehensive immunophenotypic analysis on single cell suspensions from secondary lymphoid organs of conditional $Utx^{fl/fl}$ mutant and $Utx^{+/+}$ control mice.

Utx inactivation led to a modest yet significant decrease of the fractions of $CD19^+$ B cells in peripheral lymphoid organs including spleen, mesenteric lymph nodes (MLNs) and Peyer's patches (PPs), corresponding respectively to a reduction of 20%, 40% and 50% of the pool of B cells (Figure 23).

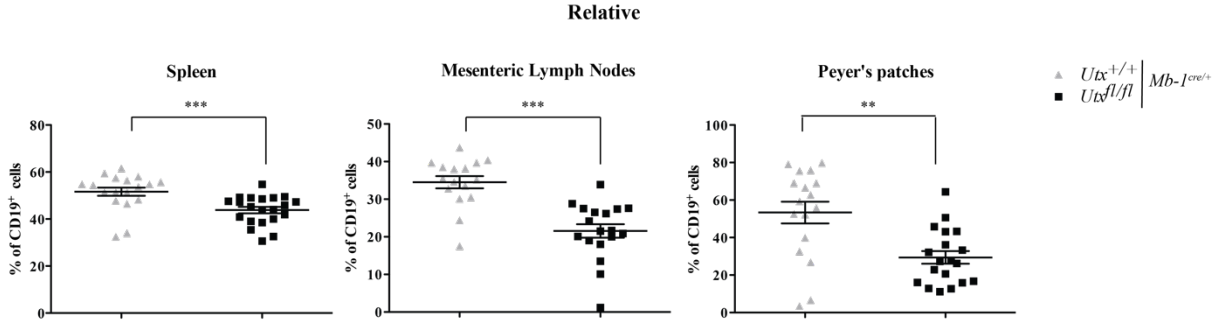


Figure 23. Reduced representation of B cells in secondary lymphoid organs of *Utx* mutant mice

Frequency of $CD19^+$ B cells in the indicated secondary lymphoid organs of *Utx* control (grey triangles) and mutant (black squares) mice. Each dot corresponds to a mouse. Lines represent mean values ± SEM (Non-parametric Mann Whitney test; *** p< 0,001).

Utx extinction had also a (mild) impact on total number of splenic B cells, which were reduced by 15% when compared to controls. The difference was not statistically significant, probably due to the high intra-group variability (Figure 24a). PPs B cell number in *Utx* deficient mice showed a stronger impairment, dropping by 70% when compared to controls (Figure 24a). These data, together with reduced B cell fractions measured in mesenteric lymph nodes of *Utx* conditional mutant mice point to a possible role of UTX in the recruitment and/or maintenance

of B lymphocytes in gut-associated lymphoid tissues. This hypothesis is further supported by the notion that numbers of B cells in other lymph nodes such as inguinal lymph nodes were comparable between $Utx^{fl/fl}$ and $Utx^{+/+}$ mice (Figure 24b).

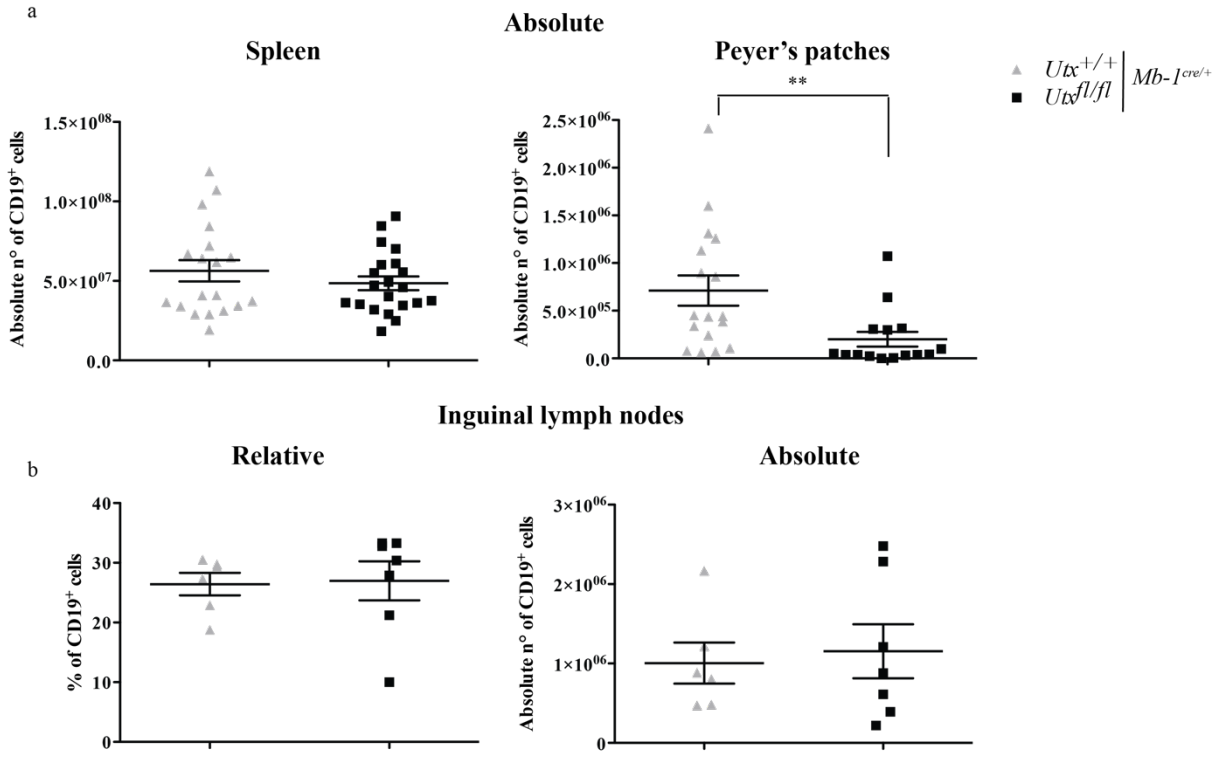


Figure 24. Quantification of B cell numbers in secondary lymphoid organs of *Utx* control and mutant mice

a. Absolute number of $CD19^+$ B cells in the spleen and Peyer's patches of *Utx* control (grey triangles; n=19) and mutant (black squares; n=21) mice were calculated based on flow cytometric analyses. b. Frequency (left) and absolute number (right) of gated $CD19^+$ B cells in inguinal lymph nodes of *Utx* control (grey triangles; n=6) and mutant (black squares; n=7) mice. Each dot represents a mouse. Lines indicate the mean values ± SEM. (Non-parametric Mann Whitney test; ** p< 0,01).

To rule out the possibility that mature B cells in peripheral lymphoid organs of *Utx* mutant mice were variants that had escaped Cre mediated recombination, we compared *Utx* exon 3 copy number assessed by quantitative genomic PCR analysing in splenic $CD19^+$ B cells from $Utx^{+/+}$ and $Utx^{fl/fl}$ mutant animals. The data revealed that B cells isolated from the spleen of *Utx* conditional mutants had undergone over 90% recombination efficiency at the *Utx* locus (Figure 25). Overall, these data are compatible with a scenario in which UTX fine tunes peripheral B cell homeostasis impacting primarily on the number of B cells residing in gut-associated lymphoid tissues.

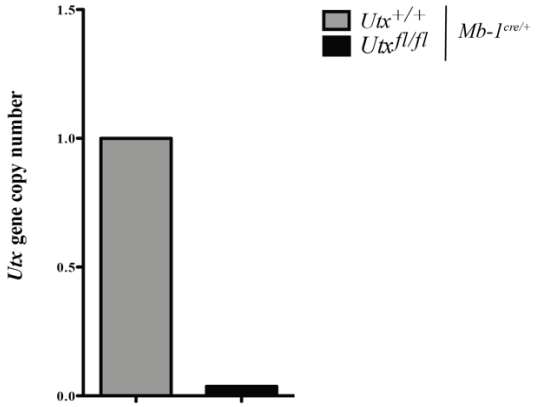


Figure 25. Efficiency of Cre-mediated recombination of the *Utx floxed* allele in splenic B cells of *Utx* conditional mutant mice

Genomic qPCR analysis to determine the *Utx* gene copy number in $CD19^+$ B cells purified from the spleen of *Utx* control (grey bar; n=4) and mutant (black bar; n=9) mice. Data are normalized to the copy number of the *Gapdh* gene and shown as relative to those of the *Utx* allele in *Mb-1*$^{cre/+}$ control B cells. Results are representative of 3 independent experiments.

3.3.2.3. Reduced numbers of immature B cells in the spleen of B-cell specific *Utx* mutants

Utx mutant mice suffer from a substantial reduction in the fraction of circulating B cells. To assess whether such disturbance correlated with an altered number of transitional B cells homing to the spleen, we performed flow cytometric analysis on single cell suspensions retrieved from this lymphoid organ of *Utx* control and mutant mice. Analysis of the data revealed that both the fraction and absolute numbers of splenic $B220^{lo}AA4.1^+$ transitional/immature B cells suffered from a 25-30% reduction in *Utx* conditional mutant mice (Figure 26). These data hint to a regulation of UTX on the migration of newly generated B cells to the spleen.

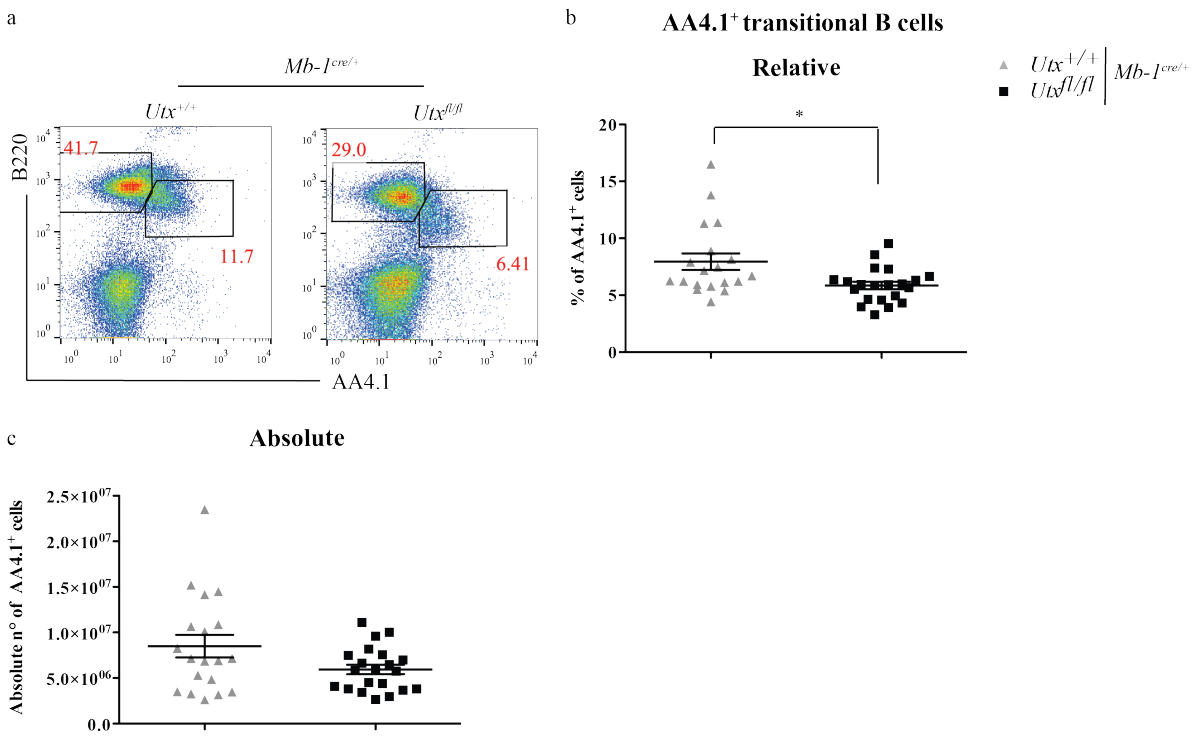


Figure 26. Transitional B cells are reduced in the spleen of *Utx* conditional mutant mice

a. Representative FACS analysis of $B220^{lo}AA4.1^{+}$ transitional B cells in the spleen of *Utx* control (left) and mutant (right) mice. Numbers indicate frequencies of boxed cells. Data are representative of 9 independent experiments. Frequency (b) and absolute numbers (c) of gated $B220^{lo}AA4.1^{+}$ transitional B cells in *Utx* control (grey triangles; n= 19) and mutant (black squares; n=21) mice. Each dot represents one mouse. Lines represent mean values ± SEM.

3.3.2.4. *Utx* deficiency interferes with peripheral B cell differentiation

B cell maturation is completed in the spleen giving rise to follicular (FO) B cells residing in primary follicles of the white pulp and to marginal zone (MZ) B cells residing outside of the marginal sinus, in close proximity to the blood stream (Lopes-Carvalho and Kearney 2004). To determine whether *Utx* inactivation affected peripheral B cell differentiation, single cell suspensions from the spleen of control and *Utx* mutant mice were subjected to flow cytometric analysis using markers distinguishing FO from MZ B cells. Extinction of *Utx* expression caused a significant decrease in the fraction, and a 25% contraction in the number of $CD19^{+}CD23^{+}CD21^{lo}$ FO B cells. Conversely, both percentages and absolute number (60%) of $CD19^{+}CD23^{+}CD21^{hi}$ MZ B cells significantly increased in *Utx* conditional mutant mice (Figures 27 and 28). We confirmed the increase in MZ B assessing the expression status of two additional MZ B cell markers, Cd1d and CD38 (Figure 29) (Sonoda and Stein-Streilein 2002; Vences-Catalan and Santos-Argumedo 2011).

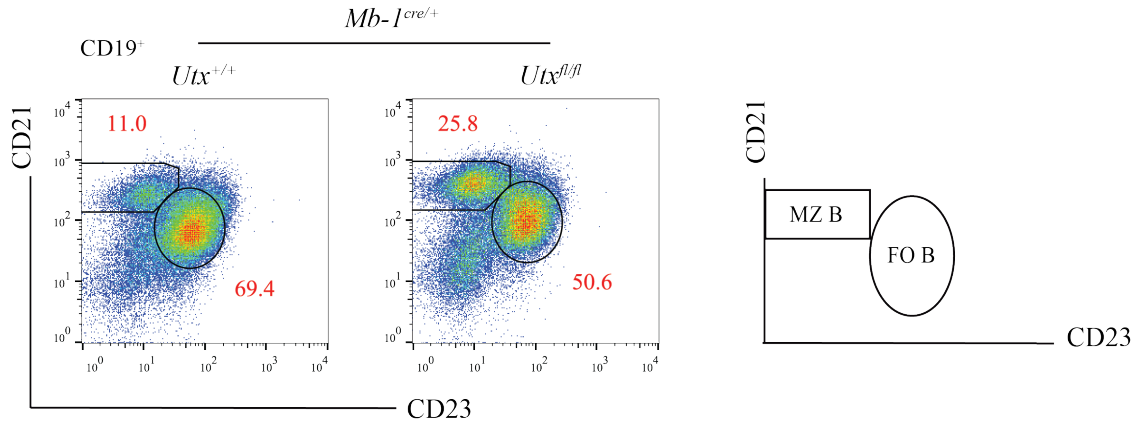


Figure 27. *Utx* deficiency affects the proportion of splenic follicular and marginal zone B cells

Representative flow cytometric analysis of $CD19^+$ gated B cells in the spleen of *Utx* control (left) mutant (right) mice, stained for the CD23 and CD21 markers. Numbers indicate frequencies of follicular ($CD21^+CD23^+$) and marginal zone ($CD21^{hi}CD23^{lo}$) B cells. Data are representative of 10 independent experiments.

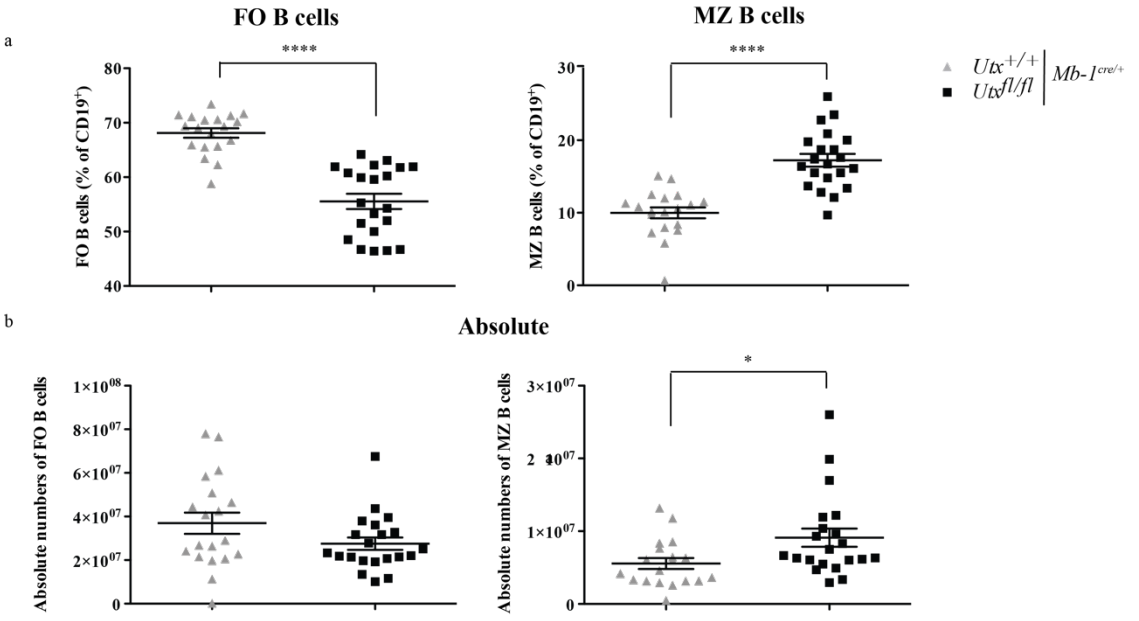


Figure 28. Numbers and frequencies of splenic mature B cell subsets are altered in *Utx* conditional mutant mice

Frequencies (a) and absolute numbers (b) of gated $CD19^+$ B cells in the spleen of Ut^x control (grey triangles) and mutant (black squares) mice. Each dot represents a mouse. Lines indicate the mean values ± SEM. (Non-parametric Mann Whitney test; * $p< 0.05$).

To assess whether the increase in MZ B cells scored by flow cytometry in the spleen of *Utx* mutant mice effectively lead to an increase in the size of the B cell pool residing in the MZ area, we performed immunofluoresce (IF) analysis on splenic sections of $Utx^{-/-}$ and $Utx^{+/+}$mice. Specifically, we used antibodies reactive against respectively B220, to detect B cells, and MOMA-1, to visualize metallophilic macrophages lining the marginal sinus (Kraal and Janse 1986)2. Surprisingly, quantification of the surface area occupied by B cells residing in the MZ

failed to reveal major differences between *Utx* control and mutant animals (Figure 30 and 31). All together, these results postulate an influence of UTX on the expression of markers distinguishing FO from MZ B cells without this affecting significantly the fraction of B cells effectively reaching the MZ.

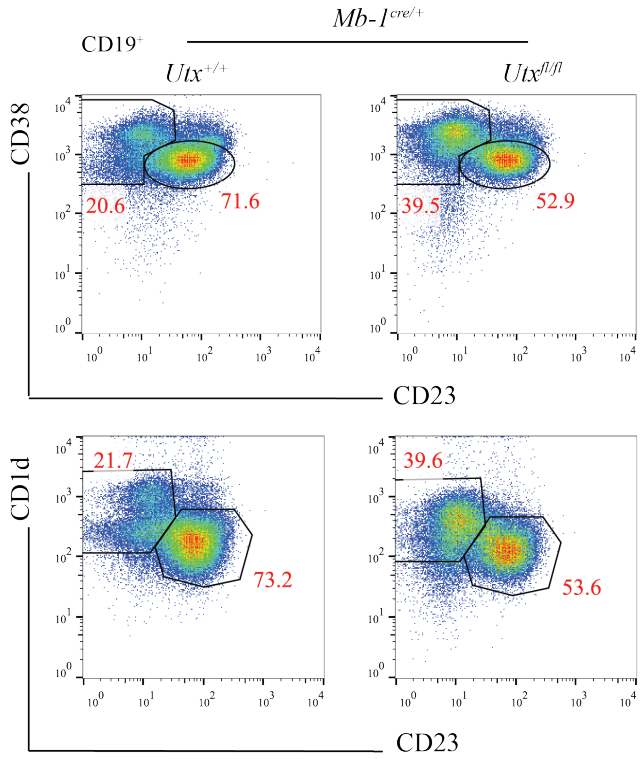


Figure 29. Analysis of FO and MZ B cells using complementary surface markers in *Utx* control and mutant mice

Representative flow cytometric analysis of $CD19^+$ gated B cells in the spleen of 4-months-old *Utx* control (left) and mutant (right) mice, stained respectively for the CD38/CD23 (upper panels) or CD1d/CD23 surface marker combinations (lower panels). MZ B cells are $CD23^{lo}CD38^{hi}CD1d^{hi}$ B cells, whereas FO B cells are $CD23^+CD38^{lo}CD1d^{lo}$ B cells. Numbers indicate frequency of boxed cells. Data are representative of 10 independent experiments.

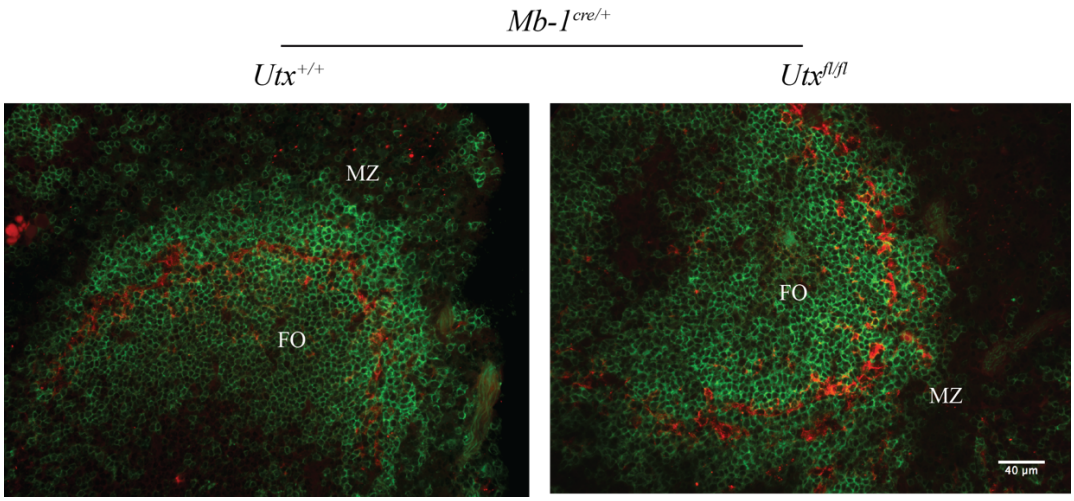


Figure 30. *Utx* mutant B cells home to splenic primary follicles and reach the marginal zone
Immunufluorescence analysis of splenic sections from *Utx* control (left) and mutant (right) mice stained for B220 (green) and MOMA-1 (red). Representative B cell follicles (FO) and the marginal zone (MZ) are displayed (10X magnification).

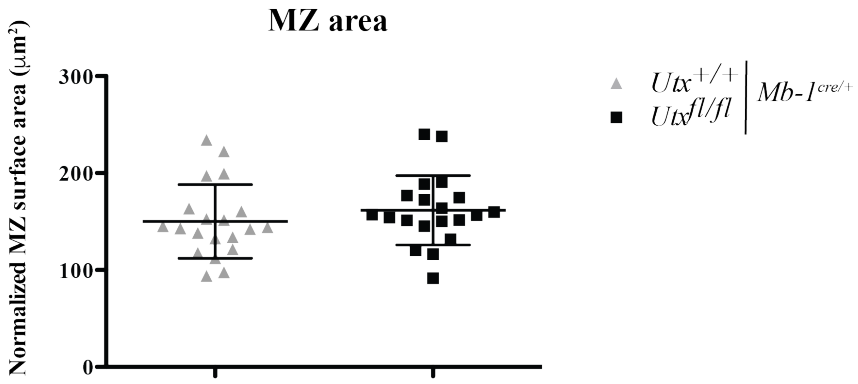


Figure 31. Measurement of the marginal zone area in *Utx* control and mutant mice
Quantification of the marginal zone area in *Utx* control (grey triangles) and mutant (black squares) mutant animals. Each value represents the marginal zone area normalized to the corresponding follicle circumference. Results are reported as mean ± SEM of a total of 10 measurements per sample, from 2 independent animals for each genotype.

We next assessed whether disruption of *Utx* expression influences the development of B-1 B cells, which mostly reside in body cavity sierosa. Flow cytometric analyses of peritoneal cavity lavages showed comparable fractions and numbers of total $CD19^+$ B cells between $Utx^{fl/fl}$ and $Utx^{+/+}$ mice (Figure 32). Among the B cells, *Utx* mutant mice showed increased frequencies of $CD19^{hi}B220^{lo}$ B-1 B cells at the expense of a reduced fraction of $CD19^+B220^+$ B-2 B cells (Figure 33 and 34). These results, combined with previous observations made on single cell suspensions analysed from the spleen and gut associated lymphoid tissues hint to a disturbance of *Utx*-deficient B-2 B cells to recirculate through secondary lymphoid organs.

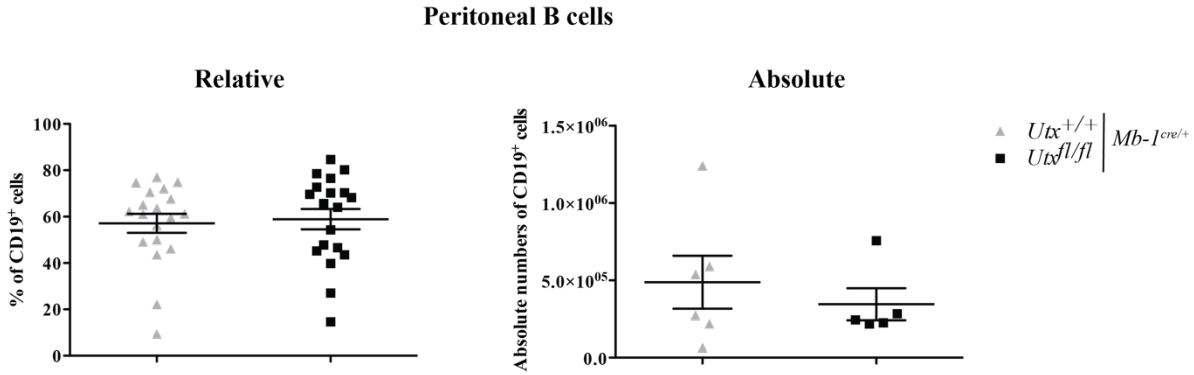


Figure 32. Frequencies and absolute number of B cells in peritoneal cavity lavages of *Utx* control and mutant mice

Frequencies (left) and absolute numbers (right) of CD19$^+$ B cells in the peritoneum of *Utx* control (grey squares) and mutant (black squares) mice, as assessed by flow cytometric analysis. Each dot represents an animal. Lines indicate mean values ± SEM.

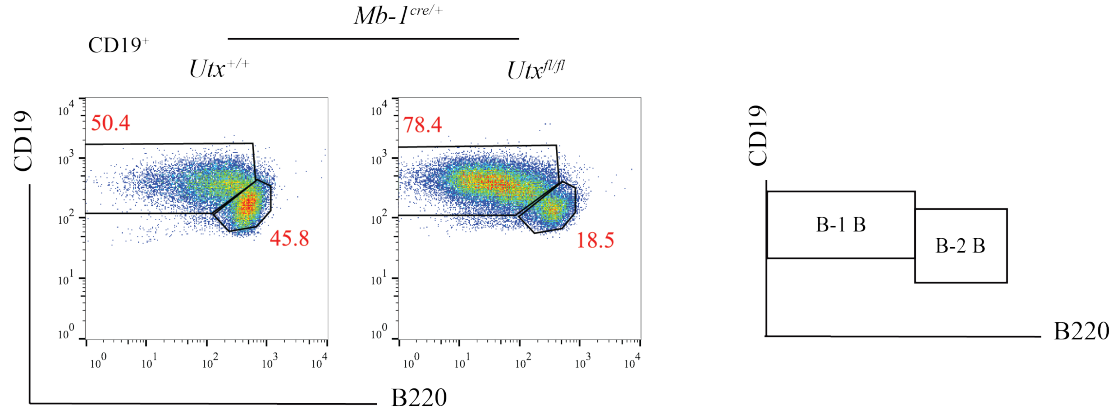


Figure 33. The B-1/B-2 B cell ratio is altered in *Utx* conditional mutant mice

Representative flow cytometric analyses of *Utx* control (left) and mutant Right) peritoneal cavity lavages stained for the indicated surface markers. CD19^{hi}B220^{lo} B-1 B cells are distinguished from CD19$^+$B220$^+$ B-2 B cells. Numbers indicate frequencies of boxed B cells among CD19$^+$ gated B cells.

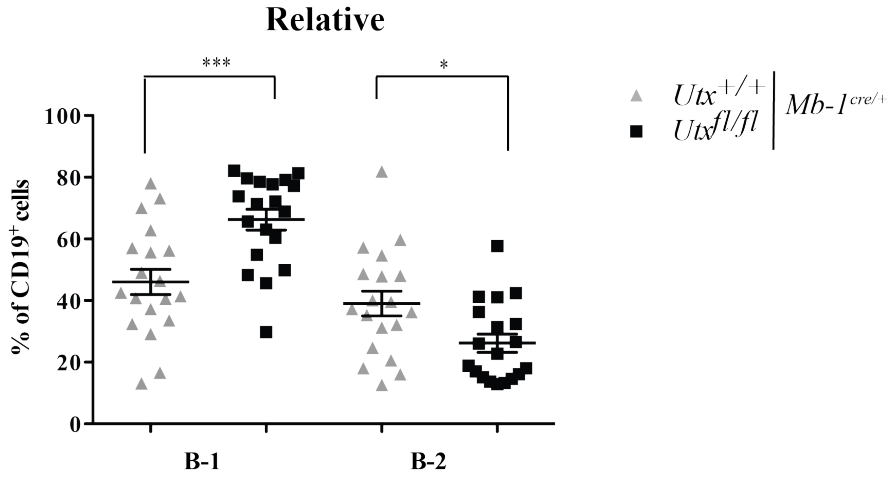


Figure 34. Distribution of B cells among the B-1 and B-2 B cell subsets is altered in the peritoneum of *Utx* mutant animals

Frequencies of the B-1 ($CD19^{hi}B220^{lo}$) and B-2 ($CD19^{+}B220^{+}$) B cell subsets, among peritoneal cavity $CD19^{+}$ gated B cells of *Utx* control (grey triangles) and mutant (black squares) mice, as determined by flow cytometric analysis. Lines represent mean values ± SEM (Non-parametric Mann Whitney test; * $p < 0.05$, *** $p < 0.001$).

3.3.2.5. Peripheral B cell homeostasis in the absence of UTX

3.3.2.5.1. B cell turnover is altered in the absence of functional Utx

The reduction in numbers of mature and immature B cell measured in the spleen and peripheral blood of Utx deficient mice, together with a decrease of recirculating mature B cells detected in the BM are compatible with a scenario in which UTX controls the turnover of mature resting B cells. To test this possibility, we performed *in vivo* BrdU labelling assays. The latter approach allows the *in vivo* investigation of the effects of specific insults, like the induction of a genetic mutation, on population dynamics (Allman, Ferguson et al. 1993). To this aim, BrdU was administered in the drinking water of *Utx* control and mutant mice (n=3 for each genotype) for 6 days after which animals were sacrificed and BrdU incorporation was measured by flow cytometry in both BM and SPL B cell subsets (Figure 35).

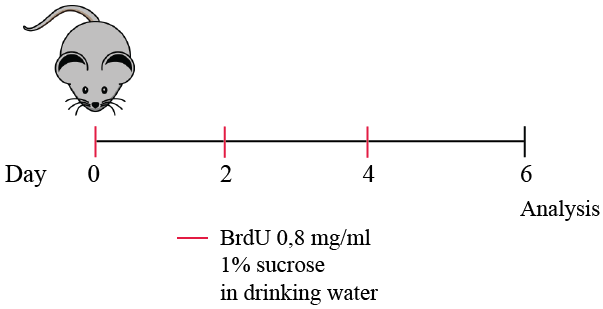


Figure 35. *In vivo* BrdU labelling: experimental plan

BrdU (0,8 mg/ml) was administered to mice in the drinking water and replaced every other day. Mice were sacrificed after 6 days.

Genotype	Samples	BrdU$^+$ cells (% of CD19$^+$ B cells)		
		Progenitor B (B220^{lo}IgM$^-$)	Immature B (B220^{lo}IgM$^+$)	Recirculating B (B220^{hi}IgM$^+$)
Utx$^{+/+}$; *Mb-1*$^{Cre/+}$	1	88.3	76.3	19.1
	2	72.4	60.0	13.5
	3	77.7	70.4	28.9
Utx $^{fl/fl}$; *Mb-1*$^{Cre/+}$	1	42.6	43.6	36.4
	2	70.5	72.3	38.5
	3	74.7	56.4	26.1
Statistics- Unpaired t-test				
Utx $^{fl/fl}$ *vs Utx*$^{+/+}$		NS	NS	NS

Table 16. BrdU$^+$ labelled recirculating B cells are increased in the BM of *Utx* mutant mice

Summary of BrdU incorporation data among the indicated BM B cells subsets in *Utx* control (*n*=3) and mutant (*n*=3) animals, as assessed by flow cytometric analysis. (Unpaired t-test; NS= not significant).

Genotype	Samples	BrdU$^+$ cells (% of CD19$^+$ B cells)			
		Immature (B220^{lo}AA4.1$^+$)	Mature (B220^{hi}AA4.1$^-$)	Follicular B (CD23$^+$CD21$^+$)	Marginal zone B (CD21^{hi}CD23^{lo})
Utx$^{+/+}$; *Mb-1*$^{Cre/+}$	1	66.9	8.470	7.78	11.5
	2	71	10	7.90	14.10
	3	77.5	9.6	7.98	12.60
Utx $^{fl/fl}$; *Mb-1*$^{Cre/+}$	1	37.6	6.4	4.66	6.43
	2	53	11	6.54	11.7
	3	54.40	16.5	7.35	13.9
Statistics- Unpaired t-test					
Utx $^{fl/fl}$ *vs Utx*$^{+/+}$		*	NS	NS	NS

Table 17. Recently immigrated immature B cells are underrepresented in the spleen of *Utx* mutant animals

Summary of BrdU incorporation data among the indicated splenic B cells subsets in *Utx* control (n=3) and mutant (n=3) animals, as assessed by flow cytometric analysis. (Unpaired t-test; * $p < 0.05$).

Data shown in Table 16 summarize the results. After 6 days of BrdU labelling between 70% and 80% of B220^{lo}IgM$^-$ progenitor B cells incorporated BrdU in both *Utx* WT and KO animals, in line with previous data (Allman, Ferguson et al. 1993). In the BM, a modest reduction in the

fraction of $BrdU^+$ $B220^{lo}IgM^+$ immature cells was detected in *Utx* deficient mice when compared to the corresponding population of controls. Instead, the percentage of $BrdU^+$ recirculating mature B cells ($B220^{hi}IgM^+$) displayed a modest increase in *Utx* KO mice when compared to controls (Table 16). Conversely, in the SPL, the fraction of BrdU-incorporating $B220^{lo}AA4.1^+$ immature B cells of *Utx* deficient mice was lower than in the controls, whereas the incorporation of BrdU in the mature B cell subsets was largely unaffected by *Utx* deficiency (Table 17). The BrdU incorporation results together with the data on absolute numbers of B cell subsets in the BM and in the SPL of *Utx* control and mutant mice, are compatible with a scenario in which UTX exerts at least two distinct functions: 1) to contribute to the pre-B to immature B cell transition, and 2) to promote the egress of newly generated immature B cells from the BM.

3.3.2.5.2. Sphingosine-1-phosphate receptor 1 expression is reduced in *Utx* deficient B cells

The reduction in mature and immature B cells measured in the SPL of *Utx* mutant mice was associated to a decrease in the proportion of $B220^+$ B cells scored in the blood, and to a contraction of the recirculating B cell compartment in the BM. Together, these data led us to hypothesize that UTX may influence the recirculation of B lymphocytes through the lymphopoietic system. To investigate the molecular determinants possibly responsible for the altered distribution of Utx mutant B cells among primary and secondary lymphoid organs, I focused my attention to the analysis of the Sphingosine-1-phosphate receptor 1 (S1PR1). S1PR1 is responsible for egress of both B- and T-lymphocytes from the thymus, spleen and lymph nodes (Cinamon, Matloubian et al. 2004). Moreover, S1PR1 provides a critical signal for the release of newly generated B cells from the BM into the blood and from there to the spleen (Pereira, Kelly et al. 2009). Importantly, *S1pr1* complementation rescued the defects in egress from the thymus of JMJD3/UTX double KO thymocytes ((Manna, Kim et al. 2015). Therefore, I quantified *S1pr1* transcripts in $CD19^+$ mature B cells purified from the spleen of $Utx^{+/+}$; $Mb\text{-}1^{cre/+/}$controls and $Utx^{fl/fl}$; $Mb\text{-}1^{cre/+}$ conditional mutant mice. As shown in Figure 36, *S1pr1* mRNA levels were significantly reduced in *Utx* mutant B cells when compared to those of control mice. These data, combined with previous evidence identifying the *S1pr1* gene as a transcriptional target of UTX in thymocytes, are suggestive of a regulation of UTX on the egress of newly formed B cells from the BM to the blood, and ultimately to the spleen (Thieme, Gyarfas et al. 2013; Manna, Kim et al. 2015) through the control of *S1pr1* expression. Furthermore, since S1PR1 has been also implicated in promoting the egress of B cells from the spleen (Matloubian, Lo et al. 2004; Pham, Baluk et al. 2010; Arnon, Xu et al. 2011), its

downregulation in *Utx* deficient B cells may contribute to the general decrease in B cell numbers observed in other secondary lymphoid organs.

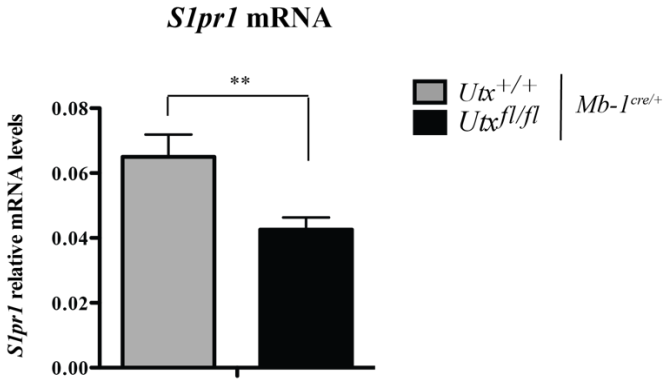


Figure 36. *Utx* mutant follicular B cells express lower *S1pr1* transcripts

S1pr1 transcript levels measured by RT-qPCR in sorted $CD19^{+}CD23^{+}CD21^{+}$ splenic follicular B cells from *Utx* control (grey bar; *n*=4) and mutant (black bar; *n*=4) animals. *S1pr1* transcript levels were normalized to those of the house-keeping gene *Rplp0*. (t test; ** p< 0,01).

3.3.2.5.3. *Utx* deficient B cells express less BAFF-R and display blunted responses to BAFF *in vitro*

The BAFF receptor (BAFF-R) is expressed on the surface of mature B cells. It is responsible for transmitting a key survival signal to these cells upon binding to the Tumor Necrosis Factor family member BAFF/BLyS produced in secondary lymphoid organs by different cell types including Follicular Dendritic Cells (Schiemann, Gommerman et al. 2001; Gorelik, Gilbride et al. 2003; Allen and Cyster 2008; Scholz, Crowley et al. 2008). We hypothesized that the reduction in mature B cell numbers seen in the spleen and in other secondary lymphoid organs of *Utx* mutant mice could also depend on a poor response of these cells to BAFF. To address this point, I first measured the expression of the BAFF-R in *Utx* mutant splenic B cells. Transcripts for *Baffr,* as revealed by RNA-sequencing analyses, were reduced in *Utx* mutant B cells (Figure 37a). More importantly, flow cytometric analyses using an anti-BAFF-R antibody revealed lower expression of BAFF-R protein on the surface of *Utx* mutant B cells (Figure 37b).

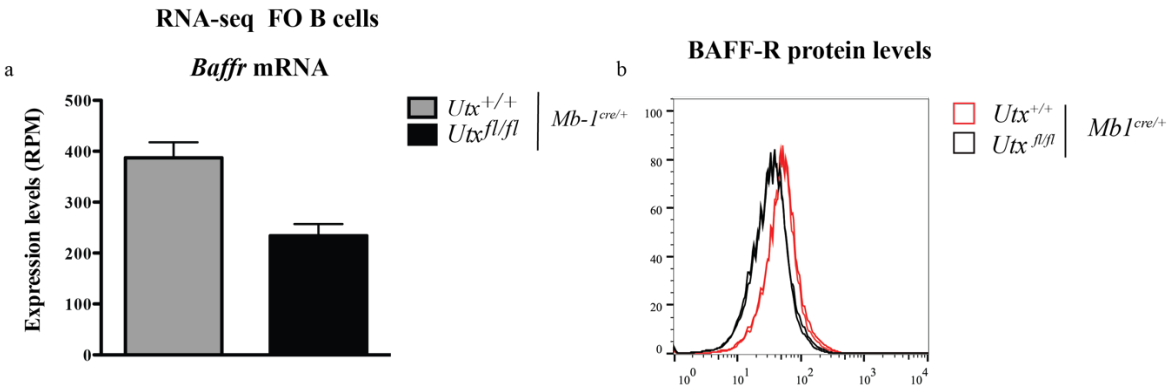


Figure 37. BAFF-R transcript and protein levels are reduced in *Utx* mutant mice

a. Baffr transcripts assessed by RNA-sequencing (RPMs: Reads Per Million mapped fragments) in *Utx* control (grey bar; n= 3) and mutant (black bar; n=3) sorted splenic follicular ($CD19^+$ $CD23^+CD21^+$) B cells. b. BAFFR protein levels measured by flow cytometry in $CD19^+$ gated *Utx* control (red line; n= 2) and mutant (black line; n=2) splenic B cells. Data are representative of 2 independent experiments.

To assess whether reduced BAFF-R expression had any functional consequence, I measured the survival response of *Utx* control and mutant B cells *in vitro* upon stimulation with BAFF. Specifically, splenic B cells purified through a depletion protocol by magnetic cell sorting from the spleen of *Utx* control and mutant mice were cultured *in vitro* in the presence of BAFF (6 ng/ml) and counted every second day, for the following 8 days. Unstimulated resting B cells were plated as a negative control. Whereas untreated B cells rapidly disappeared from the culture regardless of the *Utx* genotype, BAFF-stimulated B cells differed in their response according to the *Utx* genotype. Indeed, the lack of UTX impaired the capacity of the B cells to effectively respond to BAFF, resulting in fewer B cells measured at different time points of the culture (Figure 38). Hence, *Utx* inactivation reduces BAFF-R expression in splenic B cells, which is associated to a blunted response of the cells to the pro-survival factor BAFF.

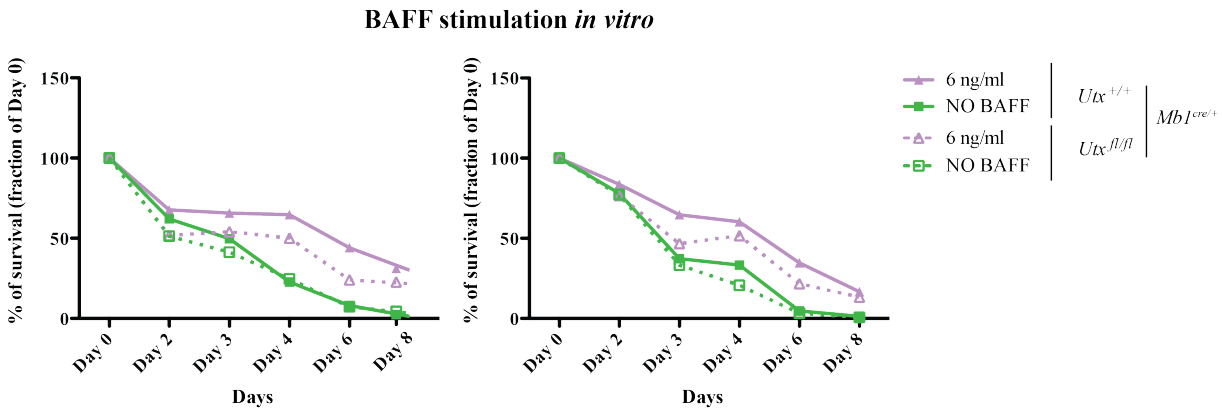


Figure 38. *Utx* mutant B cells survive less to *in vitro* BAFF stimulation

Fractions of live *Utx* control (continuous line) and mutant (dashed line) splenic $CD19^+$ purified B cells detected at the indicated time points of *in vitro* cultures, in the presence (purple lines) or absence (green lines) of BAFF stimulation (6 ng/ml) in two independent experiments. Data are represented as percentages of live cells at the onset (Day-0) of the *in vitro* culture.

3.3.2.5.4. A subset of NF-κB target genes is deregulated in *Utx* mutant B cells

The partial defect in the response of UTX mutant B cells to BAFF could extend beyond its regulation of BAFF-R expression. Given the importance of the NF-κB signalling pathway in mediating BAFF-induced survival signals, we tested whether UTX controlled the expression of one or more components of this pathway. Indeed, transcriptomic profiling of splenic FO B cells sorted from *Utx* control and conditional mutant mice (on the 129/SV X C57BL/6 mixed genetic background) revealed reduced expression of several members of both the canonical and alternative pathway. These included the transcription factors *Nfkb1, Nfkb2, c-Rel* and the upstream regulator of the pathway *IKK2 (*Figure 39).

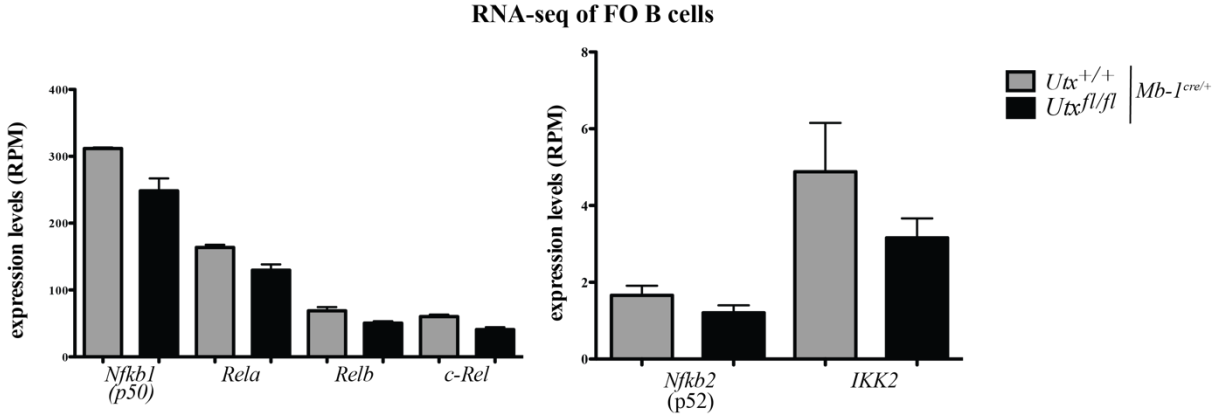


Figure 39. Transcripts for NF-κB transcription factors and effectors are reduced in *Utx* mutant FO B cells

Transcript levels for the indicated NF-κB transcription factors and effectors as assessed by RNA-sequencing (RPM: Reads Per Million mapped fragments) in *Utx* control (grey bars; *n*=3) and mutant (black bars; *n*=3) sorted FO ($CD21^+CD23^+$) B cells.

This observation predicted that NF-κB-controlled gene expression would be (at least partially) affected upon *Utx* inactivation. Intersection of the list of genes downregulated in *Utx* mutant FO B cells (407) with several published datasets (Heise, De Silva et al. 2014; De Silva, Silva et al. 2016) of genes transcriptionally downregulated upon KO of specific subunits of both the canonical and the alternative NF-κB pathway, revealed a substantial overlap (Supplementary material -Table 20). Specifically, around forty bona-fide targets induced by NF-κB were deregulated in Utx mutant B cells (Figure 40). Shared genes included regulators of Toll-like receptor, cytokine receptor and MAPK signalling pathways (*Map3k8, Map4k1, Mapk11, Stat4, Bcl9, Irak3*), metabolism (*Cmpk2, Slc4a7, Dcaf12),* chemotaxis (*Ccr7*) and immune responses (*Dhx58, Ddx58, Ifit2, Ifit3, Zbp1, Ebi3, Il17ra*) (Supplementary material -Table 20).

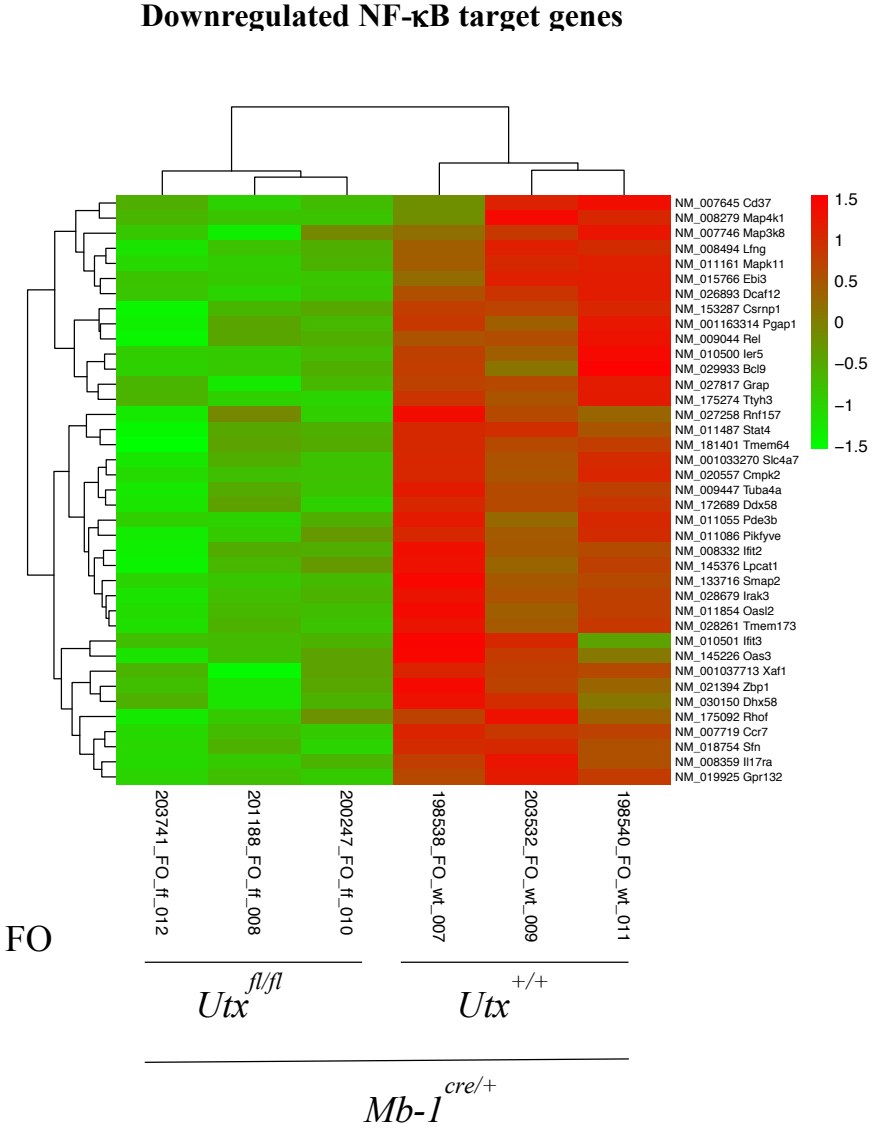


Figure 40. Reduced expression of a subset of NF-κB induced genes in *Utx* mutant follicular B cells

Heatmap representation of expression levels of a subset of previously identified NF-κB target genes (fold change < -1,2; adjusted p-value <0,05) in *Utx* control (*n*=3) and mutant (*n*=3) sorted FO ($CD19^+CD21^+CD23^+$) B cells.

Together, our results are consistent with a role of UTX in the regulation of the NF-κB pathway. The partial interference with this pathway may influence the ability of NF-κB to sustain peripheral B cell homeostasis and other functions of B cells once they are recruited into an immune response.

3.4. The role of UTX in T-cell dependent B cell responses

3.4.1. UTX limits the number of GC B cells and the size of GCs

Utx is expressed throughout B cell development including in B cells recruited to participate to the germinal center (GC) reaction during an adaptive immune response. Hence, we asked whether *Utx* deficiency influenced GC B cell responses. To address this question, $Utx^{fl/fl}$; $Mb\text{-}1^{cre/+}$ control and $Utx^{fl/fl}$; $Mb\text{-}1^{cre/+}$ compound mutants were immunized intraperitoneally with the T-cell dependent antigen 4-hydroxy-3-nitrophenyl (NP) coupled to chicken gamma globulin (CGG) in alum. GC B cells were analyzed 14 days post-immunization, at the peak of the immune response, by staining single cells suspensions from the spleen with antibodies recognizing GC B cell markers. *Utx* conditional mutant mice displayed a modest increase in the fraction and overall numbers (25%) of splenic $CD19^{+}CD38^{lo}FAS^{hi}$ GC B cells when compared to controls (Figure 41).

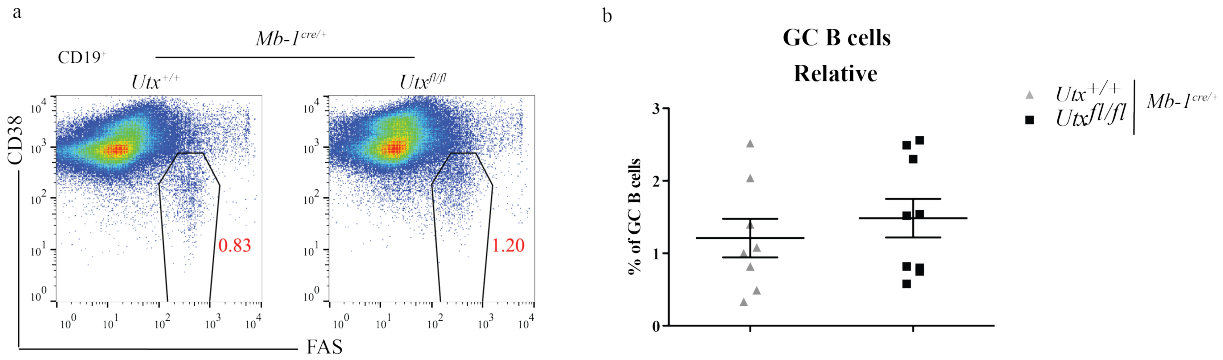


Figure 41. Modest increase in the fraction of GC B cells upon *Utx* inactivation

a. Representative flow cytometric analysis of splenic GC B cells analysed 14 days after NP-CGG immunization in *Utx* control (left; *n*=4) and mutant (right; *n*=4) animals. Numbers indicate frequencies of boxed $CD38^{lo}Fas^{hi}$ GC B cells. b. Summary of GC B cell frequencies in *Utx* control (grey triangles; *n*= 8) and mutant (black squares; *n*=9) mice immunized 14 days earlier with NP-CGG. Each dots represent one animal; lines represent mean values ± SEM.

To validate these results, we performed histological analyses on formalin fixed paraffin-embedded splenic sections of *Utx* KO and control animals immunized with either NP-CGG or sheep red blood cells (SRBC) (data not shown). As marker, we followed the expression of the transcription factor BCL6 which is strongly increased in GC B cells. *Utx* deficient mice

displayed an increased number of BCL6$^+$ GCs/tissue section, which is in line with flow cytometric data (Figure 42). Moreover, the average size of splenic GCs increased two-fold in *Utx* deficient mice when compared to controls. We confirmed that, likewise follicular B cells, the fraction of B cells recruited into the GC during an immune response was depleted of *Utx* in conditional mutant mice by performing quantitative genomic PCR for *Utx* exon 3 on sorted GC B cells (Figure 43).

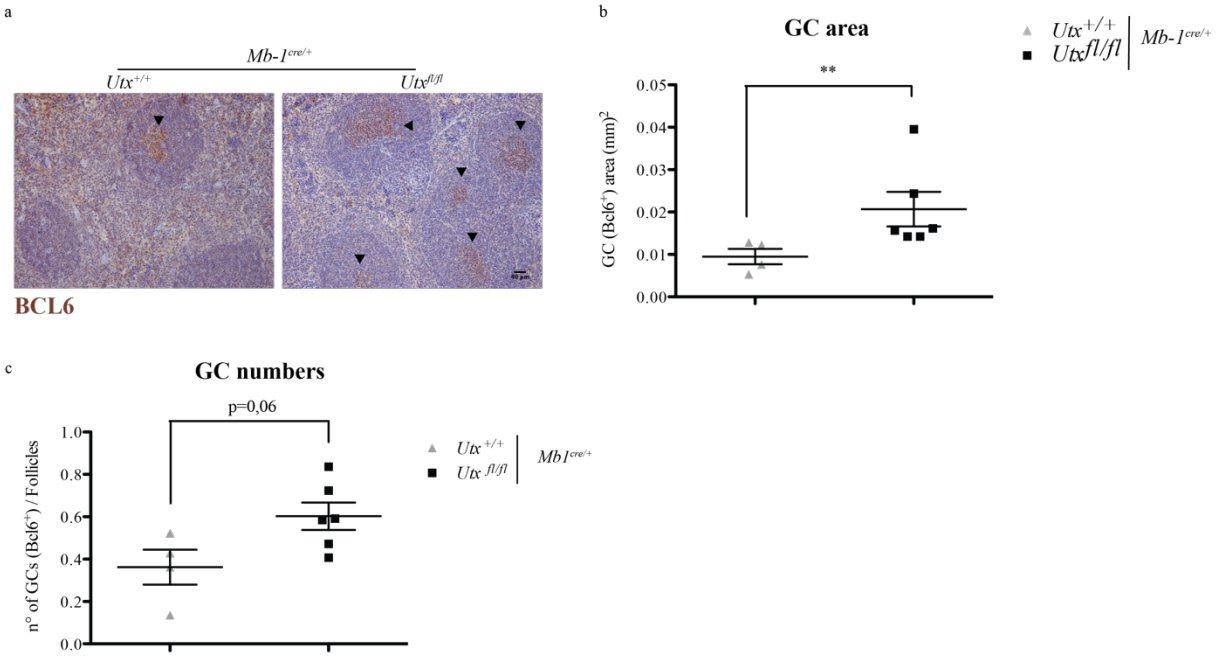


Figure 42 Increased average size of splenic BCL6$^+$ GCs in *Utx* mutant mice

a. Representative immunohistochemical analysis of paraffin-embedded splenic sections of day-14 NP-CGG-immunized *Utx* control (left) and mutant (right)animals, stained with an anti-BCL6 antibody. Individual germinal centers are indicted with arrows (10 X magnification). Sections were counterstained with hematoxylin (purple). b. Summary of the data relative to the numbers of BCL6$^+$ germinal centers per splenic section detected at day 14 in NP-CGG immunized *Utx* control (grey triangles; n=4) and mutant (black squares; n=4) animals. Data are represented as ratio between the number of BCL6$^+$ germinal center foci and the number of B cell follicles. Lines indicate mean values ± S.D. (non-parametric Mann Whitney test; p value is indicated). c. Average area of splenic BCL6$^+$ GCs detected 14 days after NP-CGG immunization of *Utx* control (grey triangles; n=4) and mutant (black squares; n=4) animals. Each dot represents the average GC area in individual animals. Lines indicate mean values ± S.D. (non-parametric Mann Whitney test; * p <0.01).

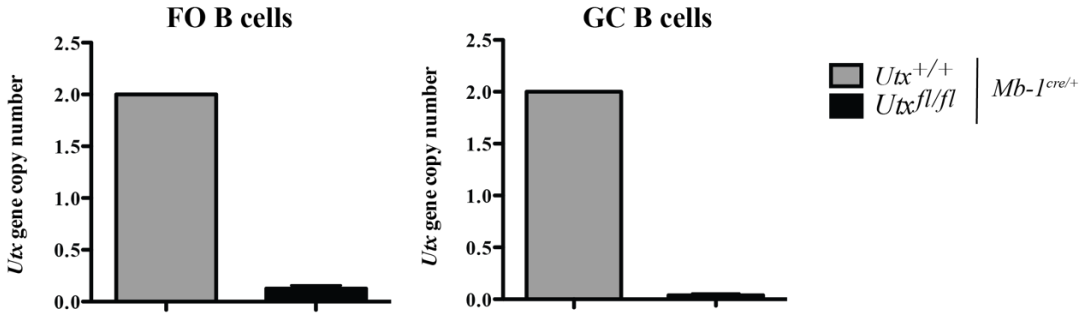


Figure 43. Close-to-complete Cre-mediated recombination of the *Utx* floxed allele in GC B cells of *Utx*$^{fl/fl}$; *Mb-1*$^{cre/+}$ mutant mice

Genomic qPCR analysis to determine *Utx* copy number respectively in sorted splenic CD19^{+}CD38^{+}Fas^{lo} FO (left) B cells and CD19^{+}CD38^{lo}Fas^{hi} GC B cells (right) of representative *Utx* control (grey bars; n=4) and mutant (black bars; n=4) animals. Germinal center B cells were purified by cell sorting 8 days after SRBCs immunization. *Utx* copy number results are normalized to those of the *Gapdh* gene and displayed as mean value ± S.D. of biological replicates.

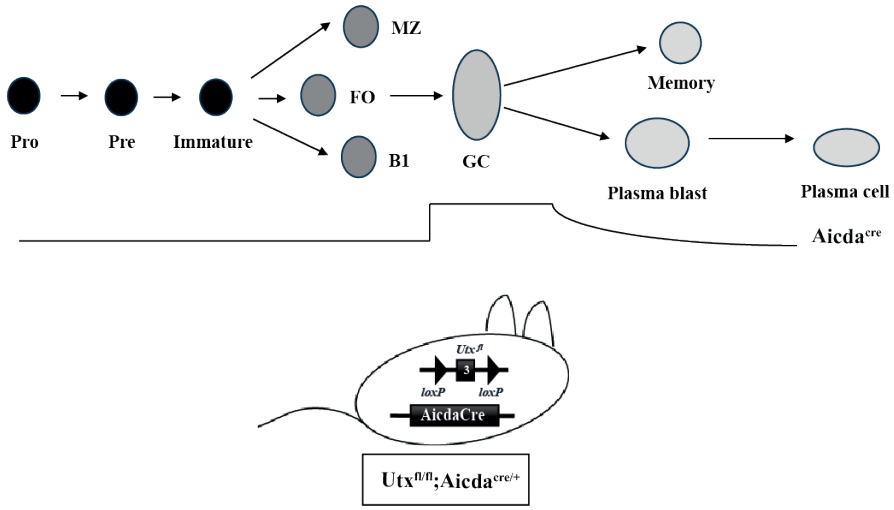


Figure 44. Germinal center B-cell specific *Utx* inactivation

Onset of Cre-mediated recombination in *Utx*$^{fl/fl}$; *Aicda*^{cre} experimental mice.

The inactivation of *Utx* starting from the pro-B/pre-B stage may have influenced the biology of mutant pre-GC B cells, which in turn could affect the biology of GC B cells (Zhang, Dominguez-Sola et al. 2015). Therefore, we tested whether acute inactivation of *Utx* in GC B cells would also lead to expansion of this population. For this purpose, *Utx* conditional knockout mice were bred to GC.

B cell specific *Aicda*^{cre} BAC transgenic mice (Kwon, Hutter et al. 2008). As for pan-B cell specific inactivation of *Utx*, GC B cell-specific extinction of UTX function was measured only in female mice (on a 129/SV X C57BL/6 mixed genetic background) comparing them to sex-matched *Aicda*^{cre} controls (Figure 44).

In *Utx*$^{fl/fl}$; *Aicda*^{cre} compound mutant mice, splenic GC B cells measured 8 days post SRBCs immunization were 50% increased compared to their *Utx* proficient counterparts (Figure 45a-b). Even stronger effects were seen analysing the fraction of GC B cells retrieved from MLNs (60% increase) and PPs (80% increase; Figure 45). These results indicate that inhibition of UTX either in GC B cells or in their direct progenitors favours expansion of the GC B cell pool upon immunization with T-cell dependent antigens.

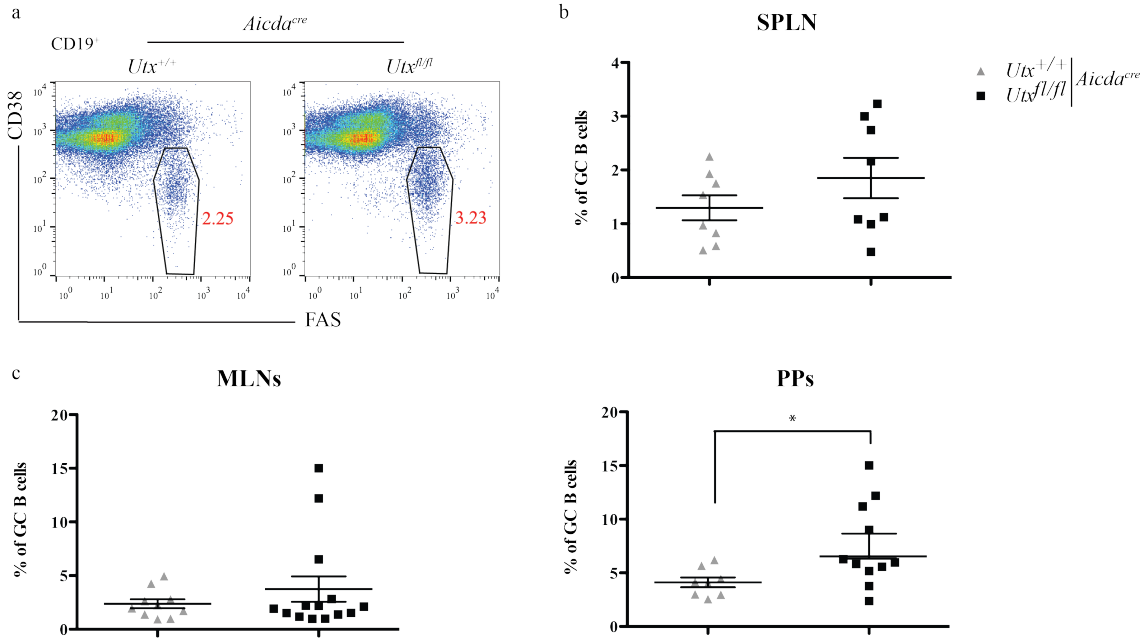


Figure 45. Increased GC B cell frequency in spleen and GALT of *Utx*$^{fl/fl}$; *Aicda*^{cre} immunized mice

a. Representative flow cytometric analysis of CD19^{+} pre-gated splenic GC B cells in *Utx* control (left) and mutant (right) mice, 8 days after immunization with sheep red blood cells (SRBC). Numbers indicate frequencies of boxed GC B cells (CD19^{+}CD38^{lo}Fas^{hi}). Data are representative of 5 independent experiments. b. Summary of data on the frequency of splenic CD19^{+}CD38^{lo}Fas^{hi} GC B cells in *Utx* control (grey triangles; n=9) and mutant (black squares; n=9) mice, analyzed eight days after SRBC immunization. c. Frequencies of GC B cells assessed by flow cytometric analysis in MLNs (left) and PPs of *Utx* control (grey triangles; n=10 for MLNs; n=8 for PPs,) and mutant (black squares; n=14 for MLNs; n=11 for PP) mice. Each dot corresponds to one mouse; lines represent mean values ± SEM (non-parametric Mann Whitney test; * p<0,05).

3.4.2. UTX restricts the pool of germinal center centroblasts

Germinal centers consist of a dark zone, consisting of B cells (also called centroblasts, CB) actively proliferating and which incorporate at high frequency mutations into the immunoglobulin heavy and light chain variable region genes, and a light zone, where cell-cycle arrested B cells (also called centrocytes, CC) undergo antigen-driven selection (Victora and Nussenzweig 2012). In order to test whether the lack of *Utx* affected the distribution of B cells within the CB and CC fractions, we analyzed these subpopulations in the spleen of *Utx* mutant

and control mice 14 days after NP-CGG immunization by flow cytometry. In particular, we took advantage of the CD86 and CXCR4 markers, whose differential expression allows to discriminate CBs from CCs (Victora, Schwickert et al. 2010). Inactivation of *Utx* led to an increase in the fraction of $CXCR4^{hi}CD86^{lo}$ centroblasts at the expense of the pool of $CXCR4^{lo}CD86^{hi}$ centrocytes (Victora, Schwickert et al. 2010) (Figure 46).

In support of these findings, transcriptomic analyses from the bulk population of GC B cells sorted from the spleen of *Utx* control and mutant mice (on the 129/SV X C57BL/6J mixed genetic background) indicated that a subset of genes differentially expressed between control and mutant GC B cells also discriminates normal CBs from CCs (Victora, Schwickert et al. 2010) (Figure 47).

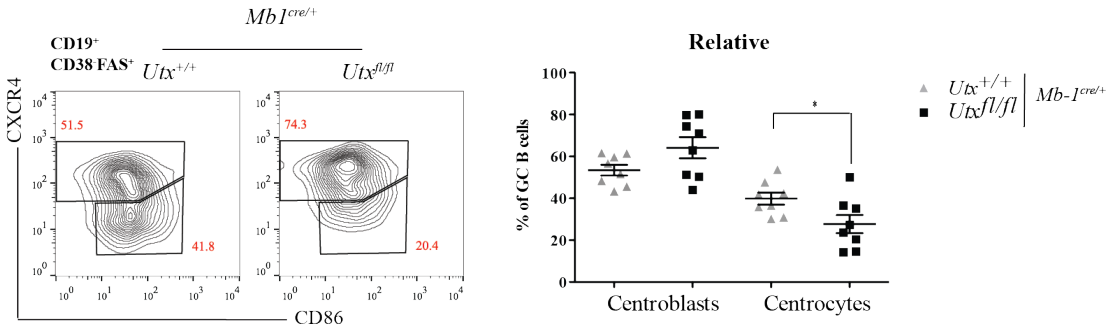


Figure 46. *Utx* inactivation leads to an increase in the germinal center centroblast fraction

Frequencies of boxed centroblasts ($CXCR4^{hi}CD86^{lo}$) and centrocytes ($CXCR4^{lo}CD86^{hi}$ cells) among gated $CD19^{+}FAS^{hi}$ GC B cells, in the spleen of *Utx* control (left; n=8) and mutant (right; n=8) mice, 14 days post NP-CGG immunization, as assessed by flow cytometric analysis. Lines represent mean values ± SEM (non-parametric Mann Whitney test; * $p < 0.05$).

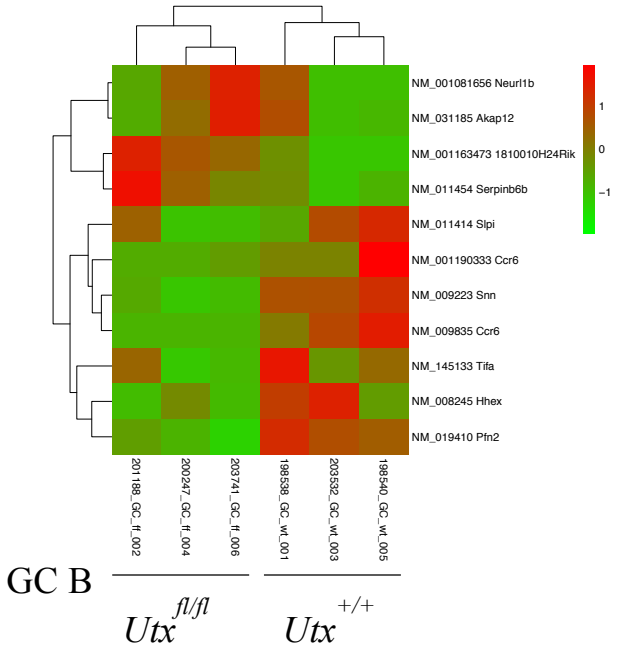


Figure 47. *Utx* mutant GC B cells express preferentially centroblast-associated genes

Heatmap representation of transcript levels in *Utx* control (right; *n*=3) and mutant (left; *n*=3) sorted GC B cells of a selected list genes chosen for their differential expression between control centroblasts and centrocytes, revealed by RNA-sequencing.

A further evidence supporting an enrichment among *Utx* deficient GC B cells of the centroblast pool came from the BCL6 protein levels. In accordance with the knowledge that BCL6 protein levels are higher in CBs than CCs, intracellular flow-cytometric analyses on gated $CD19^{+}CD95^{hi}CD38^{lo}$ GC B cells revealed higher average levels of BCL6 protein in *Utx* mutant mice when compared to controls (Figure 48).

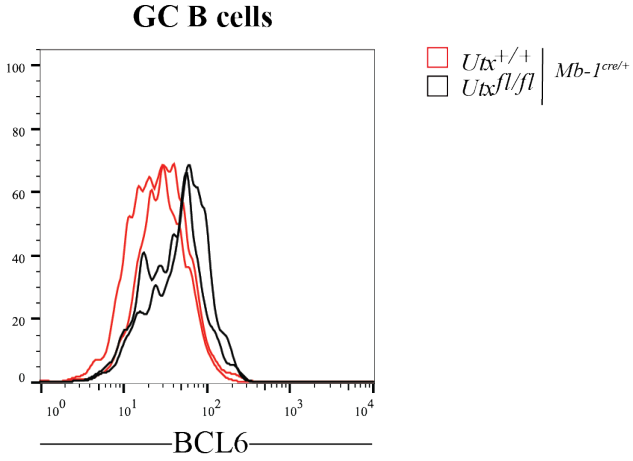


Figure 48. Higher average expression of BCL6 protein in *Utx* mutant GC B cells

Quantification of BCL6 protein levels in gated $CD19^{+}CD38^{lo}FAS^{hi}$ lymph node GC B cells in *Utx* control (red line; n=2) and mutant (black line; n=2;) mice, as revealed by intracellular flow cytometric analysis.

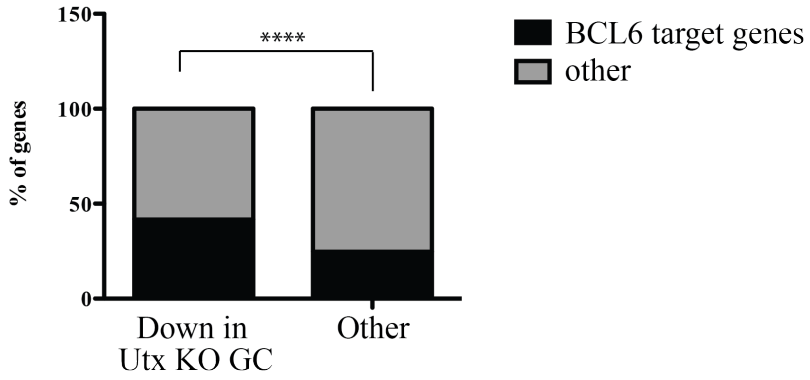


Figure 49. *Utx* mutant GC B cells express lower levels of BCL6 repressed genes. Fraction of previously described BCL6 target genes (black bars) whose expression is downregulated in *Utx* mutant (*Utx*$^{fl/fl}$*; Mb-1*$^{cre/+}$) GC B cells (*n*= 3) when compared to the corresponding subset (*n*=3) of *Utx* control (*Utx*$^{+/+}$*; Mb-1*$^{cre/+}$) mice, as assessed by RNA-sequencing (fold change < -1,2; adjusted p-value <0,05). As comparison, we represented the fraction of BCL6 target genes not affected by *Utx* inactivation. Grey bars indicate the fraction of non-BCL6 target genes in each of the 2 indicated datasets.

A stronger representation of BCL6^{hi} CBs among GC B cells of *Utx* mutant mice correlated with lower levels of expression of a subset of BCL6 repressed genes (Basso, Saito et al. 2010) measured in bulk GC B cell fractions of *Utx* mutant mice when compared to controls (Figure 49).

3.4.3. *Utx* deficiency alters GC responses in gut associated lymphoid tissues

Gut-associated lymphoid tissues (GALTs) exert an important function in mucosal immunity. Here, the daily encounter with antigens from the gut lumen triggers the continuous recruitment of naïve B cells into GCs in PPs and MLNs. The output of GALT GCs are predominantly IgA-expressing plasma blasts, which home to the intestinal lamina propria from where they secrete large amounts of IgA, which are ultimately released in the gut lumen to prevent the dissemination of both commensal and pathogenic microbial organisms. To assess whether *Utx* deficiency affected chronic GCs formed in GALT, we performed flow cytometric analysis on single cell suspensions retrieved from PPs and MLNs. The frequencies of CD19^{+}CD38^{lo}FAS^{hi} GC B cells were significantly increased in both lymphoid organs (Figure 50).

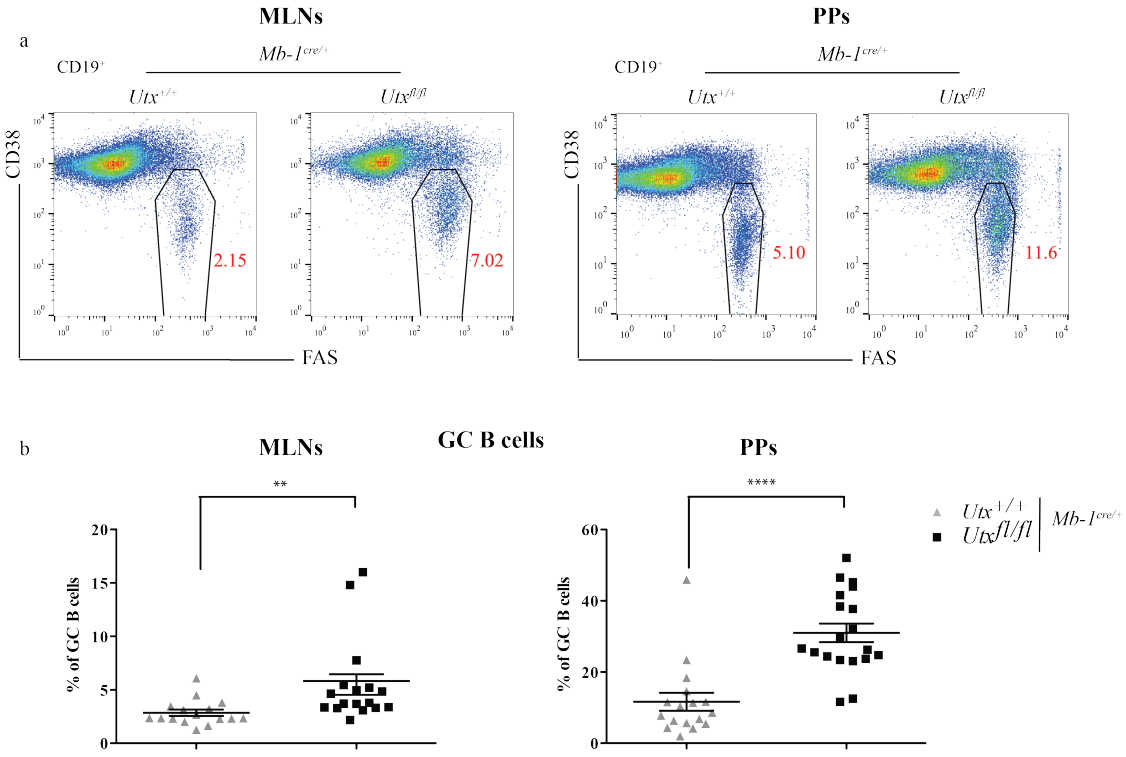


Figure 50. The frequency of GC B cells is increased in GALT of *Utx* mutant mice

a. Representative flow cytometric analyses of $CD19^+$ pre-gated GC B cells in components of the GALT, in *Utx* control (left; n=11) and mutant (right; n=11) animals. Numbers indicate frequencies of boxed GC B cells. **b.** Summary of data on frequencies of GC B cells among gated $CD19^+$ B cells in the indicated lymphoid organs of *Utx* control (grey triangles; n=8) and mutant (black squares; n=9) animals at day-14 post NP-CGG immunization, as assessed by flow cytometric analysis. Each dot represents one animal; lines represent mean values ± SEM

These results prompted us to investigate whether the pool of IgA PBs residing in the intestinal lamina propria was affected by *Utx* inactivation. Surprisingly, in contrast to the strong increase in the fraction of GALT GC B cells, immunohistochemical analyses of intestinal villi revealed a striking reduction of IgA^+ PBs in these animals (Figure 51).

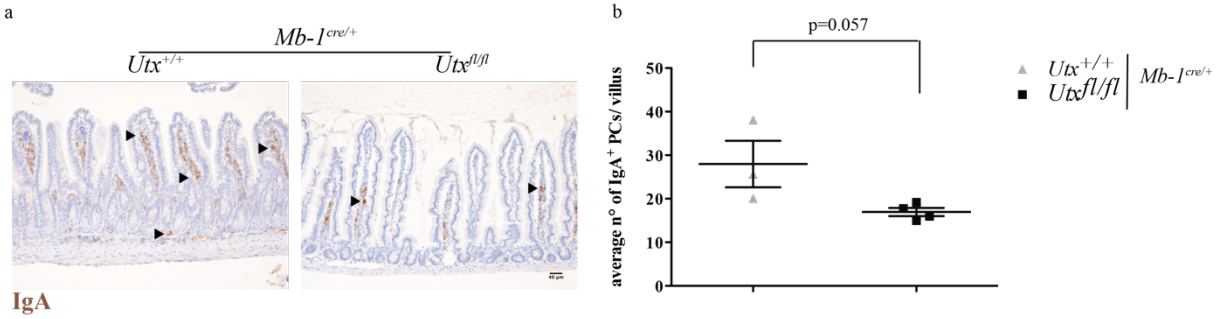


Figure 51. *Utx* deficient mice have less IgA$^+$ PCs in small intestine lamina propria

a. Representative immunohistochemical analysis of paraffin-embedded small intestine sections stained with an anti-IgA antibody (brown) retrieved from *Utx* control (left) and mutant (right) animals. IgA-secreting plasma cells are indicated with arrowheads (10X magnification). Sections were counterstained with hematoxylin (purple). b. Summary of the data on the quantification of the average number of IgA$^+$ PCs per intestinal villus, measured in *Utx* control (n=3) and mutant (n=4) animals. Each dot represents the average number of IgA-secreting plasma cells per mouse. Lines represent mean values ± SEM.

Moreover, transcriptomic analyses from GC B cells showed that *Utx* inactivation interfered with normal expression of regulators of B cell chemotaxis in GALT (*Ccr7, Ccr6*), plasma blast homing to the intestinal lamina propria, (*Itgβ7* and *Itgα4*), and triggering of IgA CSR (*TACI*) (Figure 52). Taken together, our results indicate that Utx exerts a crucial control over gut B cell immunity acting at multiple levels. Whereas it limits the size of the GC centroblast pool, it positively regulates important determinants of: 1) the migration of B cells to and within GALT, 2) IgA isotype switching as well as 3) homing of IgA PBs to the intestinal lamina propria.

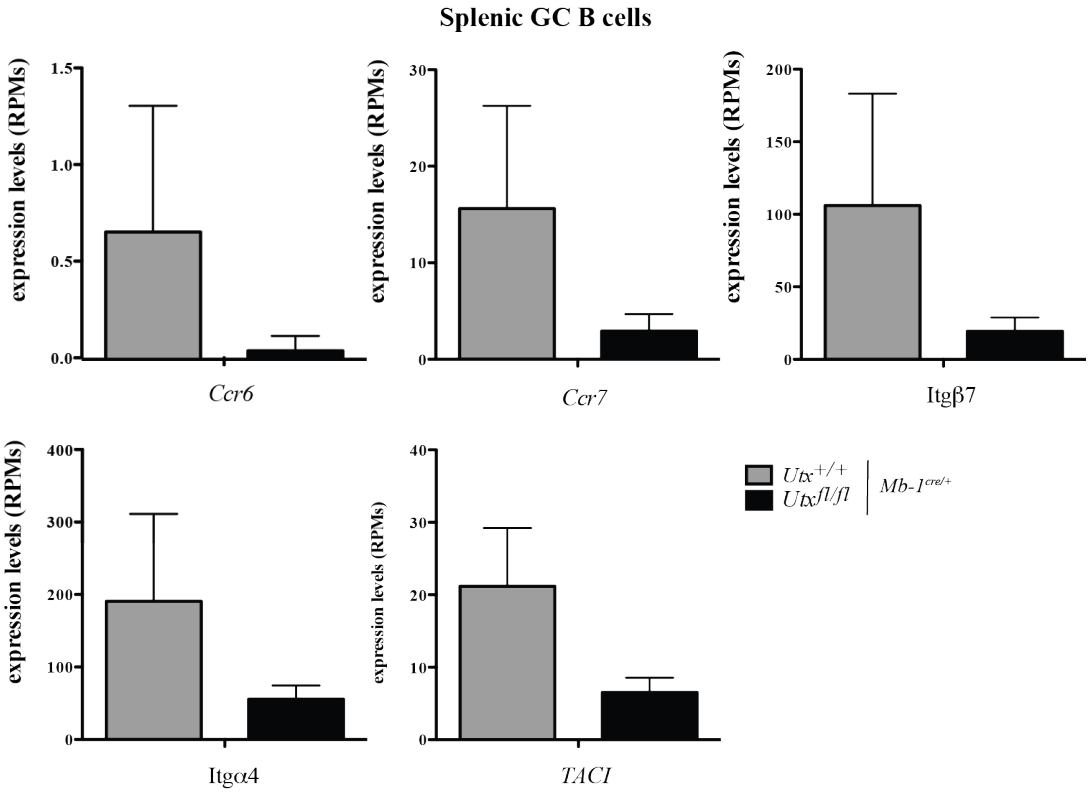


Figure 52. Reduced transcript levels for homing receptors and *TACI* in *Utx* mutant GC B cells
Transcript levels of selected genes controlling B cells migration in sorted *Utx* control (grey bars; n=3) and mutant (black bars; n=3) splenic GC B cells, as assessed by RNA-sequencing (RPMs: Reads Per Million mapped fragments). Expression of the Tumor Necrosis Factor (TNF) receptor superfamily member TACI, controlling IgA isotype switching was also included in the analysis. All genes resulted significantly downregulated (fold change < -1,2; adjusted p- value <0,05). Lines represent mean values ± S.D.

3.4.4. Immunoglobulin somatic hypermutation and clonal selection in *Utx* mutant GC B cells

Utx deficiency in mature B cells increases the pool of GC B cells, and in particular that of CBs. The latter result prompted us to investigate the consequences of *Utx* deficiency on the process of Ig somatic hypermutation (SHM) and antigen-driven clonal selection. Upon immunization with NP-CGG, in C57BL/6 mice, B cells expressing the V_H186.2 Ig V gene are preferentially recruited into the GC reaction (Cumano and Rajewsky 1986). Here, during clonal selection, NP-specific B cells carrying selected point mutations are gradually expanded as a result of increased affinity of their B cell receptors for the antigen NP. We sorted splenic GC B cells from $Utx^{fl/fl}$; $Mb\text{-}1^{cre/+}$ mutant and $Utx^{+/+}$; $Mb\text{-}1^{cre/+}$ control mice 14 days post NP-CGG immunization. From these cells, V_H186.2-bearing IgH V gene rearrangements were specifically amplified by genomic PCR, cloned and subjected to Sanger sequencing. Results of the analysis are depicted in Table 18 and are representative of 2 mice/group. IgH V gene mutation frequency

was slightly reduced in Utx mutant GC B cells when compared to controls (1,58% versus 2,17%), with clonal complexity comparable between the two experimental groups as revealed by analysis of the CDR3 region (Table 18).

	Samples (nr)	Unique V_H rearrang. /total	Mutation spectrum/ V_H rerrang. (nr)	Mutation Frequency (%)	TGG ⇒ TTG (W33L; %)
***Utx*$^{+/+}$GC**	2	30/33	1-26	2,17	53,3
***Utx*$^{fl/fl}$ GC**	2	23/27	1-15	1,58	12,7

Table 18. IgH SHM analysis and clonal selection in Utx control and mutant GC B cells

Analysis of somatic mutations in V_H186.2-bearing V_H rearrangements cloned from *Utx* control (*Utx*$^{+/+}$; *Mb-1*$^{cre/+}$; *n*=2) and mutant (*Utx*$^{fl/fl}$; *Mb-1*$^{Cre/+}$; *n*=2) sorted GC B cells at day-14 post NP-CGG immunization. Uniqueness of V_H rearrangements was assessed through CDR3 sequence analysis. Mutation frequency and antigen-driven clonal selection was calculated as described in the Methods section.

Antigen-driven affinity maturation was measured focusing the attention to the mutational spectrum of codon-33 of the V_H186.2 gene (Weiss and Rajewsky 1990). Strikingly, the frequency of unique V_H rearrangements bearing a tryptophan-to leucine (W33L) substitution at codon-33, which confers a 10-fold higher affinity of the BCR for NP, were reduced from 53,3% to 12,7% in *Utx* mutants (Table 18). These results suggest that whereas the somatic hypermutation machinery is largely independent from UTX function, its loss greatly interferes with the capacity to positively select GC B cells carrying high-affinity BCRs.

3.4.5. Altered serum Ig titers in B cell specific *Utx* mutant mice

To investigate the contribution of UTX to antibody responses, we first measured by ELISA serum immunoglobulin titers in *Utx*$^{fl/fl}$*; Mb-1*$^{cre/+}$ mutant and *Utx*$^{+/+}$*; Mb-1*$^{cre/+}$ control mice (on the 129/SV X C57BL/6J mixed genetic background), in resting conditions. *Utx* mutant animals displayed a consistent and significant decrease in IgG1, IgG2b and IgA serum titers. IgG3 levels also decreased in Utx mutant animals, yet more marginally (Figure 53). Conversely, *Utx* loss led to significantly higher IgM serum titers when compared to control mice (Figure 53). Preliminary data on the first set of *Utx* mutant mice on the pure C57BL/6J background have confirmed these results (data not shown). Together, our data point to a contribution of UTX to the process of Ig class switching and are reminiscent of a (mild) hyper-IgM immunodeficiency.

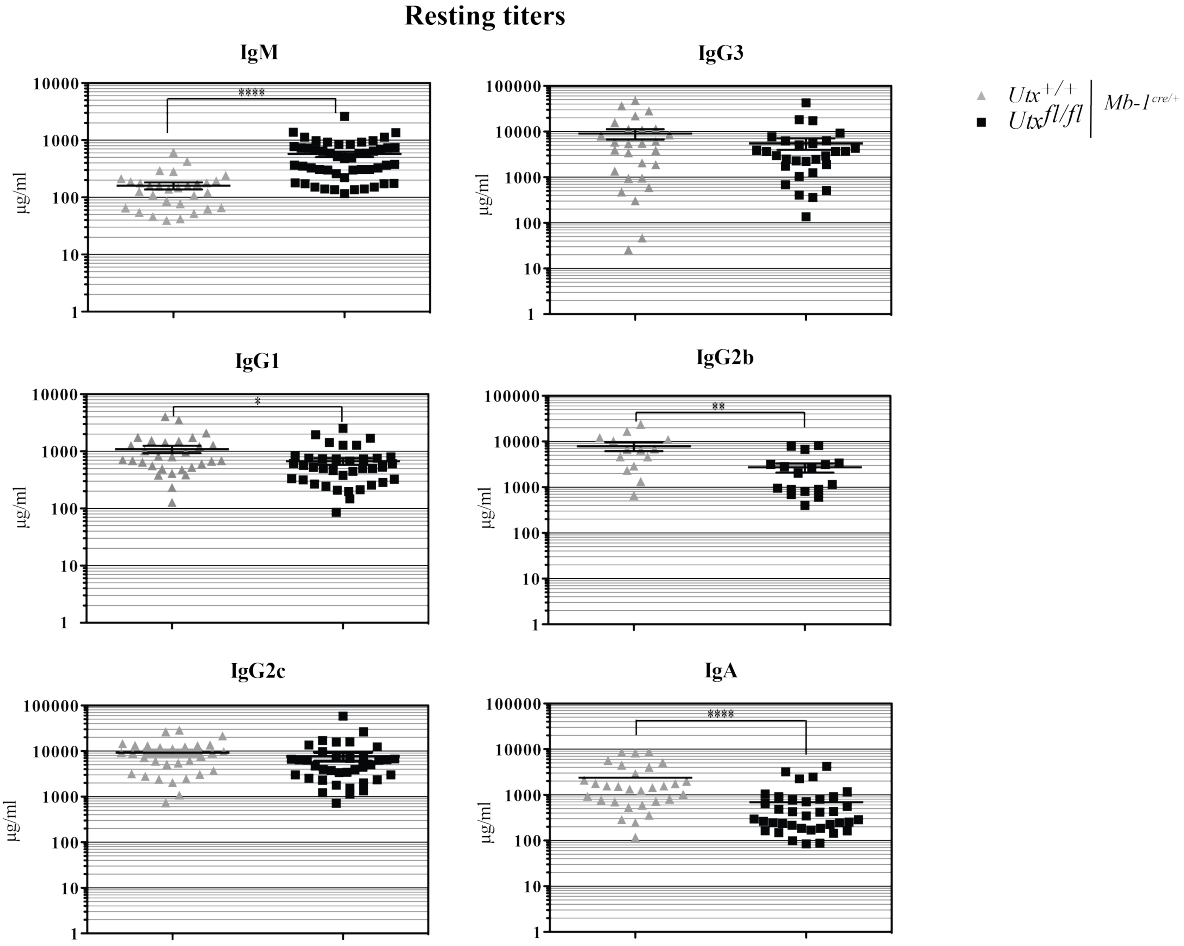


Figure 53. *Utx* KO mice exhibit altered serum antibody titers in resting conditions Quantification of Ig serum titers in un-immunized *Utx* control (grey triangles; n=30 for IgM, IgA and IgG1 and n=27 for IgG3) and mutant (black squares; n=50 for IgM, n=37 for IgA and IgG1 and n=29 for IgG3) mice, as assessed by ELISA. Each dot corresponds to one mouse. Lines represent mean values ± SEM. (non-parametric Mann-Whitney test; * p< 0.05; ** p<0.1 **** p< 0.0001).

3.4.6. Effect of *Utx* deficiency on the production of antigen-specific IgM and IgG1 antibodies and antibody-secreting cells

3.4.6.1. Primary antibody responses

Impaired selection in *Utx* mutant mice of GC B cell variants expressing high-affinity BCRs predicts that mutant animals will suffer from impaired production of terminally differentiated plasma cells secreting antigen-specific high-affinity immunoglobulins. To address this point, we measured NP-specific IgM and IgG1 serum titers in cohorts of *Utx* mutant (*Utx*$^{fl/fl}$*; Mb-1*$^{cre/+}$) and control animals immunized with NP-CGG. ELISA assays were performed on serum retrieved from the animals at different time points after immunization (Figure 54).

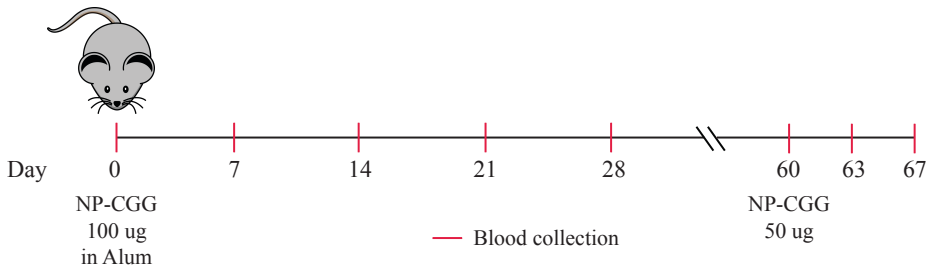


Figure 54. Sera collection scheme for the analysis or primary and secondary T-cell dependent antibody responses

In contrast to the failure of *Utx* mutant GC B cells to properly select variants expressing high-affinity BCRs, both low- and high-affinity soluble anti-NP IgM and IgG1 antibodies were by-and-large unaffected by *Utx* inactivation (Figure 55). Hence, the interference with clonal selection of GC B cells resulting from *Utx* inactivation does not prevent terminal differentiation of PCs secreting high affinity antigen-specific antibodies.

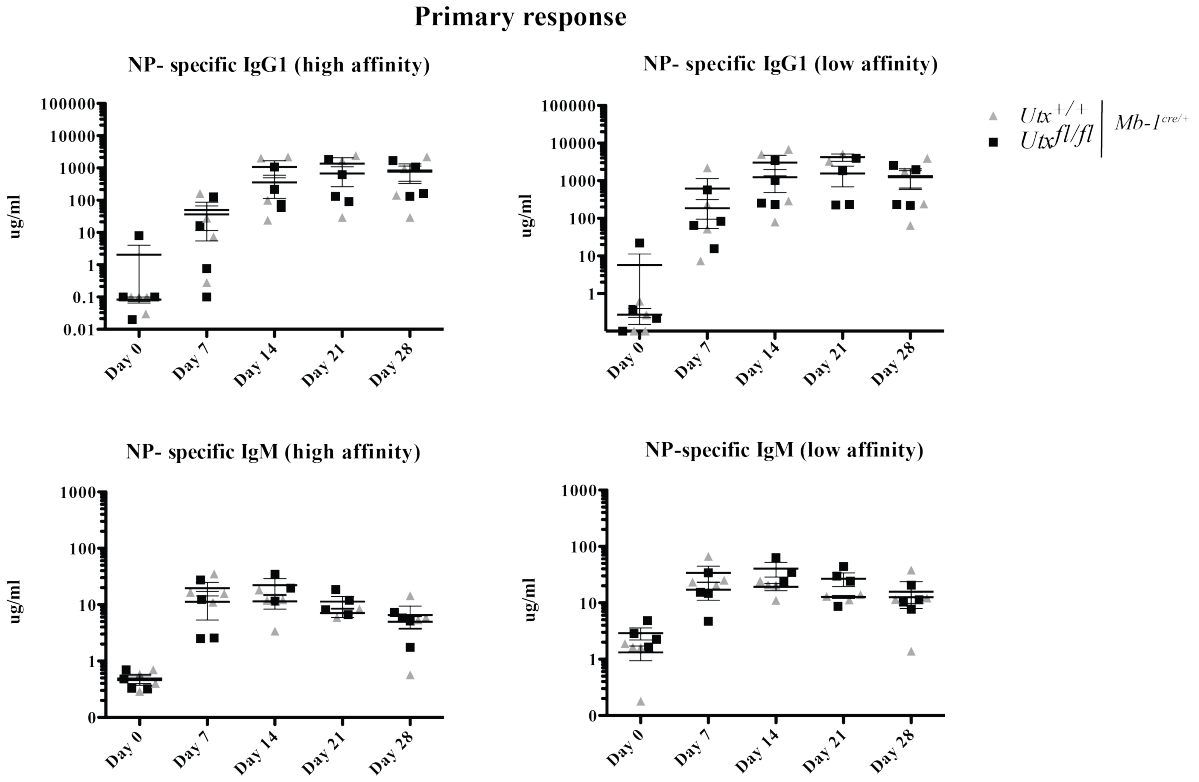


Figure 55. Normal antigen-specific IgM and IgG1 antibody responses in *Utx* mutant mice after immunization with alum-precipitated NP-CGG

Quantification by ELISA of respectively total and high-affinity NP-specific IgM and IgG1 serum titers in *Utx* control (grey triangles; *n*=4) and mutant (black squares; *n*=4) mice, at the indicated time points after immunization with alum-precipitated NP_{28}-CGG.

3.4.6.2. Secondary antibody responses

Recall antibody responses are mostly contributed by the activation of previously generated high-affinity, antigen-specific long-lived memory B cells which differentiate into antibody-secreting plasma cells. To address the ability of *Utx* mutant mice to mount a recall response, NP-CGG immunized $Utx^{fl/fl}$; $Mb\text{-}1^{cre/+}$ mutant mice and controls were boosted 60 days later with a second (lower) dose of NP-CGG in the absence of adjuvant. Blood sera were collected respectively 3 and 7 days following secondary immunization and NP-specific high-affinity and low-affinity IgG1 and IgM antibodies were quantified by ELISA (Figure 54). As shown in Figure 56, high- and low-affinity NP-specific IgM and IgG1 secondary antibody titers were largely unaffected by *Utx* inactivation This result suggests that the formation of antigen-selected long-lived high affinity memory B cells, as well as their capacity to directly differentiate into PCs is largely unaffected by *Utx* inactivation.

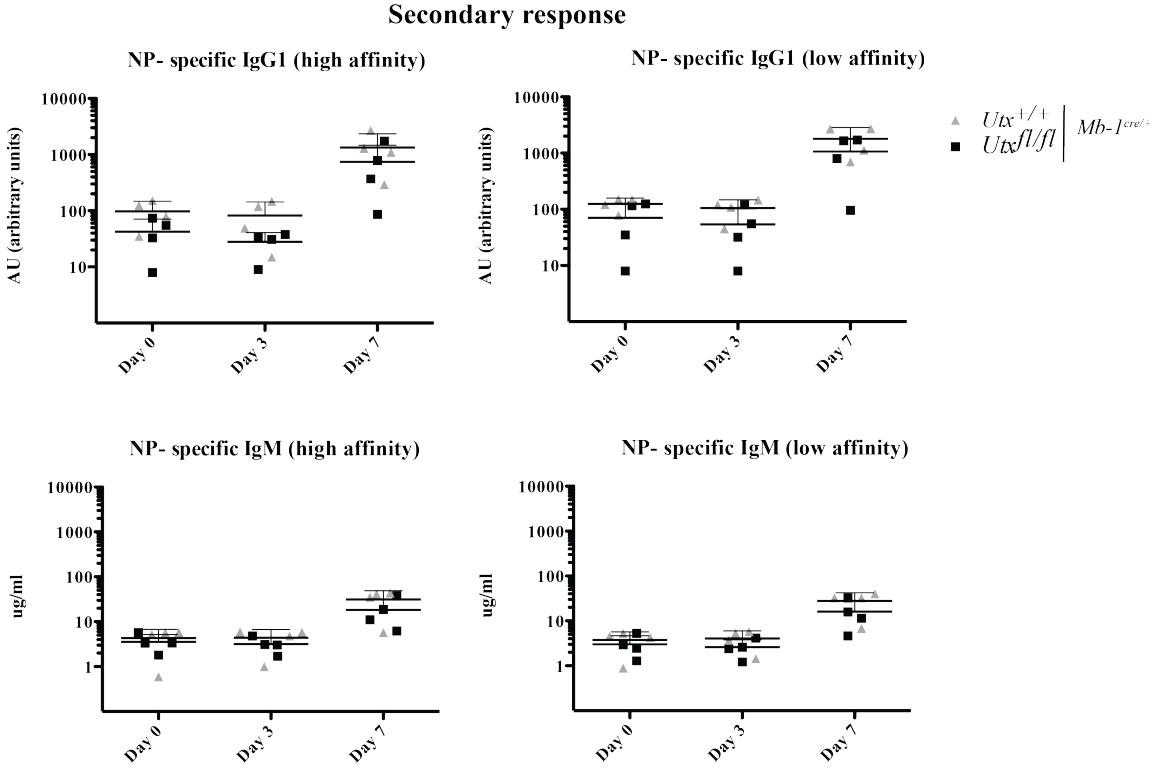


Figure 56. Recall antigen-specific IgM and IgG1 antibody responses are comparable between *Utx* control and mutant mice

Quantification by ELISA of respectively total (low affinity) and high-affinity NP-specific IgM and IgG1 serum titers in *Utx* control (grey triangles; n=4) and mutant (black squares; n=4) mice, at the indicated time points after secondary NP_{28}-CGG immunization (performed 60 days after the first).

3.4.6.3. Formation of antigen-specific plasma cells in vivo in Utx mutant animals

In secondary antibody responses, memory B cells get activated in response to re-encounter of the antigen, triggering ultimately a differentiation program leading them to become antibody-secreting PCs. To study whether the lack of *Utx* could affect the process of terminal differentiation from memory B cells, $Utx^{fl/fl}$; $Mb\text{-}1^{cre/+}$ mutant and $Utx^{+/+}$; $Mb\text{-}1^{cre/+}$ mice were immunized with alum-precipitated NP-CGG, boosted 60 days later again with lower doses of the same antigen in the absence of adjuvant, and, ultimately, sacrificed in order to assess by flow cytometry the fraction of NP-specific PCs in the spleen 7 days after antigen re-challenge (Figure 57).

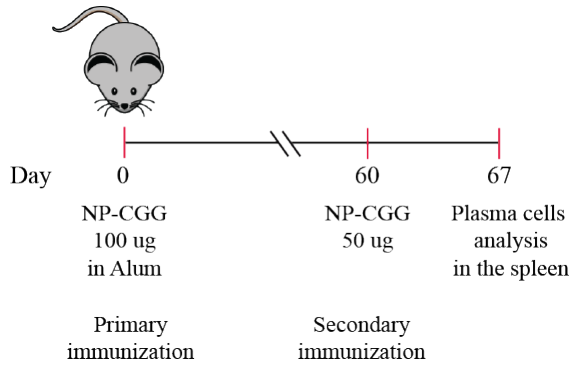


Figure 57. Timeline for the analysis of antigen-specific plasma cells *in vivo*

Flow cytometric analyses revealed an 80% reduction in the frequencies and a 70% reduction in the number of splenic MHC II^-, $CD11c^-$, $Ter119^-$, $CD4^-$, $CD8^-$, $CD3^-$, $Gr1^-CD19^-$ $Pax5^{lo}$ NIP^+ *bona fide* newly generated PCs, in *Utx* mutant mice when compared to controls (Figure 58). The combination of the data on antigen-specific antibody titers and those on the numbers of newly formed antigen-specific PCs in B-lineage mutant *Utx* mice are compatible with a scenario in which *Utx* deficiency negatively interferes with the formation of antigen-specific PCs. However, a partial penetrance of the phenotype allows residual *Utx* defective antigen-specific PCs to homeostatically expand and ultimately achieve the release of normal titers of antigen-specific antibodies.

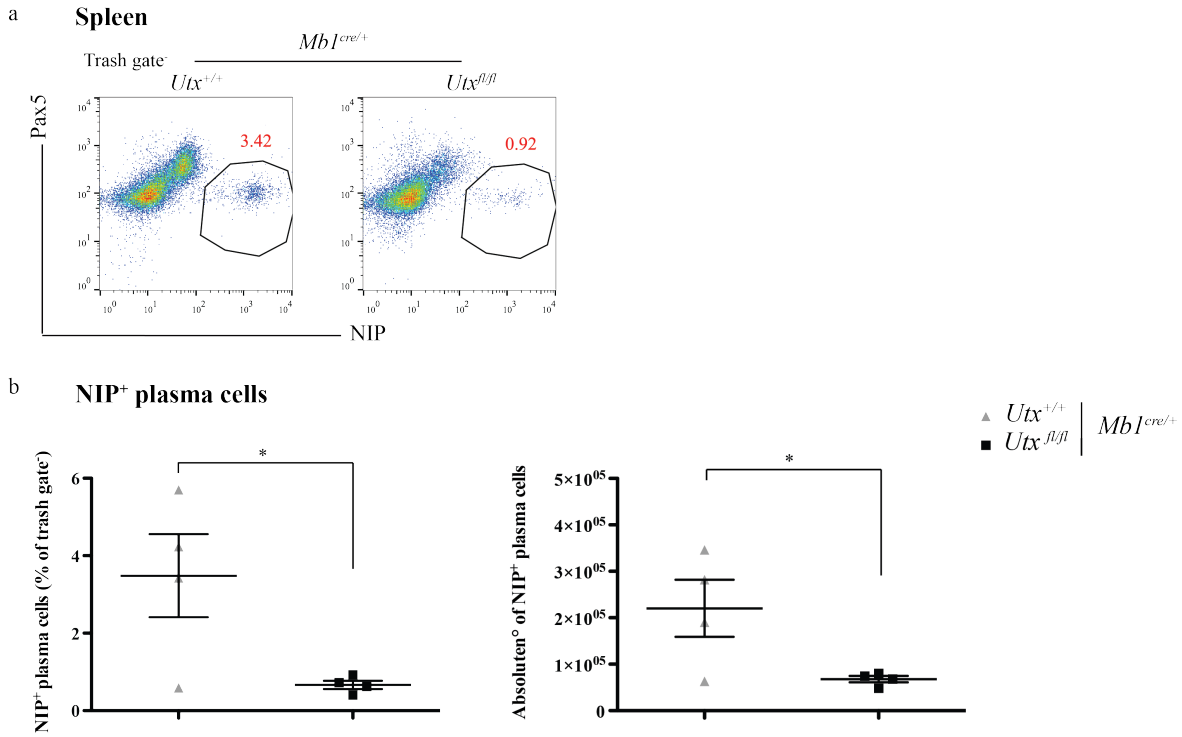


Figure 58. Newly formed antigen-specific plasma cells are reduced in the spleen of *Utx* mutant mice after recall immunization with the T-cell dependent antigen NP-CGG

a. Representative flow cytometric analysis of MHC II$^-$, CD11c$^-$, Ter119$^-$, CD4$^-$, CD8$^-$, CD3$^-$, Gr1$^-$CD19$^-$ pre-gated splenic cells (trash gate) stained for the transcription factor PAX5 and for NIP. Boxed Pax5^{lo}NIP$^+$ cells were considered *bona fide* PBs identified 7 days after boosting with NP-CGG of *Utx* control (left; n=4) and mutant (right; n=4) animals. b. Frequencies (left) and absolute numbers (right) of gated Pax5^{lo}NIP$^+$ PBs in the spleen of of *Utx* control (left; n=4) and mutant (right; n=4) animals. Each dot represents a mouse. Lines indicate the mean values ± SEM. (t-test; * p< 0.05).

3.5. Effects of *Utx* inactivation on terminal B cell differentiation

3.5.1. *Utx* expression is rapidly downregulated in B cells undergoing terminal differentiation

Data shown in Figure 58 suggest a possible defect in the generation of antigen-specific plasma cells. To support this hypothesis, *ex vivo* isolated primary B cells from *Utx* control mice were subjected to *in vitro* stimulation with either lipopolysaccharide or a combination of CD40 activation and IL21. Total RNA extracted from control B cells at different time points after the initial stimulation was reverse transcribed and cDNA employed in quantitative RT-PCR analyses to measure Utx transcripts.

In response to LPS stimulation, *Utx* mRNA levels remained steady for the first two hours. By 4 hours of stimulation *Utx* transcripts were 2-fold downregulated, with later time points failing to detect further changes in expression (Figure 59a). In a similar fashion, taking advantage of

the so-called induced germinal center-like B cell (iGB) *in vitro* culture system, in which primary B cells are activated through the CD40 receptor in combination with BAFF and IL4 for the first four days and IL21 for the following four (Nojima, Haniuda et al. 2011), we could observe a rapid downregulation of *Utx* transcripts soon after the induction of PC differentiation (Figure 59b, c). Taken together, these results point to a possible role of UTX in the very early stages of PC differentiation.

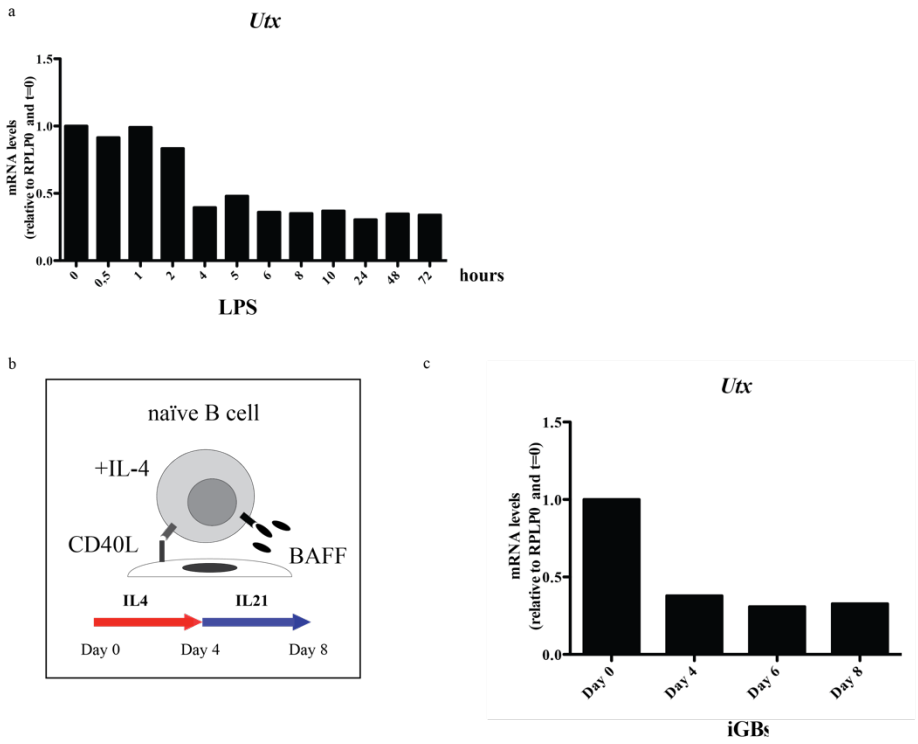


Figure 59. *Utx* expression is downregulated upon B cell activation

a. Quantitative RT-PCR analysis of *Utx* transcript levels in splenic B cells isolated from C57BL/6J mice and stimulated in vitro with LPS (20µg/ml) for the indicated time. *Utx* mRNA levels are normalized to those of the housekeeping gene *Rplp0* and represented as relative to the ones measured in resting B cells (t=0). b. (Left) Schematic representation of the iGB culture system. (Right) Quantitative RT-PCR analysis of *Utx* transcript levels in splenic B cells isolated from C57BL/6J mice and subjected to the iGB *in vitro* culture system for the indicated time. *Utx* mRNA levels are normalized to those of the housekeeping gene *Rplp0* and represented as relative to the ones measured in resting B cells (day 0).

3.5.2. Transcripts for PC transcription factors *Prdm1* and *Irf4* are reduced in *Utx* mutant GC B cells

In the GC, a minor antigen-selected fraction of B cells differentiates into long-lived antibody-secreting PCs (Victora, Schwickert et al. 2010). The transcriptional program driving terminal differentiation of rare antigen-selected GC B cells is linked to the downregulation of the B cell master regulator *Pax5* together with the extinction of the GC B cell master regulator *Bcl6*. At the same time, transcription factors necessary to initiate and sustain the PC differentiation program include *Irf4, Blimp-1/Prdm1* and *Xbp-1* (Gupta, Anthony et al. 2001; Klein, Casola et

al. 2006). Several reports have suggested a role for Polycomb Repressive Complex 2 in the silencing of the *Irf4* and *Prdm1* genes in cells lacking expression (or expressing low levels) of these transcription factors (Caganova, Carrisi et al. 2013). At the same time, studies in macrophages have identified *Irf4* as a direct target of the H3K27me3 demethylase JMJD3, in line with unpublished work from our group showing that *Jmjd3* mutant B cells fail to upregulate *Irf4* upon *in vitro* induction of PC differentiation (Rahmat and Casola, unpublished work).
Together these studies postulate a contribution of UTX in modulating the expression of *Prdm1* and *Irf4* in B cells triggered to differentiate to plasma cells such as a subset of GC B cells. To test this hypothesis, $CD19^{+}CD38^{lo}Fas^{hi}$ GC B cells were sorted from SRBC immunized *Utx*$^{fl/fl}$; *Mb-1cre/+*$^{/+}$ conditional mutant and control mice (on the 129/SV x C57BL/6 genetic background) and subjected to transcriptomic profiling. We found that upon *Utx* inactivation transcript levels for both *Irf4* and *Prdm1* were modestly reduced in the bulk of GC B cells when compared to controls (Figure 60). Given that only a minor fraction of GC B cells undergoes terminal differentiation (and therefore induce high *Prdm1* and *Irf4* gene transcription), our results predict that *Utx* deficiency causes an underrepresentation in the GC of B cells upregulating PC transcription factors *Irf4 and Prdm1* to initiate the terminal differentiation program.

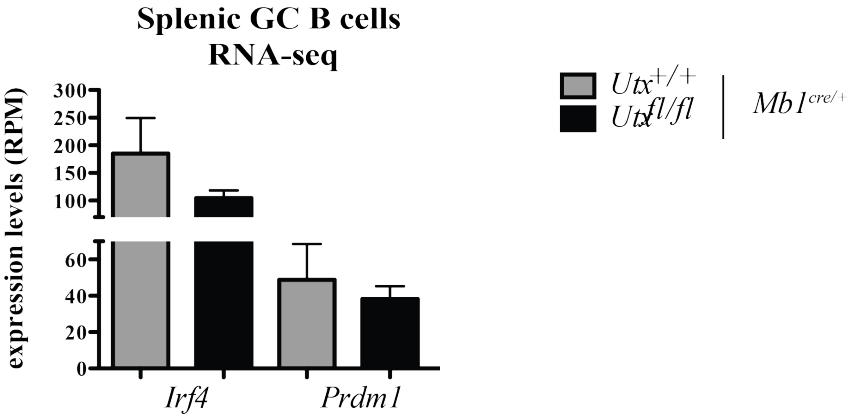


Figure 60. Reduced *Irf4* and *Prdm1* transcript levels in *Utx* mutant GC B cells
Transcript levels of *Irf4* and *Prdm1* transcription factors in *Utx* control (grey bars; *n*=3) and mutant (black bars; *n*=3) germinal center B cells, as assessed by RNA-sequencing (RPM: Reads Per Million mapped fragments). Bars represent mean values ± S.D.

3.5.3. UTX is required for *Irf4* upregulation in activated B cells

The reduction in *Irf4* transcript levels measured in the bulk population of *Utx* mutant GC B cells may reflect the relative enrichment of the centroblast fraction which expresses lower levels of *Prdm1* and *Irf4*. Therefore, to test whether UTX directly influences the levels of *Irf4*, *ex vivo* isolated primary B cells were stimulated in vitro with LPS and monitored for IRF4 expression.

To this end, we measured by intracellular flow cytometry the levels of IRF4 protein in *Utx* proficient (*Utx*$^{fl/fl}$*; Mb-1*$^{cre/+}$) and mutant (*Utx*$^{fl/fl}$*; Mb-1*$^{cre/+}$*)* B cell cultures. The results of this analysis revealed that upon *Utx* inactivation primary B cells activated with LPS for 3 days showed a defect in the upregulation of IRF4 expression (Figure 61a). The failure to upregulate IRF4 was confirmed in *Utx* KO iGBs cultures stimulated with CD40L and IL21 (Figure 61b). To further validate these results, IRF4 protein levels were measured by immunoblotting analyzing protein lysates extracted from *Utx* control and mutant iGB cultures stimulated respectively for two and four days with CD40L and IL21 (Figure 61c). The decrease in IRF4 protein levels correlated with a down-regulation of *Irf4* transcripts measured by qPCR in *Utx* mutant iGB cells stimulated with CD40L and IL21 (Figure 62). Interestingly, *Irf4* transcript levels were found unaffected in *Utx* mutant resting B cells prior to their stimulation with LPS (day 0 in Figure 62), consistently with transcriptomic analyses performed on FO B cells, where *Irf4* gene was not significantly deregulated upon *Utx* inactivation (data not shown). These results, together, indicate that UTX plays an important role in the induction of *Irf4* gene expression in B cells committed to undergo terminal differentiation upon stimulation with LPS or CD40L+IL21.

3.5.4 *In vitro* plasma blast differentiation in the absence of *Utx*

Next, we investigated the impact of impaired upregulation of *Irf4* expression on *in vitro* induced plasma cell differentiation. To address this, *Utx*-proficient and -defective B cell cultures were stimulated *in vitro* with LPS for three days, after which cells were assessed by flow cytometry for expression of IRF4 and the plasma cell marker CD138/Syndecan-1. This analysis allowed to follow distinct subsets of B cells differing in the levels of IRF4 and/or CD138 (Figure 63). In particular, *Utx* inactivation led to an enrichment of a population of IRF4^{lo}CD138^{-} B cells at the expense of the subset of IRF4^{hi} CD138^{-} activated B cells (Figure 63a). Similar results were observed when primary B cells from *Utx* mutant mice were activated *in vitro* with CD40L+IL-21 (Figure 63b).

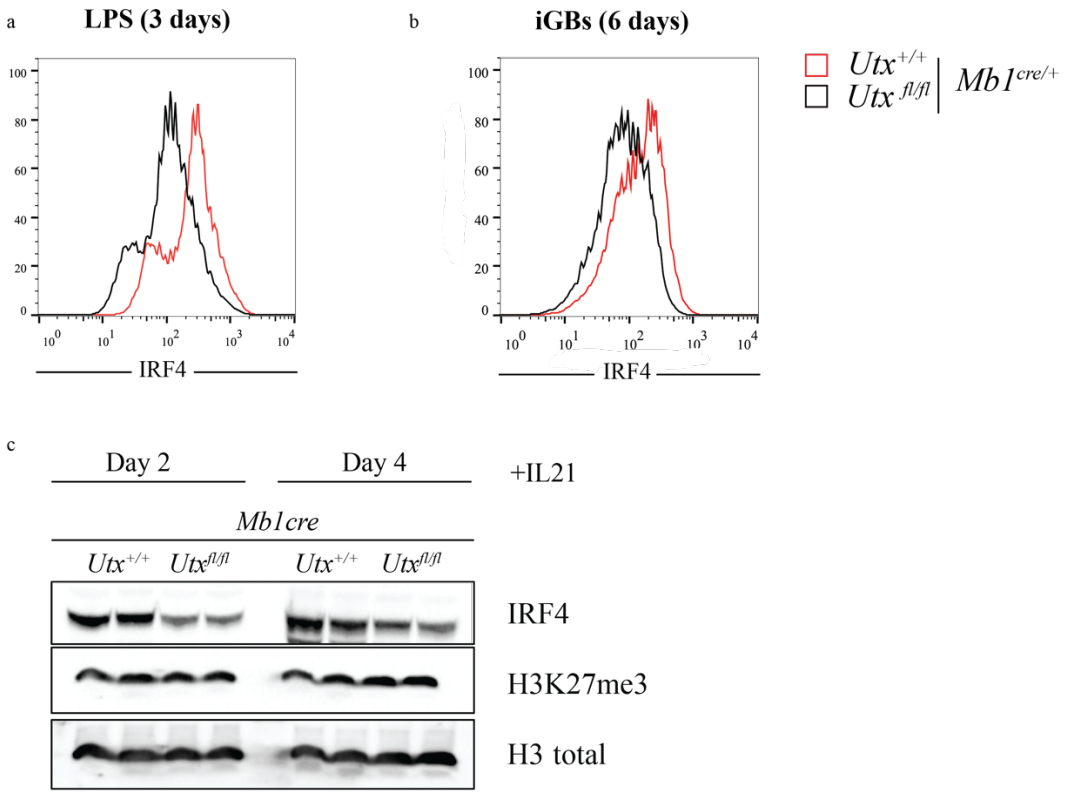


Figure 61. Reduced IRF4 protein levels in *Utx* mutant *in-vitro* activated B cells

a. Quantification of IRF4 protein levels in purified splenic B cells of *Utx* control (red line; n=3) and mutant (black line; n=3) mice activated *in vitro* for three days with LPS (2,5 µg/ml), as assessed by intracellular flow cytometric analysis. Data are representative of 3 independent experiments. b. IRF4 protein levels in *Utx* control (red line) and mutant (black line) iGB *in vitro* cultures at day-6 of CD40L stimulation (including two days in the presence of IL-21). Data are representative of 2 independent experiments. **c.** Immunoblotting analysis of IRF4 and H3K27me3 levels in *Utx* control (n=2) and mutant (n=2) iGB cultures stimulated respectively for 2 and 4 days with IL-21. Histone H3 acted as loading control. Data are representative of 2 independent experiments.

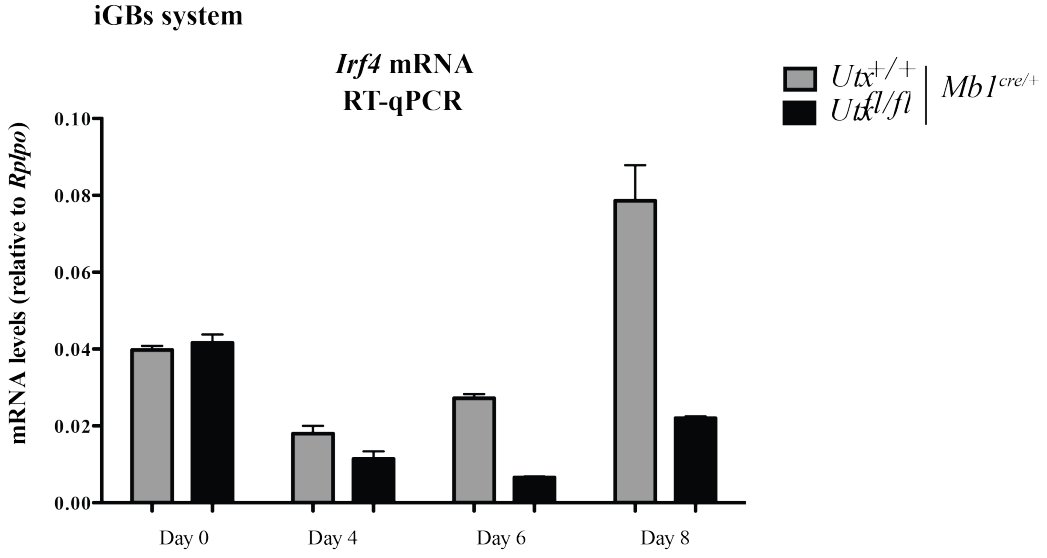


Figure 62. *Irf4* transcript levels are reduced in *Utx* mutant B cells after CD40/IL21 stimulation

Quantitative RT-PCR analysis of *Irf4* transcript levels in *Utx* control and mutant iGB cultures, analysed at the indicated time points. *Irf4* mRNA levels are normalized to those of the housekeeping gene *Rplp0*. Bars represent the mean value of 3 replicates ± S.D.

Conversely, the fraction of IRF4^{hi}CD138^{+} plasma blasts was only modestly affected in *Utx* mutant B cell cultures stimulated with CD40L+IL21 and unaffected in B cells upon LPS activation. The latter result is suggestive of a primary defect in B cell activation suffered by *Utx* mutant B cells, which coincides with a defect to upregulate IRF4 expression. Once *Utx* mutant cells succeed to become activated and to upregulate IRF4 levels, the transition from an activated B cell to a *bona fide* CD138^{+} IRF4^{hi} plasma blast can successfully proceed.

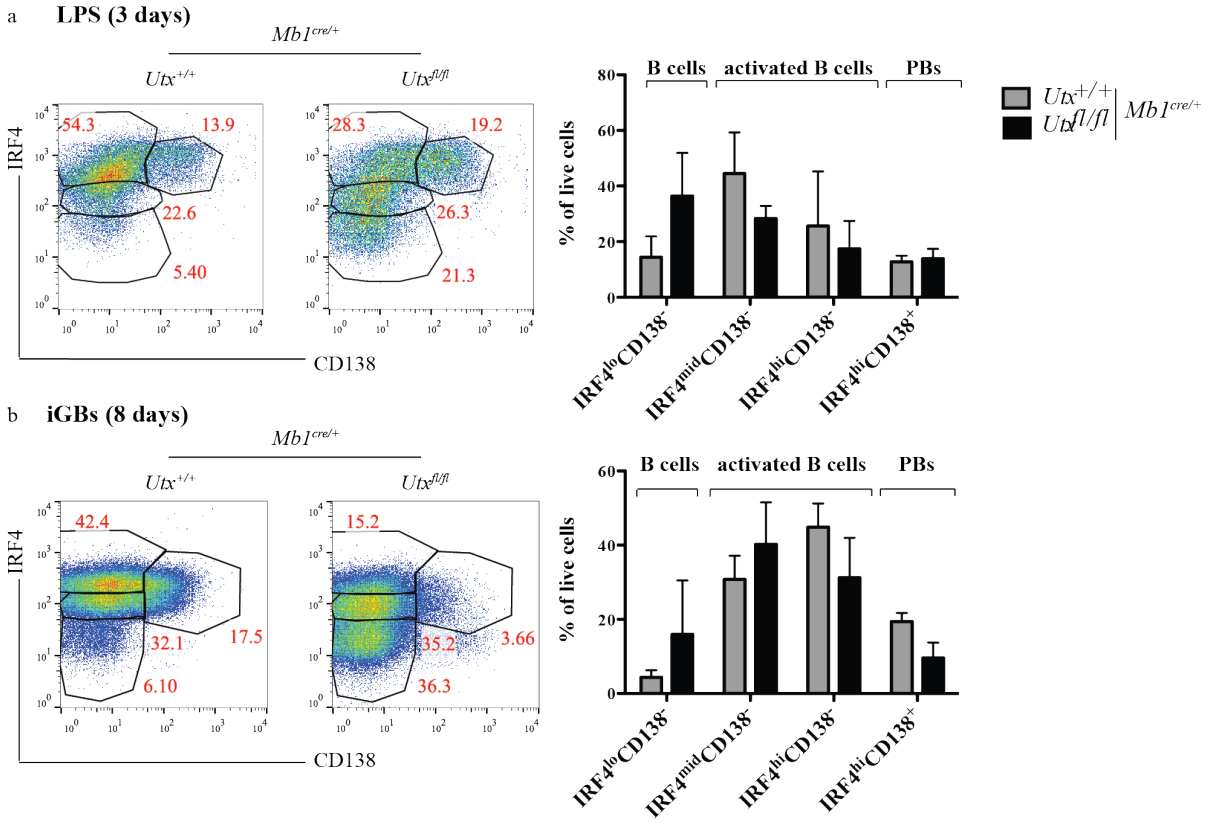


Figure 63. *In vitro* plasmablast differentiation in the absence of *Utx*

a. (Left) Representative flow cytometric analyses of *Utx* control (left; n=4) and mutant (right; n=4) splenic B cells stimulated *in vitro* either for three days in the presence of LPS, or for eight days with CD40L and IL-21. Numbers indicate frequencies of boxed CD138^{-}IRF4^{lo} resting B cells, CD138^{-} IRF4$^{mid/hi}$ activated B cells and CD138^{+} IRF4^{hi} plasma blasts. Right: summary of the data shown in the left panel. Bars indicate average frequencies +/- SEM and are representative of 3 independent experiments. For iGB cultures, data are representative of 2 independent experiments.

3.5.5. *Prdm1* gene expression in *Utx* mutant B cells undergoing PC differentiation *in vitro*

The defect of a fraction of *Utx* mutant B cells to effectively upregulate IRF4 expression in response to either LPS of CD40L +IL21 stimulation could be linked to interferences with *Prdm1*/BLIMP1 upregulation in these cells (Sciammas, Shaffer et al. 2006) To address this point, BLIMP1 protein levels were quantified by intracellular flow cytometric analysis in *in vitro* cultures of *Utx* control and mutant B cells stimulated with LPS. BLIMP1 levels increased to the same extent in *Utx* KO activated B cells compared to controls, thus ruling out the possibility that a defect in BLIMP1 upregulation is involved in the impaired IRF4 induction observed in a subset of *Utx* KO B cells (Figure 64).

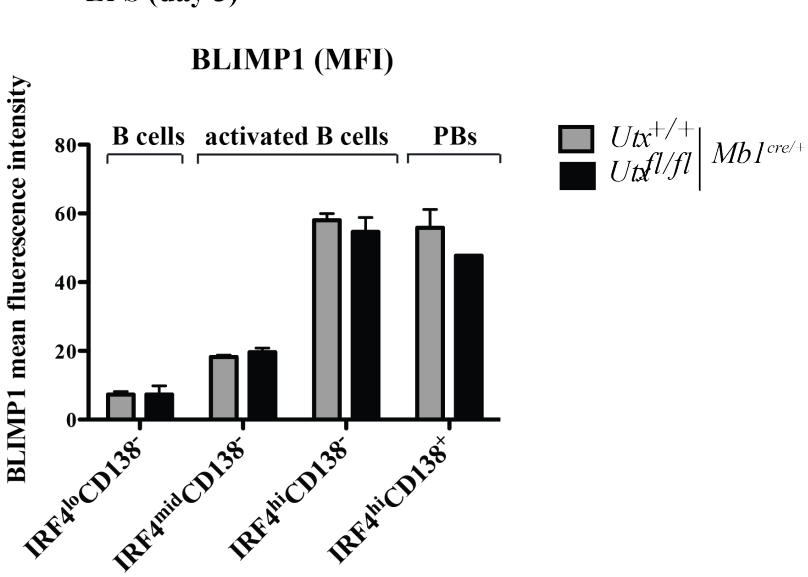


Figure 64. *In vitro* BLIMP1 upregulation in bona fide activated B cells and plasma blasts is not affected by *Utx* loss

BLIMP1 expression levels shown as mean fluorescence intensity measured by FACS analyses in each of the indicated B cells populations, gated according to IRF4 and CD138 expression at day 3 upon LPS stimulation, as displayed in Figure 53. Grey bars represent $Utx^{+/+}$control while black bars represent $Utx^{fl/fl}$ conditional mutant samples.

3.6. The impact of *Utx* deficiency on immunoglobulin isotype switching

3.6.1. *Utx* deficiency affects fractions of isotype-switched cells upon *in vitro* stimulation

IRF4 has been implicated in the regulation of Ig isotype switching, possibly by inducing the expression of Activation-Induced cytidine Deaminase (AID) (Klein, Casola et al. 2006). Given the impaired IRF4 upregulation in *Utx* mutant B cells upon activation, and the reduced serum titers of isotype-switched antibodies in *Utx* mutant mice, we postulated that *Utx* controls Ig isotype switching, possibly through the regulation of IRF4 expression. To closely monitor the effect of UTX on Ig class switch recombination, we measured the fraction of isotype-switched B cells generated in vitro in B cell cultures from *Utx* control and mutant mice activated with different stimuli. Upon *in vitro* stimulation with LPS, *Utx* mutant B cells showed a significant reduction in the proportion of IgG3-switched B cells (Figure 65a). A milder effect on Ig isotype switching was observed when *Utx* mutant B cells were stimulated with LPS+IL4 to generate IgG1-expressing B cells (Figure 65b). A partial defect in IgG1 (and possibly of IgE) class switching was also observed when *Utx* mutant B cells were stimulated with CD40L and IL4 in the presence of BAFF (Figure 65c). This defect coincided with a corresponding increase in the fraction of unswitched IgM^+ cells. These results point to a role of *Utx* in the generation of isotype-switched B cells, in particular those expressing IgG3 and IgA isotypes (see below).

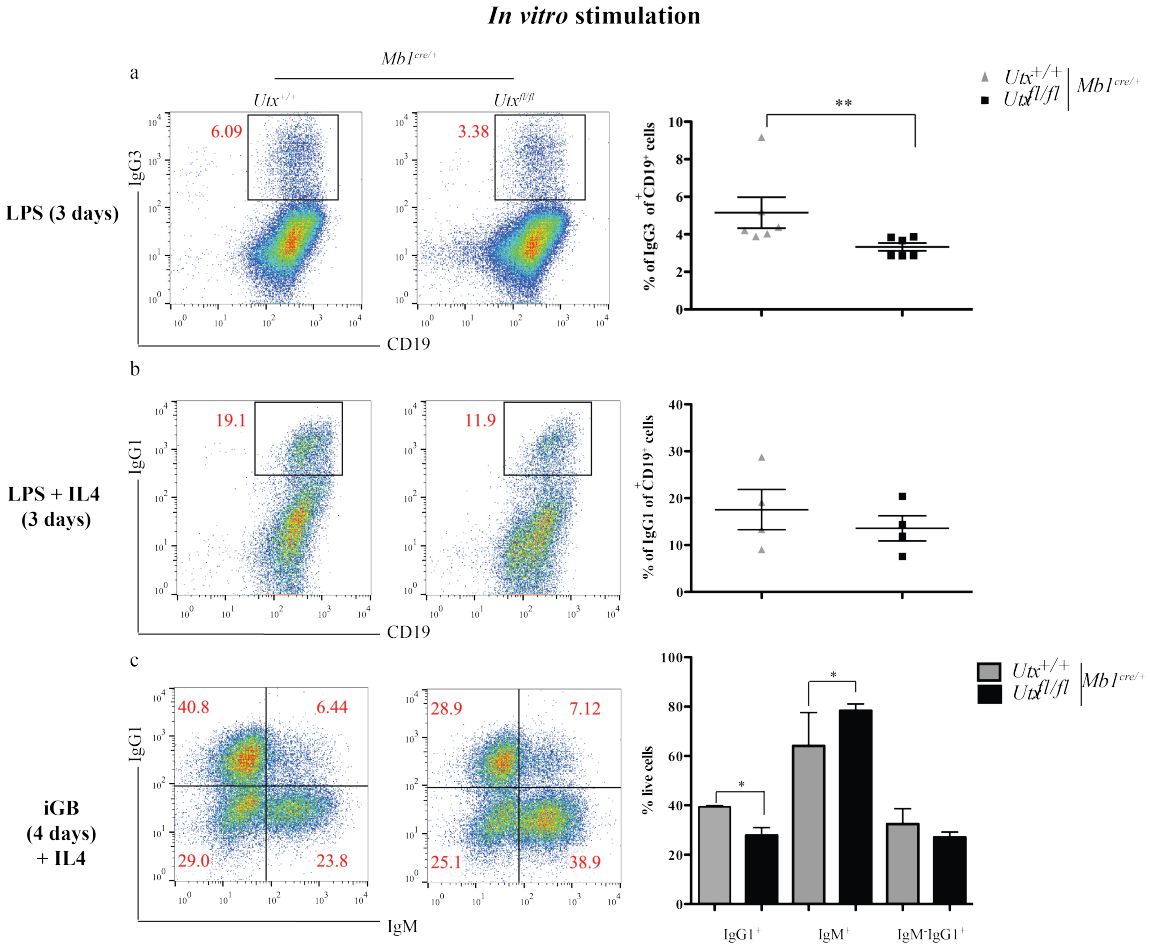


Figure 65. *In vitro* IgG3 and IgG1 isotype switching is impaired in *Utx* mutant B cells

Representative flow cytometric analysis of *in-vitro* activated *Utx* control (left; *n*=6 for LPS stimulations and *n*=4 for LPS+IL-4 and CD40L +IL-4 stimulations) and mutant (right; *n*=6 for LPS stimulations and *n*=4 for LPS+IL-4 and CD40L +IL-4 stimulations) B cells stimulated *in vitro* in the indicated fashion, and analysed by flow cytometry for the indicated surface markers and immunoglobulin isotypes. Numbers indicate frequency of B cells in the corresponding quadrants. Each dot corresponds to one mouse. Histogram bars represent summary of flow cytometric data. (non-parametric Mann-Whitney test * $p< 0.05$; ** $p< 0.01$)

3.6.2. *Utx* mutant B cells show suboptimal activation upon stimulation with TLR agonists

Immunoglobulin isotype switching is linked to cell division (Hasbold, Gett et al. 1999; Hasbold, Corcoran et al. 2004). Therefore, we investigated whether *Utx* inactivation influenced the number of divisions that B cell go through in response to mitogenic stimuli triggering Ig CSR. To this end, we purified resting B cells from the spleen of *Utx* mutant (*Utx$^{fl/fl}$; Mb-1$^{cre/+}$*) and control (*Utx$^{+/+}$; Mb-1$^{cre/+}$*) mice and cultured them for 4 days in the presence of LPS +/- IL4 or with CD40L+ IL4 or with the mitogen α–RP105. Growth curve analysis revealed subtle differences in the proliferative response of the bulk population of activated *Utx* proficient and mutant B cells (Figure 66). To monitor the proliferative response of individual *in-vitro* activated

B cells, the latter were labelled with carboxyfluorescein succinimidyl esther (CFSE) (Hasbold, Corcoran et al. 2004) prior to LPS stimulation and monitored by flow cytometric analysis over the 4 days of culture. The majority of both *Utx* mutant and control B cells responded to the mitogen by undergoing one or multiple rounds of cell division (Figure 67). However, quantification of the proportions of cells that had completed a certain number of divisions revealed an average 2-fold increase in the fraction of *Utx* mutant cells that had divided fewer times when compared to controls (Figure 67). This result was reproduced in 2 experiments, even if the proportion of cells undergoing fewer divisions in *Utx* mutant B cell cultures differed a bit depending on culture conditions and activation efficiency.

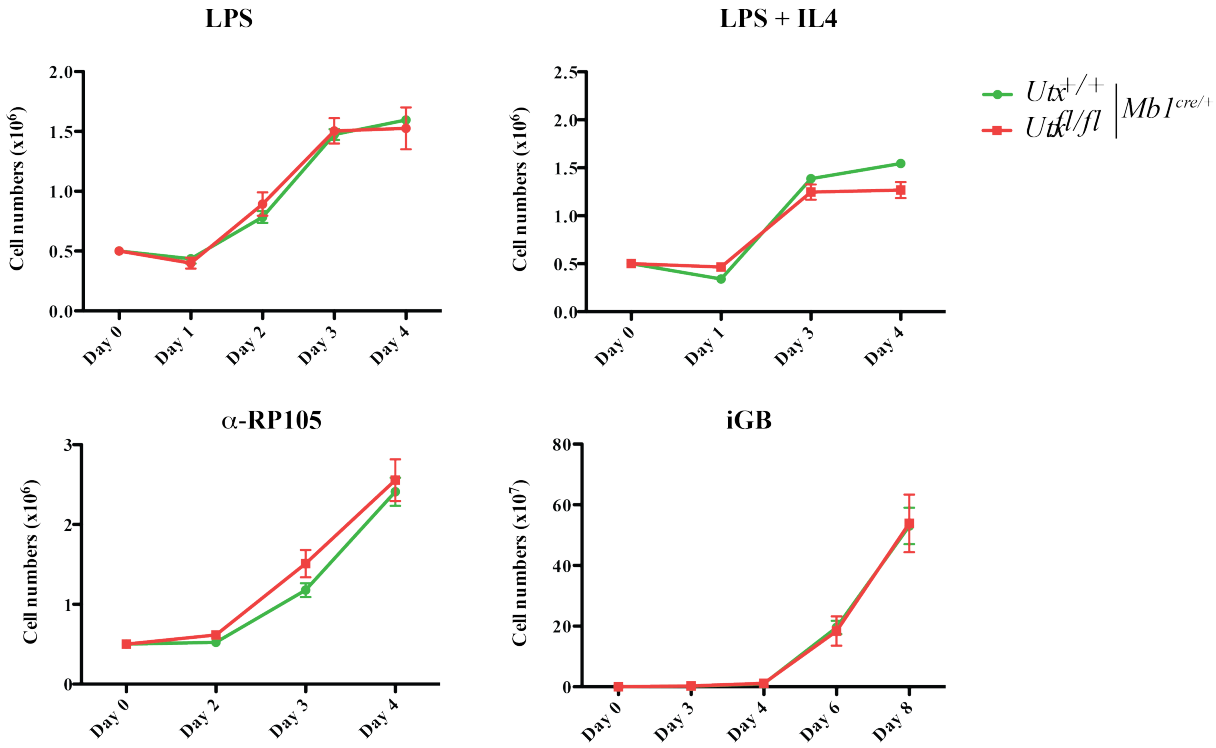


Figure 66. Growth curves of *in vitro* stimulated Utx control and mutant B cells

Representative growth curve analyses of *Utx* control (green line; n=6 for LPS stimulations; n=4 for LPS+IL-4 stimulations and n=2 for α-RP105 stimulations) and mutant (red line; n=6 for LPS stimulations; n=4 for LPS+IL-4 stimulations and n=2 for α-RP105 stimulations) splenic B cells stimulated *in vitro* with the indicated mitogens, and for the indicated time points.

3.6.3. Defective IgG3 isotype switching in *Utx* KO B cells is independent of cell proliferation abnormalities

The failure of a subset of *Utx* mutant B cells to accomplish a higher number of cell divisions after LPS activation could explain the reduced frequency of IgG3-switched B cells in these cultures. To test this hypothesis, *Utx* control and mutant B cells were labelled with CFSE and stimulated in vitro with LPS. After three days from the initial stimulation, cells were analyzed by flow cytometry to determine the frequency of IgG3 switched B cells that underwent a defined number of cell divisions assessed through CFSE dilution measurements. A significant reduction in the frequency of $IgG3^+$ B cells was consistently observed among *Utx* mutant B cells that had completed the same number of cell divisions as their *Utx* proficient counterparts (Figure 68). Hence, the defect of IgG3 isotype switching observed in *Utx* mutant B cell cultures stimulated with LPS is not dependent on defects in proliferation seen for these cells.

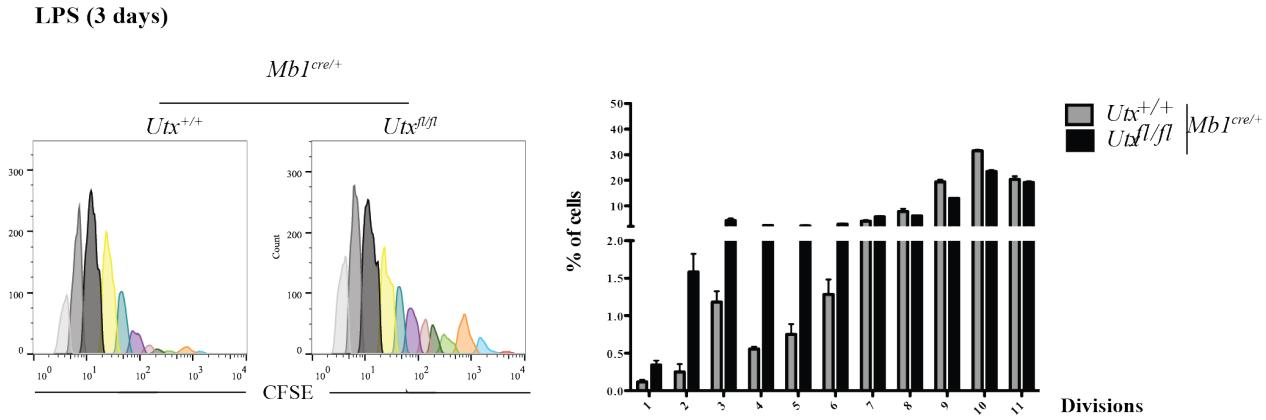


Figure 67. Delayed cell division of a subset of *Utx* mutant B cells stimulated *in vitro* with LPS a. Representative flow cytometric analysis of CFSE-labelled *Utx* control (left; n=2) and mutant (right; n=2) B cells stimulated *in vitro* for 3 days with LPS. B cells were gated on the basis of the degree of CFSE dilution they went through as a result of consecutive cell divisions. Each histogram represents the fraction of B cells that had completed a certain number of cell divisions. b. Quantification of the fraction of *Utx* control and mutant B cells that had undergone the indicated number of cell divisions defined on the basis of the degree of CFSE dilution. Bars represent mean values of 3 replicates ± SEM.

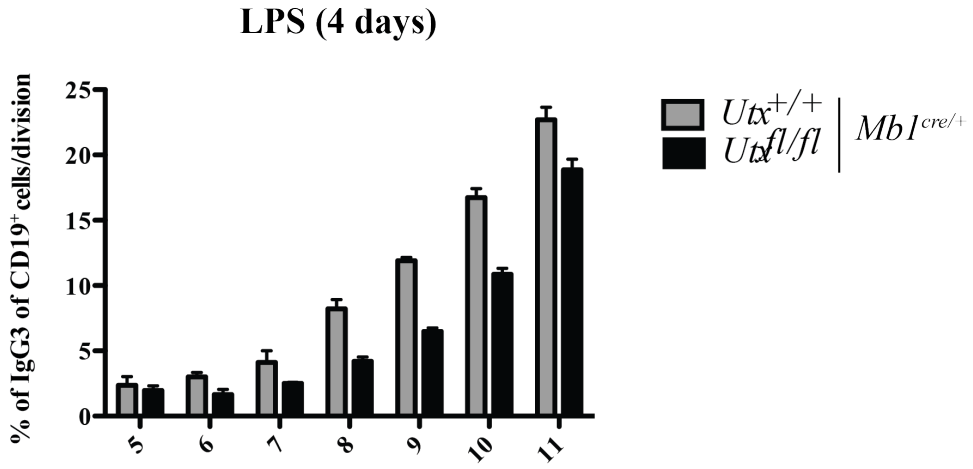


Figure 68. Impaired switching to IgG3 of *Utx* mutant B cells does not depend on defects in cell proliferation

Comparison of the frequency of IgG3-switched B cells in day-4 LPS-stimulated *Utx* control (grey bars) and mutant (black bars) *in vitro* B cell cultures, grouped according to the number of the indicated cell divisions, as assessed by CFSE-dilution assays. Bars represent mean values of 3 technical replicates ± SEM.

3.6.4. The immunoglobulin heavy chain locus is accessible to AID in the absence of *Utx*

Having excluded a role for impaired cell division in the defect of IgG3 isotype switching observed in *Utx* mutant B cell cultures stimulated with LPS, we turned our attention to other possible mechanisms explaining this defect.

Onset of Ig isotype switching is accompanied by activation of germline/sterile transcripts (GLTs) starting from IgH constant region genes placed downstream of Cμ. Transcription at these sites, which is essential for Ig CSR (Radbruch, Burger et al. 1986) is positively regulated by the activity of the MLL/Trithorax complex (Daniel, Santos et al. 2010), which may require the contribution of UTX. Therefore, we tested whether *Utx* mutant B cells, upon activation with LPS, displayed defects in Cγ3 germline transcription. Specifically, *Utx* control and mutant B cells were isolated from the spleen and stimulated *in vitro* with LPS for 24 hours to capture Cγ3 GLTs (Radbruch, Burger et al. 1986). Quantitative RT-PCR analysis revealed comparable levels of Iγ3–Cγ3 GLTs between *Utx* control and mutant B cells stimulated with LPS (Figure 69). Moreover, *Aicda* transcript levels assessed by qPCR 24 hours after LPS +/- IL4 stimulation, were comparable between *Utx* control and mutant B cells (Figure 70).

Together, these results exclude a major contribution of UTX to the onset of Ig CSR through the regulation of *Aicda* expression and induction of Ig heavy chain gene GLTs.

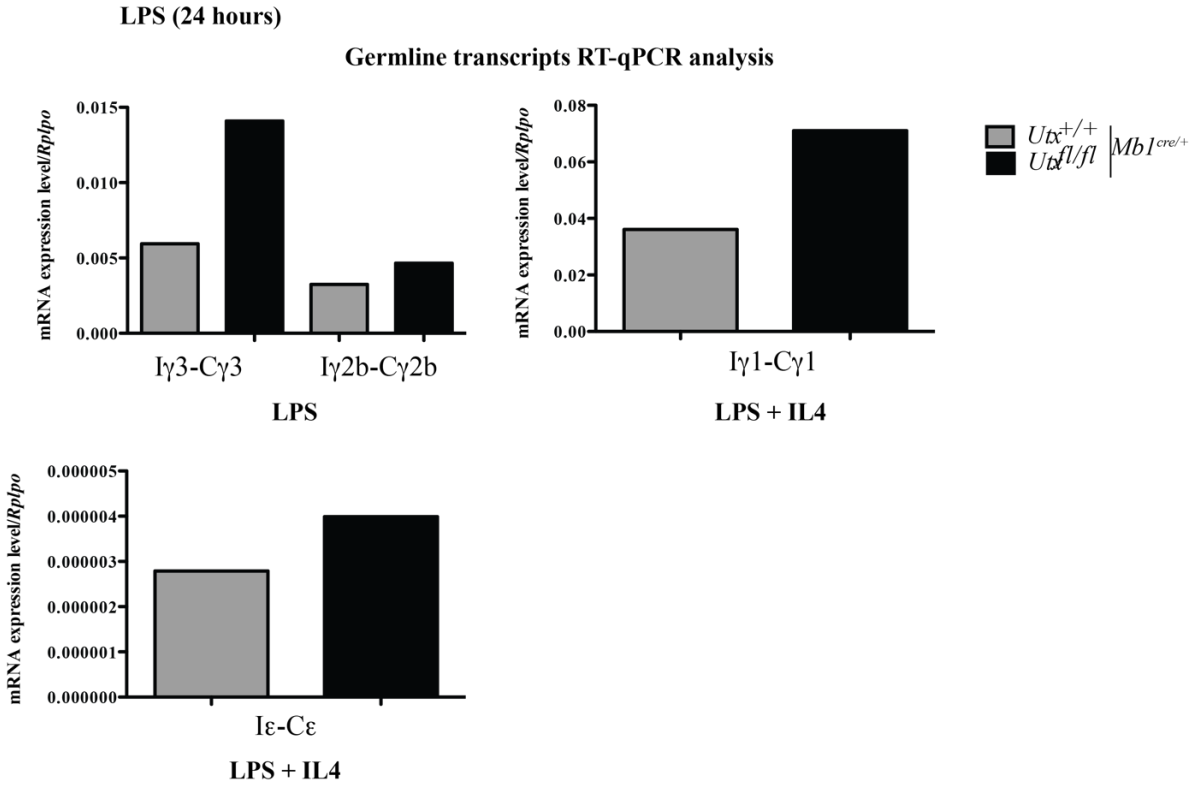


Figure 69. Normal expression of Ig C_H germline transcripts in *Utx* mutant activated B cells

Quantitative RT-PCR analysis of Iγ3-Cγ3, Iγ2b-Cγ2b, Iγ1-Cγ1 and Iε–Cε C_H germline transcripts in representative *Utx* control and mutant B cells stimulated *in vitro* for 24h as indicated. C_H germline transcripts are normalized to those of the housekeeping gene *Rplp0*.

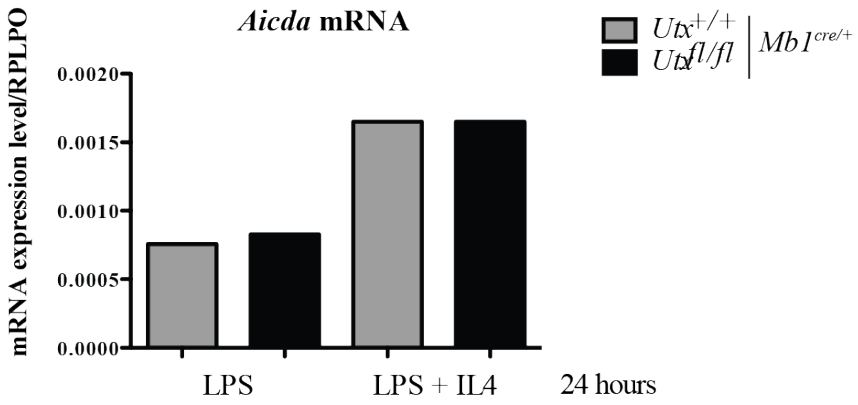


Figure 70. *Aicda* expression is comparable between *Utx* control and mutant B cells stimulated *in vitro* with LPS

Quantitative RT-PCR analysis of *Aicda* transcripts in representative *Utx* control (grey bars; n=2) and mutant (black bars; n=2) splenic B cells stimulated for 24h as indicated. *Aicda* mRNA levels are normalized to those of the housekeeping gene *Rplp0*.

3.6.5. Isotype-switched *Utx* KO B cells die comparably to their control counterpart

To assess whether the reduced percentages of isotype-switched B cells measured in the absence of *Utx* could be explained by increased apoptosis of these cells, *Utx* control and mutant B cells isolated three days after LPS stimulation were stained with the CaspGLOW™ fluorescein active caspase staining kit. Flow cytometric analysis of activated B cells excluded that the fraction of *Utx* mutant IgG3$^+$ B cells was enriched for apoptotic cells (Figure 71).

In summary, Utx deficiency leads to a partial defect in IgG3 class switching which is independent of defects in: a) cell division, b) AID expression, c) C_H germline transcription and 4) survival. Whether UTX controls the late stages of the Ig CSR process will need to be tested in forthcoming experiments.

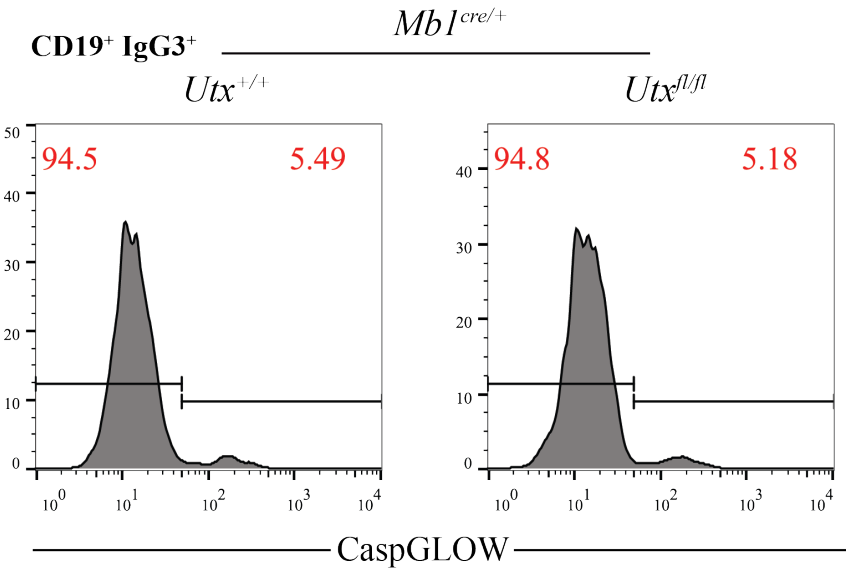


Figure 71. The fraction of apoptotic IgG3-switched B cells remains unaffected by *Utx* inactivation

Frequency of pre-gated CD19$^+$IgG3$^+$ B cells binding to the fluorescent-labelled inhibitor of active caspases VAD-FMK at day-3 of LPS stimulation of *Utx* control (left) and mutant (right) B cells. Numbers show frequencies of gated cells. Data are representative of 2 independent experiments.

3.7. *Utx* deficiency affects selective transcriptional networks in mature B cells

To gain insights into the molecular mechanisms by which UTX controls the transcriptional networks influencing B cell differentiation and function, we performed transcriptomic profiling of sorted splenic FO B and GC B cells from *Utx* deficient and control mice, isolated 8 days after SRBC immunization. Bioinformatic analysis of RNA-sequencing data allowed to identify 469 upregulated and 417 downregulated genes in mutant FO B cells when they were compared to their *Utx* proficient counterpart. The loss of *Utx* in GC B cells led to the upregulation of 58

genes and to the downregulation of 110. (Table 19). Differentially expressed genes (DEGs) identified in these analyses were selected for an expression difference between *Utx* mutant and control samples of 1.2-fold and an adjusted p-value<0.05. In order to better elucidate the impact of *Utx* loss on the transcriptional profile of resting and GC B cells, we classified DEGs on the basis of their fold change expression difference between *Utx* deficient and proficient B cells. Table 19 summarizes the numbers of downregulated and upregulated genes that were selected for an expression difference greater than 1.5, 2, 2.5 or 3 folds, when comparing *Utx* mutant to control FO and GC B cells, respectively. Our results revealed that in FO B cells most of the transcriptionally downregulated genes were mildly affected in the absence of *Utx*, showing a decrease in their expression levels smaller than 2-fold. Instead, in GC B cells, most of the downregulated genes displayed an expression difference between *Utx* mutant and controls that was greater than 2-fold (Table 19). Milder differences were probably not statistically significant because of high intra-group variability among both $Utx^{fl/fl}$ mutant and control GC B cells. Considering upregulated genes, the expression of half of them was more than 2-fold increased in *Utx* deficient compared to proficient FO B cells, whereas in GC B cells most of the upregulated genes showed an expression difference that was greater than 2-fold between mutant and controls (Table 19). These evidences suggest that overall the absence of *Utx* mildly impacts on the transcriptional profiles of resting and activated B cells and support the view of UTX playing important roles both as a transcriptional activator and repressor in B cells.

Cell type	**Gene subsets**	**Differentially expressed genes (nr)**					
	Down in *Utx* mutant B cells	**FC<-1,2**	**FC<-1,5**	**FC<-1,8**	**FC<-2**	**FC<-2,5**	**FC<-3**
FO		417	235	127	75	34	17
GC		110	110	108	107	76	45
	Up in *Utx* mutant B cells	**FC>1,2**	**FC>1,5**	**FC>1,8**	**FC>2**	**FC>2,5**	**FC>3**
FO		469	415	302	201	93	36
GC		58	58	56	52	37	18

Table 19. Genes differentially expressed between *Utx* control and mutant B cells

Numbers of genes that are respectively down- (top) and up-regulated (bottom) in *Utx* mutant (*n*=3) FO and GC B cells when compared to those of *Utx* control (n=3) mice, as assessed by RNA-sequencing. Differentially expressed genes (DEGs) reported in the table were filtered according to an adjusted p-value<0,05 and the indicated fold changes.

We next decided to focus our attention on DEGs whose difference in expression between *Utx* mutant and control cells was more than 1.5 folds, in order to exclude very mild differences that are likely not functionally relevant and could potentially affect our conclusions.

Pathway analysis performed on the downregulated genes in *Utx* mutant FO B cells revealed significant enrichment for genes of the Toll-like receptor signalling (TLR) pathway via MYD88 (e.g. *Dusp4, Irak3, Mapk11*); *Utx* loss led also to significant downregulation of genes identified as NF-κB targets (Figure 72) (Supplementary material -Table 20). Instead, genes downregulated in *Utx* defective GC B cells were enriched for categories involving chemotaxis (e.g. *Ccr7, Ccr6*) (Figure 73). Genes downregulated in both *Utx* KO FO and GC B cells were enriched for categories related to PPs biology and IgA production in the intestine (e.g. *Ccr7, Tnfrsf13b/TACI*, *Itgβ7, Itga4*). Moreover, intersection of the list of genes downregulated in both *Utx* mutant B and GC B cells with published data sets of ChIP-sequencing experiments, revealed a significant enrichment for IRF8 targets (Figures 72, 73). The latter result, combined with our evidences showing a defect in induction of IRF4 in a subset of *Utx* mutant activated B cells, point to a possible dysregulation of genes controlled by the IRF4/IRF8 transcriptional axis, which critically contributes to the regulation of B cell differentiation, Ig isotype switching and germinal center B cell responses (Feng, Wang et al. 2011; Xu, Chaudhri et al. 2015).

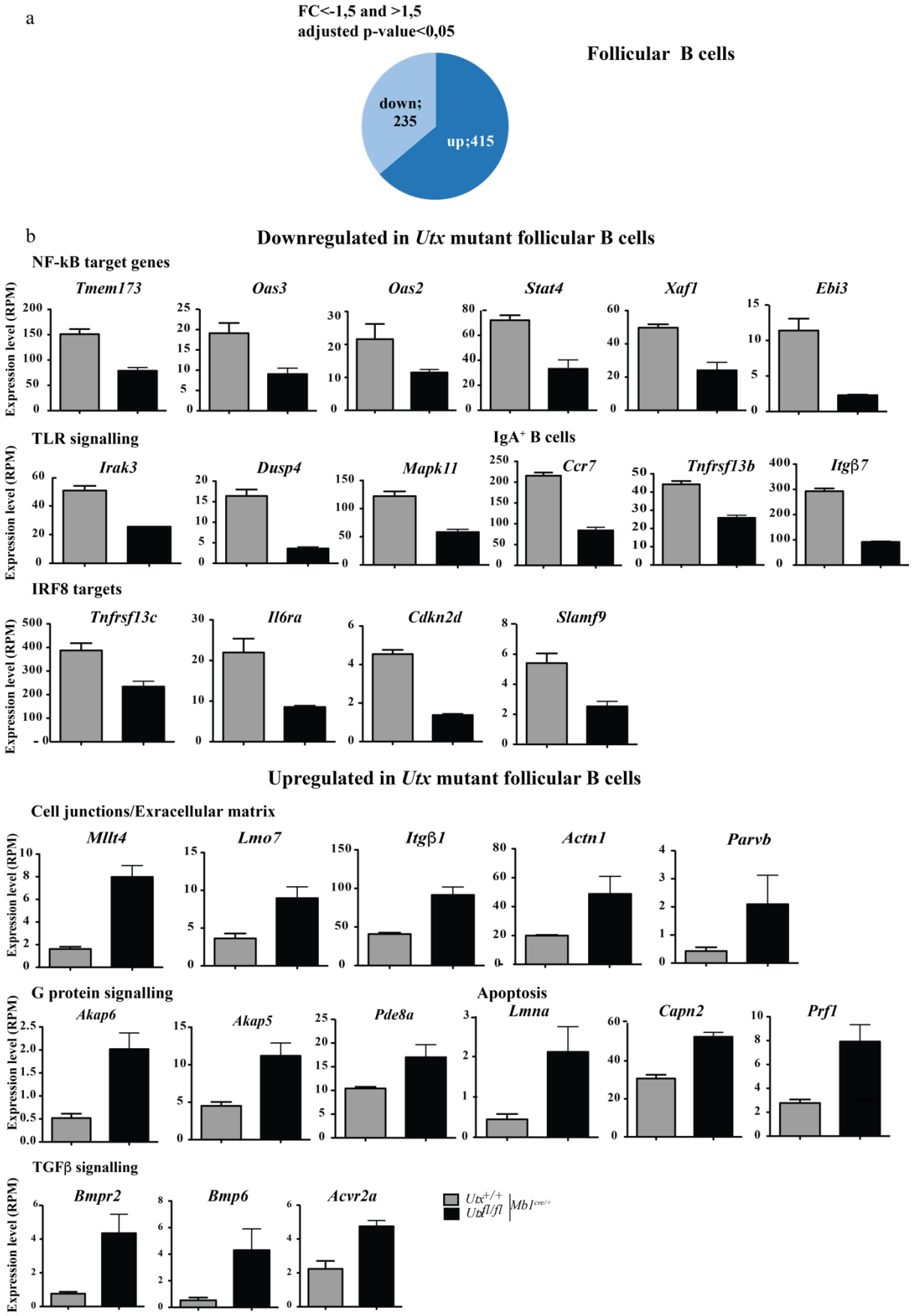

a
FC<-1,5 and >1,5
adjusted p-value<0,05
Follicular B cells
down; 235
up;415
b
Downregulated in Utx mutant follicular B cells
NF-kB target genes
Tmem173
Oas3
Oas2
Stat4
Xaf1
Ebi3
Expression level (RPM)
TLR signalling
IgA+ B cells
Irak3
Dusp4
Mapk11
Ccr7
Tnfrsf13b
Itgβ7
IRF8 targets
Tnfrsf13c
Il6ra
Cdkn2d
Slamf9
Upregulated in Utx mutant follicular B cells
Cell junctions/Exracellular matrix
Mllt4
Lmo7
Itgβ1
Actn1
Parvb
G protein signalling
Apoptosis
Akap6
Akap5
Pde8a
Lmna
Capn2
Prf1
TGFβ signalling
Bmpr2
Bmp6
Acvr2a
Utx+/+ Mb1cre/+
Utxfl/fl Mb1cre/+

Figure 72. Genes controlled by UTX in follicular B cells

a. Pie chart representations of genes that are respectively down- (light blue) and up-regulated (dark blue) in *Utx* mutant (*n*=3) FO B cells when compared to the corresponding cells of *Utx* controls (n=3), as assessed by RNA sequencing. b. Transcript levels of selected genes belonging to specific functional categories, respectively down- and up-regulated in *Utx* mutant follicular B cells, when compared to control B cells of the same subset, as revealed by bioinformatic analysis of RNA sequencing data (RPMs: Reads Per Million mapped fragments; fold change >1,5; adjusted p-value <0,05). Bars represent mean values ± S.D

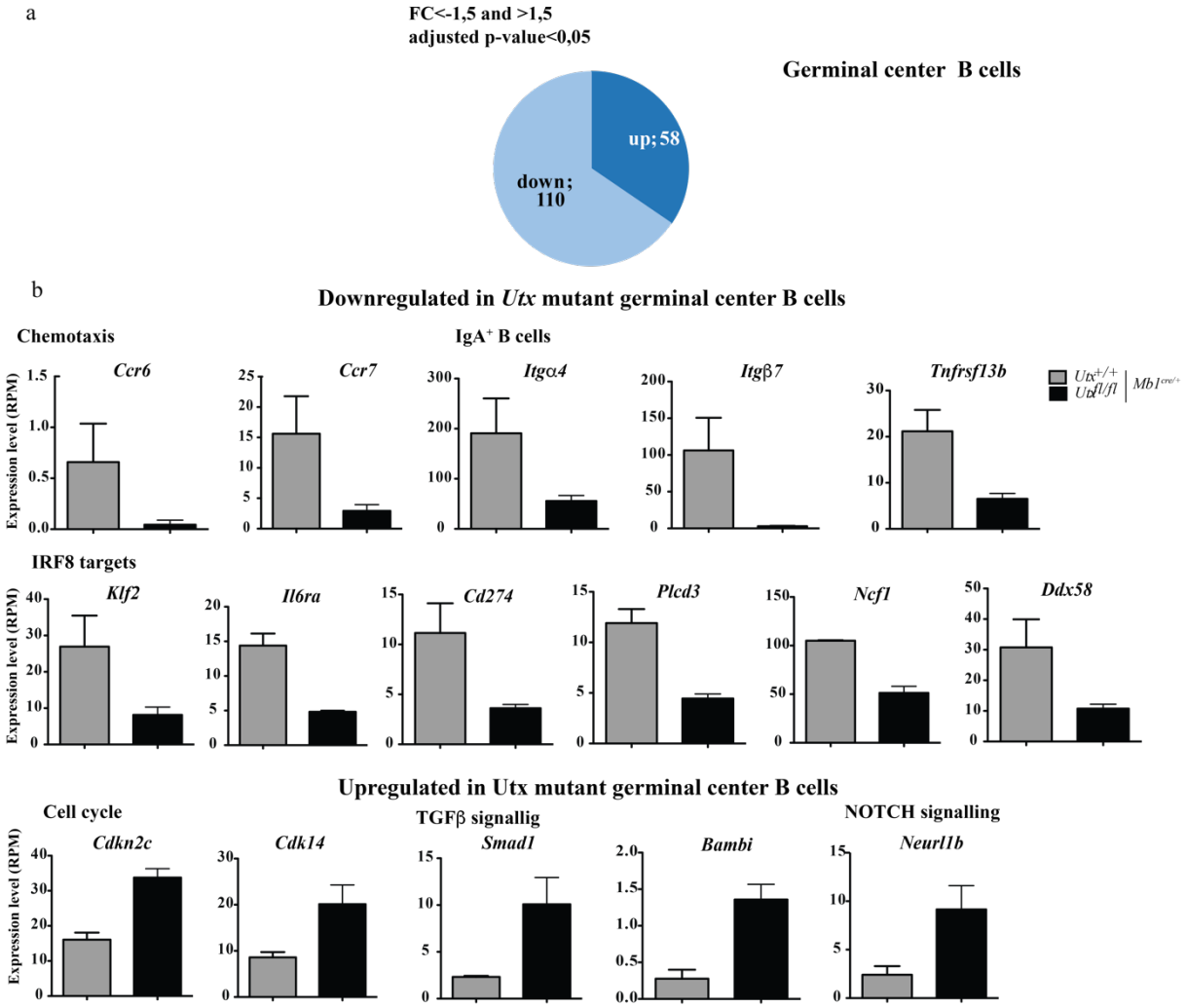


Figure 73. Genes controlled by UTX in GC B cells

Pie chart representation of genes that are respectively down- (light blue) and up-regulated (dark blue) in *Utx* mutant (*n*=3) germinal center B cells when compared to the corresponding cells of *Utx* controls (*n*=3), as assessed by RNA sequencing. b. Transcript levels of selected genes belonging to specific functional categories, respectively down- and up-regulated in *Utx* mutant germinal center B cells, when compared to control B cells of the same subset, as revealed by bioinformatic analysis of RNA sequencing data (RPMs: Reads Per Million mapped fragments; fold change >1,5; adjusted p-value <0,05). Bars represent mean values ± S.D.

Genes upregulated in *Utx* mutant FO B cells were enriched for categories related to molecular effectors of cellular junctions (*Mllt4, Lmo7*) and of interaction with the extracellular matrix (*Itgb1, Actn1, Parvb)*, effectors of G protein signalling (*Akap6, Akap5, Pde8a),* mediators of apoptosis *(Lmna, Capn2, Prf1)* and of TGFβ signalling *(Bmpr2, Bmp6, Acvr2a)* (Figure 72). Pathway analysis performed on the few upregulated genes in *Utx* deficient GC B cells revealed enrichment for members of TGFβ signalling (*Smad1, Bambi*), NOTCH signalling (*Neurl1b)* and the cell cycle regulators *Cdk14* and *Cdkn2c* (Figure 73).

3.8. The chromatin landscape of UTX mutant B cells

3.8.1. Effects of *Utx* inactivation on global H3K27 and H3K4 trimethylation

UTX catalyzes H3K27me3 demethylation and interacts with the H3K4 methyltransferase KMT2D to sustain gene expression (Lee, Villa et al. 2007). Therefore, we hypothesized that *Utx* deficiency could affect H3K27 and/or H3K4 methylation levels in B cells. To address this point, we measured the global levels of H3K27me3, H3K4me3 and H3K4me1 by immunoblotting in purified CD19^{+} splenic B cells of *Utx* mutant (*Utx$^{fl/fl}$; Mb-1$^{cre/+}$)* and control (*Utx$^{+/+}$; Mb-1$^{cre/+}$)* mice (on 129/SV x C57BL/6J mixed genetic background). Quantification of the data revealed that *Utx* deficient B cells displayed levels of H3K27me3 and H3K4me3 similar to those of controls (Figure 75). This result excludes that UTX has a major impact on genome wide H3K27 and H3K4 methylation, hinting, instead, to locus-specific effects.

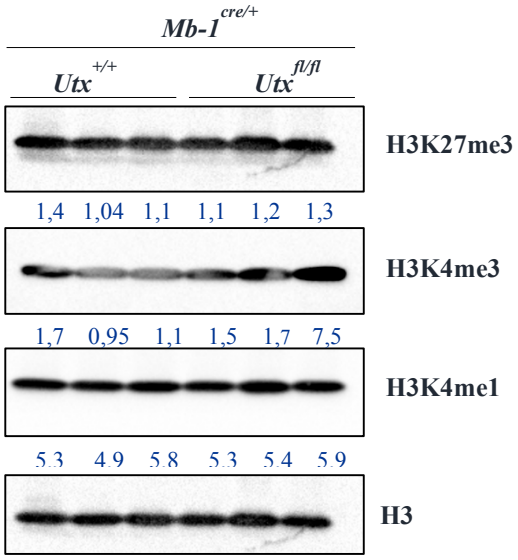


Figure 74. Global H3K27 trimethylation and H3K4 mono/thrimethylation are unaffected in *Utx* mutant B cells

Immunoblotting analyses of H3K27me3, H3K4me3 and H3K4me1 levels in purified resting CD19^{+} splenic B cells of representative *Utx* control (left; *n*=3) and mutant (right; *n*=3) mice. Histone H3 was used as a loading control. Numbers indicate normalized levels of the indicated forms of methylated Histone H3.

3.8.2. *Utx* deficiency does not perturb H3K4me3 deposition at promoter regions both in resting and GC B cells

Several recent studies have unravelled the contribution of UTX to the shaping of the epigenetic landscape of T cell progenitors and invariant Natural Killer T cells, acting at specific genomic regions (Cook, Shpargel et al. 2015; Manna, Kim et al. 2015; Beyaz, Kim et al. 2017). These evidences suggested to us that similar mechanisms may operate during B cell differentiation. To address this point, we mapped in *Utx* control and mutant B cells the genome-wide distribution of different histone H3 post-translational modifications by performing Chromatin Immunoprecipitation, coupled to ultra-deep sequencing of the immunoprecipitated material (ChIP-seq). We started with the genome wide profiling of H3K4me3 on total splenic $CD19^+$ B cells and on sorted GC B cells (129/SV x C57BL/6J mixed genetic background), as changes in this mark have been commonly associated with the loss of MLL complexes components (Zhang, Dominguez-Sola et al. 2015). Bioinformatic analysis of the data identified 11076 and 13195 genes marked by H3K4me3 in a region of +/- 1.5 kb around their TSS, in wildtype $CD19^+$ and GC B cells, respectively. The majority of these genes retained the mark upon *Utx* deletion in both $CD19^+$ resting B cells and in GC B cells (Figure 76). In *Utx* mutant $CD19^+$ B cells, less than 5% of genes (n=350) were not identified as marked by H3K4me3 at the promoter region, whereas only 37 genes were not called by MACS as $H3K4me3^+$ in mutant GC B cells when compared to controls and these percentages suggest that they are most probably randomic. Therefore, loss of *Utx* did not associate with deposition of H3K4me3 at new target genes neither in resting $CD19^+$ cells nor in GC B cells (Figure 76).

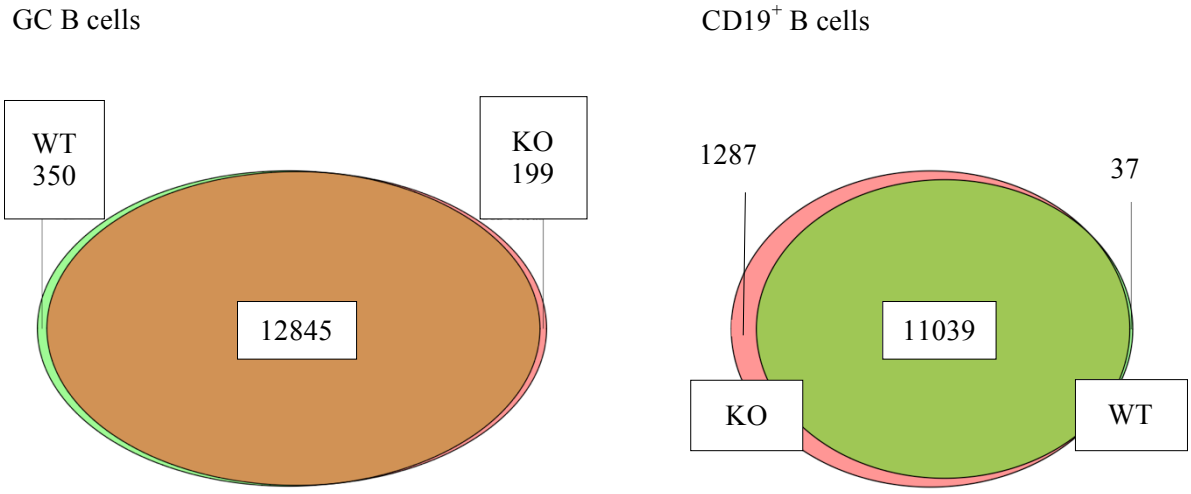


Figure 75. H3K4me3 distribution at promoter regions in *Utx* proficient and mutant B cells

Venn diagram representation of the number of genes showing H3K4me3 deposition at the promoter region (TSS +/- 1,5 kb) in *Utx* control (n=3) and mutant (n=3) GC B cells (left) and$CD19^+$ splenic B cells (right), respectively.

3.8.3. Effects of *Utx* inactivation on the expression of genes marked by H3K4me3 and/or H3K27me3 in resting and GC B cells

In an effort to reconstruct the genome-wide landscape of H3K27 trimethylation, I performed H3K27me3 ChIP-sequencing in both $CD19^+$ B cells and in GC B cells obtained from *Utx* control mice. Pooling data from two H3K27me3 Chip-seq assays performed previously in our laboratory with the ones I performed for the present study, I generated a comprehensive list of genomic regions around the TSS (+/- 5Kb) marked by H3K27me3 in *Utx* proficient $CD19^+$ and GC B cells. To determine the impact of *Utx* inactivation on the expression of genes marked in both *Utx* proficient and mutant cells by H3K4me3 (n= 11039 in FO; n=12845 in GC B cells), H3K27me3 (n= 4157 in GC B cells) or by both histone marks (n= 2473 in GC B cells), we compared their average expression in *Utx* control and mutant B cells. The analysis revealed that in both FO and GC B cells the average expression of genes marked respectively by H3K4me3, H3K27me3 or by both is not significantly affected by *Utx* inactivation (Figure 77). This result suggests that the putative regulation exerted by UTX on target gene expression does not affect the activity of Polycomb complex at the promoter of target genes.

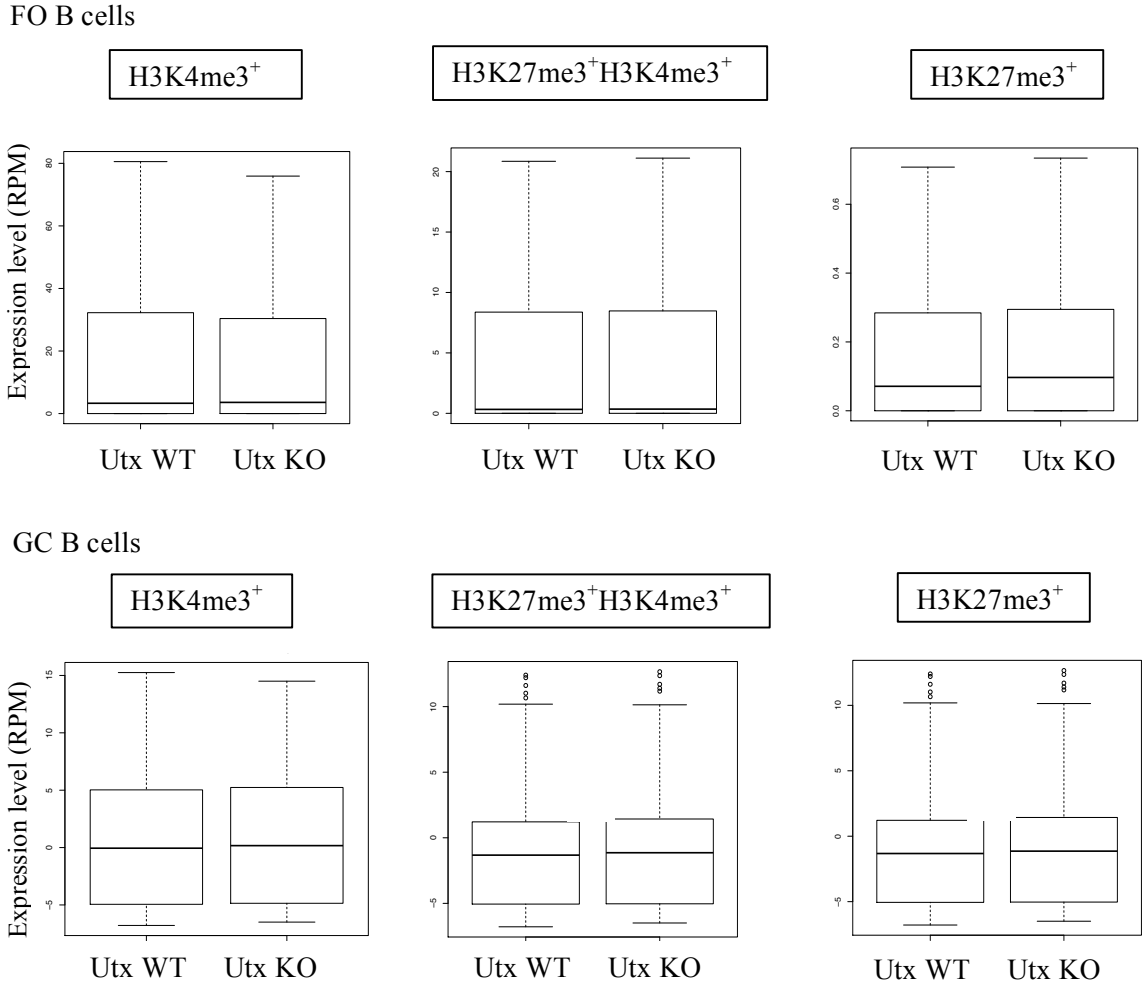


Figure 76. Expression of H3K4me3- and/or H3K27me3-marked genes in *Utx* proficient and deficient B cells

Boxplot representation of the average expression of genes displaying the indicated histone mark(s) at the promoter region in resting B cells or germinal center B cells, assessed respectively in *Utx* control (Utx WT) and mutant *(Utx* KO) B cells through RNA sequencing analyses. The list of bivalent genes (H3K4me3$^+$ and H3K27me3$^+$) in GC B cells was obtained after merging data from 3 independent experiments. Data on bivalent genes in FO B cells were retrieved from datasets previously published by our group (Caganova, Carrisi et al. 2013).

3.8.4. H3K27 acetylation is affected at promoter regions in *Utx* deficient resting and GC B cells

Histone H3 lysine-27 acetylation (H3K27ac) is a histone mark commonly associated with transcribed regions of the genome. To assess whether *Utx* deficiency affected the distribution around the TSS of H3K27ac, we performed ChIP-seq assays for these histone marks in purified CD19$^+$ resting B cells and in sorted GC B cells.

Bioinformatic analyses of the data revealed that over 96% of H3K27ac target genes (n= 8651) were shared between *Utx* proficient and mutant CD19$^+$ B cells (Figure 78). Instead, genes selectively marked by H3K27ac in *Utx* control or mutant CD19$^+$ B cells were respectively 302 and 1257, making up less than 4% and 14%, respectively, of the total number of target genes found in these cells. Similar observations were made analyzing GC B cells. In these cells, 92% of H3K27ac targets overlapped between *Utx* control and mutant B cells. Moreover, 680 genes (8,4% of total) were specifically marked by H3K27ac in *Utx* control B cells, whereas their mutant counterparts carried 623 marked genes (7,7% of total) which likely displayed lower levels of the histone mark in control B cells.

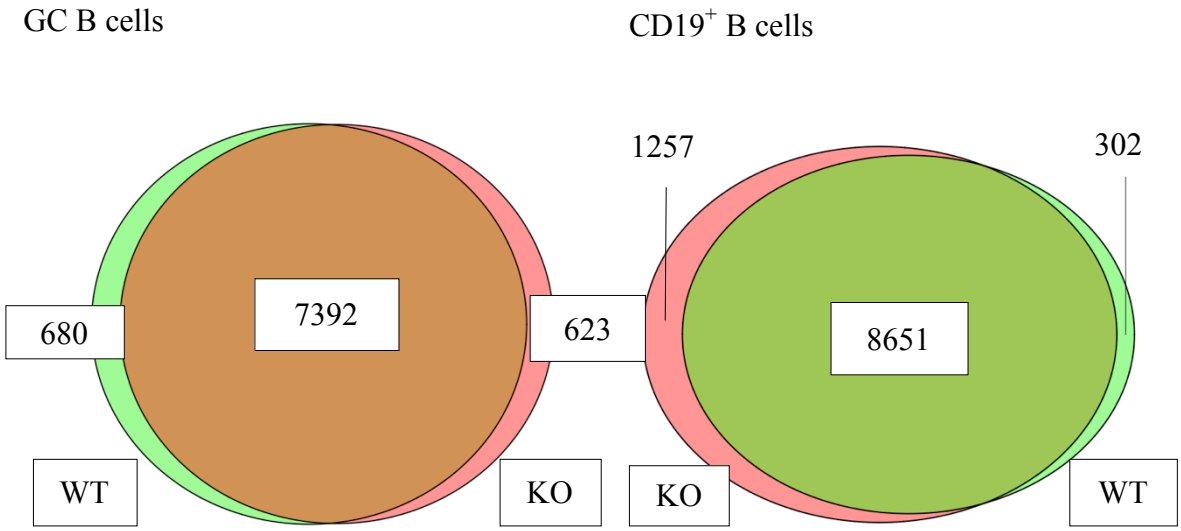


Figure 77. H3K27ac distribution at promoter regions in *Utx* proficient and mutant B cells

Venn diagram representation of the number of genes showing deposition of H3K27ac at the promoter region (TSS +/- 1,5 kb) in *Utx* control (n=3) and mutant (n=3) GC B cells (left) and CD19$^+$ splenic B cells (right). GC B cells were sorted from 4 independent *Utx* control and mutant mice. CD19$^+$ B cells were purified from 3 *Utx* control and mutant mice.

To further validate the differences in H3K27ac deposition at the promoters of target genes in the absence of *Utx*, we assessed read density distribution around the TSS of genes defined as commonly marked by H3K27ac both in *Utx* control and mutant B and GC B cells, H3K27ac$^+$ only in *Utx* control and H3K27ac$^+$ only in *Utx* mutant B and GC B cells. Results, depicted in Figure 79, suggest that the levels of H3K27ac mark are lower in *Utx* mutant B and GC B cells for the specific subset of genes where MACS algorithm did not identify a peak in *Utx* mutant samples (302 in CD19$^+$ B cells and 680 in GC B cells). On the other hand, genes defined as H3K27ac$^+$ at their promoters only in *Utx* mutant B and GC B cells (1257 in CD19$^+$ B cells and 623 in GC B cells) carried higher levels of the mark compared to their control counterparts. These data support a scenario whereby *Utx* is important to control the deposition of the H3K27ac mark at the promoter of specific subsets of genes. Further experiments will be needed in order to assess whether the lack of *Utx* may influence the balance between acetylation and trimethylation of H3K27 residues, potentially influencing the transcriptional status of target genes.

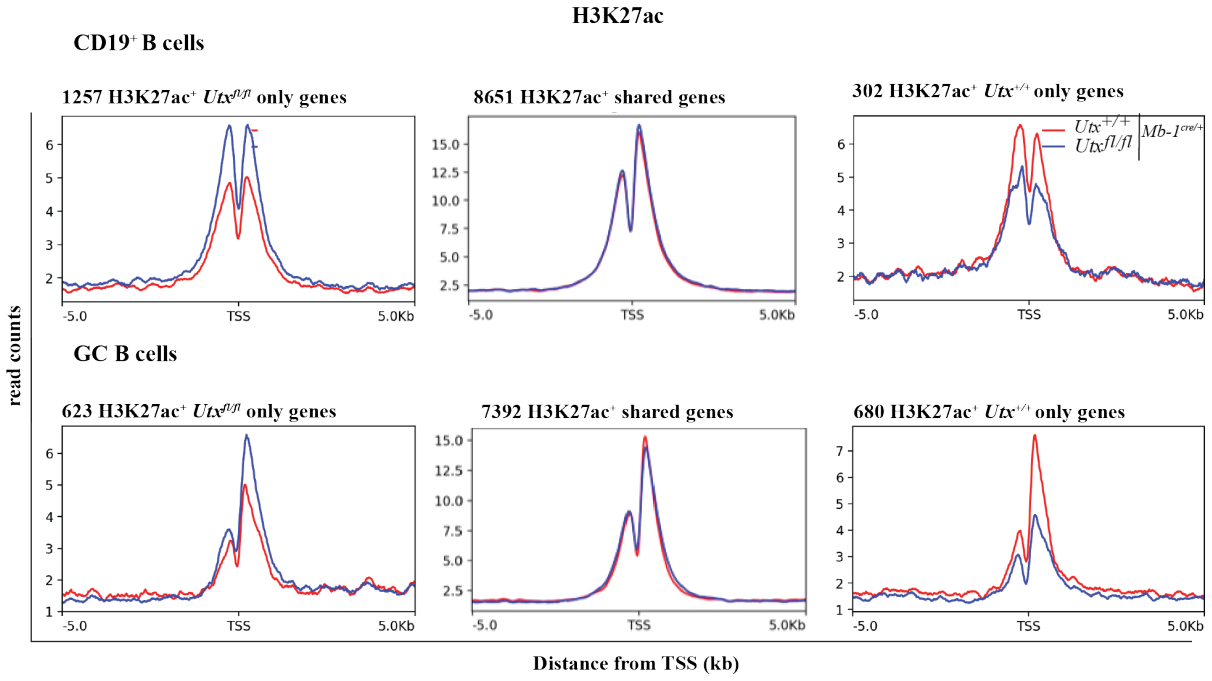


Figure 78. H3K27ac distribution across differentially acetylated promoter regions in *Utx* mutant and control B and GC B cells.

Average read counts of H3K27ac enrichment at the promoter region (TSS +/- 5 Kb) of the indicated subset of genes in *Utx* control (red line) and mutant (blue line) CD19+ (upper panels) and germinal center B cells (lower

panels). Two distinct groups of genes representing those marked preferentially by H3K27ac in either *Utx* mutant (left columns) or control (right columns) B cells are shown. Genes where H3K27ac deposition at the promoter region remained largely unaffected by *Utx* inactivation, were also included in the representation (shared genes; central column).

To estimate the effects of aberrant H3K27ac levels on target gene expression in *Utx* mutant B cells, we intersected the list of genes with lower or higher H3K27ac levels at their promoters, following *Utx* inactivation, with those differentially expressed between *Utx* control and mutant FO and GC B cells, respectively. By doing so, we identified 17 and 13 genes which, upon *Utx* inactivation, were downregulated as well as bearing lower levels of H3K27ac at the promoter region respectively in FO and GC B cells (examples shown in Figure 80 a). Concomitantly, 90 genes were upregulated and carried higher levels of H3K27ac at their promoters in FO B cells (an example is shown in Figure 80 b), whereas only 5 genes fell in the same category in GC B cells.

These results suggest that the regulation of H3K27ac levels at the promoter regions of *Utx* target genes represents a very limited mechanism through which *Utx* can sustain the expression of its transcriptional targets. Future experiments, like ChIP-sequencing profiles for H3K4me1 of *Utx* control and mutant B cells will be crucial to map intergenic regulatory regions like enhancers in B cells, in determining the impact of the lack of *Utx* at these regions and whether this represents the main mechanism through which UTX regulates gene expression.

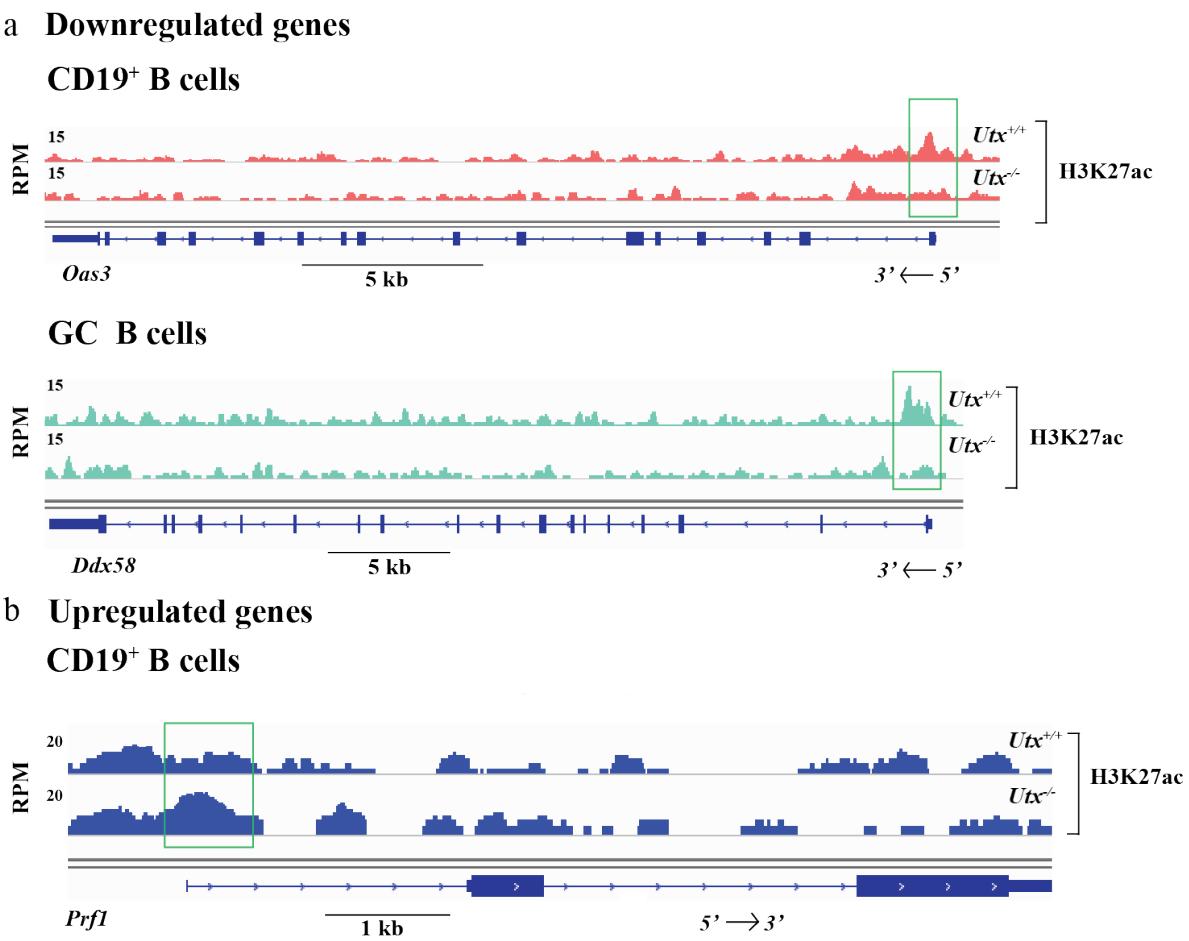


Figure 79. Changes in H3K27ac levels at promoters of representative Utx-controlled genes, in *Utx* mutant B cells

Changes in H3K27ac deposition at the promoter of representative Utx-regulated genes. The upper and mid H3K27ac distribution profiles (a) refer to genes (*Oas3* and *Ddx58*) that are downregulated in *Utx* mutant resting ($CD19^+$) and germinal center (GC B cells) B cells, respectively. The lower profiles (b) refer to the H3K27ac distribution profile of the *Prf1* gene that is upregulated in *Utx* mutant resting B cells. H3K27ac distribution across the selected genes is represented together with the exon-intron structure of the same genes. Green boxes highlight promoter regions where the H3K27ac peak was called by the MACS-2 algorithm. Read density is depicted as RPM value.

.

4. Discussion

This study has addressed the role of the demethylase UTX/*Kdm6a* in B lymphopoiesis and in adaptive B cell immune responses. Gene expression analyses performed on purified murine B cell subsets revealed that *Utx* is expressed throughout B cell development, with stronger expression detected in pro- and pre-B cells and in short lived plasma blasts. This result is compatible with UTX playing a role at multiple stages of B cell differentiation. Using a B-cell specific conditional knock-out approach, starting from pro-B cells, we show that UTX finely tunes B cell development, optimizing the output of B cells from the bone marrow and influencing peripheral B cell subset differentiation and recirculation. The loss of *Utx* function coincided with decreased numbers of FO B cells in the spleen at the expense of cells displaying a marginal zone B cell surface phenotype. Notably, the latter increase did not coincide with an expansion of the splenic MZ, as assessed by histological analysis of the spleen. Moreover, in response to *Utx* inactivation, the distribution of B cells through primary and secondary lymphoid organs was substantially altered, particularly in GALTs such as PPs and MLNs.

Another consistent finding of our study relates to the expansion of the GC B cells population in B-cell specific *Utx* mutant mice in response to immunization with T-cell dependent antigens including NP-CGG and sheep red blood cells. The increase in GC B cells was also observed when *Utx* was selectively inactivated in AID-expressing GC B cells, thus pointing to a GC B cell-specific contribution of UTX to the dynamics of GC B cell responses. An increase in the fraction of GC B cells was particularly evident in rudimental PPs of B-cell specific *Utx* mutant mice, which suffered at the same time from a significant defect in serum IgA titers and in the establishment of a normal pool of IgA-secreting PCs in the intestinal lamina propria. Within the GC, *Utx* deficiency led to a striking expansion of the proliferating compartment of $BCL6^{+}CXCR4^{+}CD83^{-}$ centroblasts at the expense of the population of centrocytes undergoing antigen-driven selection. The alteration in the centroblast/centrocyte ratio correlated with a weaker selection of B cells bearing high affinity mutations, without affecting, however, the capacity of *Utx* mutant mice to generate high-affinity antibody secreting plasma cells. Nevertheless, a closer look at the early stages of PC differentiation *in vivo* revealed a partial defect of *Utx* mutant mice to generate a normal pool of antigen-specific PCs.

Conditional inactivation of *Utx* throughout B cell lymphopoiesis, interfered with the capacity of mutant mice to produce normal levels of isotype-switched antibodies. This defect correlated with a substantial increase in serum levels of IgM, reproducing the serological defects seen in patients affected by hyper-IgM immunodeficiencies. *In vitro* studies aiming to determine a possible contribution of UTX to the process of Ig isotype switching suggest a contribution of the demethylase to optimal activation and proliferation of B cells, to the execution of terminal steps of the Ig class switch recombination process, and possibly to its influence on the induction

of transcription factors such as *Irf4* whose contribution to Ig CSR has been previously demonstrated.

Data generated from the analysis of *Utx* conditional mutant mice will be discussed in detail in the next sections, discussing the results in the frame of existing knowledge. Our findings represent the first attempt to unveil the role of UTX in B cell development and immune responses.

4.1. UTX in early B cell development

The lack of information on the role of UTX in B cell development, combined with the expression of the demethylase throughout B cell development motivated us to investigate its function starting from progenitor B cells. To this aim, mice carrying *Utx* floxed alleles were crossed to *Mb-1*$^{cre/+}$ knock-in animals, which express Cre recombinase starting from the pro-B cell stage (Hobeika, Thiemann et al. 2006). We decided to focus our attention on the analysis of female animals given that the *Utx* gene maps on the X-chromosome, and previous data had hypothesized a possible functional redundancy between UTX and the Y-chromosome-linked UTY paralogue (Shpargel, Sengoku et al. 2012; Wang, Lee et al. 2012). Quantitative genomic PCR data revealed that most pro-B cells (B220^{lo} IgM^{-}CD43^{+}), and over 80% of pre-B cells (B220^{lo}IgM^{-}CD25^{+}) and immature B cells (B220^{lo}IgM^{+}) had undergone Cre-mediated recombination, thus excluding toxic effects of *Utx* loss in early stages of B cell lymphopoiesis. This result, together with the observation that the total number of BM B cells was unaffected in *Utx* conditional mutant mice, indicates that the demethylase is not essential for early B cell development. Similar results were recently observed in our group studying mice mutant in B cells for the only other described H3K27me3 demethylase, JMJD3/*Kdm6b* (Rahmat and Casola, personal communication). Hence, we cannot exclude a degree of functional redundancy between UTX and JMJD3 in the regulation of the early stages of B cell development, including a possible influence of these enzymes to the process V(D)J recombination. Indeed, previous reports have suggested a role for H3K27 trimethylation in the regulation of V_H gene accessibility during the process of VDJ recombination (Xu, Schaffer et al. 2008). In this context, the lack of H3K27me3 demethylase activity resulting from *Utx* and/or *Jmjd3* deficiency could alter the V_H gene usage and thereby the IgH repertoire expressed by developing mutant B cells.

Utx inactivation impacted on the number of the progenitor B cell pool, affecting primarily the pre-B cell subset, which expanded in the BM of mutant mice. This result is compatible with a role for UTX in the proliferation of pre-B cells. The loss of *Utx* has been previously associated to enhanced proliferation in neural progenitors (Lei and Jiao 2018), as well as in several types of malignant tumors (van Haaften, Dalgliesh et al. 2009; Ntziachristos, Tsirigos et al. 2014;

Van der Meulen, Sanghvi et al. 2015). Interestingly, recent work using Eμ-MYC lymphoma-prone mice has proposed a contribution for *Utx* inactivation in lymphomagenesis through the upregulation of the SRC-like kinase BLK. Increased BLK expression (leading to its possible constitutive activation) may mimic pre-BCR signalling, thereby enhancing pre-B cells proliferation (Tretter, Ross et al. 2003; Li, Zhang et al. 2018). In forthcoming experiments, we will test this hypothesis by short-term *in vivo* BrdU labelling experiments. We will also establish from the BM of *Utx* control and mutant mice IL7-driven progenitor B cell cultures *in vitro* to closely monitor the impact of *Utx* inactivation on pre-BCR signalling. The relevance for *Utx* in progenitor B cell differentiation could derive from the positive regulation exerted by the demethylase on the induction of the transcription factor IRF4. Indeed, IRF4, together with IRF8, limits pre-B cells expansion and attenuates IL7-signalling to facilitate Ig light chain rearrangements and hence the progression to the immature B cell stage (Lu 2008; Ma, Pathak et al. 2008). Interestingly, the loss of JMJD3 was associated to a contraction in size of the pre-B cell compartment, pointing to antagonistic functions of the two H3K27me3 demethylases in early B cell development (Rahmat and Casola, unpublished results).

A comprehensive evaluation of the numbers of B cells found in the blood circulation and in primary and secondary lymphoid organs suggests that UTX controls B cell homeostasis. Indeed, in *Utx* mutant mice, the reduced fraction of recirculating B cells in the BM combined with a sharp decrease in the fraction of B cells circulating in the blood and with a reduction in the size of the immature B cell pool found in the spleen, point to a regulation operated by UTX on the egress (exit) from and entry into the BM of B cells. This scenario predicts an accumulation of newly generated immature B cells in the BM of *Utx* mutant mice. However, this increase was not observed, possibly because at the same time, *Utx* deficiency caused a partial defect in the pre-B to immature B cell transition.

In summary, *Utx* deficiency starting from progenitors interferes with the early stages of B cell lymphopoiesis sustaining, on the one hand, pre-B cell expansion and, on the other, preventing newly generated immature B cells to egress from the BM.

4.2. UTX and peripheral B cell differentiation and maintenance

Immunophenotypic analyses of single cell suspensions from secondary lymphoid organs have unravelled important contributions of UTX to peripheral B cells differentiation.

The inactivation of *Utx* caused a reduction in the proportion and in the numbers of splenic $CD19^+$ B cells starting from the immature B cell stage, which was accompanied by an even stronger contraction of the B cell pool in GALT. These observations recapitulate previous findings on B cell-specific mutants for the H3K4 methyltransferase *Kmt2d* (MLL4) (Ortega-Molina, Boss et al. 2015; Zhang, Dominguez-Sola et al. 2015). In particular, Zhang and

colleagues found a significant reduction in the pool of splenic and lymph node B cells in *Kmt2d* conditional mutant animal, which was associated to fewer recirculating mature B cells present in the BM (Zhang, Dominguez-Sola et al. 2015). Interestingly, whereas *Kmt2d* mutant mice displayed these defects preferentially upon immunization, *Utx* knock out animals showed similar alterations already in resting conditions. The striking similarities between *Kmt2d* and *Utx* deficient mice in terms of aberrant distribution of B cells between primary and secondary lymphoid organs speak for the action of these two enzymes within the same macromolecular complex.

The normal distribution of splenic B cells between the FO and MZ B cell subsets was disturbed by the lack of *Utx*. Specifically, *Utx* deficient animals showed a mild contraction in the FO B cell pool, which was counterbalanced by an increase in the number of *bona fide* MZ B cells defined on the basis of several surface markers including CD23, CD21, CD1d and CD38. Surprisingly, a higher number of MZ B cells in the spleen of *Utx* mutant mice did not coincide with a corresponding increase in the average MZ surface area measured by immunofluorescence analysis. These results can be reconciled hypothesizing a defect of MZ B cells to re-circulate from the follicle to the MZ area, as will be discussed below.

The consistent reduction in resting mature FO B cells observed in the spleen of *Utx* mutant mice could, at least partially, depend on impaired survival of these cells. We tested this hypothesis, by measuring the expression in *Utx* control and mutant B cells of the Tumor Necrosis Factor (TNF) receptor family member BAFFR, which is crucial to mediate the survival of mature B cells by binding to its cognate ligand BAFF/BlyS (Harless, Lentz et al. 2001; Schiemann, Gommerman et al. 2001). Indeed, we found that UTX positively regulates BAFFR protein levels in mature B cells, through the control of *Baffr* gene expression. Importantly, the reduced expression of BAFFR in *Utx* mutant peripheral B cells limited their response *in vitro* to soluble BAFF, accelerating their disappearance over time. These results are compatible with a role for UTX in controlling mature B cell homeostasis by optimizing its response to the survival factor BAFF. On the other hand, the close-to-normal turnover of FO B cells detected in *Utx* mutant mice, as revealed by *in vivo* BrdU labelling experiments suggests that under the stringent selection pressure required to persist in secondary lymphoid organs, mature B cells may set in place compensatory mechanisms for *Utx* deficiency. This hypothesis will be tested in the future, by performing competitive bone marrow reconstitution assays.

Transcriptional profiling comparing resting mature splenic B cells from *Utx* control and mutant mice, assigned to UTX a specific function in the control of the NF-κB signaling pathway. Indeed, *Utx* mutant B cells expressed lower transcript levels for several NF-κB family members including *cRel, Nfkb1(p105) and Nfkb2(p100)*. A major upstream regulator of the NF-κb canonical pathway, *IKK2*, was also downregulated in B cells in response to *Utx* inactivation.

How could interference with NF-κB signalling impact on peripheral B cell homeostasis? One possible pathway suffering from sub-optimal NF-κB signalling is initiated by the BAFFR in response to the binding to BAFF. Indeed, activation of the alternative (*Nfkb1*) NF-κb signalling pathway triggered by BAFF binding could suffer from reduced levels of *Nfkb2*. Future analyses aiming to study the transcriptional response to *in vitro* BAFF stimulation in *Utx* mutant B cells will unveil the extent to which inactivation of the demethylase prevents the full-blown activation of the anti-apoptotic response in these cells.

Interference with the canonical pathway suggested by the reduced levels of *Ikk2* measured in *Utx* defective B cells could instead interfere with B cell maturation. Indeed, studies with different mouse mutants lacking essential modulators of the canonical NF-κB signalling pathway including *NEMO, IKK/IKK2* or *cRel/Rela* double deficiency suffered from major developmental problems arresting B cell differentiation at the transitional T1 stage. (Franzoso, Carlson et al. 1997). Whereas *Utx* mutant B cells displayed a substantially milder effect on peripheral B cell maturation than the one observed in NF-kB mutants, the reduced expression in demethylase mutant B cells of a critical subset of NF-kB targets, supports a scenario in which the differentiation of short lived transitional B cells into long lived FO B cells requires optimal NF-kB signalling, which is guaranteed by UTX function. Canonical NF-kB signalling is less relevant for the maintenance of FO B cells, which mainly requires activation of the Phosphoinositide 3' kinase signalling pathway emanating from the BCR (Franzoso, Carlson et al. 1997). Whereas Utx mutant B cells displayed a substantially milder effect on peripheral B cell maturation than the one observed in NF-κb mutants, the reduced expression in demethylase mutant B cells of a critical subset of Nf-κb targets, supports a scenario in which the differentiation of short-lived transitional B cells into long-lived FO B cells requires optimal NF-κb signalling, which is guaranteed by Utx function. Canonical NF-κb signalling is less relevant for the maintenance of FO B cells, which mainly requires activation of the Phosphoinositide 3' kinase signalling pathway emanating from the BCR (Grossmann, Metcalf et al. 1999; Claudio, Brown et al. 2006; Derudder, Cadera et al. 2009; Srinivasan, Sasaki et al. 2009; Gerondakis and Siebenlist 2010; Derudder, Herzog et al. 2016). Altogether, our data are compatible with a scenario in which UTX supports the transitional to mature B cell differentiation step, by controlling both the canonical and alternative NF-κB signalling pathway exerting its action at multiple levels, including the regulation on the expression of *Baffr*, NF-κb signalling effectors (*Ikk2*) and transcription factors (*cRel*) and, possibly, of downstream target genes (*Ccr7, Irak3, Mapk11, Cd37, Xaf1*). Future experiments will reveal whether UTX directly targets these genes forming a complex with the H3K4 methyltransfrase KMT2D. Whereas *Utx* mutant B cells displayed a substantially milder effect on peripheral B cell

maturation than the one observed in NF-kB mutants, the reduced expression in demethylase mutant B cells of a critical subset of NF-kB targets, supports a scenario in which the differentiation of short lived transitional B cells into long lived FO B cells requires optimal NF-kB signalling, which is guaranteed by UTX function. Canonical NF-kB signalling is less relevant for the maintenance of FO B cells, which mainly requires activation of the Phosphoinositide 3' kinase signalling pathway emanating from the BCR

The lack of *Utx* in B cells altered the ratio between splenic FO and MZ B cells, as assessed by flow cytometric analysis. This change was in part contributed by a (mild) contraction in the FO B cell pool, and, on the other, by an increase in the number of bona fide MZ B cells. However, histological analyses on spleen sections of *Utx* control and mutant mice failed to reveal major differences in the surface area occupied by the MZ. We will confirm the result, complementing the current immunofluorescence analyses with a new set of experiments using a combination of the MOMA1 antibody, marking metallophilic macrophages lining the marginal sinus, with anti-IgM labelling of B cells present both within and outside the primary follicles. The results could be explained by hypothesizing an aberrant expression in *Utx* mutant B cells of the genes coding for the markers we used to distinguish FO from MZ B cells, including *Cd19, Cd21, Cd23, Cd38* and *Cd1d*. This scenario will be tested verifying whether any of the listed genes are directly targeted by UTX through its binding at the promoter and/or enhancer regions, by performing UTX ChIP-seq assays on *Utx* wild-type FO B cells. We will also attempt to acutely inactivate *Utx* in resting $Utx^{fl/fl}$ FO B cells *in vitro* using a tamoxifen-inducible R26-$CreER_{T2}$ allele, followed by their re-introduction into B-cell deficient JHT mice, or monitoring them for several days in culture upon stimulation of the cells with BAFF. *Utx* mutant B cells retrieved from transplanted animals or from BAFF-stimulated *in vitro* cultures will be tested by flow cytometry and gene expression analysis for changes in the expression of the markers distinguishing FO from MZ B cells.

An alternative hypothesis to explain the inconsistencies between flow cytometric and histological analysis is linked to the possibility that UTX may control the continuous shuttling of MZ B cells between the follicle and the MZ. In support of this scenario, we found that *Utx* mutant splenic B cells expressed lower levels of the Sphingosine 1 phosphate receptor-1 (*S1pr1*). These results are in accordance with recent data showing that S1PR1 is a direct target of both UTX and JMJD3 in other cell types including thymocytes (Manna, Kim et al. 2015). S1PR1 is essential to localize B cells into the MZ area (Cinamon, Matloubian et al. 2004). Moreover, MZ B cells continuously shuttle between the MZ area and the follicles where they deliver antigen uptaken from the blood stream (Cinamon, Zachariah et al. 2008). Importantly, the return of MZ B cells to the MZ is strictly S1PR1-dependent. Based on this knowledge and on our findings, we could hypothesize that lower levels of *S1pr1* may impound *Utx* mutant MZ

B cells into the follicle preventing their effective return to the MZ area. To test this hypothesis, we will measure the capacity of both FO and MZ B cells to migrate to a gradient of Sphingosine 1 phosphate (S1P) using transwell chambers as described in (Allende, Tuymetova et al. 2010). Should the experiment unveil a defective migration of *Utx* mutant B cells, we will attempt to restore expression of S1PR1 in these cells by bone marrow reconstitution experiments using as donors *Utx* mutant stem cells reconstituted with lentiviral vectors expressing *S1pr1*.

Why are *bona fide* MZ B cells increased in numbers in *Utx* mutant mice? One possibility comes from recent work by the Klein group highlighting the property of IRF4 defective mature B cells to acquire a MZ B cell identity on the bases of enhanced activation of the NOTCH-2 pathway. Interestingly, transcriptome data revealed that in resting $CD19^{+}$ B cells, *Utx* deficiency caused downregulation of genes controlled by the IRF4/IRF8 transcriptional axis suggesting a possible interference with IRF4/IRF8 expression/function in these cells. Despite the significant impairment of a fraction of *Utx* mutant splenic B cells to upregulate IRF4 expression in response to activation with LPS or CD40 ligation, we failed to detect measurable differences in IRF4 levels in *Utx* mutant resting mature B cells. Hence, our data are compatible with a possible defect in IRF4 controlled gene expression. To test this hypothesis, we will profile genome wide IRF4 distribution in *Utx* mutant resting mature B cells and compare it to that of their control counterparts. Given the importance of the NOTCH2 transcriptional pathway in the control of MZ B cell differentiation (Saito, Chiba et al. 2003), we will test whether proteolytic NOTCH2 activation as well as expression of NOTCH2 target genes is already detectable in FO B cells of *Utx* mutant mice.

Immunophenotypic analysis of B cells retrieved from peritoneal cavity lavages revealed a significant enrichment in the proportion of B-1 B cells. This was mainly dependent on the reduction in the number of $CD19^{+}B220^{+}$ B-2 B cells, while $CD19^{hi}B220^{lo}$ B-1 B cells remained largely unaffected in numbers by *Utx* deficiency. These results confirm once more the impaired representation of resting B-2 B cells in secondary lymphoid organs of B-cell specific *Utx* mutant mice. Instead, development and possibly maintenance of B-1 B cells appears to be independent of UTX function. The knowledge that differently from B-2 B cells, B-1 B cells do not depend on BAFF for their maintenance (Mackay and Schneider 2009; Gerondakis and Siebenlist 2010) could help to explain why homeostasis of the latter cells remained unperturbed in *Utx* mutant mice. *Utx* mutant mice did not reproduce the severe defect in B-1 B cells generation observed in mice mutant for *Nfkb1* or *cRel*, excluding a major impairment in the activation of NF-κB signalling through these factors in demethylase mutant B-1 B cells (Pohl, Gugasyan et al. 2002; Thome 2004; Gerondakis, Grumont et al. 2006).

Peripheral B cell maturation is strongly influenced by the strength of the signal emanating from the B cell antigen receptor (Casola, Otipoby et al. 2004; Casola 2007; Pillai and Cariappa 2009).

Indeed, whereas, strong BCR signals facilitate B-1 B development, weaker ones are compatible with B-2B and MZ B cell development. Given the under-representation of B-2 B cells while B-1 B cells were largely unaffected, we could speculate that *Utx* inactivation in progenitors of B-1 and B-2 B lineage cells may exert on these cells a different effect, by potentiating the BCR signal strength. In particular, whereas increased BCR signal strength could prevent B-2 progenitors from effective development, it would facilitate that of B-1 B cells. *Utx* deficiency may influence BCR signalling strength by interfering in pro-B cells with the accessibility of the RAG recombination machinery to the Immunoglobulin V_H locus. Specifically, *Utx* inactivation could influence the usage of D_H proximal versus distal V_H gene families as substrates of recombination, favouring the former. The bias usage of V_H genes could result from the failure of *Utx* mutant progenitor B cells to undergo IgH locus contraction. D_H proximal V_H genes, which confer auto/self-reactive specificities to newly generated BCRs, are preferentially enriched in B-1 B cells, while they are counter selected during the development of B-2 B cell progenitors (Kantor 1996). To test a possible contribution of UTX to the establishment of the primary IgH repertoire, we will determine by next generation sequencing technology the relative usage of D_H proximal and distal V_H genes in IgH V gene rearrangements amplified from pre-B cells (prior to selection) as well as mature B-2 B cells of controls and *Utx* B-cell specific mutant mice.

4.3. UTX and B cell migration

The reduction in mature and immature B cells measured in the spleen of *Utx* mutant mice was associated to a decrease in the fraction of $B220^+$ B cells detected in the blood, and to a contraction of the recirculating mature B cell compartment in the BM, whereas immature B cell were mildly overrepresented in this organ. Moreover, *in vivo* BrdU labelling experiments revealed in the BM a slower rate of replacement of newly generated *Utx* deficient immature B cell, which together with fewer of these B cells detected in the spleen, pointed to a longer persistence within the BM.

These observations led us to hypothesize that *Utx* controls the distribution of B lymphocytes among the various lymphoid organs possibly through a direct influence on their migratory capacities. Two families of G-protein coupled receptors play essential roles in controlling B-lymphocyte migration through secondary lymphoid organs: chemokine receptors and sphingosine-1-phosphate (S1p) receptors. Whereas chemokine receptor CXCR5 binding to CXCL13 and (to a lesser degree) CCR7 recognizing CCL19 and CCL21, favour the migration of B cells from the blood stream into in the white pulp and their retention within the follicle (Forster, Emrich et al. 1994; Pereira, Kelly et al. 2009; Gatto, Wood et al. 2011), sphingosine-1-phosphate (S1P) receptors promote the active egress of cells from lymphoid structures into

the circulation (Allende, Tuymetova et al. 2010; Arnon and Cyster 2014). In particular, two independent studies have revealed that S1PR1 in B cells is required for the exit of immature B cell from the BM to the blood (Pereira, Kelly et al. 2009). These results are highly reminiscent of the defects seen in B-cell specific *Utx* mutant mice. Interestingly, Manna and colleagues have recently reported that in thymocytes UTX and JMJD3 are required to egress from the thymus and reach the spleen, by favouring *S1pr1* gene expression (Manna, Kim et al. 2015). In agreement with these findings, our work shows that *Utx* deficient splenic B cells express lower levels of *S1pr1* transcripts. Based on previous data (Cinamon, Matloubian et al. 2004; Allende, Tuymetova et al. 2010; Arnon, Xu et al. 2011), we envision at least two distinct stages in the life of *Utx*-defective B cells when reduction in *S1pr1* expression may significantly affect their distribution. In the BM, newly generated *Utx* defective immature B cells may encounter a defect in the capacity to first enter the blood stream, which is necessary to reach secondary lymphoid organs such as the spleen. Once arrived in the spleen, *Utx* deficiency may impair the initial migration of B cells to the MZ and the subsequent shuttling of MZ B cells from between the follicle and the MZ area. As discussed above, such scenario will be validated measuring the *in vitro* migratory capacity of *Utx* mutant B cells upon stimulation with S1P, and by testing whether restoration of normal S1PR1 levels starting from immature B cells can normalize the defects in B cell distribution in different secondary lymphoid organs seen in *Utx* mutant mice. Mechanistically, we will determine whether, as in thymocytes, UTX controls *S1pr1* gene expression by modulating H3K27me3 levels at the promoter region, and /or by affecting the chromatin state at distal enhancer regions (Manna, Kim et al. 2015).

We report a significant reduction in the number of B cells present in MLNs and PPs of *Utx* mutant mice, suggesting a role for UTX in the homing of B cells to these sites. Lymphocyte entry into GALT requires the adhesion of the cells to high endothelial venules (HEV) and involves a cascade of chemokine-mediated integrin activations. In particular, the adhesion molecule Integrin α4β7 (ITGα4β7), which is constitutively expressed on the surface of B- and T-cells, plays a crucial role in controlling lymphocyte migration into the PP and MLNs by binding to MAdCAM-1, which is expressed on HEVs. Importantly, *Utx* inactivation reduced the level of expression of *Itgβ7* in mature B cells. This defect may be responsible for the reduced representation of B cells in GALTs, as well as that of IgA-secreting PCs in the intestinal lamina propria (Farstad, Halstensen et al. 1995). The migratory disturbances suffered by *Utx* mutant B cells are also possibly linked to the reduced expression of chemokine receptor *Ccr6*. Indeed, CCR6 was recently shown to guide the migration of activated PP B cells to the sub epithelial dome (SED), where interaction with dendritic cells is necessary to trigger IgA class witch recombination (Reboldi, Arnon et al. 2016). Finally, *Utx* mutant mature B cells showed reduced expression of the chemokine receptors *Ccr7* and *Cxcr4*. Defects of *Ccr7* expression could

impact on the migration of B cells into lymph nodes and PPs as suggested by data on *Ccr7* deficient mice (Forster, Schubel et al. 1999). Instead, *Cxcr4* downregulation could on one hand interfere with the capacity of B cells to form follicles in PPs (Nie, Waite et al. 2004) but most importantly it could influence the migration into the bone marrow of terminally differentiated PCs (Tokoyoda, Hauser et al. 2010). All together, these studies unveil an influence of UTX on general mechanisms of lymphocyte migration affecting both the entry into, and the exit from, primary and secondary lymphoid organs, with a possible strong impact on gut-associated immune responses.

Chemotaxis assays will be crucial to validate the possible migratory defects of *Utx* mutant B cells. Also, through ChIP-seq and ChIP-qPCR assays on *Utx* mutant resting and activated B cells, we will determine to which extent UTX exerts a direct control over the regulation of one or more migration-associated genes acting at the promoter level and/or by modulating enhancer accessibility.

4.4. UTX and T-cell dependent immune responses

Several reports including ours have unveiled a role for the H3K27 methyltransferase EZH2 in the control of GC B cell responses (Beguelin, Popovic et al. 2013; Caganova, Carrisi et al. 2013). Hence, we hypothesized that UTX, through its H3K27me3 demethylase function, could regulate GC B cell responses by counteracting the function of EZH2. In line with this prediction, we observed a consistent increase in the fraction of B cells carrying markers typical of GC B cells, in response to *Utx* inactivation. This was true both for GC B cell responses triggered in the spleen in response to the immunization with T-cell dependent antigens such as NP-CGG or SRBC, and for those spontaneously occurring in PPs and MLNs in response to microflora stimulation. The close-to-complete Cre-mediated recombination of the *Utx* conditional allele in GC B cells from *Utx* mutant mice establish the full capacity of *Utx* null B cells to contribute to the GC reaction. The increased fraction of *bone fide* GC B cells was confirmed by histological analysis of spleen sections in *Utx* control and mutant mice after immunization with T-cell dependent antigens, which revealed a consistent increase in the surface area occupied by BCL6-expressing GC B cells. The increase in the fraction of GC B cells observed in *Utx* conditional mutant mice closely resembles that observed after Cre-mediated inactivation of *Kmt2d* in all B cells using the CD19-cre transgene (Zhang, Dominguez-Sola et al. 2015). The latter observation suggests a role for *Utx* in cooperating with the MLL4/Thrithorax complex to sustain GC B cell biology (Ortega-Molina, Boss et al. 2015; Zhang, Dominguez-Sola et al. 2015). Interestingly, whereas *Kmt2d* inactivation starting from GC B cells failed to unveil major differences in the GC B cells fractions of control and mutant mice (Zhang, Dominguez-Sola et al. 2015), GC B cell-specific inactivation of *Utx* was

sufficient to increase the fraction of GC B cells in the mutant mice. The discrepancies between the two set of data could depend on the temporal onset of Cre-mediated recombination which could slightly differ between the Cγ1-cre and *Aicda*^{cre} transgenes, on differences in the stability of the two proteins, as well as on gene-specific effects of the knock-out on GC B cells and/or their immediate activated B cell precursor.

Using CXCR4 and CD86 as surface markers to discriminate centroblasts (CXCR4^{hi}CD86^{lo}) from centrocytes (CXCR4^{lo}CD86^{hi}), we observed a significant increase in the centroblast subset in response to U*tx* inactivation. These results were in accordance with a higher frequency in *Utx* mutant mice of GC B cells expressing high levels of BCL6. Moreover, transcriptomic profiling comparing *Utx* control to mutant GC B cells revealed lower expression of BCL6 target genes in the mutant cells, compatible with a higher proportion of centroblasts contributing to the pool of *Utx* defective GC B cells. The increased proportion of centroblasts following *Utx* inactivation may result from extensive proliferation and/or improved survival of these cells and from the failure to migrate to the light zone and/or to antagonize the activity of BCL6 and FOXO1 transcription factors. Future investigations will address these points, performing *in vivo* BrdU labelling experiments to assess proliferation, and the monitoring of apoptosis by measuring the fraction of GC B cells expressing activated caspases. We will also determine the impact of *Utx* deficiency on the fraction of positively selected centrocytes upregulating c-MYC expression, which will be assessed by flow cytometric analysis.

Transcriptional profiling of GC B cells identified a failure of *Utx* mutant cells to sustain the transcriptional activity of the IRF8/IRF4 axis, possibly acting at different stages of the GC reaction. Indeed, UTX may sustain the transcriptional activity of IRF8, which is primarily expressed in centroblasts (Shukla and Lu 2014), as a category of IRF8 target genes was significantly enriched among those that were downregulated in *Utx* mutant GC B cells. These included genes involved in signalling and chemotactic receptors (*Ccr6, Ccr7*) Instead, in centrocytes, where IRF8 is downregulated, UTX may sustains IRF4 function, (Klein, Casola et al. 2006; Shukla and Lu 2014; Xu, Chaudhri et al. 2015) to facilitate terminal differentiation and immunoglobulin isotype switching. Indeed, transcriptomic data revealed lower *Irf4* transcript levels in the bulk of *Utx* mutant GC B cells. Moreover, defects in the upregulation of IRF4 protein levels, possibly associated to less efficient activation, were observed when *Utx* mutant B cells were stimulated *in vitro* with CD40L+IL21, mimicking TF_H-derived signals delivered to positively selected centrocytes.

Hints on the profound changes occurring in GC B cell selection in response to *Utx* inactivation come from the analysis of immunoglobulin V gene rearrangement analysis. Indeed, upon immunization with the T-cell dependent antigen NP-CGG, we observed that *Utx* mutant mice

had a profound defect in selecting GC B cells bearing high-affinity anti-NP BCRs. Indeed, differently from control GC B cells, the V_H186.2 gene rearrangements cloned from *Utx* mutant GC B cells lacked in most cases point mutations causing a tryptophan to leucine substitution in codon-33 which confers a 10-fold increase in the affinity of the BCR for NP. This result combined with a largely unaffected rate of Ig somatic mutations is suggestive of the limited power of *Utx* mutant GCs to select B cells on the basis of the affinity of their BCRs. This result could depend on the limited time spent by *Utx* mutant GC B cells in the light zone where selection takes place. Alternatively, *Utx* mutant centrocytes may suffer from defects in antigen presentation, and/or from the failure to correctly signal through the BCR and/or CD40 receptors, providing thereby the same chances to low- and high-affinity B cells to survive, to possibly initiate further rounds of proliferation in the dark zone and/or to exit from the GC differentiating into memory B cells or antibody-secreting PCs (Victora and Nussenzweig 2012). Surprisingly, the failure of *Utx* mutant mice to preferentially select (and hence expand) GC B cells carrying high affinity BCRs did not prevent these animals from producing antigen-specific high-affinity antibodies in response to immunization. Indeed, following NP-CGG immunization, the rise in high-affinity anti-NP IgM and IgG1 serum titers was largely comparable between *Utx* control and mutant mice. Hence, the loose antigen-driven selection of GC B cells measured in *Utx* mutant mice does not prevent a possibly rare fraction of these cells expressing high-affinity antigen-specific BCR to differentiate into antibody-secreting PCs. To obtain a realistic estimate of the output of antigen-specific antibody-secreting cells released from the GC in the absence of *Utx*, future investigation will be focused on the careful quantification by ELISPOT assays and flow cytometric determinations of the fractions of total and antigen-specific antibody-secreting cells present in the spleen and bone marrow, at different time points following immunization.

Beside antibody-secreting PCs, the other major cellular output of the GC reaction consists of long-lived, antigen-selected, high-affinity memory B cells (Kurosaki, Kometani et al. 2015). These cells recirculate through secondary lymphoid organs and represent the primary subset of B cells recruited into recall immune responses (Kurosaki, Kometani et al. 2015). Upon secondary antigenic challenge, a fraction of memory B cells, mostly IgM-expressing (Dogan, Bertocci et al. 2009), are recruited into the GC reaction, while another subset, frequently expressing isotype switched BCRs, (Dogan, Bertocci et al. 2009) directly differentiate into antibody-secreting PCs. How does *Utx* inactivation influence the generation from the GC of high-affinity memory B cells? Furthermore, can *Utx* mutant memory B cells differentiate into antibody-secreting PCs upon antigen re-challenge? We have started to answer to these questions. Specifically, *Utx* control and mutant mice were immunized a first time with alum-precipitated NP_{27}-CGG and rechallenged 60 days later the animals with NP_{28}-CGG in the

absence of adjuvant. The comparison of the serum titers of high-affinity anti-NP IgG1 before and two days after antigenic rechallenge revealed a comparable rise of IgG1 titers in the serum of *Utx* control and mutant mice. From this preliminary experiment, we conclude that high-affinity IgG1 memory B cells can be generated in *Utx* mutant animals, and that the latter can differentiate into IgG1 antibody-secreting PCs. Future experiments will be focused on quantitative measurement by flow cytometric analysis of the numbers of antigen-specific isotype-switched memory B cells produced in *Utx* mutant mice after primary immunization with the T cell dependent antigen NP-CGG. Also, ELISPOT assay combined with flow cytometric assays will unveil the extent to which *Utx* inactivation regulates the number of antigen-specific plasma cells generated from memory B cells present both in the spleen and the bone marrow at different time points after secondary immunization.

4.5. UTX and immunoglobulin isotype switching

Basal immunoglobulin serum titers revealed alterations for different immunoglobulin isotypes in B-cell specific *Utx* mutant mice. In particular, the levels of IgG1, IgG2b and, most strikingly, IgA were reduced in *Utx* mutant animals. IgG3 serum titers were also consistently lower in *Utx* mutant animals when compared to controls, despite not reaching statistical significance. Conversely, IgM titers were increased in the latter animals when compared to controls. These results are consistent with a defect of *Ut*x mutant B cells to undergo immunoglobulin isotype switching, contributing to the establishment of a possible hyper-IgM immunodeficiency.

Defects in Ig isotype switching may result in one or more defects affecting, directly or indirectly, the protein machinery catalyzing this process. We excluded a contribution of AID to the defect of Ig CSR since the rate of Ig somatic hypermutation was unaffected in *Utx* mutant GC B cells. Moreover, *Aicda* transcripts were not deregulated in *Utx* mutant GC B cells. To monitor in more detail B cells undergoing Ig isotype switching, we performed a series of *in vitro* activation studies, stimulating control and *Utx* mutant B cells with different combinations of mitogens and cytokines to redirect isotype switching to specific immunoglobulin classes. These studies confirmed a defect of *Utx* mutant B cells to complete Ig isotype switching in due time. In particular, LPS cultures revealed a significant reduction in IgG3-expressing B cells at day 3 of the culture. In a similar fashion, *in vitro* stimulation with CD40L in the presence of IL4 and BAFF revealed a substantial delay of *Utx* mutant B cells to become IgG1 and IgE-expressing B cells.

Since Ig CSR strictly depends on the capacity of B cells to undergo repeated cell divisions (Hodgkin, Lee et al. 1996), we analyzed the proliferative capacity of *Utx* control and mutant B cells after LPS stimulation or CD40 ligation. These studies excluded gross differences in the growth behaviour of *Utx* control and mutant B cells. However, a closer look to individual B

cells using CFSE labelling revealed that *Utx* mutant cultures stimulated with LPS consisted of a larger fraction of B cells that had undergone fewer cell divisions (less than 5). The limited contribution of the latter population to the total B cell pool may explain why absolute numbers in *Utx* mutant cultures were comparable to those of *Utx* controls. Importantly, when we measured the fraction of LPS activated B cells that switched to IgG3, clustering them according to the number of cell divisions they went through, we failed to observe major differences between *Utx* control and mutant B cell cultures. All together, these data are compatible with a scenario in which loss of *Utx* increases the threshold for B cell activation. The B cells overcoming this activation barrier, proliferate vigorously and complete the process of Ig isotype switching. Interestingly, unpublished work from our group has revealed that JMJD3 mutant B cells stimulated *in vitro* with LPS also displayed a defect in cell activation. In this case, demethylase mutant B cells showed a defect in completing the first cell cycle after stimulation, which led to a delay in the exponential growth of the cells (Rahmat and Casola unpublished results).

Mechanistically, we tested whether the impaired capacity of *Utx* mutant B cells to undergo Ig CSR was related to changes in expression at the IgH constant region genes. Given the importance of C_H germline transcription for triggering AID-dependent Ig isotype switching (Stavnezer-Nordgren and Sirlin 1986), we quantified in LPS-activated B cells from *Utx* control and mutant cultures, *Igh-γ3* germline transcripts, 24 h post-stimulation. Transcripts starting from the sterile Iγ3 promoter were comparable in levels between *Utx* control and mutant B cells. This result excludes that *Utx* is involved in the initiation of the Ig CSR process. Recent work has hinted to a role for the component of the mixed-lineage leukemia 3 (MLL3)/MLL4 chromatin-modifying complex, PTIP in the process of Ig CSR through the regulation of C_H germline transcription (Starnes, Su et al. 2016). Our data exclude that such function depends on UTX. Future studies will reveal whether UTX influences Ig CSR by facilitating the occurrence of breaks at C_H switch regions and/or by supporting the non-homologous end joining (NHEJ) DNA repair machinery to finalize the joining between distal IgH switch regions. For this, we will initially compare the levels of C_H circle and post-switched transcripts in *Utx* control and mutant B cells which are produced in B cells that have respectively undergone breaks at Ig switch regions or have rejoined them (Kinoshita, Harigai et al. 2001).

Finally, we tested whether the lower frequency of Ig-isotype switched B cells observed in *Utx* mutant cultures could depend on increased sensitivity of these cells to undergo apoptosis, possibly in relation to the DNA damage caused by single-strand and/or double strand DNA breaks caused by AID. To address this point, we measured the fraction of B cells expressing activated forms of Caspases as readout of ongoing apoptosis. These experiments indicated that

Utx deficiency had not impact on apoptosis of B cells undergoing Ig CSR in response to LPS stimulation.

One possible molecular determinant responsible for the defects in Ig CSR observed in *Utx* mutant B cells is the transcription factor IRF4. Indeed, upon LPS stimulation or CD40 ligation *Utx* mutant B cells suffered from a defect in inducing the expression of the *Irf4* gene. As a matter of facts, we scored the accumulation in *Utx* mutant cultures of a substantial fraction of B cells with low IRF4 protein levels. IRF4 has been shown to regulate Ig CSR, acting downstream of germline transcription of C_H regions. Indeed, as reported by Klein et al, *Irf4* mutant B cells stimulated *in vitro* with LPS+ IL4 expressed normal *Igh-γ1* sterile transcripts, while displaying considerably lower levels of circle Iγ1-Cμ, and post-switch *Iμ-Cγ1* transcripts (Klein, Casola et al. 2006). The accumulation of $IRF4^{lo}$ cells upon *in vitro* stimulation did not prevent *Utx* mutant B cells, stimulated *in vitro* with LPS or *in vivo* in GC B cells, from upregulating *Aicda* gene expression, excluding the latter as possible mechanism for the defect in Ig CSR seen in *Utx* mutant mice. Future investigations will attempt to normalize IRF4 expression levels through lentiviral complementation assays in LPS-activated *Utx* mutant B cells in order to test whether this is sufficient to normalize Ig isotype switching.

Utx mutant mice suffered from a significant decrease in serum IgA titers. Importantly, similar defects are observed in patients suffering from the Kabuki syndrome, which is linked to inactivating mutations of either the *KMT2D* or *UTX*/*KDM6A* genes (Lindsley, Saal et al. 2016). KS patients suffer from a mild immunodeficiency mainly related to disturbances in gut mucosal immunity (Lin, Lee et al. 2015). Therefore, *Utx* mutant mice represent an ideal model system to understand the molecular bases underlying the immune defects related to IgA deficiency observed in KS patients. Transcriptomic profiling of primary *Utx* mutant B cells, including both resting B cells and GC B cells, identified multiple genes involved in the generation of IgA-expressing B cells that were downregulated in response to *Utx* inactivation. First, *Utx* mutant B cells suffered from a downregulation of the TNFR family member TACI. Expression of TACI in lamina propria B cells is crucial to mediate IgA switching in response to stimulation with APRIL, which is locally released by dendritic cells (He, Xu et al. 2007; Fagarasan, Kawamoto et al. 2010). Second, *Utx* mutant B cells expressed lower levels of the chemokine receptor *Ccr6*. In PPs, CCR6 expression on B cells is crucial for their migration towards the sub-epithelial dome where interactions with dendritic cells is a crucial step to become IgA-expressing B cells (Reboldi, Arnon et al. 2016). Third, *Utx* mutant B cells suffered from weaker expression of the integrin *Itgβ7*. This defect is expected to limit the migration of B cells to PPs and MLNs, which are the primary sites for IgA switching (Wagner, Lohler et al. 1996; Mora, Iwata et al. 2006) (Dullaers, Li et al. 2009). Moreover, *Utx* mutant PBs generated in PP GCs may encounter difficulties to reach the intestinal lamina propria, where they secrete IgA that ultimately reaches

the intestinal lumen (Mora, Iwata et al. 2006; Dullaers, Li et al. 2009). In support of this, we observed a substantial reduction in IgA-expressing PCs in the intestinal lamina propria of *Utx* mutant mice. Future studies based on UTX and MLL4 ChIP-seq or ChIP-qPCR at target genes in *Utx* proficient B cells will be needed to assess whether genes transcriptionally controlled by UTX and involved in the generation of IgA-expressing B cells are also UTX/MLL direct targets.

4.6. UTX and plasma cell differentiation

Expression analysis suggested a role for UTX in the early stages of PC differentiation. Indeed, expression of the *Utx* gene transiently increased in $CD138^{+}CD19^{lo}$ PBs, before getting substantially downmodulated at later stages of the terminal differentiation program. We analyzed terminal differentiation both *in vitro* and *in vivo,* upon immunization of *Utx* mutant mice with T-cell dependent antigens.

The disturbed pattern of secreted immunoglobulins observed in *Utx* mutant mice renders any conclusive statement on PC function difficult to draw. Indeed, in these mice the increased IgM titers counteracted corresponding defects in the serum levels of isotype-switched immunoglobulins. Under these conditions, homeostatic expansion of selected subsets of PCs to guarantee normal secreted antibody levels may hinder underlying defects in PC differentiation. To overcome these limitations, we performed a series of *in vitro* experiments meant to monitor the early steps of PC differentiation through the stimulation of B cells with either LPS or a combination of CD40 ligation and IL21. In particular, we monitored the dynamics of expression of two major determinants of the PC differentiation program, namely IRF4 and BLIMP1/*Prdm1*. The choice to study these two transcription factors comes from previous evidences, including some from our own group, indicating that the *Prdm1* and *Irf4* genes are marked by H3K27me3 in resting B cells. Based on this, we hypothesized that the H3K27 demethylase function of *Utx* could contribute to the upregulation of IRF4 and BLIMP1 expression by erasing the H3K27me3 mark.

Flow cytometric determination of BLIMP1 protein levels excluded major effects of *Utx* inactivation on the induction of the *Prdm1* gene in B cells activated with LPS. On the contrary, we observed a substantial fraction of LPS activated B cells coming from *Utx* mutant cultures that failed to induce IRF4 protein levels. This was observed performing flow cytometric analyses and immunoblotting analyses on the bulk B cell population upon *in vitro* stimulation. Results were largely reproduced in *Utx* mutant B cell cultures activated with CD40 ligation and IL21 stimulation, which mimic signals delivered by T_{FH} to B cells in the GC. In support of this, transcriptomic profiling revealed lower transcript levels for *Irf4* in *Utx* mutant GC B cells when compared to controls, whereas the reduction of *Prdm1* transcripts in the same mutants was

marginal. These data are consistent with a scenario whereby UTX facilitates full activation of B cells, concomitantly inducing *Irf4* gene expression, which is required to trigger PC differentiation (Klein, Casola et al. 2006). In the absence of *Utx*, fewer B cells succeed to express the levels of IRF4 required to initiate terminal differentiation. Conversely, once B cells reach high IRF4 expression, they can proceed to become CD138-expressing PBs and sustain high IRF4 levels in the absence of *Utx*. How could UTX influence the initial rise in IRF4 expression upon activation? One possible scenario is linked to the recruitment of UTX at *Irf4* regulatory regions where it may affect H3K27 methylation/acetylation levels, thereby sustaining its expression (Caganova, Carrisi et al. 2013). This will be addressed measuring by ChIP-qPCR, the H3K27me3 and H3K27ac levels at the promoter of the *Irf4* gene in *Utx* mutant B cells after LPS activation. Should we observe higher H3K27me3 levels at the *Irf4* locus in these cells, we will test whether pharmacological inhibition of EZH2 can restore IRF4 expression and thereby optimal PC differentiation in *Utx* mutant cultures (Ezponda, Dupere-Richer et al. 2017).

Given the partial defect suffered by *Utx* mutant B cells to upregulate IRF4 in response to stimuli triggering terminal differentiation, we were surprised to see that upon immunization with T-cell dependent antigens, *Utx* mutant mice produced comparable levels of high-affinity antigen-specific, IgM an IgG1 antibodies. This scenario suggests that in *Utx* mutant mice compensatory mechanisms may operate *in vivo* to ensure activated B cells to effectively upregulate *Irf4* expression in order to differentiate into antibody-secreting cells. To test this hypothesis, we will compare by flow cytometry IRF4 expression levels in newly generated $CD138^{+}$ $B220^{lo}$ $CD19^{lo}$ PBs from *Utx* control and mutant mice soon (e.g. 24h -72h) after immunization with either T-cell dependent (NP-CGG) or -independent antigens (LPS).

One candidate demethylase capable of replacing UTX function in B cells in the regulation of *Irf4* gene induction is JMJD3. Indeed, several reports have assigned to JMJD3 a role in the positive regulation of *Irf4* gene expression in normal cells (Satoh, Takeuchi et al. 2010). This hypothesis is further supported by unpublished work from our own group, which revealed lower *Irf4* expression in *Jmjd3* mutant B cells stimulated with LPS (Rahmat and Casola, personal communication). To test whether JMJD3 can, at least partially, replace UTX function in *Utx* mutant B cells, we will measure IRF4 protein levels in *Utx/Jmjd3* double mutant B cells stimulated both *in vitro* and *in vivo* with LPS. These experiments will be performed using $Jmjd3^{fl/fl}Utx^{fl/fl}$; $Mb\text{-}1^{cre/+}$ compound mutant mice which are becoming available in our laboratory.

In vitro LPS stimulation assays have revealed that once B cells succeed to express high levels of IRF4 protein, the differentiation towards CD138-expressing PCs can proceed regardless of *Utx* expression. This is consistent with the observation that in PCs *Utx* levels are significantly

downregulated. The results are also compatible with a scenario whereby a possibly limited output *in vivo* of precursor PCs/PBs resulting from *Utx* inactivation is counteracted by the homeostatic expansion of terminally differentiated PCs (or by homeostatic increase in the rate of antibody secretion/cell) still generated despite *Utx* deficiency. The latter PCs may account for the production of normal titers of antigen-specific anti-NP IgM and IgG1 antibodies produced in *Utx* mutant mice after NP-CGG immunization. In support of this hypothesis, we observed that whereas the fraction of NP-specific PBs identified two days after secondary NP-CGG immunization were reduced in *Utx* mutant mice, anti-NP IgG1 titers produced by secondary PCs (namely those differentiating from memory B cells) in these animals were comparable to those of controls. Altogether, *in vitro* and *in vivo* studies are suggestive of a distinct defect suffered by *Utx* mutant B cells in the early stages of PC differentiation, possibly linked to the failure to reach full-blown activation and effectively upregulate the PC master regulator IRF4.

4.7. The gene expression profile and chromatin landscape of mature B cells lacking *Utx*

Bioinformatics analysis of RNA-seq data, setting a relatively low cut-off for the fold change in gene expression (FC > 1.2 an adjusted p-value <0.05) revealed a relatively similar number of genes respectively up- and downregulated in both resting and GC B cells of *Utx* mutant mice when compared to the corresponding subsets of control animals. A more conservative call for differentially expressed genes (FC > 1.5 and adjusted p-value < 0.05; Figure 72) revealed a lower number of genes down regulated in *Utx* mutant B cells, while the list of upregulated genes remained largely unaffected (Figure 72). Similar results were recently observed analyzing *Utx*-deficient hematopoietic stem and progenitor cells (Gozdecka, Meduri et al. 2018). Together, these results indicate that UTX acts both as a positive and negative regulator of gene expression. The impact of *Utx* deficiency on gene expression was influenced by the state of activation of the mature B cells. Indeed, whereas in resting B cells, *Utx* deficiency caused mild effects on gene expression, with the majority of the downregulated genes displaying fold changes lower than 2, in GC B cells the loss of the demethylase exerted a more robust detrimental effect on gene expression, with the majority showing differences in expression stronger than two-fold. In resting B cells, *Utx* loss significantly (FC<-1.5; q value<0.05) affected the expression of NF-κB target genes (*Zbp1, Ebi3, Oas3, Slc4a7, Oas2*) as well as genes involved in MYD88-dependent TLR signalling (*Dusp4, Irak3, Mapk11*). Instead, in GC B cells the lack of the demethylase consistently reduced the expression of genes involved in chemotaxis (*Ccr7, Ccr6*). Categories of genes significantly downregulated in both *Utx* mutant resting and GC B cells

included those implicated in the biology of IgA-expressing B cells (*Ccr7, Tnfrsf13b/TACI*, *Itgβ7* and *Itgα4*), as well as targets of the IRF4/IRF8 transcriptional axis (*Slamf9, Il6ra, Cd274, Cdkn2d, Ncf1, Tnfrsf13c*).

In resting B cells, *Utx* deficiency caused a mild increase in the expression of around 300 genes, with differences ranging between 1.2 and 1.8 folds. In contrast, *Utx* mutant GC B cells displayed a more robust increase in the expression of a limited set (~ 50) of genes. Resting B cells lacking *Utx* increased preferentially the expression of genes coding for proteins involved in cellular junctions (*Mllt4, Lmo7*), interaction with the extracellular matrix (*Itgb1, Actn1, Parvb,*), G protein-coupled receptor signalling (*Akap6, Akap5, Pde8a*), apoptosis (*Lmna, Capn2, Prf1*) and TGFβ signalling (*Bmpr2, Bmp6, Acvr2a*). In *Utx* mutant GC B cells the very few upregulated included members of TGFβ signalling (*Smad1, Bambi)*, NOTCH signalling (*Neurl1b*) and regulators of the cell cycle such as *Cdk14* and *Cdkn2c*. The mild effects on gene expression consequent of *Utx* inactivation are not unexpected. Indeed, mild changes in gene expression (FC > 1.5) have been also described as a consequence of *Kmt2d* inactivation in resting and GC B cells (Zhang, Dominguez-Sola et al. 2015). Similarly, *Crebbp* mutant GC B cells exhibited around 1000 of differentially expressed genes with FC >1.2, of which only 200 represented bona fide direct targets (Zhang, Vlasevska et al. 2017). Similarly, *Crebbp* mutant GC B cells exhibited around 1000 of differentially expressed genes with FC >1.2, of which only 200 represented bona fide direct targets.

From our data, it emerges a picture in which *Utx* impacts on B cell biology primarily influencing B cell migration and B cell activation in response to TLR signalling, mostly through the regulation of NF-κB and IRF4/8 controlled gene expression. A striking enrichment for genes implicated in the generation and function of IgA-expressing B cells among those regulated by *Utx* predicted a major impact of *Utx* deficiency on IgA-associated mucosal immunity. Indeed, *Utx* deficient mice suffered from significantly lower IgA serum titers, underrepresented B cell populations in GALT and poor recruitment of IgA-secreting PCs to the intestinal lamina propria. These combined defects may alter the relationship between the organism and the microbiota colonizing the intestine, with possible direct and indirect influences on local and systemic immunity. This will represent a major focus of my future investigations, as it may help understand the immune dysfunction suffered by Kabuki Syndrome patients carrying mutations in the *UTX/KDM6A* gene.

In the present study, we began to reconstruct in *Utx* mutant B cells the genome-wide distribution of H3K4me3 and H3K27ac, to explore the effects of *Utx* deficiency on the epigenetic landscape of B cells. Taking into account the reported interaction of UTX with the H3K4 methyltransferase MLL4/KMT2D (Cho, Hong et al. 2007), we expected to find changes in the

number of genes marked by H3K4me3 in *Utx* mutant B cells. Instead, both in resting and GC B cells the repertoire of H3K4me3-marked genes was largely unaffected by *Utx* inactivation. Whereas these results exclude major redistribution of the MLL4 complexes in the absence of *Utx*, we cannot exclude that the absence of the demethylase causes fine changes in the degree of deposition of this mark at target genes. The answer to this question will come performing quantitative ChIP-seq assays or by ChIP-qPCR analyses on candidate genes.

Genes downregulated in *Utx* mutant B cells remained marked by H3K4me3 at the promoter region. This result suggests that UTX controls target gene expression without necessarily affecting its epigenetic state at the promoter region. In line with these conclusions, we observed that the groups of genes marked in wild-type B cells respectively by H3K4me3, H3K27me3/H3K4me3 and H3K27me3 taken as a whole, did not significantly change their expression in the *Utx* mutant counterparts. These results are compatible with a scenario in which UTX operates in a cell-type-, stage- and gene-specific fashion.

The existence of a chromatin complex composed of UTX, MLL4 and the histone acetyltransferase p300 (Wang, Tang et al. 2017), prompted us to profile the genome-wide distribution of H3K27 acetylation in *Utx* mutant resting and GC B cells. Preliminary bioinformatics analyses of ChIP-seq data identified a specific subset of genes with lower H3K27ac levels at the promoter in *Ut*x mutant mature (302 genes) and GC B cells (680 genes). A small fraction of these genes was also significantly transcriptionally downregulated respectively in *Utx* mutant resting (17 genes) and GC B cells (13 genes) compared to their control counterparts. At the same time, we identified a subset of genes carrying higher H3K27ac levels in *Utx* mutant B (1257 genes) and GC B cells (623) with a minor fraction (around 10-15%) being transcriptionally upregulated in *Utx* deficient B cells. All together, these results suggest that UTX fine tunes the levels of H3K27ac at the promoter of at least a subset of target genes modulating thereby their expression level. These results do not exclude the possibility that UTX may influence gene expression modulating chromatin accessibility through changes in the deposition of other histone marks. In this context, future experiments will be focused on assessing the impact of *Utx* deficiency on the genome-wide distribution of H3K27me3 in B cells and, more in general, on the fine balance between H3K27 acetylation and methylation at promoters of target genes. Additionally, several recent reports have highlighted the importance of UTX in regulating in different cell types the accessibility of distal regulatory regions including enhancers and, possibly, super enhancers (Beyaz, Kim et al. 2017; Gozdecka, Meduri et al. 2018). UTX has been linked to the regulation of enhancer activity and gene activation via coordination of COMPASS-mediated H3K4me1 deposition and CREBBP/p300-mediated H3K27ac deposition (Wang, Tang et al. 2017). To this end, ChIP-sequencing profiling of enhancer-associated H3K4me1, catalyzed by the MLL3/KMT2C and MLL4/KMT2D

methyltransferases (Hu, Gao et al. 2013), will be performed comparing *Utx* control to mutant B cells. The intersection between H3K4me1 and H3K27ac genome wide distribution profiles will allow us to reconstruct the repertoire of H3K27ac^{+}H3K4me1^{+} promoter-distal regions functionally linked to enhancer regions in both wildtype and *Utx* mutant B cells. The reconstruction of a high-fidelity genome wide map of active enhancers in both *Utx* control and mutant B cells will also benefit from data obtained from the Assay for Transposase Accessible Chromatin (ATAC)-coupled to ultra-deep sequencing (Buenrostro, Giresi et al. 2013).

Recently, Beyaz and colleagues reported an accumulation of H3K27me3 at so called super enhancer regions of *Utx*-mutant iNKT cells (Beyaz, Kim et al. 2017). Enrichment of this repressive histone mark at these sites was associated to loss in chromatin accessibility and transcriptional downregulation of putative target genes. Hence, it is possible that at least part of the contribution of UTX to the regulation of target gene expression is operated through a fine modulation of H3K27me3 levels at distal regulatory regions. Future studies aiming to score in a quantitative fashion through ChIP-seq assays possible changes in H3K27me3 deposition at intergenic regions in response to *Utx* inactivation will help to solve this question.

4.8. UTX and B cell transformation

Several types of solid cancers including tumors of the urogenital tract (urothelial bladder cancer, renal clear cell carcinoma), brain (medulloblastoma and glioblastoma) and blood (acute lymphoid leukemia, chronic myelomonocytic leukemia and multiple myeloma) display mutations, deletions or downregulation of the *Utx* gene (van Haaften, Dalgliesh et al. 2009; Van der Meulen, Speleman et al. 2014). These data render UTX a candidate tumor suppressor. Recent studies in the mouse model have corroborated this hypothesis (Van der Meulen, Sanghvi et al. 2015; Wu, Tian et al. 2018). In particular, using the E*μ*-MYC lymphoma-prone model, it has been shown that loss of *Utx* significantly accelerates B cell lymphomagenesis. *Utx* deficiency also changed the spectrum of this disease, shifting the lymphomas from a B cell progenitor-type to a more immature B cell type tumor. Also, *Eμ-MYC; Utx*$^{-/-}$ lymphomas became significantly more aggressive than their *Utx* proficient counterparts, disseminating more frequently into non-lymphoid organs including the brain. In all mouse tumor models, in which UTX tumor suppressor function was investigated, the inactivation of the demethyalse accelerated tumorigenesis driven by deregulated expression/activity of proto-oncogenes such as *Myc* and *Ras* (Li, Zhang et al. 2018; Wu, Tian et al. 2018). Instead, *Utx* deficiency alone had minor effects on malignant transformation. These results point to UTX as a facilitator/enhancer of oncogene-driver transformation. In line with these results, we failed to observe any sign of malignant B cell transformation in B cell specific *Utx* mutant mice monitored so far up to 12-

month of age. However, the increased fraction of GC centroblasts, consequent to *Utx* inactivation, could represent a pre-neoplastic lesion, predisposing to the occurrence of GC B-cell derived lymphomas. Enlarged GCs were also described in transgenic animals expressing a gain-of-function mutant allele for the Polycomb gene *Ezh2*, which is frequently selected in Follicular lymphoma and Diffuse Large B cell lymphoma (Morin, Johnson et al. 2010; McCabe, Ott et al. 2012; Beguelin, Popovic et al. 2013). Hence, in GC B cells the potentiation of the H3K27 methylation axis either by loss of *Utx* or by gain-of-function mutations of *Ezh2* may facilitate malignant transformation driven by oncogenes such as BCL6 and BCL2. To test this hypothesis, we are currently breeding conditional *Utx* mutant mice to lymphoma-prone animals carrying either the *VavP-Bcl2* transgene (Egle, Harris et al. 2004) promoting Follicular lymphoma, or the *Iμ-HABCL6* knock-in allele, which promotes Diffuse Large B cell lymphomas (Cattoretti, Pasqualucci et al. 2005). Interestingly, the *Efnb1* gene has been found upregulated in *Utx* mutant FO B cells and GC B cells and also highly induced in *Utx*-mutant lymphomas, suggesting that it could contribute to the aggressiveness and enhance the dissemination of *Utx* KO *Eμ-MYC* lymphomas.

4.9. What did we learn from studying UTX function in B cells?

Motivated by the growing body of evidences highlighting critical roles in lymphopoiesis for components of the Polycomb Repressive complexes and for the MLL family of methyltransferases, we decided to elucidate the functional role in B cell development of the related family of H3K27 demethylases through the analysis of B-cell specific *Utx* conditional knockout-mice. The investigations led us to unveil distinct roles of UTX at different stages of B cell development. Whereas in early lymphopoiesis, *Utx* loss impacted on the size of the pre-B cell compartment favouring its expansion, in peripheral B cell maturation the lack of the demethylase impinged on the size of the peripheral pool of resting B-2 B cells, combined with a possible migratory defect that prevented the cells from effective seeding of secondary lymphoid organs, an in particular of GALTs. The mild yet consistent impairment of *Utx* mutant mature resting B cells to respond to the pro-survival factor BAFF, possibly contributed by defects in NF-κB function, could, on the long run interfere with their homeostasis.

A major finding of our studies relates to the disturbance in *Utx* mutant B cells of the expression of different classes of genes controlling intra- and extravasation of B cells from the blood, and in particular their homing to PPs and MLNs. These, together with findings linking UTX function to the expression of genes promoting IgA isotype switching and migration of IgA plasma cells to the intestinal lamina propria, establish a crucial role for UTX in the control of IgA-associated B cell immunity. Importantly, similar defects have been observed in Kabuki Syndrome patients, who, in a fraction of cases carry inactivating mutations in the *UTX gene*.

Hence, B-cell specific *Utx* mutant mice represent an ideal model system to study the molecular bases for the humoral immune disorders by Kabuki Syndrome patients.

Molecular analysis performed on *Utx* mutant B cells unveiled the transcription factor IRF4 as a possible relevant molecular determinant of at least some of the developmental and functional defects of these cells. Reduced IRF4 expression may contribute to impaired Ig isotype switching, defective triggering of terminal differentiation in response to LPS or CD40L+IL21 stimulation and possibly to an enlargement of the pool of *bona fide* MZ B cells.

Preliminary studies of genome wide mapping of selected histone marks revealed a minor contribution of UTX to the shaping of the repertoire of gene promoters marked by H3K4me3. Instead, *Utx* deficiency affected the degree of H3K27 acetylation at the promoter of a subset of its targets possibly contributing to the fine tuning of their expression. These studies highlight the necessity to perform, as next step, a careful quantitative assessment in *Utx* mutant B cells of the deposition of histone marks including H3K4me3, H3K27me3, H3K27ac and H3K4me1 at both promoter regions as well as distal regulatory regions such as enhancers and super-enhancers.

In summary, the data so far obtained from studies in B-cell specific *Utx* knock-out mice highlight an important contribution of *Utx* in ensuring an effective progression of B cells through both early and late stages of development, via fine tuning of expression of a selected set of genes controlling cell migration, cell survival, antibody isotype switching, and optimal activation in response to both T-cell dependent and -independent antigens.

4.10. Future goals

Throughout the discussion I have already listed the set of experiments I believe are needed to fill in our current knowledge gaps on the function of UTX in B cell development and B cell immune responses. A summary of these experiments with an experimental plan is outlined below:

4.10.1. Role of UTX in pre-B cells and in the control of S1PR1-induced B cell migration

To address these questions, we will perform a short *in vivo* BrdU labelling pulse experiments to measure the fraction of proliferating cells in the bone marrow pre-B cell compartment. We will also dedicate a cohort of mice for a brief pulse of BrdU labelling *in vivo* followed by a short chase phase to determine the time needed for pre-B cells to transit to the IgM^+ immature B cell stage. To test the sensitivity of *Utx* mutant B cells to Sphingosine-1 phosphate (S1P) induced migration, we will perform *in vitro* 3 hours chemotaxis assays with total bone marrow cells using transwell chambers and flow cytometry to characterize the populations responding to S1P. Similar experiments will be repeated with splenic B cells from *Utx* control and mutant

mice. S1PR1 deficient immature B cells failing to leave the BM could undergo apoptosis (Allende, Tuymetova et al. 2010). To test this, we will perform stainings for the expression of activated caspases analyzing different BM B cell subsets in controls and *Utx* mutant mice.

4.10.2. To study the effects of *Utx* inactivation on NF-κB signalling in response to BAFF/BCR stimulation

Initially, we will validate RNA seq data, performing qRT-PCR assays for genes coding for NF-κB family members and downstream targets that were found downregulated in *Utx* mutant resting and GC B cells. Next, we will test a possible defect in the alternative NF-κB signalling pathway resulting from *Utx* deficiency upon BAFF stimulation. For this, we will measure by immunoblotting analyses the levels of both p100/*Nfκb2* and of its processed, active form p52 in resting B cells before and after BAFF stimulation. This analysis will be completed by qRT-PCR assays for targets of p52 including pro-survival genes *Bcl2* and *Mcl1* and pro-apoptotic ones like *Bim, Bax Bad, Puma*, and *Bcl2l11*.

4.10.3. To assess the competitive fitness of *Utx* mutant B cells

To test this hypothesis, I will generate mixed BM chimeras, in which *Utx* knock-out and wild type cells will compete in the same environment. These experiments will be instrumental to unveil possible defects in the fitness of mature resting *Utx* mutant B cells, when they have to compete with *Utx* proficient cells. BM chimeras will also unveil whether *Utx* mutant GC B cells have an advantage over their wild type counterparts in expanding within the GC, and whether recruitment of these cells into the memory or PC compartments and the maintenance of the later subsets is influenced by *Utx* deficiency.

4.10.4. To study how *Utx* deficiency deregulates the transcriptional network sustaining GC B cell function

To answer this question, we will initially perform *in vivo* BrdU labelling experiments to measure the fractions of *Utx* control and mutant GC B cells in active proliferation. I will also assess by flow cytometry, measuring activated caspase expression, the frequency of *Utx* deficient and proficient GC B cells undergoing programmed cell death. *Utx* may also influence the dynamics of GC responses. To address this point, I will dedicate different cohorts of mice to an immunization protocol using NP-CGG. In these mice, I will quantify the frequency of GC B cells by flow cytometry, and the number and size of GCs by histological examination, at different time points after the immunization.

To investigate in greater detail the transcriptional networks operative in GC B cells in the absence of *Utx*, I will combine staining for GC B cells with fluorescent-labelled antibodies to measure by intracellular flow cytometry the expression respectively of PAX5, BCL6, IRF4 and

BLIMP1 transcription factors. The goal of these studies is to obtain, at single cell level resolution, information on how *Utx* deficiency interferes with the expression of transcription factors controlling the transition from centroblast to centrocytes and the committment to PC differentiation.

In particular, to address the status of IRF4 and IRF8 transcriptional activity in *Utx* mutant GC B cells, I will measure by qRT-PCR analysis the expression of a representative set of target genes respectively in FACS-sorted centroblasts and centrocytes retrived from *Utx* control and mutant mice. Should we observe a substantial influence of *Utx* deficiency on IRF4 controlled gene expression, I will study to what extent UTX and IRF4 share a similar subset of target genes. To this aim, I will use *in vitro* activated B cells stimulated with LPS to perform UTX and IRF4 ChIP-seq assays respectively on $IRF4^{lo}CD19^{+}CD138^{-}$ pre-activated B cells, $IRF4^{hi}CDl9^{+}CD138^{-}$ activated B cells and $IRF4^{hi}CDl9^{lo}CD138^{+}$ PBs purified from control cultures. Genes (and/or their distal regulatory regions) recruiting both UTX and IRF4 will be investigated by qRT-PCR analysis for the extent to which they are modulated in response to *Utx* inactivation.

To investigate how *Utx* inactivation affects the output of the GC reaction, we will measure by ELISPOT and flow cytometry the number of antibody-secreting PCs present in the BM and spleen at different time points after immunization with either T-cell dependent (NP-CGG) or -independent type-1 (NP-LPS) antigens. This analysis will be extended at several months (at least four) after the immunization to estimate a possible influence of *Utx* deficiency on the maintenance of long-lived memory B cells.

4.10.5. To determine whether the failure to effectively induce IRF4 expression upon activation is responsible for the defect in immunoglobulin isotype switching seen in *Utx* mutant B cells

To address this point, primary resting B cells isolated from *Utx* mutant and control spleens will be activated with LPS and transduced with lentiviral vectors expressing IRF4 in combination the GFP reporter gene. We will measure whether restored IRF4 expression in *Utx* mutant B cell is sufficient to normalize Ig isotype switching to IgG3.

We will also test whether *Utx* deficiency interferes with the late stages of Ig CSR following the initial breaks at Ig switch regions induced by AID. To this end, we will quantify Cμ circle (*Iγ3-Cμ*) and post-switch (*Iμ-Cγ3*) transcripts by qRT-PCR analysis in *Utx* control and mutant B cells stimulated in vitro with LPS.

4.10.6 To define the landscape of UTX direct targets in resting and activated mature B cells

To address this question, I will perform UTX ChIP-seq assays on chromatin extracted from wildtype resting splenic B cells and from B cells activated *in vitro* with LPS. In a preliminary experiment, I have used with little success the antibody our group developed in house.

Therefore, I will resume to a commercially available source of UTX antibody, which has been used to map genome wide distribution of UTX in iNKT cells (Beyaz, Kim et al. 2017). The list of UTX binding sites will be intersected with the list of genes differentially expressed between control and *Utx* mutant B cells, to ultimately reveal the repertoire of target genes transcriptionally controlled by UTX. I will try to perform similar experiments on GC B cells. However, the limiting number of the cells may limit the feasibility of this experiment.

To establish the repertoire of distal regulatory regions under the control of UTX in mature B cells, we will first generate a map of chromosome regions marked by H3K27ac and H3K4me1, by performing H3K4me1 ChIP sequencing profiling of mature B cells of wild type mice, intersect it with ATAC-seq data that will be obtained from resting and LPS-activated B cells and with NET-CAGE data generated from these cells in collaboration with Dr Murakawa (Riken Institute, Yokohama). Chromosome coordinates sharing all these chromatin features (e.g. regions marked by H3K27ac and H3K4me1, $ATAC^{+}$ and transcribed) will be considered *bona fide* active enhancers. The status of the latter regions will then be investigated in the same set of B cells, this time lacking *Utx*. Through these analyses, we expect to find the repertoire of distal regulatory regions under the control of UTX in resting and LPS-activated B cells.

4.9.7. Functional redundancy between UTX and JMJD3 in B cell development and activation

To address this question, I will perform a comprehensive immunophenotypic analysis of B cell populations in primary and secondary lymphoid organs including GALT comparing respectively control animals, JMJD3-only KO mice (*Jmjd3*$^{fl/fl}$*; Mb-1*$^{cre/+}$), *Utx*-only KO mice (*Utx*$^{fl/fl}$*; Mb-1*$^{cre/+}$*)* and JMJD3/UTX dKO mice (*Jmjd3*$^{fl/fl}$*; Utx*$^{fl/fl}$*; Mb-1*$^{cre/+}$). I will compare numbers and frequencies of various B cell subsets as well as their capacity to: 1) form GCs upon immunization with T-cell dependent antigens, 2) undergo Ig isotype switching both in vitro and in vivo; 3) generate short- and long-lived PCs and memory B cells.

4.10.8. To establish the role of UTX catalytic activity in B cell development and GC responses

Several reports have postulated that UTX function may also be exerted independently of its catalytic activity (Miller, Mohn et al. 2010; Shpargel, Sengoku et al. 2012; Wang, Lee et al. 2012).

Therefore, I wish to define how UTX catalytic activity contributes to the role of UTX in B cell development and activation during an immune response.

To address this question, I will analyze mice developed in the laboratory of Dr Kai Ge (NIH, Bethesda, USA) carrying three distinct mutations within the catalytic domain of UTX preventing its function (Wang, Lee et al. 2012). The latter animals have been instrumental to assess the relevance of UTX catalytic activity for mouse craniofacial development and muscle regeneration (Shpargel, Starmer et al. 2017) (Faralli, Wang et al. 2016). Analysis of B cell

development and GC responses in UTX catalytic dead animals will be performed in collaboration with Dr Ge and Dr Li (Childrens Hospital, Boston, USA) who has kindly agreed to provide us with the animals needed to perform the experiments. Specifically, in UTX catalytic-dead mice, I intend to perform four sets of experiments as outlined below:

1) A comprehensive immunophenotypic analysis of B cells retrieved from primary and secondary lymphoid organs including GALT.

2) Transcriptional profiling and ChIP-seq assays (in order of priority: UTX, H3K27me3, H3K27ac, H3K4me1 and H3K4me3) on mature resting and LPS-activated B cells

3) *In vitro* Ig isotype switching assays after stimulation of the B cells with either LPS, LPS+ IL4, or CD40L + IL4.

4) *In vitro* PC differentiation after stimulation with either LPS or CD40L+ IL21.

5. Supplementary information

Table 20. List of NF-κB transcriptional target genes downregulated in *Utx* KO FO B cells

Functional category	Symbol	log2FC	Adjusted p-value
Apoptosis	Xaf1	-0,882386022	0,000486655
Trafficking	Ccr7	-1,218804085	2,82E-13
Metabolism	Slc4a7	-0,660031197	0,000428032
	Pgap1	-0,624229289	0,002643833
	Cmpk2	-0,831342564	3,92E-05
	Ebi3	-1,942899504	6,83E-17
Transcription	Rel	-0,472719682	0,024834128
Cytoskeleton	Tuba4a	-0,412798932	0,033190959
Protein degradation	Dcaf12	-0,374102297	0,017906926
Immune responses	Il17ra	-0,461999578	0,001769831
	Cd37	-0,33950634	0,04984451
	Tmem173	-0,825397016	8,80E-06
	Irak3	-0,869248141	9,30E-06
	Map3k8	-0,577689028	0,011115134
	Ddx58	-0,469518043	0,014066875
	Zbp1	-0,524890392	0,020371768
	Oas3	-0,889056753	0,001218873
	Oasl2	-0,826205749	0,000482477
	Dhx58	-0,569443694	0,010624535
Signalling	Grap	-0,408792313	0,005960047
	Rhof	-0,494208991	0,008724161
	Csrnp1	-0,671741068	0,000790589
	Ttyh3	-0,463547664	0,005976762
	Map4k1	-0,386496953	0,027308638
	Lfng	-1,067404898	4,21E-08
	Mapk11	-0,96141955	6,51E-11
	Stat4	-0,919331428	0,000609456
	Pde3b	-0,668809133	0,000507211
	Pikfyve	-0,640719047	0,000889705
	Sfn	-0,613758188	0,000780417
	Bcl9	-0,516013973	0,004777158
Miscellanous	Ier5	-0,531246765	0,000314678
	Tmem64	-0,76110265	0,003899255
	Gpr132	-1,230742788	2,09E-15
	Rnf157	-0,66962771	0,016279756
	Smap2	-0,569402588	0,0008611
	6230427J02Rik	-1,256896861	7,08E-07
	Lpcat1	-0,631354822	0,006337271

6. References

- Abidi, F., M. Miano, J. Murray and C. Schwartz (2007). "A novel mutation in the PHF8 gene is associated with X-linked mental retardation with cleft lip/cleft palate." Clin Genet 72(1): 19-22.
- Adolfsson, J., O. J. Borge, D. Bryder, K. Theilgaard-Monch, I. Astrand-Grundstrom, E. Sitnicka, Y. Sasaki and S. E. Jacobsen (2001). "Upregulation of Flt3 expression within the bone marrow Lin(-)Sca1(+)c-kit(+) stem cell compartment is accompanied by loss of self-renewal capacity." Immunity 15(4): 659-669.
- Adolfsson, J., R. Mansson, N. Buza-Vidas, A. Hultquist, K. Liuba, C. T. Jensen, D. Bryder, L. Yang, O. J. Borge, L. A. Thoren, K. Anderson, E. Sitnicka, Y. Sasaki, M. Sigvardsson and S. E. Jacobsen (2005). "Identification of Flt3+ lympho-myeloid stem cells lacking erythro-megakaryocytic potential a revised road map for adult blood lineage commitment." Cell 121(2): 295-306.
- Agger, K., P. A. C. Cloos, J. Christensen, D. Pasini, S. Rose, J. Rappsilber, I. Issaeva, E. Canaani, A. E. Salcini and K. Helin (2007). "UTX and JMJD3 are histone H3K27 demethylases involved in HOX gene regulation and development." Nature 449: 731-734.
- Allen, C. D., K. M. Ansel, C. Low, R. Lesley, H. Tamamura, N. Fujii and J. G. Cyster (2004). "Germinal center dark and light zone organization is mediated by CXCR4 and CXCR5." Nat Immunol 5(9): 943-952.
- Allen, C. D. C. and J. G. Cyster (2008). "Follicular dendritic cell networks of primary follicles and germinal centers: Phenotype and function." Seminars in Immunology 20(1): 14-25.
- Allende, M. L., G. Tuymetova, B. G. Lee, E. Bonifacino, Y.-P. Wu and R. L. Proia (2010). "S1P1 receptor directs the release of immature B cells from bone marrow into blood." The Journal of experimental medicine 207(5): 1113-1124.
- Allman, D., R. C. Lindsley, W. DeMuth, K. Rudd, S. A. Shinton and R. R. Hardy (2001). "Resolution of three nonproliferative immature splenic B cell subsets reveals multiple selection points during peripheral B cell maturation." J Immunol 167(12): 6834-6840.
- Allman, D. M., S. E. Ferguson and M. P. Cancro (1992). "Peripheral B cell maturation. I. Immature peripheral B cells in adults are heat-stable antigenhi and exhibit unique signaling characteristics." J Immunol 149(8): 2533-2540.
- Allman, D. M., S. E. Ferguson, V. M. Lentz and M. P. Cancro (1993). "Peripheral B cell maturation. II. Heat-stable antigen(hi) splenic B cells are an immature developmental intermediate in the production of long-lived marrow-derived B cells." J Immunol 151(9): 4431-4444.
- Almaden, J. V., R. Tsui, Y. C. Liu, H. Birnbaum, M. N. Shokhirev, K. A. Ngo, J. C. Davis-Turak, D. Otero, S. Basak, R. C. Rickert and A. Hoffmann (2014). "A pathway switch directs BAFF signaling to distinct NFkappaB transcription factors in maturing and proliferating B cells." Cell Rep 9(6): 2098-2111.
- Alugupalli, K. R., J. M. Leong, R. T. Woodland, M. Muramatsu, T. Honjo and R. M. Gerstein (2004). "B1b lymphocytes confer T cell-independent long-lasting immunity." Immunity 21(3): 379-390.
- Anders, S., P. T. Pyl and W. Huber (2015). "HTSeq--a Python framework to work with high-throughput sequencing data." Bioinformatics 31(2): 166-169.
- Ang, Y. S., S. Y. Tsai, D. F. Lee, J. Monk, J. Su, K. Ratnakumar, J. Ding, Y. Ge, H. Darr, B. Chang, J. Wang, M. Rendl, E. Bernstein, C. Schaniel and I. R. Lemischka (2011). "Wdr5 mediates self-renewal and reprogramming via the embryonic stem cell core transcriptional network." Cell 145(2): 183-197.
- Angelin-Duclos, C., G. Cattoretti, K. I. Lin and K. Calame (2000). "Commitment of B lymphocytes to a plasma cell fate is associated with Blimp-1 expression in vivo." J Immunol 165(10): 5462-5471.
- Annunziato, A. T., M. B. Eason and C. A. Perry (1995). "Relationship between Methylation and Acetylation of Arginine-Rich Histones in Cycling and Arrested HeLa Cells." Biochemistry 34(9): 2916-2924.
- Armstrong, L., A. Abd El Moneim, K. Aleck, D. J. Aughton, C. Baumann, S. R. Braddock, G. Gillessen-Kaesbach, J. M. Graham, Jr., T. A. Grebe, K. W. Gripp, B. D. Hall, R. Hennekam, A. Hunter, K. Keppler-Noreuil, D. Lacombe, A. E. Lin, J. E. Ming, N. M. Kokitsu-Nakata, S. M.

Nikkel, N. Philip, A. Raas-Rothschild, A. Sommer, A. Verloes, C. Walter, D. Wieczorek, M. S. Williams, E. Zackai and J. E. Allanson (2005). "Further delineation of Kabuki syndrome in 48 well-defined new individuals." Am J Med Genet A 132a(3): 265-272.

- Arnon, T. I. and J. G. Cyster (2014). "Blood, sphingosine-1-phosphate and lymphocyte migration dynamics in the spleen." Curr Top Microbiol Immunol 378: 107-128.
- Arnon, T. I., Y. Xu, C. Lo, T. Pham, J. An, S. Coughlin, G. W. Dorn and J. G. Cyster (2011). "GRK2-dependent S1PR1 desensitization is required for lymphocytes to overcome their attraction to blood." Science 333(6051): 1898-1903.
- Arpin, C., J. Dechanet, C. Van Kooten, P. Merville, G. Grouard, F. Briere, J. Banchereau and Y. J. Liu (1995). "Generation of memory B cells and plasma cells in vitro." Science 268(5211): 720-722.
- Austenaa, L., I. Barozzi, A. Chronowska, A. Termanini, R. Ostuni, E. Prosperini, A. F. Stewart, G. Testa and G. Natoli (2012). "The histone methyltransferase Wbp7 controls macrophage function through GPI glycolipid anchor synthesis." Immunity 36(4): 572-585.
- Ayton, P. M. and M. L. Cleary (2003). "Transformation of myeloid progenitors by MLL oncoproteins is dependent on Hoxa7 and Hoxa9." Genes Dev 17(18): 2298-2307.
- Banka, S., D. Lederer, V. Benoit, E. Jenkins, E. Howard, S. Bunstone, B. Kerr, S. McKee, I. C. Lloyd, D. Shears, H. Stewart, S. M. White, R. Savarirayan, G. M. Mancini, D. Beysen, R. D. Cohn, B. Grisart, I. Maystadt and D. Donnai (2015). "Novel KDM6A (UTX) mutations and a clinical and molecular review of the X-linked Kabuki syndrome (KS2)." Clin Genet 87(3): 252-258.
- Basso, K. and R. Dalla-Favera (2010). "BCL6: master regulator of the germinal center reaction and key oncogene in B cell lymphomagenesis." Adv Immunol 105: 193-210.
- Basso, K., M. Saito, P. Sumazin, A. A. Margolin, K. Wang, W. K. Lim, Y. Kitagawa, C. Schneider, M. J. Alvarez, A. Califano and R. Dalla-Favera (2010). "Integrated biochemical and computational approach identifies BCL6 direct target genes controlling multiple pathways in normal germinal center B cells." Blood 115(5): 975-984.
- Basu, U., J. Chaudhuri, C. Alpert, S. Dutt, S. Ranganath, G. Li, J. P. Schrum, J. P. Manis and F. W. Alt (2005). "The AID antibody diversification enzyme is regulated by protein kinase A phosphorylation." Nature 438(7067): 508-511.
- Baumgarth, N. (2011). "The double life of a B-1 cell: self-reactivity selects for protective effector functions." Nat Rev Immunol 11(1): 34-46.
- Beguelin, W., R. Popovic, M. Teater, Y. Jiang, K. L. Bunting, M. Rosen, H. Shen, S. N. Yang, L. Wang, T. Ezponda, E. Martinez-Garcia, H. Zhang, Y. Zheng, S. K. Verma, M. T. McCabe, H. M. Ott, G. S. Van Aller, R. G. Kruger, Y. Liu, C. F. McHugh, D. W. Scott, Y. R. Chung, N. Kelleher, R. Shaknovich, C. L. Creasy, R. D. Gascoyne, K. K. Wong, L. Cerchietti, R. L. Levine, O. Abdel-Wahab, J. D. Licht, O. Elemento and A. M. Melnick (2013). "EZH2 is required for germinal center formation and somatic EZH2 mutations promote lymphoid transformation." Cancer Cell 23(5): 677-692.
- Béguelin, W., M. A. Rivas, M. T. Calvo Fernández, M. Teater, A. Purwada, D. Redmond, H. Shen, M. F. Challman, O. Elemento, A. Singh and A. M. Melnick (2017). "EZH2 enables germinal centre formation through epigenetic silencing of CDKN1A and an Rb-E2F1 feedback loop." Nature Communications 8(1): 877.
- Berek, C., A. Berger and M. Apel (1991). "Maturation of the immune response in germinal centers." Cell 67(6): 1121-1129.
- Berg, E. L., L. M. McEvoy, C. Berlin, R. F. Bargatze and E. C. Butcher (1993). "L-selectin-mediated lymphocyte rolling on MAdCAM-1." Nature 366: 695.
- Bernstein, B. E., T. S. Mikkelsen, X. Xie, M. Kamal, D. J. Huebert, J. Cuff, B. Fry, A. Meissner, M. Wernig, K. Plath, R. Jaenisch, A. Wagschal, R. Feil, S. L. Schreiber and E. S. Lander (2006). "A bivalent chromatin structure marks key developmental genes in embryonic stem cells." Cell 125(2): 315-326.
- Beyaz, S., J. H. Kim, L. Pinello, M. E. Xifaras, Y. Hu, J. Huang, M. A. Kerenyi, P. P. Das, R. A. Barnitz, A. Herault, R. Dogum, W. N. Haining, O. H. Yilmaz, E. Passegue, G. C. Yuan, S. H. Orkin and F. Winau (2017). "The histone demethylase UTX regulates the lineage-specific epigenetic program of invariant natural killer T cells." Nat Immunol 18(2): 184-195.
- Blackledge, N. P., N. R. Rose and R. J. Klose (2015). "Targeting Polycomb systems to regulate gene expression: modifications to a complex story." Nat Rev Mol Cell Biol 16(11): 643-649.

- Blobel, G. A., S. Kadauke, E. Wang, A. W. Lau, J. Zuber, M. M. Chou and C. R. Vakoc (2009). "A reconfigured pattern of MLL occupancy within mitotic chromatin promotes rapid transcriptional reactivation following mitotic exit." Mol Cell 36(6): 970-983.
- Bossen, C. and P. Schneider (2006). "BAFF, APRIL and their receptors: structure, function and signaling." Semin Immunol 18(5): 263-275.
- Bouillet, P., D. Metcalf, D. C. Huang, D. M. Tarlinton, T. W. Kay, F. Kontgen, J. M. Adams and A. Strasser (1999). "Proapoptotic Bcl-2 relative Bim required for certain apoptotic responses, leukocyte homeostasis, and to preclude autoimmunity." Science 286(5445): 1735-1738.
- Bowman, E. P., N. A. Kuklin, K. R. Youngman, N. H. Lazarus, E. J. Kunkel, J. Pan, H. B. Greenberg and E. C. Butcher (2002). "The intestinal chemokine thymus-expressed chemokine (CCL25) attracts IgA antibody-secreting cells." The Journal of experimental medicine 195(2): 269-275.
- Boyer, L. A., K. Plath, J. Zeitlinger, T. Brambrink, L. A. Medeiros, T. I. Lee, S. S. Levine, M. Wernig, A. Tajonar, M. K. Ray, G. W. Bell, A. P. Otte, M. Vidal, D. K. Gifford, R. A. Young and R. Jaenisch (2006). "Polycomb complexes repress developmental regulators in murine embryonic stem cells." Nature 441(7091): 349-353.
- Bracken, A. P., N. Dietrich, D. Pasini, K. H. Hansen and K. Helin (2006). "Genome-wide mapping of Polycomb target genes unravels their roles in cell fate transitions." Genes & development 20(9): 1123-1136.
- Brandtzaeg, P., T. S. Halstensen, K. Kett, P. Krajci, D. Kvale, T. O. Rognum, H. Scott and L. M. Sollid (1989). "Immunobiology and immunopathology of human gut mucosa: humoral immunity and intraepithelial lymphocytes." Gastroenterology 97(6): 1562-1584.
- Brandtzaeg, P. and F. E. Johansen (2005). "Mucosal B cells: phenotypic characteristics, transcriptional regulation, and homing properties." Immunol Rev 206: 32-63.
- Brelinska, R. and C. Pilgrim (1982). "The significance of the subcompartments of the marginal zone for directing lymphocyte traffic within the splenic pulp of the rat." Cell Tissue Res 226(1): 155-165.
- Buenrostro, J. D., P. G. Giresi, L. C. Zaba, H. Y. Chang and W. J. Greenleaf (2013). "Transposition of native chromatin for fast and sensitive epigenomic profiling of open chromatin, DNA-binding proteins and nucleosome position." Nat Methods 10(12): 1213-1218.
- Burgold, T., N. Voituron, M. Caganova, P. P. Tripathi, C. Menuet, B. K. Tusi, F. Spreafico, M. Bevengut, C. Gestreau, S. Buontempo, A. Simeone, L. Kruidenier, G. Natoli, S. Casola, G. Hilaire and G. Testa (2012). "The H3K27 demethylase JMJD3 is required for maintenance of the embryonic respiratory neuronal network, neonatal breathing, and survival." Cell Rep 2(5): 1244-1258.
- Byvoet, P., G. R. Shepherd, J. M. Hardin and B. J. Noland (1972). "The distribution and turnover of labeled methyl groups in histone fractions of cultured mammalian cells." Arch Biochem Biophys 148(2): 558-567.
- Caganova, M., C. Carrisi, G. Varano, F. Mainoldi, F. Zanardi, P. L. Germain, L. George, F. Alberghini, L. Ferrarini, A. K. Talukder, M. Ponzoni, G. Testa, T. Nojima, C. Doglioni, D. Kitamura, K. M. Toellner, I. H. Su and S. Casola (2013). "Germinal center dysregulation by histone methyltransferase EZH2 promotes lymphomagenesis." Journal of Clinical Investigation 123: 5009-5022.
- Calfon, M., H. Zeng, F. Urano, J. H. Till, S. R. Hubbard, H. P. Harding, S. G. Clark and D. Ron (2002). "IRE1 couples endoplasmic reticulum load to secretory capacity by processing the XBP-1 mRNA." Nature 415(6867): 92-96.
- Cao, F., E. C. Townsend, H. Karatas, J. Xu, L. Li, S. Lee, L. Liu, Y. Chen, P. Ouillette, J. Zhu, J. L. Hess, P. Atadja, M. Lei, Z. S. Qin, S. Malek, S. Wang and Y. Dou (2014). "Targeting MLL1 H3K4 methyltransferase activity in mixed-lineage leukemia." Molecular cell 53(2): 247-261.
- Cariappa, A., C. Boboila, S. T. Moran, H. Liu, H. N. Shi and S. Pillai (2007). "The recirculating B cell pool contains two functionally distinct, long-lived, posttransitional, follicular B cell populations." J Immunol 179(4): 2270-2281.
- Casellas, R., A. Nussenzweig, R. Wuerffel, R. Pelanda, A. Reichlin, H. Suh, X. F. Qin, E. Besmer, A. Kenter, K. Rajewsky and M. C. Nussenzweig (1998). "Ku80 is required for immunoglobulin isotype switching." The EMBO journal 17(8): 2404-2411.

- Casola, S. (2007). "Control of peripheral B-cell development." Current opinion in immunology 19(2): 143-149.
- Casola, S., K. L. Otipoby, M. Alimzhanov, S. Humme, N. Uyttersprot, J. L. Kutok, M. C. Carroll and K. Rajewsky (2004). "B cell receptor signal strength determines B cell fate." Nature immunology 5(3): 317-327.
- Cattoretti, G., L. Pasqualucci, G. Ballon, W. Tam, S. V. Nandula, Q. Shen, T. Mo, V. V. Murty and R. Dalla-Favera (2005). "Deregulated BCL6 expression recapitulates the pathogenesis of human diffuse large B cell lymphomas in mice." Cancer Cell 7(5): 445-455.
- Chagraoui, J., J. Hébert, S. Girard and G. Sauvageau (2011). "An anticlastogenic function for the Polycomb Group gene Bmi1." Proceedings of the National Academy of Sciences 108(13): 5284-5289.
- Chamberlain, S. J., D. Yee and T. Magnuson (2008). "Polycomb repressive complex 2 is dispensable for maintenance of embryonic stem cell pluripotency." Stem Cells 26(6): 1496-1505.
- Chang, S. K., B. K. Arendt, J. R. Darce, X. Wu and D. F. Jelinek (2006). "A role for BLyS in the activation of innate immune cells." Blood 108(8): 2687-2694.
- Chang, S. K., S. A. Mihalcik and D. F. Jelinek (2008). "B lymphocyte stimulator regulates adaptive immune responses by directly promoting dendritic cell maturation." J Immunol 180(11): 7394-7403.
- Chapman, M. A., M. S. Lawrence, J. J. Keats, K. Cibulskis, C. Sougnez, A. C. Schinzel, C. L. Harview, J.-P. Brunet, G. J. Ahmann, M. Adli, K. C. Anderson, K. G. Ardlie, D. Auclair, A. Baker, P. L. Bergsagel, B. E. Bernstein, Y. Drier, R. Fonseca, S. B. Gabriel, C. C. Hofmeister, S. Jagannath, A. J. Jakubowiak, A. Krishnan, J. Levy, T. Liefeld, S. Lonial, S. Mahan, B. Mfuko, S. Monti, L. M. Perkins, R. Onofrio, T. J. Pugh, S. V. Rajkumar, A. H. Ramos, D. S. Siegel, A. Sivachenko, A. K. Stewart, S. Trudel, R. Vij, D. Voet, W. Winckler, T. Zimmerman, J. Carpten, J. Trent, W. C. Hahn, L. A. Garraway, M. Meyerson, E. S. Lander, G. Getz and T. R. Golub (2011). "Initial genome sequencing and analysis of multiple myeloma." Nature 471: 467.
- Chaudhuri, J., C. Khuong and F. W. Alt (2004). "Replication protein A interacts with AID to promote deamination of somatic hypermutation targets." Nature 430(7003): 992-998.
- Chen, C. C., S. M. Jeon, P. T. Bhaskar, V. Nogueira, D. Sundararajan, I. Tonic, Y. Park and N. Hay (2010). "FoxOs inhibit mTORC1 and activate Akt by inducing the expression of Sestrin3 and Rictor." Dev Cell 18(4): 592-604.
- Chen, E. Y., C. M. Tan, Y. Kou, Q. Duan, Z. Wang, G. V. Meirelles, N. R. Clark and A. Ma'ayan (2013). "Enrichr: interactive and collaborative HTML5 gene list enrichment analysis tool." BMC Bioinformatics 14: 128.
- Chen, H. and P. C. Boutros (2011). "VennDiagram: a package for the generation of highly-customizable Venn and Euler diagrams in R." BMC Bioinformatics 12: 35.
- Chen, H., X. Gu, I. H. Su, R. Bottino, J. L. Contreras, A. Tarakhovsky and S. K. Kim (2009). "Polycomb protein Ezh2 regulates pancreatic beta-cell Ink4a/Arf expression and regeneration in diabetes mellitus." Genes Dev 23(8): 975-985.
- Chiba, K., Y. Yanagawa, Y. Masubuchi, H. Kataoka, T. Kawaguchi, M. Ohtsuki and Y. Hoshino (1998). "FTY720, a novel immunosuppressant, induces sequestration of circulating mature lymphocytes by acceleration of lymphocyte homing in rats. I. FTY720 selectively decreases the number of circulating mature lymphocytes by acceleration of lymphocyte homing." J Immunol 160(10): 5037-5044.
- Cho, Y. W., T. Hong, S. Hong, H. Guo, H. Yu, D. Kim, T. Guszczynski, G. R. Dressler, T. D. Copeland, M. Kalkum and K. Ge (2007). "PTIP associates with MLL3- and MLL4-containing histone H3 lysine 4 methyltransferase complex." J Biol Chem 282(28): 20395-20406.
- Christoffersen, C., H. Obinata, S. B. Kumaraswamy, S. Galvani, J. Ahnstrom, M. Sevvana, C. Egerer-Sieber, Y. A. Muller, T. Hla, L. B. Nielsen and B. Dahlback (2011). "Endothelium-protective sphingosine-1-phosphate provided by HDL-associated apolipoprotein M." Proc Natl Acad Sci U S A 108(23): 9613-9618.
- Chung, J. B., R. A. Sater, M. L. Fields, J. Erikson and J. G. Monroe (2002). "CD23 defines two distinct subsets of immature B cells which differ in their responses to T cell help signals." Int Immunol 14(2): 157-166.

- Cinamon, G., M. Matloubian, M. J. Lesneski, Y. Xu, C. Low, T. Lu, R. L. Proia and J. G. Cyster (2004). "Sphingosine 1-phosphate receptor 1 promotes B cell localization in the splenic marginal zone." Nat Immunol 5(7): 713-720.
- Cinamon, G., M. A. Zachariah, O. M. Lam, F. W. Foss, Jr. and J. G. Cyster (2008). "Follicular shuttling of marginal zone B cells facilitates antigen transport." Nature immunology 9(1): 54-62.
- Claudio, E., K. Brown and U. Siebenlist (2006). "NF-κB guides the survival and differentiation of developing lymphocytes." Cell Death And Differentiation 13: 697.
- Cloos, P. A., J. Christensen, K. Agger and K. Helin (2008). "Erasing the methyl mark: histone demethylases at the center of cellular differentiation and disease." Genes Dev 22(9): 1115-1140.
- Cloos, P. A., J. Christensen, K. Agger, A. Maiolica, J. Rappsilber, T. Antal, K. H. Hansen and K. Helin (2006). "The putative oncogene GASC1 demethylates tri- and dimethylated lysine 9 on histone H3." Nature 442(7100): 307-311.
- Cobaleda, C., A. Schebesta, A. Delogu and M. Busslinger (2007). "Pax5: the guardian of B cell identity and function." Nat Immunol 8(5): 463-470.
- Cook, Kevin D., Karl B. Shpargel, J. Starmer, F. Whitfield-Larry, B. Conley, Denise E. Allard, Julia E. Rager, Rebecca C. Fry, Marsha L. Davenport, T. Magnuson, Jason K. Whitmire and Maureen A. Su (2015). "T Follicular Helper Cell-Dependent Clearance of a Persistent Virus Infection Requires T Cell Expression of the Histone Demethylase UTX." Immunity 43(4): 703-714.
- Cooper, S., M. Dienstbier, R. Hassan, L. Schermelleh, J. Sharif, N. P. Blackledge, V. De Marco, S. Elderkin, H. Koseki, R. Klose, A. Heger and N. Brockdorff (2014). "Targeting polycomb to pericentric heterochromatin in embryonic stem cells reveals a role for H2AK119u1 in PRC2 recruitment." Cell Rep 7(5): 1456-1470.
- Copur, Ö. and J. Müller (2013). "The histone H3-K27 demethylase Utx regulates HOX gene expression in Drosophila in a temporally restricted manner." Development (Cambridge, England) 140(16): 3478-3485.
- Crouch, E. E., Z. Li, M. Takizawa, S. Fichtner-Feigl, P. Gourzi, C. Montano, L. Feigenbaum, P. Wilson, S. Janz, F. N. Papavasiliou and R. Casellas (2007). "Regulation of AID expression in the immune response." The Journal of experimental medicine 204(5): 1145-1156.
- Crowley, J. E., J. L. Scholz, W. J. Quinn, 3rd, J. E. Stadanlick, J. F. Treml, L. S. Treml, Y. Hao, R. Goenka, P. J. O'Neill, A. H. Matthews, R. F. Parsons and M. P. Cancro (2008). "Homeostatic control of B lymphocyte subsets." Immunol Res 42(1-3): 75-83.
- Cumano, A. and K. Rajewsky (1986). "Clonal recruitment and somatic mutation in the generation of immunological memory to the hapten NP." Embo j 5(10): 2459-2468.
- Cyster, J. G. (2005). "Chemokines, sphingosine-1-phosphate, and cell migration in secondary lymphoid organs." Annu Rev Immunol 23: 127-159.
- Daniel, J. A., M. A. Santos, Z. Wang, C. Zang, K. R. Schwab, M. Jankovic, D. Filsuf, H. T. Chen, A. Gazumyan, A. Yamane, Y. W. Cho, H. W. Sun, K. Ge, W. Peng, M. C. Nussenzweig, R. Casellas, G. R. Dressler, K. Zhao and A. Nussenzweig (2010). "PTIP promotes chromatin changes critical for immunoglobulin class switch recombination." Science 329(5994): 917-923.
- Darce, J. R., B. K. Arendt, X. Wu and D. F. Jelinek (2007). "Regulated expression of BAFF-binding receptors during human B cell differentiation." J Immunol 179(11): 7276-7286.
- Davie, J. R. and L. C. Murphy (1990). "Level of ubiquitinated histone H2B in chromatin is coupled to ongoing transcription." Biochemistry 29(20): 4752-4757.
- De Keersmaecker, K., Z. K. Atak, N. Li, C. Vicente, S. Patchett, T. Girardi, V. Gianfelici, E. Geerdens, E. Clappier, M. Porcu, I. Lahortiga, R. Lucà, J. Yan, G. Hulselmans, H. Vranckx, R. Vandepoel, B. Sweron, K. Jacobs, N. Mentens, I. Wlodarska, B. Cauwelier, J. Cloos, J. Soulier, A. Uyttebroeck, C. Bagni, B. A. Hassan, P. Vandenberghe, A. W. Johnson, S. Aerts and J. Cools (2012). "Exome sequencing identifies mutation in CNOT3 and ribosomal genes RPL5 and RPL10 in T-cell acute lymphoblastic leukemia." Nature Genetics 45: 186.
- De Santa, F., M. G. Totaro, E. Prosperini, S. Notarbartolo, G. Testa and G. Natoli (2007). "The histone H3 lysine-27 demethylase Jmjd3 links inflammation to inhibition of polycomb-mediated gene silencing." Cell 130(6): 1083-1094.
- De Silva, N. S., K. Silva, M. M. Anderson, G. Bhagat and U. Klein (2016). "Impairment of Mature B Cell Maintenance upon Combined Deletion of the Alternative NF-kappaB Transcription Factors RELB and NF-kappaB2 in B Cells." J Immunol 196(6): 2591-2601.

- Dedeoglu, F., B. Horwitz, J. Chaudhuri, F. W. Alt and R. S. Geha (2004). "Induction of activation-induced cytidine deaminase gene expression by IL-4 and CD40 ligation is dependent on STAT6 and NFkappaB." International immunology 16(3): 395-404.
- Delogu, A., A. Schebesta, Q. Sun, K. Aschenbrenner, T. Perlot and M. Busslinger (2006). "Gene repression by Pax5 in B cells is essential for blood cell homeostasis and is reversed in plasma cells." Immunity 24(3): 269-281.
- Dengler, H. S., G. V. Baracho, S. A. Omori, S. Bruckner, K. C. Arden, D. H. Castrillon, R. A. DePinho and R. C. Rickert (2008). "Distinct functions for the transcription factor Foxo1 at various stages of B cell differentiation." Nat Immunol 9(12): 1388-1398.
- Denissov, S., H. Hofemeister, H. Marks, A. Kranz, G. Ciotta, S. Singh, K. Anastassiadis, H. G. Stunnenberg and A. F. Stewart (2014). "Mll2 is required for H3K4 trimethylation on bivalent promoters in embryonic stem cells, whereas Mll1 is redundant." Development 141(3): 526-537.
- Dent, A. L., A. L. Shaffer, X. Yu, D. Allman and L. M. Staudt (1997). "Control of inflammation, cytokine expression, and germinal center formation by BCL-6." Science 276(5312): 589-592.
- Derudder, E., E. J. Cadera, J. C. Vahl, J. Wang, C. J. Fox, S. Zha, G. van Loo, M. Pasparakis, M. S. Schlissel, M. Schmidt-Supprian and K. Rajewsky (2009). "Development of immunoglobulin lambda-chain-positive B cells, but not editing of immunoglobulin kappa-chain, depends on NF-kappaB signals." Nature immunology 10(6): 647-654.
- Derudder, E., S. Herzog, V. Labi, T. Yasuda, K. Kochert, M. Janz, A. Villunger, M. Schmidt-Supprian and K. Rajewsky (2016). "Canonical NF-kappaB signaling is uniquely required for the long-term persistence of functional mature B cells." Proc Natl Acad Sci U S A 113(18): 5065-5070.
- Dhordain, P., R. J. Lin, S. Quief, D. Lantoine, J. P. Kerckaert, R. M. Evans and O. Albagli (1998). "The LAZ3(BCL-6) oncoprotein recruits a SMRT/mSIN3A/histone deacetylase containing complex to mediate transcriptional repression." Nucleic acids research 26(20): 4645-4651.
- Di Croce, L. and K. Helin (2013). "Transcriptional regulation by Polycomb group proteins." Nat Struct Mol Biol 20(10): 1147-1155.
- Di Noia, J. and M. S. Neuberger (2002). "Altering the pathway of immunoglobulin hypermutation by inhibiting uracil-DNA glycosylase." Nature 419(6902): 43-48.
- Di Noia, J. M. and M. S. Neuberger (2007). "Molecular mechanisms of antibody somatic hypermutation." Annual review of biochemistry 76: 1-22.
- Difilippantonio, M. J., J. Zhu, H. T. Chen, E. Meffre, M. C. Nussenzweig, E. E. Max, T. Ried and A. Nussenzweig (2000). "DNA repair protein Ku80 suppresses chromosomal aberrations and malignant transformation." Nature 404(6777): 510-514.
- Dobenecker, M. W., J. K. Kim, J. Marcello, T. C. Fang, R. Prinjha, R. Bosselut and A. Tarakhovsky (2015). "Coupling of T cell receptor specificity to natural killer T cell development by bivalent histone H3 methylation." J Exp Med 212(3): 297-306.
- Dogan, I., B. Bertocci, V. Vilmont, F. Delbos, J. Megret, S. Storck, C. A. Reynaud and J. C. Weill (2009). "Multiple layers of B cell memory with different effector functions." Nat Immunol 10(12): 1292-1299.
- Dominguez-Sola, D., J. Kung, A. B. Holmes, V. A. Wells, T. Mo, K. Basso and R. Dalla-Favera (2015). "The FOXO1 Transcription Factor Instructs the Germinal Center Dark Zone Program." Immunity 43(6): 1064-1074.
- Dou, Y., T. A. Milne, A. J. Tackett, E. R. Smith, A. Fukuda, J. Wysocka, C. D. Allis, B. T. Chait, J. L. Hess and R. G. Roeder (2005). "Physical association and coordinate function of the H3 K4 methyltransferase MLL1 and the H4 K16 acetyltransferase MOF." Cell 121(6): 873-885.
- Dullaers, M., D. Li, Y. Xue, L. Ni, I. Gayet, R. Morita, H. Ueno, K. A. Palucka, J. Banchereau and S. Oh (2009). "A T Cell-Dependent Mechanism for the Induction of Human Mucosal Homing Immunoglobulin A-Secreting Plasmablasts." Immunity 30(1): 120-129.
- Duy, C., J. J. Yu, R. Nahar, S. Swaminathan, S. M. Kweon, J. M. Polo, E. Valls, L. Klemm, S. Shojaee, L. Cerchietti, W. Schuh, H. M. Jack, C. Hurtz, P. Ramezani-Rad, S. Herzog, H. Jumaa, H. P. Koeffler, I. M. de Alboran, A. M. Melnick, B. H. Ye and M. Muschen (2010). "BCL6 is critical for the development of a diverse primary B cell repertoire." J Exp Med 207(6): 1209-1221.
- Eastman, Q. M., T. M. Leu and D. G. Schatz (1996). "Initiation of V(D)J recombination in vitro obeying the 12/23 rule." Nature 380(6569): 85-88.

- Edry, E. and D. Melamed (2004). "Receptor editing in positive and negative selection of B lymphopoiesis." J Immunol 173(7): 4265-4271.
- Egle, A., A. W. Harris, M. L. Bath, L. O'Reilly and S. Cory (2004). "VavP-Bcl2 transgenic mice develop follicular lymphoma preceded by germinal center hyperplasia." Blood 103(6): 2276-2283.
- Ezponda, T., D. Dupere-Richer, C. M. Will, E. C. Small, N. Varghese, T. Patel, B. Nabet, R. Popovic, J. Oyer, M. Bulic, Y. Zheng, X. Huang, M. Y. Shah, S. Maji, A. Riva, M. Occhionorelli, G. Tonon, N. Kelleher, J. Keats and J. D. Licht (2017). "UTX/KDM6A Loss Enhances the Malignant Phenotype of Multiple Myeloma and Sensitizes Cells to EZH2 inhibition." Cell Rep 21(3): 628-640.
- Fagarasan, S. and T. Honjo (2003). "Intestinal IgA synthesis: regulation of front-line body defences." Nat Rev Immunol 3(1): 63-72.
- Fagarasan, S., S. Kawamoto, O. Kanagawa and K. Suzuki (2010). "Adaptive immune regulation in the gut: T cell-dependent and T cell-independent IgA synthesis." Annu Rev Immunol 28: 243-273.
- Fan, T., S. Jiang, N. Chung, A. Alikhan, C. Ni, C.-C. R. Lee and T. J. Hornyak (2011). "EZH2-dependent suppression of a cellular senescence phenotype in melanoma cells by inhibition of p21/CDKN1A expression." Molecular cancer research : MCR 9(4): 418-429.
- Faralli, H., C. Wang, K. Nakka, A. Benyoucef, S. Sebastian, L. Zhuang, A. Chu, C. G. Palii, C. Liu, B. Camellato, M. Brand, K. Ge and F. J. Dilworth (2016). "UTX demethylase activity is required for satellite cell-mediated muscle regeneration." J Clin Invest 126(4): 1555-1565.
- Farstad, I. N., T. S. Halstensen, A. I. Lazarovits, J. Norstein, O. Fausa and P. Brandtzaeg (1995). "Human intestinal B-cell blasts and plasma cells express the mucosal homing receptor integrin alpha 4 beta 7." Scand J Immunol 42(6): 662-672.
- Feng, J., H. Wang, D. M. Shin, M. Masiuk, C. F. Qi and H. C. Morse, 3rd (2011). "IFN regulatory factor 8 restricts the size of the marginal zone and follicular B cell pools." J Immunol 186(3): 1458-1466.
- Forsberg, E. C., T. Serwold, S. Kogan, I. L. Weissman and E. Passegue (2006). "New evidence supporting megakaryocyte-erythrocyte potential of flk2/flt3+ multipotent hematopoietic progenitors." Cell 126(2): 415-426.
- Forster, R., T. Emrich, E. Kremmer and M. Lipp (1994). "Expression of the G-protein--coupled receptor BLR1 defines mature, recirculating B cells and a subset of T-helper memory cells." Blood 84(3): 830-840.
- Forster, R., A. E. Mattis, E. Kremmer, E. Wolf, G. Brem and M. Lipp (1996). "A putative chemokine receptor, BLR1, directs B cell migration to defined lymphoid organs and specific anatomic compartments of the spleen." Cell 87(6): 1037-1047.
- Forster, R., A. Schubel, D. Breitfeld, E. Kremmer, I. Renner-Muller, E. Wolf and M. Lipp (1999). "CCR7 coordinates the primary immune response by establishing functional microenvironments in secondary lymphoid organs." Cell 99(1): 23-33.
- Fortschegger, K., P. de Graaf, N. S. Outchkourov, F. M. A. van Schaik, H. T. M. Timmers and R. Shiekhattar (2010). "PHF8 targets histone methylation and RNA polymerase II to activate transcription." Molecular and cellular biology 30(13): 3286-3298.
- Franco, S., M. Gostissa, S. Zha, D. B. Lombard, M. M. Murphy, A. A. Zarrin, C. Yan, S. Tepsuporn, J. C. Morales, M. M. Adams, Z. Lou, C. H. Bassing, J. P. Manis, J. Chen, P. B. Carpenter and F. W. Alt (2006). "H2AX prevents DNA breaks from progressing to chromosome breaks and translocations." Molecular cell 21(2): 201-214.
- Franzoso, G., L. Carlson, L. Xing, L. Poljak, E. W. Shores, K. D. Brown, A. Leonardi, T. Tran, B. F. Boyce and U. Siebenlist (1997). "Requirement for NF-kappaB in osteoclast and B-cell development." Genes Dev 11(24): 3482-3496.
- Fujita, N., D. L. Jaye, C. Geigerman, A. Akyildiz, M. R. Mooney, J. M. Boss and P. A. Wade (2004). "MTA3 and the Mi-2/NuRD complex regulate cell fate during B lymphocyte differentiation." Cell 119(1): 75-86.
- Fukuda, T., T. Yoshida, S. Okada, M. Hatano, T. Miki, K. Ishibashi, S. Okabe, H. Koseki, S. Hirosawa, M. Taniguchi, N. Miyasaka and T. Tokuhisa (1997). "Disruption of the Bcl6 gene results in an impaired germinal center formation." J Exp Med 186(3): 439-448.

- Fuxa, M. and M. Busslinger (2007). "Reporter gene insertions reveal a strictly B lymphoid-specific expression pattern of Pax5 in support of its B cell identity function." J Immunol 178(5): 3031-3037.
- Fuxa, M., J. Skok, A. Souabni, G. Salvagiotto, E. Roldan and M. Busslinger (2004). "Pax5 induces V-to-DJ rearrangements and locus contraction of the immunoglobulin heavy-chain gene." Genes & development 18(4): 411-422.
- Gao, Z., J. Zhang, R. Bonasio, F. Strino, A. Sawai, F. Parisi, Y. Kluger and D. Reinberg (2012). "PCGF homologs, CBX proteins, and RYBP define functionally distinct PRC1 family complexes." Mol Cell 45(3): 344-356.
- Gardam, S. and R. Brink (2014). "Non-Canonical NF-κB Signaling Initiated by BAFF Influences B Cell Biology at Multiple Junctures." Frontiers in immunology 4: 509-509.
- Gass, J. N., N. M. Gifford and J. W. Brewer (2002). "Activation of an unfolded protein response during differentiation of antibody-secreting B cells." The Journal of biological chemistry 277(50): 49047-49054.
- Gatto, D., K. Wood and R. Brink (2011). "EBI2 Operates Independently of but in Cooperation with CXCR5 and CCR7 To Direct B Cell Migration and Organization in Follicles and the Germinal Center." The Journal of Immunology 187(9): 4621-4628.
- Gerondakis, S., R. Grumont, R. Gugasyan, L. Wong, I. Isomura, W. Ho and A. Banerjee (2006). "Unravelling the complexities of the NF-kappaB signalling pathway using mouse knockout and transgenic models." Oncogene 25(51): 6781-6799.
- Gerondakis, S. and U. Siebenlist (2010). "Roles of the NF-kappaB pathway in lymphocyte development and function." Cold Spring Harbor perspectives in biology 2(5): a000182-a000182.
- Gieni, R. S. and M. J. Hendzel (2009). "Polycomb group protein gene silencing, non-coding RNA, stem cells, and cancer." Biochem Cell Biol 87(5): 711-746.
- Ginjala, V., K. Nacerddine, A. Kulkarni, J. Oza, S. J. Hill, M. Yao, E. Citterio, M. van Lohuizen and S. Ganesan (2011). "BMI1 is recruited to DNA breaks and contributes to DNA damage-induced H2A ubiquitination and repair." Mol Cell Biol 31(10): 1972-1982.
- Glaser, S., J. Schaft, S. Lubitz, K. Vintersten, F. van der Hoeven, K. R. Tufteland, R. Aasland, K. Anastassiadis, S. L. Ang and A. F. Stewart (2006). "Multiple epigenetic maintenance factors implicated by the loss of Mll2 in mouse development." Development 133(8): 1423-1432.
- Gonda, H., M. Sugai, Y. Nambu, T. Katakai, Y. Agata, K. J. Mori, Y. Yokota and A. Shimizu (2003). "The balance between Pax5 and Id2 activities is the key to AID gene expression." The Journal of experimental medicine 198(9): 1427-1437.
- Gorelik, L., K. Gilbride, M. Dobles, S. L. Kalled, D. Zandman and M. L. Scott (2003). "Normal B Cell Homeostasis Requires B Cell Activation Factor Production by Radiation-resistant Cells." The Journal of Experimental Medicine 198: 937-945.
- Gorman, J. R. and F. W. Alt (1998). "Regulation of immunoglobulin light chain isotype expression." Adv Immunol 69: 113-181.
- Gozdecka, M., E. Meduri, M. Mazan, K. Tzelepis, M. Dudek, A. J. Knights, M. Pardo, L. Yu, J. S. Choudhary, E. Metzakopian, V. Iyer, H. Yun, N. Park, I. Varela, R. Bautista, G. Collord, O. Dovey, D. A. Garyfallos, E. De Braekeleer, S. Kondo, J. Cooper, B. Gottgens, L. Bullinger, P. A. Northcott, D. Adams, G. S. Vassiliou and B. J. P. Huntly (2018). "UTX-mediated enhancer and chromatin remodeling suppresses myeloid leukemogenesis through noncatalytic inverse regulation of ETS and GATA programs." Nat Genet 50(6): 883-894.
- Greenfield, A., L. Carrel, D. Pennisi, C. Philippe, N. Quaderi, P. Siggers, K. Steiner, P. P. Tam, A. P. Monaco, H. F. Willard and P. Koopman (1998). "The UTX gene escapes X inactivation in mice and humans." Hum Mol Genet 7(4): 737-742.
- Grigorova, I. L., S. R. Schwab, T. G. Phan, T. H. Pham, T. Okada and J. G. Cyster (2009). "Cortical sinus probing, S1P1-dependent entry and flow-based capture of egressing T cells." Nat Immunol 10(1): 58-65.
- Grossmann, M., D. Metcalf, J. Merryfull, A. Beg, D. Baltimore and S. Gerondakis (1999). "The combined absence of the transcription factors Rel and RelA leads to multiple hemopoietic cell defects." Proceedings of the National Academy of Sciences of the United States of America 96(21): 11848-11853.
- Grunstein, M. (1997). "Histone acetylation in chromatin structure and transcription." Nature 389(6649): 349-352.

- Gui, Y., G. Guo, Y. Huang, X. Hu, A. Tang, S. Gao, R. Wu, C. Chen, X. Li, L. Zhou, M. He, Z. Li, X. Sun, W. Jia, J. Chen, S. Yang, F. Zhou, X. Zhao, S. Wan, R. Ye, C. Liang, Z. Liu, P. Huang, C. Liu, H. Jiang, Y. Wang, H. Zheng, L. Sun, X. Liu, Z. Jiang, D. Feng, J. Chen, S. Wu, J. Zou, Z. Zhang, R. Yang, J. Zhao, C. Xu, W. Yin, Z. Guan, J. Ye, H. Zhang, J. Li, K. Kristiansen, M. L. Nickerson, D. Theodorescu, Y. Li, X. Zhang, S. Li, J. Wang, H. Yang, J. Wang and Z. Cai (2011). "Frequent mutations of chromatin remodeling genes in transitional cell carcinoma of the bladder." Nat Genet 43(9): 875-878.
- Guo, C., C. C. Chang, M. Wortham, L. H. Chen, D. N. Kernagis, X. Qin, Y. W. Cho, J. T. Chi, G. A. Grant, R. E. McLendon, H. Yan, K. Ge, N. Papadopoulos, D. D. Bigner and Y. He (2012). "Global identification of MLL2-targeted loci reveals MLL2's role in diverse signaling pathways." Proc Natl Acad Sci U S A 109(43): 17603-17608.
- Guo, L., X. Li, J. X. Huang, H. Y. Huang, Y. Y. Zhang, S. W. Qian, H. Zhu, Y. D. Zhang, Y. Liu, Y. Liu, K. K. Wang and Q. Q. Tang (2012). "Histone demethylase Kdm4b functions as a co-factor of C/EBPβ to promote mitotic clonal expansion during differentiation of 3T3-L1 preadipocytes." Cell death and differentiation 19(12): 1917-1927.
- Guo, M., M. J. Price, D. G. Patterson, B. G. Barwick, R. R. Haines, A. K. Kania, J. E. Bradley, T. D. Randall, J. M. Boss and C. D. Scharer (2017). "EZH2 Represses the B Cell Transcriptional Program and Regulates Antibody-Secreting Cell Metabolism and Antibody Production." The Journal of Immunology.
- Guo, W. J., S. Datta, V. Band and G. P. Dimri (2007). "Mel-18, a polycomb group protein, regulates cell proliferation and senescence via transcriptional repression of Bmi-1 and c-Myc oncoproteins." Mol Biol Cell 18(2): 536-546.
- Gupta, S., A. Anthony and A. B. Pernis (2001). "Stage-specific modulation of IFN-regulatory factor 4 function by Kruppel-type zinc finger proteins." J Immunol 166(10): 6104-6111.
- Gutzeit, C., G. Magri and A. Cerutti (2014). "Intestinal IgA production and its role in host-microbe interaction." Immunol Rev 260(1): 76-85.
- Haas, K. M., J. C. Poe, D. A. Steeber and T. F. Tedder (2005). "B-1a and B-1b cells exhibit distinct developmental requirements and have unique functional roles in innate and adaptive immunity to S. pneumoniae." Immunity 23(1): 7-18.
- Hagman, J. and K. Lukin (2006). "Transcription factors drive B cell development." Curr Opin Immunol 18(2): 127-134.
- Hardy, R. R. (2006). "B-1 B cell development." J Immunol 177(5): 2749-2754.
- Hardy, R. R., C. E. Carmack, S. A. Shinton, J. D. Kemp and K. Hayakawa (1991). "Resolution and characterization of pro-B and pre-pro-B cell stages in normal mouse bone marrow." The Journal of Experimental Medicine 173(5): 1213-1225.
- Harless, S. M., V. M. Lentz, A. P. Sah, B. L. Hsu, K. Clise-Dwyer, D. M. Hilbert, C. E. Hayes and M. P. Cancro (2001). "Competition for BLyS-mediated signaling through Bcmd/BR3 regulates peripheral B lymphocyte numbers." Curr Biol 11(24): 1986-1989.
- Hasbold, J., L. M. Corcoran, D. M. Tarlinton, S. G. Tangye and P. D. Hodgkin (2004). "Evidence from the generation of immunoglobulin G-secreting cells that stochastic mechanisms regulate lymphocyte differentiation." Nat Immunol 5(1): 55-63.
- Hasbold, J., A. V. Gett, J. S. Rush, E. Deenick, D. Avery, J. Jun and P. D. Hodgkin (1999). "Quantitative analysis of lymphocyte differentiation and proliferation in vitro using carboxyfluorescein diacetate succinimidyl ester." Immunol Cell Biol 77(6): 516-522.
- Hatzi, K., Y. Jiang, C. Huang, F. Garrett-Bakelman, M. D. Gearhart, E. G. Giannopoulou, P. Zumbo, K. Kirouac, S. Bhaskara, J. M. Polo, M. Kormaksson, A. D. Mackerell, Jr., F. Xue, C. E. Mason, S. W. Hiebert, G. G. Prive, L. Cerchietti, V. J. Bardwell, O. Elemento and A. Melnick (2013). "A Hybrid Mechanism of Action for BCL6 in B Cells Defined by Formation of Functionally Distinct Complexes at Enhancers and Promoters." Cell Rep 4(3): 578-588.
- Hauser, A. E., G. F. Debes, S. Arce, G. Cassese, A. Hamann, A. Radbruch and R. A. Manz (2002). "Chemotactic responsiveness toward ligands for CXCR3 and CXCR4 is regulated on plasma blasts during the time course of a memory immune response." J Immunol 169(3): 1277-1282.
- He, B., W. Xu, P. A. Santini, A. D. Polydorides, A. Chiu, J. Estrella, M. Shan, A. Chadburn, V. Villanacci, A. Plebani, D. M. Knowles, M. Rescigno and A. Cerutti (2007). "Intestinal Bacteria Trigger T Cell-Independent Immunoglobulin A2 Class Switching by Inducing Epithelial-Cell Secretion of the Cytokine APRIL." Immunity 26(6): 812-826.

- He, J., L. Shen, M. Wan, O. Taranova, H. Wu and Y. Zhang (2013). "Kdm2b maintains murine embryonic stem cell status by recruiting PRC1 complex to CpG islands of developmental genes." Nat Cell Biol 15(4): 373-384.
- Heise, N., N. S. De Silva, K. Silva, A. Carette, G. Simonetti, M. Pasparakis and U. Klein (2014). "Germinal center B cell maintenance and differentiation are controlled by distinct NF-kappaB transcription factor subunits." J Exp Med 211(10): 2103-2118.
- Hemming, S., D. Cakouros, S. Isenmann, L. Cooper, D. Menicanin, A. Zannettino and S. Gronthos (2014). "EZH2 and KDM6A Act as an Epigenetic Switch to Regulate Mesenchymal Stem Cell Lineage Specification." STEM CELLS 32(3): 802-815.
- Herz, H.-M., M. Mohan, A. S. Garruss, K. Liang, Y.-H. Takahashi, K. Mickey, O. Voets, C. P. Verrijzer and A. Shilatifard (2012). "Enhancer-associated H3K4 monomethylation by Trithorax-related, the Drosophila homolog of mammalian Mll3/Mll4." Genes & development 26(23): 2604-2620.
- Herz, H. M., L. D. Madden, Z. Chen, C. Bolduc, E. Buff, R. Gupta, R. Davuluri, A. Shilatifard, I. K. Hariharan and A. Bergmann (2010). "The H3K27me3 demethylase dUTX is a suppressor of Notch- and Rb-dependent tumors in Drosophila." Mol Cell Biol 30(10): 2485-2497.
- Herzog, S., E. Hug, S. Meixlsperger, J. H. Paik, R. A. DePinho, M. Reth and H. Jumaa (2008). "SLP-65 regulates immunoglobulin light chain gene recombination through the PI(3)K-PKB-Foxo pathway." Nat Immunol 9(6): 623-631.
- Hillringhaus, L., W. W. Yue, N. R. Rose, S. S. Ng, C. Gileadi, C. Loenarz, S. H. Bello, J. E. Bray, C. J. Schofield and U. Oppermann (2011). "Structural and evolutionary basis for the dual substrate selectivity of human KDM4 histone demethylase family." J Biol Chem 286(48): 41616-41625.
- Hobeika, E., S. Thiemann, B. Storch, H. Jumaa, P. J. Nielsen, R. Pelanda and M. Reth (2006). "Testing gene function early in the B cell lineage in mb1-cre mice." Proc Natl Acad Sci U S A 103(37): 13789-13794.
- Hodgkin, P. D., J. H. Lee and A. B. Lyons (1996). "B cell differentiation and isotype switching is related to division cycle number." J Exp Med 184(1): 277-281.
- Hoffman, J. D., K. L. Ciprero, K. E. Sullivan, P. B. Kaplan, D. M. McDonald-McGinn, E. H. Zackai and J. E. Ming (2005). "Immune abnormalities are a frequent manifestation of Kabuki syndrome." Am J Med Genet A 135(3): 278-281.
- Hong, S., Y. W. Cho, L. R. Yu, H. Yu, T. D. Veenstra and K. Ge (2007). "Identification of JmjC domain-containing UTX and JMJD3 as histone H3 lysine 27 demethylases." Proc Natl Acad Sci U S A 104(47): 18439-18444.
- Horton, J. R., A. K. Upadhyay, H. H. Qi, X. Zhang, Y. Shi and X. Cheng (2010). "Enzymatic and structural insights for substrate specificity of a family of jumonji histone lysine demethylases." Nat Struct Mol Biol 17(1): 38-43.
- Hu, D., X. Gao, M. A. Morgan, H. M. Herz, E. R. Smith and A. Shilatifard (2013). "The MLL3/MLL4 branches of the COMPASS family function as major histone H3K4 monomethylases at enhancers." Mol Cell Biol 33(23): 4745-4754.
- Huang, C., Y. Xiang, Y. Wang, X. Li, L. Xu, Z. Zhu, T. Zhang, Q. Zhu, K. Zhang, N. Jing and C. D. Chen (2010). "Dual-specificity histone demethylase KIAA1718 (KDM7A) regulates neural differentiation through FGF4." Cell Res 20(2): 154-165.
- Huynh, K. D. and V. J. Bardwell (1998). "The BCL-6 POZ domain and other POZ domains interact with the co-repressors N-CoR and SMRT." Oncogene 17(19): 2473-2484.
- Ikuta, K. and I. L. Weissman (1992). "Evidence that hematopoietic stem cells express mouse c-kit but do not depend on steel factor for their generation." Proceedings of the National Academy of Sciences of the United States of America 89(4): 1502-1506.
- Inagaki, T., M. Tachibana, K. Magoori, H. Kudo, T. Tanaka, M. Okamura, M. Naito, T. Kodama, Y. Shinkai and J. Sakai (2009). "Obesity and metabolic syndrome in histone demethylase JHDM2a-deficient mice." Genes Cells 14(8): 991-1001.
- Ingham, P. and R. Whittle (1980). "Trithorax: A new homoeotic mutation of Drosophila melanogaster causing transformations of abdominal and thoracic imaginal segments." Molecular and General Genetics MGG 179(3): 607-614.
- Ingham, P. W. (1985). "A clonal analysis of the requirement for the trithorax gene in the diversification of segments in Drosophila." J Embryol Exp Morphol 89: 349-365.

- Inoue, T., R. Shinnakasu, W. Ise, C. Kawai, T. Egawa and T. Kurosaki (2017). "The transcription factor Foxo1 controls germinal center B cell proliferation in response to T cell help." J Exp Med 214(4): 1181-1198.
- Ismail, I. H., C. Andrin, D. McDonald and M. J. Hendzel (2010). "BMI1-mediated histone ubiquitylation promotes DNA double-strand break repair." The Journal of Cell Biology 191(1): 45-60.
- Itoh-Nakadai, A., R. Hikota, A. Muto, K. Kometani, M. Watanabe-Matsui, Y. Sato, M. Kobayashi, A. Nakamura, Y. Miura, Y. Yano, S. Tashiro, J. Sun, T. Ikawa, K. Ochiai, T. Kurosaki and K. Igarashi (2014). "The transcription repressors Bach2 and Bach1 promote B cell development by repressing the myeloid program." Nat Immunol 15(12): 1171-1180.
- Iwakoshi, N. N., A. H. Lee, P. Vallabhajosyula, K. L. Otipoby, K. Rajewsky and L. H. Glimcher (2003). "Plasma cell differentiation and the unfolded protein response intersect at the transcription factor XBP-1." Nature immunology 4(4): 321-329.
- Jacob, J., G. Kelsoe, K. Rajewsky and U. Weiss (1991). "Intraclonal generation of antibody mutants in germinal centres." Nature 354: 389.
- Jankowska, A. M., H. Makishima, R. V. Tiu, H. Szpurka, Y. Huang, F. Traina, V. Visconte, Y. Sugimoto, C. Prince, C. O'Keefe, E. D. Hsi, A. List, M. A. Sekeres, A. Rao, M. A. McDevitt and J. P. Maciejewski (2011). "Mutational spectrum analysis of chronic myelomonocytic leukemia includes genes associated with epigenetic regulation: UTX, EZH2, and DNMT3A." Blood 118(14): 3932-3941.
- Jansen, J. G., P. Langerak, A. Tsaalbi-Shtylik, P. van den Berk, H. Jacobs and N. de Wind (2006). "Strand-biased defect in C/G transversions in hypermutating immunoglobulin genes in Rev1-deficient mice." The Journal of experimental medicine 203(2): 319-323.
- Jenuwein, T. and C. D. Allis (2001). "Translating the histone code." Science 293(5532): 1074-1080.
- Jiang, W., J. Wang and Y. Zhang (2013). "Histone H3K27me3 demethylases KDM6A and KDM6B modulate definitive endoderm differentiation from human ESCs by regulating WNT signaling pathway." Cell research 23(1): 122-130.
- Johnson, K., D. L. Pflugh, D. Yu, D. G. Hesslein, K. I. Lin, A. L. Bothwell, A. Thomas-Tikhonenko, D. G. Schatz and K. Calame (2004). "B cell-specific loss of histone 3 lysine 9 methylation in the V(H) locus depends on Pax5." Nature immunology 5(8): 853-861.
- Jones, D. T., N. Jager, M. Kool, T. Zichner, B. Hutter, M. Sultan, Y. J. Cho, T. J. Pugh, V. Hovestadt, A. M. Stutz, T. Rausch, H. J. Warnatz, M. Ryzhova, S. Bender, D. Sturm, S. Pleier, H. Cin, E. Pfaff, L. Sieber, A. Wittmann, M. Remke, H. Witt, S. Hutter, T. Tzaridis, J. Weischenfeldt, B. Raeder, M. Avci, V. Amstislavskiy, M. Zapatka, U. D. Weber, Q. Wang, B. Lasitschka, C. C. Bartholomae, M. Schmidt, C. von Kalle, V. Ast, C. Lawerenz, J. Eils, R. Kabbe, V. Benes, P. van Sluis, J. Koster, R. Volckmann, D. Shih, M. J. Betts, R. B. Russell, S. Coco, G. P. Tonini, U. Schuller, V. Hans, N. Graf, Y. J. Kim, C. Monoranu, W. Roggendorf, A. Unterberg, C. Herold-Mende, T. Milde, A. E. Kulozik, A. von Deimling, O. Witt, E. Maass, J. Rossler, M. Ebinger, M. U. Schuhmann, M. C. Fruhwald, M. Hasselblatt, N. Jabado, S. Rutkowski, A. O. von Bueren, D. Williamson, S. C. Clifford, M. G. McCabe, V. P. Collins, S. Wolf, S. Wiemann, H. Lehrach, B. Brors, W. Scheurlen, J. Felsberg, G. Reifenberger, P. A. Northcott, M. D. Taylor, M. Meyerson, S. L. Pomeroy, M. L. Yaspo, J. O. Korbel, A. Korshunov, R. Eils, S. M. Pfister and P. Lichter (2012). "Dissecting the genomic complexity underlying medulloblastoma." Nature 488(7409): 100-105.
- Kabashima, K., N. M. Haynes, Y. Xu, S. L. Nutt, M. L. Allende, R. L. Proia and J. G. Cyster (2006). "Plasma cell S1P1 expression determines secondary lymphoid organ retention versus bone marrow tropism." J Exp Med 203(12): 2683-2690.
- Kaisho, T., K. Takeda, T. Tsujimura, T. Kawai, F. Nomura, N. Terada and S. Akira (2001). "IkappaB kinase alpha is essential for mature B cell development and function." J Exp Med 193(4): 417-426.
- Kaji, T., A. Ishige, M. Hikida, J. Taka, A. Hijikata, M. Kubo, T. Nagashima, Y. Takahashi, T. Kurosaki, M. Okada, O. Ohara, K. Rajewsky and T. Takemori (2012). "Distinct cellular pathways select germline-encoded and somatically mutated antibodies into immunological memory." J Exp Med 209(11): 2079-2097.

- Kallies, A., J. Hasbold, D. M. Tarlinton, W. Dietrich, L. M. Corcoran, P. D. Hodgkin and S. L. Nutt (2004). "Plasma cell ontogeny defined by quantitative changes in blimp-1 expression." The Journal of experimental medicine 200(8): 967-977.
- Kandoth, C., M. D. McLellan, F. Vandin, K. Ye, B. Niu, C. Lu, M. Xie, Q. Zhang, J. F. McMichael, M. A. Wyczalkowski, M. D. M. Leiserson, C. A. Miller, J. S. Welch, M. J. Walter, M. C. Wendl, T. J. Ley, R. K. Wilson, B. J. Raphael and L. Ding (2013). "Mutational landscape and significance across 12 major cancer types." Nature 502: 333.
- Kantor, A. B. (1996). "V-Gene usage and N-region insertions in B-1a, B-1b and conventional B cells." Seminars in Immunology 8(1): 29-35.
- Kaplinsky, J., A. Li, A. Sun, M. Coffre, S. B. Koralov and R. Arnaout (2014). "Antibody repertoire deep sequencing reveals antigen-independent selection in maturing B cells." Proceedings of the National Academy of Sciences of the United States of America 111(25): E2622-E2629.
- Kawabe, T., T. Naka, K. Yoshida, T. Tanaka, H. Fujiwara, S. Suematsu, N. Yoshida, T. Kishimoto and H. Kikutani (1994). "The immune responses in CD40-deficient mice: impaired immunoglobulin class switching and germinal center formation." Immunity 1(3): 167-178.
- Kennison, J. A. and J. W. Tamkun (1988). "Dosage-dependent modifiers of polycomb and antennapedia mutations in Drosophila." Proc Natl Acad Sci U S A 85(21): 8136-8140.
- Kikuchi, K., A. Y. Lai, C.-L. Hsu and M. Kondo (2005). "IL-7 receptor signaling is necessary for stage transition in adult B cell development through up-regulation of EBF." The Journal of experimental medicine 201(8): 1197-1203.
- Kim, J. H., A. Sharma, S. S. Dhar, S. H. Lee, B. Gu, C. H. Chan, H. K. Lin and M. G. Lee (2014). "UTX and MLL4 coordinately regulate transcriptional programs for cell proliferation and invasiveness in breast cancer cells." Cancer Res 74(6): 1705-1717.
- Kinoshita, K., M. Harigai, S. Fagarasan, M. Muramatsu and T. Honjo (2001). "A hallmark of active class switch recombination: Transcripts directed by I promoters on looped-out circular DNAs." Proceedings of the National Academy of Sciences 98(22): 12620-12623.
- Klein, U., S. Casola, G. Cattoretti, Q. Shen, M. Lia, T. Mo, T. Ludwig, K. Rajewsky and R. Dalla-Favera (2006). "Transcription factor IRF4 controls plasma cell differentiation and class-switch recombination." Nature immunology 7(7): 773-782..
- Klein, U. and R. Dalla-Favera (2008). "Germinal centres: role in B-cell physiology and malignancy." Nature reviews. Immunology 8(1): 22-33..
- Klein, U., Y. Tu, G. A. Stolovitzky, J. L. Keller, J. Haddad, Jr., V. Miljkovic, G. Cattoretti, A. Califano and R. Dalla-Favera (2003). "Transcriptional analysis of the B cell germinal center reaction." Proc Natl Acad Sci U S A 100(5): 2639-2644.
- Klose, R. J., Q. Yan, Z. Tothova, K. Yamane, H. Erdjument-Bromage, P. Tempst, D. G. Gilliland, Y. Zhang and W. G. Kaelin Jr (2007). "The Retinoblastoma Binding Protein RBP2 Is an H3K4 Demethylase." Cell 128(5): 889-900.
- Kometani, K., R. Nakagawa, R. Shinnakasu, T. Kaji, A. Rybouchkin, S. Moriyama, K. Furukawa, H. Koseki, T. Takemori and T. Kurosaki (2013). "Repression of the transcription factor Bach2 contributes to predisposition of IgG1 memory B cells toward plasma cell differentiation." Immunity 39(1): 136-147.
- Kopan, R. and M. X. Ilagan (2009). "The canonical Notch signaling pathway: unfolding the activation mechanism." Cell 137(2): 216-233.
- Kornberg, R. D. (1974). "Chromatin structure: a repeating unit of histones and DNA." Science 184(4139): 868-871.
- Kornberg, R. D. and Y. Lorch (1999). "Twenty-five years of the nucleosome, fundamental particle of the eukaryote chromosome." Cell 98(3): 285-294.
- Koyama-Nasu, R., G. David and N. Tanese (2007). "The F-box protein Fbl10 is a novel transcriptional repressor of c-Jun." Nat Cell Biol 9(9): 1074-1080.
- Kraal, G. and M. Janse (1986). "Marginal metallophilic cells of the mouse spleen identified by a monoclonal antibody." Immunology 58(4): 665-669.
- Kraus, M., M. B. Alimzhanov, N. Rajewsky and K. Rajewsky (2004). "Survival of resting mature B lymphocytes depends on BCR signaling via the Igalpha/beta heterodimer." Cell 117(6): 787-800.

- Krieg, A. J., E. B. Rankin, D. Chan, O. Razorenova, S. Fernandez and A. J. Giaccia (2010). "Regulation of the histone demethylase JMJD1A by hypoxia-inducible factor 1 alpha enhances hypoxic gene expression and tumor growth." Mol Cell Biol 30(1): 344-353.
- Kruidenier, L., C. W. Chung, Z. Cheng, J. Liddle, K. Che, G. Joberty, M. Bantscheff, C. Bountra, A. Bridges, H. Diallo, D. Eberhard, S. Hutchinson, E. Jones, R. Katso, M. Leveridge, P. K. Mander, J. Mosley, C. Ramirez-Molina, P. Rowland, C. J. Schofield, R. J. Sheppard, J. E. Smith, C. Swales, R. Tanner, P. Thomas, A. Tumber, G. Drewes, U. Oppermann, D. J. Patel, K. Lee and D. M. Wilson (2012). "A selective jumonji H3K27 demethylase inhibitor modulates the proinflammatory macrophage response." Nature 488(7411): 404-408.
- Kuleshov, M. V., M. R. Jones, A. D. Rouillard, N. F. Fernandez, Q. Duan, Z. Wang, S. Koplev, S. L. Jenkins, K. M. Jagodnik, A. Lachmann, M. G. McDermott, C. D. Monteiro, G. W. Gundersen and A. Ma'ayan (2016). "Enrichr: a comprehensive gene set enrichment analysis web server 2016 update." Nucleic Acids Res 44(W1): W90-97.
- Kunkel, E. J., C. H. Kim, N. H. Lazarus, M. A. Vierra, D. Soler, E. P. Bowman and E. C. Butcher (2003). "CCR10 expression is a common feature of circulating and mucosal epithelial tissue IgA Ab-secreting cells." J Clin Invest 111(7): 1001-1010.
- Kuroda, K., H. Han, S. Tani, K. Tanigaki, T. Tun, T. Furukawa, Y. Taniguchi, H. Kurooka, Y. Hamada, S. Toyokuni and T. Honjo (2003). "Regulation of marginal zone B cell development by MINT, a suppressor of Notch/RBP-J signaling pathway." Immunity 18(2): 301-312.
- Kuroki, Y., Y. Suzuki, H. Chyo, A. Hata and I. Matsui (1981). "A new malformation syndrome of long palpebralfissures, large ears, depressed nasal tip, and skeletal anomalies associated with postnatal dwarfism and mental retardation." The Journal of Pediatrics 99(4): 570-573.
- Kurosaki, T., K. Kometani and W. Ise (2015). "Memory B cells." Nature Reviews Immunology 15: 149.
- Kwon, H., D. Thierry-Mieg, J. Thierry-Mieg, H. P. Kim, J. Oh, C. Tunyaplin, S. Carotta, C. E. Donovan, M. L. Goldman, P. Tailor, K. Ozato, D. E. Levy, S. L. Nutt, K. Calame and W. J. Leonard (2009). "Analysis of interleukin-21-induced Prdm1 gene regulation reveals functional cooperation of STAT3 and IRF4 transcription factors." Immunity 31(6): 941-952.
- Kwon, K., C. Hutter, Q. Sun, I. Bilic, C. Cobaleda, S. Malin and M. Busslinger (2008). "Instructive role of the transcription factor E2A in early B lymphopoiesis and germinal center B cell development." Immunity 28(6): 751-762.
- Labbé, R. M., A. Holowatyj and Z.-Q. Yang (2013). "Histone lysine demethylase (KDM) subfamily 4: structures, functions and therapeutic potential." American journal of translational research 6(1): 1-15.
- Laborda, J. (1991). "36B4 cDNA used as an estradiol-independent mRNA control is the cDNA for human acidic ribosomal phosphoprotein PO." Nucleic Acids Res 19(14): 3998.
- Lam, K. P., R. Kuhn and K. Rajewsky (1997). "In vivo ablation of surface immunoglobulin on mature B cells by inducible gene targeting results in rapid cell death." Cell 90(6): 1073-1083.
- Lan, F., P. E. Bayliss, J. L. Rinn, J. R. Whetstine, J. K. Wang, S. Chen, S. Iwase, R. Alpatov, I. Issaeva, E. Canaani, T. M. Roberts, H. Y. Chang and Y. Shi (2007). "A histone H3 lysine 27 demethylase regulates animal posterior development." Nature 449(7163): 689-694.
- Langmead, B. and S. L. Salzberg (2012). "Fast gapped-read alignment with Bowtie 2." Nature methods 9(4): 357-359.
- Lederer, D., B. Grisart, M. C. Digilio, V. Benoit, M. Crespin, S. C. Ghariani, I. Maystadt, B. Dallapiccola and C. Verellen-Dumoulin (2012). "Deletion of KDM6A, a histone demethylase interacting with MLL2, in three patients with Kabuki syndrome." Am J Hum Genet 90(1): 119-124.
- Lee, J., D. H. Kim, S. Lee, Q. H. Yang, D. K. Lee, S. K. Lee, R. G. Roeder and J. W. Lee (2009). "A tumor suppressive coactivator complex of p53 containing ASC-2 and histone H3-lysine-4 methyltransferase MLL3 or its paralogue MLL4." Proc Natl Acad Sci U S A 106(21): 8513-8518.
- Lee, J.-E., C. Wang, S. Xu, Y.-W. Cho, L. Wang, X. Feng, A. Baldridge, V. Sartorelli, L. Zhuang, W. Peng and K. Ge (2013). "H3K4 mono- and di-methyltransferase MLL4 is required for enhancer activation during cell differentiation." eLife 2: e01503-e01503.
- Lee, K., W. Tirasophon, X. Shen, M. Michalak, R. Prywes, T. Okada, H. Yoshida, K. Mori and R. J. Kaufman (2002). "IRE1-mediated unconventional mRNA splicing and S2P-mediated

ATF6 cleavage merge to regulate XBP1 in signaling the unfolded protein response." Genes Dev 16(4): 452-466.
- Lee, M. G., R. Villa, P. Trojer, J. Norman, K. P. Yan, D. Reinberg, L. Di Croce and R. Shiekhattar (2007). "Demethylation of H3K27 regulates polycomb recruitment and H2A ubiquitination." Science 318(5849): 447-450.
- Lee, S., J. W. Lee and S. K. Lee (2012). "UTX, a histone H3-lysine 27 demethylase, acts as a critical switch to activate the cardiac developmental program." Dev Cell 22(1): 25-37.
- Lee, T. I., R. G. Jenner, L. A. Boyer, M. G. Guenther, S. S. Levine, R. M. Kumar, B. Chevalier, S. E. Johnstone, M. F. Cole, K.-i. Isono, H. Koseki, T. Fuchikami, K. Abe, H. L. Murray, J. P. Zucker, B. Yuan, G. W. Bell, E. Herbolsheimer, N. M. Hannett, K. Sun, D. T. Odom, A. P. Otte, T. L. Volkert, D. P. Bartel, D. A. Melton, D. K. Gifford, R. Jaenisch and R. A. Young (2006). "Control of Developmental Regulators by Polycomb in Human Embryonic Stem Cells." Cell 125(2): 301-313.
- Lei, X. and J. Jiao (2018). "UTX Affects Neural Stem Cell Proliferation and Differentiation through PTEN Signaling." Stem cell reports 10(4): 1193-1207.
- Levine, S. S., A. Weiss, H. Erdjument-Bromage, Z. Shao, P. Tempst and R. E. Kingston (2002). "The core of the polycomb repressive complex is compositionally and functionally conserved in flies and humans." Mol Cell Biol 22(17): 6070-6078.
- Lewis, E. B. (1945). "The Relation of Repeats to Position Effect in Drosophila Melanogaster." Genetics 30(2): 137-166.
- Lewis, E. B. (1978). "A gene complex controlling segmentation in Drosophila." Nature 276: 565.
- Li, C. L. and G. R. Johnson (1995). "Murine hematopoietic stem and progenitor cells: I. Enrichment and biologic characterization." Blood 85(6): 1472-1479.
- Li, X., K. Su, C. Ji, A. J. Szalai, J. Wu, Y. Zhang, T. Zhou, R. P. Kimberly and J. C. Edberg (2008). "Immune opsonins modulate BLyS/BAFF release in a receptor-specific fashion." J Immunol 181(2): 1012-1018.
- Li, X., Y. Zhang, L. Zheng, M. Liu, C. D. Chen and H. Jiang (2018). "UTX is an escape from X-inactivation tumor-suppressor in B cell lymphoma." Nature Communications 9(1): 2720.
- Li, Z., T. Otevrel, Y. Gao, H. L. Cheng, B. Seed, T. D. Stamato, G. E. Taccioli and F. W. Alt (1995). "The XRCC4 gene encodes a novel protein involved in DNA double-strand break repair and V(D)J recombination." Cell 83(7): 1079-1089.
- Liebich, H. M., E. Gesele, C. Wirth, J. Woll, K. Jobst and A. Lakatos (1993). "Non-enzymatic glycation of histones." Biol Mass Spectrom 22(2): 121-123.
- Lin, H. and R. Grosschedl (1995). "Failure of B-cell differentiation in mice lacking the transcription factor EBF." Nature 376(6537): 263-267.
- Lin, J. L., W. I. Lee, J. L. Huang, P. K. Chen, K. C. Chan, L. J. Lo, Y. J. You, Y. F. Shih, T. Y. Tseng and M. C. Wu (2015). "Immunologic assessment and KMT2D mutation detection in Kabuki syndrome." Clin Genet 88(3): 255-260.
- Lin, K. I., C. Angelin-Duclos, T. C. Kuo and K. Calame (2002). "Blimp-1-dependent repression of Pax-5 is required for differentiation of B cells to immunoglobulin M-secreting plasma cells." Molecular and cellular biology 22(13): 4771-4780.
- Lin, Y., K. Wong and K. Calame (1997). "Repression of c-myc transcription by Blimp-1, an inducer of terminal B cell differentiation." Science 276(5312): 596-599.
- Lin, Y. C., S. Jhunjhunwala, C. Benner, S. Heinz, E. Welinder, R. Mansson, M. Sigvardsson, J. Hagman, C. A. Espinoza, J. Dutkowski, T. Ideker, C. K. Glass and C. Murre (2010). "A global network of transcription factors, involving E2A, EBF1 and Foxo1, that orchestrates B cell fate." Nat Immunol 11(7): 635-643.
- Lindsley, A. W., H. M. Saal, T. A. Burrow, R. J. Hopkin, O. Shchelochkov, P. Khandelwal, C. Xie, J. Bleesing, L. Filipovich, K. Risma, A. H. Assa'ad, P. A. Roehrs and J. A. Bernstein (2016). "Defects of B-cell terminal differentiation in patients with type-1 Kabuki syndrome." The Journal of allergy and clinical immunology 137: 179-187.e110.
- Liu, J., T. Mercher, C. Scholl, K. Brumme, D. G. Gilliland and N. Zhu (2012). "A functional role for the histone demethylase UTX in normal and malignant hematopoietic cells." Experimental hematology 40: 487-498.e483.

- Liu, M., J. L. Duke, D. J. Richter, C. G. Vinuesa, C. C. Goodnow, S. H. Kleinstein and D. G. Schatz (2008). "Two levels of protection for the B cell genome during somatic hypermutation." Nature 451(7180): 841-845.
- Livak, K. J. and T. D. Schmittgen (2001). "Analysis of relative gene expression data using real-time quantitative PCR and the 2(-Delta Delta C(T)) Method." Methods 25(4): 402-408.
- Lo, C. G., T. T. Lu and J. G. Cyster (2003). "Integrin-dependence of lymphocyte entry into the splenic white pulp." The Journal of experimental medicine 197(3): 353-361.
- Loder, F., B. Mutschler, R. J. Ray, C. J. Paige, P. Sideras, R. Torres, M. C. Lamers and R. Carsetti (1999). "B cell development in the spleen takes place in discrete steps and is determined by the quality of B cell receptor-derived signals." J Exp Med 190(1): 75-89.
- Loh, Y. H., W. Zhang, X. Chen, J. George and H. H. Ng (2007). "Jmjd1a and Jmjd2c histone H3 Lys 9 demethylases regulate self-renewal in embryonic stem cells." Genes Dev 21(20): 2545-2557.
- Lopes-Carvalho, T. and J. F. Kearney (2004). "Development and selection of marginal zone B cells." Immunological reviews 197: 192-205.
- Love, M. I., W. Huber and S. Anders (2014). "Moderated estimation of fold change and dispersion for RNA-seq data with DESeq2." Genome Biol 15(12): 550.
- Lu, R. (2008). "Interferon regulatory factor 4 and 8 in B-cell development." Trends in immunology 29(10): 487-492.
- Lu, T., M. W. Jackson, B. Wang, M. Yang, M. R. Chance, M. Miyagi, A. V. Gudkov and G. R. Stark (2010). "Regulation of NF-kappaB by NSD1/FBXL11-dependent reversible lysine methylation of p65." Proc Natl Acad Sci U S A 107(1): 46-51.
- Lu, T. T. and J. G. Cyster (2002). "Integrin-mediated long-term B cell retention in the splenic marginal zone." Science 297(5580): 409-412.
- Luger, K. (2003). "Structure and dynamic behavior of nucleosomes." Curr Opin Genet Dev 13(2): 127-135.
- Ma, S., S. Pathak, L. Trinh and R. Lu (2008). "Interferon regulatory factors 4 and 8 induce the expression of Ikaros and Aiolos to down-regulate pre-B-cell receptor and promote cell-cycle withdrawal in pre-B-cell development." Blood 111(3): 1396-1403.
- Ma, S., V. Shukla, L. Fang, K. A. Gould, S. S. Joshi and R. Lu (2013). "Accelerated development of chronic lymphocytic leukemia in New Zealand Black mice expressing a low level of interferon regulatory factor 4." J Biol Chem 288(37): 26430-26440.
- Mackay, F. and H. Leung (2006). "The role of the BAFF/APRIL system on T cell function." Semin Immunol 18(5): 284-289.
- Mackay, F. and P. Schneider (2009). "Cracking the BAFF code." Nat Rev Immunol 9(7): 491-502.
- Macpherson, A. J., K. D. McCoy, F. E. Johansen and P. Brandtzaeg (2008). "The immune geography of IgA induction and function." Mucosal Immunol 1(1): 11-22.
- Maillard, I., T. Fang and W. S. Pear (2005). "Regulation of lymphoid development, differentiation, and function by the Notch pathway." Annu Rev Immunol 23: 945-974.
- Manis, J. P., Y. Gu, R. Lansford, E. Sonoda, R. Ferrini, L. Davidson, K. Rajewsky and F. W. Alt (1998). "Ku70 is required for late B cell development and immunoglobulin heavy chain class switching." The Journal of experimental medicine 187(12): 2081-2089.
- Mann, K. M., J. M. Ward, C. C. K. Yew, A. Kovochich, D. W. Dawson, M. A. Black, B. T. Brett, T. E. Sheetz, A. J. Dupuy, D. K. Chang, A. V. Biankin, N. Waddell, K. S. Kassahn, S. M. Grimmond, A. G. Rust, D. J. Adams, N. A. Jenkins and N. G. Copeland (2012). "Sleeping Beauty mutagenesis reveals cooperating mutations and pathways in pancreatic adenocarcinoma." Proceedings of the National Academy of Sciences 109(16): 5934-5941.
- Manna, S., J. K. Kim, C. Bauge, M. Cam, Y. Zhao, J. Shetty, M. S. Vacchio, E. Castro, B. Tran, L. Tessarollo and R. Bosselut (2015). "Histone H3 Lysine 27 demethylases Jmjd3 and Utx are required for T-cell differentiation." Nat Commun 6: 8152.
- Mansour, A. A., O. Gafni, L. Weinberger, A. Zviran, M. Ayyash, Y. Rais, V. Krupalnik, M. Zerbib, D. Amann-Zalcenstein, I. Maza, S. Geula, S. Viukov, L. Holtzman, A. Pribluda, E. Canaani, S. Horn-Saban, I. Amit, N. Novershtern and J. H. Hanna (2012). "The H3K27 demethylase Utx regulates somatic and germ cell epigenetic reprogramming." Nature 488(7411): 409-413.

- Mansson, R., A. Hultquist, S. Luc, L. Yang, K. Anderson, S. Kharazi, S. Al-Hashmi, K. Liuba, L. Thoren, J. Adolfsson, N. Buza-Vidas, H. Qian, S. Soneji, T. Enver, M. Sigvardsson and S. E. Jacobsen (2007). "Molecular evidence for hierarchical transcriptional lineage priming in fetal and adult stem cells and multipotent progenitors." Immunity 26(4): 407-419.
- Margueron, R. and D. Reinberg (2011). "The Polycomb complex PRC2 and its mark in life." Nature 469: 343-349.
- Martensson, I. L. and R. Ceredig (2000). "Review article: role of the surrogate light chain and the pre-B-cell receptor in mouse B-cell development." Immunology 101(4): 435-441.
- Martin, F. and J. F. Kearney (2002). "Marginal-zone B cells." Nat Rev Immunol 2(5): 323-335.
- Martin, S. W. and C. C. Goodnow (2002). "Burst-enhancing role of the IgG membrane tail as a molecular determinant of memory." Nat Immunol 3(2): 182-188.
- Martinez-Valdez, H., C. Guret, O. de Bouteiller, I. Fugier, J. Banchereau and Y. J. Liu (1996). "Human germinal center B cells express the apoptosis-inducing genes Fas, c-myc, P53, and Bax but not the survival gene bcl-2." J Exp Med 183(3): 971-977.
- Matloubian, M., C. G. Lo, G. Cinamon, M. J. Lesneski, Y. Xu, V. Brinkmann, M. L. Allende, R. L. Proia and J. G. Cyster (2004). "Lymphocyte egress from thymus and peripheral lymphoid organs is dependent on S1P receptor 1." Nature 427(6972): 355-360.
- Matsumoto, N. and N. Niikawa (2003). "Kabuki make-up syndrome: a review." Am J Med Genet C Semin Med Genet 117c(1): 57-65.
- Matsuzawa, A., P. H. Tseng, S. Vallabhapurapu, J. L. Luo, W. Zhang, H. Wang, D. A. Vignali, E. Gallagher and M. Karin (2008). "Essential cytoplasmic translocation of a cytokine receptor-assembled signaling complex." Science 321(5889): 663-668.
- McBlane, J. F., D. C. van Gent, D. A. Ramsden, C. Romeo, C. A. Cuomo, M. Gellert and M. A. Oettinger (1995). "Cleavage at a V(D)J recombination signal requires only RAG1 and RAG2 proteins and occurs in two steps." Cell 83(3): 387-395.
- McCabe, M. T., H. M. Ott, G. Ganji, S. Korenchuk, C. Thompson, G. S. Van Aller, Y. Liu, A. P. Graves, A. Della Pietra, 3rd, E. Diaz, L. V. LaFrance, M. Mellinger, C. Duquenne, X. Tian, R. G. Kruger, C. F. McHugh, M. Brandt, W. H. Miller, D. Dhanak, S. K. Verma, P. J. Tummino and C. L. Creasy (2012). "EZH2 inhibition as a therapeutic strategy for lymphoma with EZH2-activating mutations." Nature 492(7427): 108-112.
- McManus, S., A. Ebert, G. Salvagiotto, J. Medvedovic, Q. Sun, I. Tamir, M. Jaritz, H. Tagoh and M. Busslinger (2011). "The transcription factor Pax5 regulates its target genes by recruiting chromatin-modifying proteins in committed B cells." Embo j 30(12): 2388-2404.
- Medina, K. L., J. M. Pongubala, K. L. Reddy, D. W. Lancki, R. Dekoter, M. Kieslinger, R. Grosschedl and H. Singh (2004). "Assembling a gene regulatory network for specification of the B cell fate." Dev Cell 7(4): 607-617.
- Melek, M., M. Gellert and D. C. van Gent (1998). "Rejoining of DNA by the RAG1 and RAG2 proteins." Science 280(5361): 301-303.
- Mikkelsen, T. S., M. Ku, D. B. Jaffe, B. Issac, E. Lieberman, G. Giannoukos, P. Alvarez, W. Brockman, T. K. Kim, R. P. Koche, W. Lee, E. Mendenhall, A. O'Donovan, A. Presser, C. Russ, X. Xie, A. Meissner, M. Wernig, R. Jaenisch, C. Nusbaum, E. S. Lander and B. E. Bernstein (2007). "Genome-wide maps of chromatin state in pluripotent and lineage-committed cells." Nature 448(7153): 553-560.
- Milanovic, M., N. Heise, N. S. De Silva, M. M. Anderson, K. Silva, A. Carette, F. Orelli, G. Bhagat and U. Klein (2017). "Differential requirements for the canonical NF-kappaB transcription factors c-REL and RELA during the generation and activation of mature B cells." Immunol Cell Biol 95(3): 261-271.
- Miller, S. A., S. E. Mohn and A. S. Weinmann (2010). "Jmjd3 and UTX play a demethylase-independent role in chromatin remodeling to regulate T-box family member-dependent gene expression." Mol Cell 40(4): 594-605.
- Mills, J. R., Y. Hippo, F. Robert, S. M. Chen, A. Malina, C. J. Lin, U. Trojahn, H. G. Wendel, A. Charest, R. T. Bronson, S. C. Kogan, R. Nadon, D. E. Housman, S. W. Lowe and J. Pelletier (2008). "mTORC1 promotes survival through translational control of Mcl-1." Proceedings of the National Academy of Sciences of the United States of America 105(31): 10853-10858.
- Minnich, M., H. Tagoh, P. Bönelt, E. Axelsson, M. Fischer, B. Cebolla, A. Tarakhovsky, S. L. Nutt, M. Jaritz and M. Busslinger (2016). "Multifunctional role of the transcription factor Blimp-1 in coordinating plasma cell differentiation." Nature Immunology 17: 331.

- Mo, R., S. M. Rao and Y.-J. Zhu (2006). "Identification of the MLL2 Complex as a Coactivator for Estrogen Receptor α." Journal of Biological Chemistry 281(23): 15714-15720.
- Mohan, M., H.-M. Herz, E. R. Smith, Y. Zhang, J. Jackson, M. P. Washburn, L. Florens, J. C. Eissenberg and A. Shilatifard (2011). "The COMPASS family of H3K4 methylases in Drosophila." Molecular and cellular biology 31(21): 4310-4318.
- Montecino-Rodriguez, E., H. Leathers and K. Dorshkind (2006). "Identification of a B-1 B cell-specified progenitor." Nature immunology 7(3): 293-301.
- Mora, J. R., M. Iwata, B. Eksteen, S.-Y. Song, T. Junt, B. Senman, K. L. Otipoby, A. Yokota, H. Takeuchi, P. Ricciardi-Castagnoli, K. Rajewsky, D. H. Adams and U. H. von Andrian (2006). "Generation of Gut-Homing IgA-Secreting B Cells by Intestinal Dendritic Cells." Science 314(5802): 1157-1160.
- Morales Torres, C., A. Laugesen and K. Helin (2013). "Utx Is Required for Proper Induction of Ectoderm and Mesoderm during Differentiation of Embryonic Stem Cells." PLOS ONE 8(4): e60020.
- Morey, L. and K. Helin (2010). "Polycomb group protein-mediated repression of transcription." Trends Biochem Sci 35(6): 323-332.
- Morin, R. D., N. A. Johnson, T. M. Severson, A. J. Mungall, J. An, R. Goya, J. E. Paul, M. Boyle, B. W. Woolcock, F. Kuchenbauer, D. Yap, R. K. Humphries, O. L. Griffith, S. Shah, H. Zhu, M. Kimbara, P. Shashkin, J. F. Charlot, M. Tcherpakov, R. Corbett, A. Tam, R. Varhol, D. Smailus, M. Moksa, Y. Zhao, A. Delaney, H. Qian, I. Birol, J. Schein, R. Moore, R. Holt, D. E. Horsman, J. M. Connors, S. Jones, S. Aparicio, M. Hirst, R. D. Gascoyne and M. A. Marra (2010). "Somatic mutations altering EZH2 (Tyr641) in follicular and diffuse large B-cell lymphomas of germinal-center origin." Nat Genet 42(2): 181-185.
- Morshead, K. B., D. N. Ciccone, S. D. Taverna, C. D. Allis and M. A. Oettinger (2003). "Antigen receptor loci poised for V(D)J rearrangement are broadly associated with BRG1 and flanked by peaks of histone H3 dimethylated at lysine 4." Proceedings of the National Academy of Sciences of the United States of America 100(20): 11577-11582.
- Müller, G., U. E. Höpken and M. Lipp (2003). "The impact of CCR7 and CXCR5 on lymphoid organ development and systemic immunity." Immunological Reviews 195(1): 117-135.
- Muramatsu, M., K. Kinoshita, S. Fagarasan, S. Yamada, Y. Shinkai and T. Honjo (2000). "Class switch recombination and hypermutation require activation-induced cytidine deaminase (AID), a potential RNA editing enzyme." Cell 102(5): 553-563.
- Muto, A., H. Hoshino, L. Madisen, N. Yanai, M. Obinata, H. Karasuyama, N. Hayashi, H. Nakauchi, M. Yamamoto, M. Groudine and K. Igarashi (1998). "Identification of Bach2 as a B-cell-specific partner for small maf proteins that negatively regulate the immunoglobulin heavy chain gene 3' enhancer." Embo j 17(19): 5734-5743.
- Muto, A., S. Tashiro, O. Nakajima, H. Hoshino, S. Takahashi, E. Sakoda, D. Ikebe, M. Yamamoto and K. Igarashi (2004). "The transcriptional programme of antibody class switching involves the repressor Bach2." Nature 429(6991): 566-571.
- Muto, A., S. Tashiro, H. Tsuchiya, A. Kume, M. Kanno, E. Ito, M. Yamamoto and K. Igarashi (2002). "Activation of Maf/AP-1 repressor Bach2 by oxidative stress promotes apoptosis and its interaction with promyelocytic leukemia nuclear bodies." J Biol Chem 277(23): 20724-20733.
- Nathan, D., D. E. Sterner and S. L. Berger (2003). "Histone modifications: Now summoning sumoylation." Proc Natl Acad Sci U S A 100(23): 13118-13120.
- Nemazee, D. (2006). "Receptor editing in lymphocyte development and central tolerance." Nat Rev Immunol 6(10): 728-740.
- Ng, S. S., K. L. Kavanagh, M. A. McDonough, D. Butler, E. S. Pilka, B. M. Lienard, J. E. Bray, P. Savitsky, O. Gileadi, F. von Delft, N. R. Rose, J. Offer, J. C. Scheinost, T. Borowski, M. Sundstrom, C. J. Schofield and U. Oppermann (2007). "Crystal structures of histone demethylase JMJD2A reveal basis for substrate specificity." Nature 448(7149): 87-91.
- Ngo, V. N., H. Korner, M. D. Gunn, K. N. Schmidt, D. S. Riminton, M. D. Cooper, J. L. Browning, J. D. Sedgwick and J. G. Cyster (1999). "Lymphotoxin alpha/beta and tumor necrosis factor are required for stromal cell expression of homing chemokines in B and T cell areas of the spleen." The Journal of experimental medicine 189(2): 403-412.

- Nie, Y., J. Waite, F. Brewer, M. J. Sunshine, D. R. Littman and Y. R. Zou (2004). "The role of CXCR4 in maintaining peripheral B cell compartments and humoral immunity." J Exp Med 200(9): 1145-1156.
- Niu, H., B. H. Ye and R. Dalla-Favera (1998). "Antigen receptor signaling induces MAP kinase-mediated phosphorylation and degradation of the BCL-6 transcription factor." Genes & development 12(13): 1953-1961.
- Nojima, T., K. Haniuda, T. Moutai, M. Matsudaira, S. Mizokawa, I. Shiratori, T. Azuma and D. Kitamura (2011). "In-vitro derived germinal centre B cells differentially generate memory B or plasma cells in vivo." Nat Commun 2: 465.
- Norvell, A., L. Mandik and J. G. Monroe (1995). "Engagement of the antigen-receptor on immature murine B lymphocytes results in death by apoptosis." J Immunol 154(9): 4404-4413.
- Norvell, A. and J. G. Monroe (1996). "Acquisition of surface IgD fails to protect from tolerance-induction. Both surface IgM- and surface IgD-mediated signals induce apoptosis of immature murine B lymphocytes." J Immunol 156(4): 1328-1332.
- Nowak, S. J. and V. G. Corces (2004). "Phosphorylation of histone H3: a balancing act between chromosome condensation and transcriptional activation." Trends Genet 20(4): 214-220.
- Ntziachristos, P., A. Tsirigos, G. G. Welstead, T. Trimarchi, S. Bakogianni, L. Xu, E. Loizou, L. Holmfeldt, A. Strikoudis, B. King, J. Mullenders, J. Becksfort, J. Nedjic, E. Paietta, M. S. Tallman, J. M. Rowe, G. Tonon, T. Satoh, L. Kruidenier, R. Prinjha, S. Akira, P. Van Vlierberghe, A. A. Ferrando, R. Jaenisch, C. G. Mullighan and I. Aifantis (2014). "Contrasting roles of histone 3 lysine 27 demethylases in acute lymphoblastic leukaemia." Nature 514(7523): 513-517.
- Nutt, S. L., B. Heavey, A. G. Rolink and M. Busslinger (1999). "Commitment to the B-lymphoid lineage depends on the transcription factor Pax5." Nature 401(6753): 556-562.
- Nutt, S. L. and B. L. Kee (2007). "The transcriptional regulation of B cell lineage commitment." Immunity 26(6): 715-725.
- O'Riordan, M. and R. Grosschedl (1999). "Coordinate regulation of B cell differentiation by the transcription factors EBF and E2A." Immunity 11(1): 21-31.
- Ochiai, K., M. Maienschein-Cline, G. Simonetti, J. Chen, R. Rosenthal, R. Brink, A. S. Chong, U. Klein, A. R. Dinner, H. Singh and R. Sciammas (2013). "Transcriptional regulation of germinal center B and plasma cell fates by dynamical control of IRF4." Immunity 38(5): 918-929.
- Okada, T., V. N. Ngo, E. H. Ekland, R. Forster, M. Lipp, D. R. Littman and J. G. Cyster (2002). "Chemokine requirements for B cell entry to lymph nodes and Peyer's patches." J Exp Med 196(1): 65-75.
- Opferman, J. T., A. Letai, C. Beard, M. D. Sorcinelli, C. C. Ong and S. J. Korsmeyer (2003). "Development and maintenance of B and T lymphocytes requires antiapoptotic MCL-1." Nature 426(6967): 671-676.
- Ortega-Molina, A., I. W. Boss, A. Canela, H. Pan, Y. Jiang, C. Zhao, M. Jiang, D. Hu, X. Agirre, I. Niesvizky, J. E. Lee, H. T. Chen, D. Ennishi, D. W. Scott, A. Mottok, C. Hother, S. Liu, X. J. Cao, W. Tam, R. Shaknovich, B. A. Garcia, R. D. Gascoyne, K. Ge, A. Shilatifard, O. Elemento, A. Nussenzweig, A. M. Melnick and H. G. Wendel (2015). "The histone lysine methyltransferase KMT2D sustains a gene expression program that represses B cell lymphoma development." Nat Med 21(10): 1199-1208.
- Osipovich, O., R. Milley, A. Meade, M. Tachibana, Y. Shinkai, M. S. Krangel and E. M. Oltz (2004). "Targeted inhibition of V(D)J recombination by a histone methyltransferase." Nature immunology 5(3): 309-316.
- Ota, K., K. I. Tong, K. Goto, S. Tomida, A. Komuro, Z. Wang, K. Nishio and H. Okada (2017). "The H3K27 demethylase, Utx, regulates adipogenesis in a differentiation stage-dependent manner." PLOS ONE 12(3): e0173713.
- Pabst, O. (2012). "New concepts in the generation and functions of IgA." Nature Reviews Immunology 12: 821.
- Parekh, S., J. M. Polo, R. Shaknovich, P. Juszczynski, P. Lev, S. M. Ranuncolo, Y. Yin, U. Klein, G. Cattoretti, R. Dalla Favera, M. A. Shipp and A. Melnick (2007). "BCL6 programs lymphoma cells for survival and differentiation through distinct biochemical mechanisms." Blood 110(6): 2067-2074.

- Pasini, D., A. P. Bracken, J. B. Hansen, M. Capillo and K. Helin (2007). "The polycomb group protein Suz12 is required for embryonic stem cell differentiation." Mol Cell Biol 27(10): 3769-3779.
- Pasini, D., P. A. Cloos, J. Walfridsson, L. Olsson, J. P. Bukowski, J. V. Johansen, M. Bak, N. Tommerup, J. Rappsilber and K. Helin (2010). "JARID2 regulates binding of the Polycomb repressive complex 2 to target genes in ES cells." Nature 464(7286): 306-310.
- Pasini, D., K. H. Hansen, J. Christensen, K. Agger, P. A. Cloos and K. Helin (2008). "Coordinated regulation of transcriptional repression by the RBP2 H3K4 demethylase and Polycomb-Repressive Complex 2." Genes Dev 22(10): 1345-1355.
- Pasparakis, M., M. Schmidt-Supprian and K. Rajewsky (2002). "IkappaB kinase signaling is essential for maintenance of mature B cells." J Exp Med 196(6): 743-752.
- Pasqualucci, L., Y. Kitaura, H. Gu and R. Dalla-Favera (2006). "PKA-mediated phosphorylation regulates the function of activation-induced deaminase (AID) in B cells." Proceedings of the National Academy of Sciences of the United States of America 103(2): 395-400.
- Patke, A., I. Mecklenbrauker, H. Erdjument-Bromage, P. Tempst and A. Tarakhovsky (2006). "BAFF controls B cell metabolic fitness through a PKC beta- and Akt-dependent mechanism." J Exp Med 203(11): 2551-2562.
- Pereira, J. P., L. M. Kelly, Y. Xu and J. G. Cyster (2009). "EBI2 mediates B cell segregation between the outer and centre follicle." Nature 460(7259): 1122-1126.
- Petersen, S., R. Casellas, B. Reina-San-Martin, H. T. Chen, M. J. Difilippantonio, P. C. Wilson, L. Hanitsch, A. Celeste, M. Muramatsu, D. R. Pilch, C. Redon, T. Ried, W. M. Bonner, T. Honjo, M. C. Nussenzweig and A. Nussenzweig (2001). "AID is required to initiate Nbs1/gamma-H2AX focus formation and mutations at sites of class switching." Nature 414(6864): 660-665.
- Petersen-Mahrt, S. K., R. S. Harris and M. S. Neuberger (2002). "AID mutates E. coli suggesting a DNA deamination mechanism for antibody diversification." Nature 418(6893): 99-103.
- Petrini, J. H. (1999). "The mammalian Mre11-Rad50-nbs1 protein complex: integration of functions in the cellular DNA-damage response." American journal of human genetics 64(5): 1264-1269.
- Petruk, S., Y. Sedkov, D. M. Johnston, J. W. Hodgson, K. L. Black, S. K. Kovermann, S. Beck, E. Canaani, H. W. Brock and A. Mazo (2012). "TrxG and PcG proteins but not methylated histones remain associated with DNA through replication." Cell 150(5): 922-933.
- Pham, T. H. M., P. Baluk, Y. Xu, I. Grigorova, A. J. Bankovich, R. Pappu, S. R. Coughlin, D. M. McDonald, S. R. Schwab and J. G. Cyster (2010). "Lymphatic endothelial cell sphingosine kinase activity is required for lymphocyte egress and lymphatic patterning." The Journal of experimental medicine 207(1): 17-27.
- Phan, R. T. and R. Dalla-Favera (2004). "The BCL6 proto-oncogene suppresses p53 expression in germinal-centre B cells." Nature 432(7017): 635-639.
- Phan, R. T., M. Saito, Y. Kitagawa, A. R. Means and R. Dalla-Favera (2007). "Genotoxic stress regulates expression of the proto-oncogene Bcl6 in germinal center B cells." Nat Immunol 8(10): 1132-1139.
- Pierce, S. K. and W. Liu (2013). "Encoding Immunological Memory in the Initiation of B-Cell Receptor Signaling." Cold Spring Harb Symp Quant Biol.
- Pillai, S. and A. Cariappa (2009). "The follicular versus marginal zone B lymphocyte cell fate decision." Nat Rev Immunol 9(11): 767-777.
- Pillai, S., A. Cariappa and S. T. Moran (2004). "Positive selection and lineage commitment during peripheral B-lymphocyte development." Immunol Rev 197: 206-218.
- Piunti, A. and A. Shilatifard (2016). "Epigenetic balance of gene expression by Polycomb and COMPASS families." Science 352(6290): aad9780.
- Pohl, T., R. Gugasyan, R. J. Grumont, A. Strasser, D. Metcalf, D. Tarlinton, W. Sha, D. Baltimore and S. Gerondakis (2002). "The combined absence of NF-kappa B1 and c-Rel reveals that overlapping roles for these transcription factors in the B cell lineage are restricted to the activation and function of mature cells." Proc Natl Acad Sci U S A 99(7): 4514-4519.
- Pohl, T., R. Gugasyan, R. J. Grumont, A. Strasser, D. Metcalf, D. Tarlinton, W. Sha, D. Baltimore and S. Gerondakis (2002). "The combined absence of NF-κB1 and c-Rel reveals that

overlapping roles for these transcription factors in the B cell lineage are restricted to the activation and function of mature cells." Proceedings of the National Academy of Sciences 99(7): 4514-4519.

- Polo, J. M., W. Ci, J. D. Licht and A. Melnick (2008). "Reversible disruption of BCL6 repression complexes by CD40 signaling in normal and malignant B cells." Blood 112(3): 644-651.
- Rada, C., J. M. Di Noia and M. S. Neuberger (2004). "Mismatch recognition and uracil excision provide complementary paths to both Ig switching and the A/T-focused phase of somatic mutation." Molecular cell 16(2): 163-171.
- Rada-Iglesias, A., R. Bajpai, T. Swigut, S. A. Brugmann, R. A. Flynn and J. Wysocka (2011). "A unique chromatin signature uncovers early developmental enhancers in humans." Nature 470(7333): 279-283.
- Radbruch, A., C. Burger, S. Klein and W. Muller (1986). "Control of Immunoglobulin Class Switch Recombination." Immunological Reviews 89(1): 69-84.
- Rajewsky, K. (1996). "Clonal selection and learning in the antibody system." Nature 381(6585): 751-758.
- Ramírez, F., D. P. Ryan, B. Grüning, V. Bhardwaj, F. Kilpert, A. S. Richter, S. Heyne, F. Dündar and T. Manke (2016). "deepTools2: a next generation web server for deep-sequencing data analysis." Nucleic acids research 44(W1): W160-W165.
- Ranuncolo, S. M., J. M. Polo, J. Dierov, M. Singer, T. Kuo, J. Greally, R. Green, M. Carroll and A. Melnick (2007). "Bcl-6 mediates the germinal center B cell phenotype and lymphomagenesis through transcriptional repression of the DNA-damage sensor ATR." Nature immunology 8(7): 705-714.
- Ranuncolo, S. M., J. M. Polo and A. Melnick (2008). "BCL6 represses CHEK1 and suppresses DNA damage pathways in normal and malignant B-cells." Blood Cells Mol Dis 41(1): 95-99.
- Ranuncolo, S. M., L. Wang, J. M. Polo, T. Dell'Oso, J. Dierov, T. J. Gaymes, F. Rassool, M. Carroll and A. Melnick (2008). "BCL6-mediated attenuation of DNA damage sensing triggers growth arrest and senescence through a p53-dependent pathway in a cell context-dependent manner." The Journal of biological chemistry 283(33): 22565-22572.
- Reboldi, A., T. I. Arnon, L. B. Rodda, A. Atakilit, D. Sheppard and J. G. Cyster (2016). "IgA production requires B cell interaction with subepithelial dendritic cells in Peyer's patches." Science 352(6287): aaf4822.
- Reimold, A. M., N. N. Iwakoshi, J. Manis, P. Vallabhajosyula, E. Szomolanyi-Tsuda, E. M. Gravallese, D. Friend, M. J. Grusby, F. Alt and L. H. Glimcher (2001). "Plasma cell differentiation requires the transcription factor XBP-1." Nature 412(6844): 300-307.
- Reimold, A. M., P. D. Ponath, Y. S. Li, R. R. Hardy, C. S. David, J. L. Strominger and L. H. Glimcher (1996). "Transcription factor B cell lineage-specific activator protein regulates the gene for human X-box binding protein 1." The Journal of experimental medicine 183(2): 393-401.
- Revilla, I. D. R., I. Bilic, B. Vilagos, H. Tagoh, A. Ebert, I. M. Tamir, L. Smeenk, J. Trupke, A. Sommer, M. Jaritz and M. Busslinger (2012). "The B-cell identity factor Pax5 regulates distinct transcriptional programmes in early and late B lymphopoiesis." The EMBO journal 31(14): 3130-3146.
- Revy, P., T. Muto, Y. Levy, F. Geissmann, A. Plebani, O. Sanal, N. Catalan, M. Forveille, R. Dufourcq-Labelouse, A. Gennery, I. Tezcan, F. Ersoy, H. Kayserili, A. G. Ugazio, N. Brousse, M. Muramatsu, L. D. Notarangelo, K. Kinoshita, T. Honjo, A. Fischer and A. Durandy (2000). "Activation-induced cytidine deaminase (AID) deficiency causes the autosomal recessive form of the Hyper-IgM syndrome (HIGM2)." Cell 102(5): 565-575.
- Ritchie, M. E., B. Phipson, D. Wu, Y. Hu, C. W. Law, W. Shi and G. K. Smyth (2015). "limma powers differential expression analyses for RNA-sequencing and microarray studies." Nucleic Acids Res 43(7): e47.
- Robinson, G., M. Parker, T. A. Kranenburg, C. Lu, X. Chen, L. Ding, T. N. Phoenix, E. Hedlund, L. Wei, X. Zhu, N. Chalhoub, S. J. Baker, R. Huether, R. Kriwacki, N. Curley, R. Thiruvenkatam, J. Wang, G. Wu, M. Rusch, X. Hong, J. Becksfort, P. Gupta, J. Ma, J. Easton, B. Vadodaria, A. Onar-Thomas, T. Lin, S. Li, S. Pounds, S. Paugh, D. Zhao, D. Kawauchi, M. F. Roussel, D. Finkelstein, D. W. Ellison, C. C. Lau, E. Bouffet, T. Hassall, S. Gururangan, R. Cohn, R. S. Fulton, L. L. Fulton, D. J. Dooling, K. Ochoa, A. Gajjar, E. R. Mardis, R. K. Wilson,

J. R. Downing, J. Zhang and R. J. Gilbertson (2012). "Novel mutations target distinct subgroups of medulloblastoma." Nature 488(7409): 43-48.

- Rodriguez, C. I., F. Buchholz, J. Galloway, R. Sequerra, J. Kasper, R. Ayala, A. F. Stewart and S. M. Dymecki (2000). "High-efficiency deleter mice show that FLPe is an alternative to Cre-loxP." Nat Genet 25(2): 139-140.
- Romanow, W. J., A. W. Langerak, P. Goebel, I. L. M. Wolvers-Tettero, J. J. M. van Dongen, A. J. Feeney and C. Murre (2000). "E2A and EBF Act in Synergy with the V(D)J Recombinase to Generate a Diverse Immunoglobulin Repertoire in Nonlymphoid Cells." Molecular Cell 5(2): 343-353.
- Rosen, S. D. (2004). "Ligands for L-selectin: homing, inflammation, and beyond." Annu Rev Immunol 22: 129-156.
- Saito, T., S. Chiba, M. Ichikawa, A. Kunisato, T. Asai, K. Shimizu, T. Yamaguchi, G. Yamamoto, S. Seo, K. Kumano, E. Nakagami-Yamaguchi, Y. Hamada, S. Aizawa and H. Hirai (2003). "Notch2 is preferentially expressed in mature B cells and indispensable for marginal zone B lineage development." Immunity 18(5): 675-685.
- Sander, S., V. T. Chu, T. Yasuda, A. Franklin, R. Graf, D. P. Calado, S. Li, K. Imami, M. Selbach, M. Di Virgilio, L. Bullinger and K. Rajewsky (2015). "PI3 Kinase and FOXO1 Transcription Factor Activity Differentially Control B Cells in the Germinal Center Light and Dark Zones." Immunity 43(6): 1075-1086.
- Sasaki, Y., S. Casola, J. L. Kutok, K. Rajewsky and M. Schmidt-Supprian (2004). "TNF family member B cell-activating factor (BAFF) receptor-dependent and -independent roles for BAFF in B cell physiology." J Immunol 173(4): 2245-2252.
- Sasaki, Y., E. Derudder, E. Hobeika, R. Pelanda, M. Reth, K. Rajewsky and M. Schmidt-Supprian (2006). "Canonical NF-kappaB activity, dispensable for B cell development, replaces BAFF-receptor signals and promotes B cell proliferation upon activation." Immunity 24(6): 729-739.
- Sasaki, Y. and K. Iwai (2016). "Roles of the NF-kappaB Pathway in B-Lymphocyte Biology." Curr Top Microbiol Immunol 393: 177-209.
- Satoh, T., O. Takeuchi, A. Vandenbon, K. Yasuda, Y. Tanaka, Y. Kumagai, T. Miyake, K. Matsushita, T. Okazaki, T. Saitoh, K. Honma, T. Matsuyama, K. Yui, T. Tsujimura, D. M. Standley, K. Nakanishi, K. Nakai and S. Akira (2010). "The Jmjd3-Irf4 axis regulates M2 macrophage polarization and host responses against helminth infection." Nat Immunol 11(10): 936-944.
- Sauvageau, M. and G. Sauvageau (2010). "Polycomb group proteins: multi-faceted regulators of somatic stem cells and cancer." Cell Stem Cell 7(3): 299-313.
- Sayegh, C. E., M. W. Quong, Y. Agata and C. Murre (2003). "E-proteins directly regulate expression of activation-induced deaminase in mature B cells." Nature immunology 4(6): 586-593.
- Scelfo, A., A. Piunti and D. Pasini (2015). "The controversial role of the Polycomb group proteins in transcription and cancer: how much do we not understand Polycomb proteins?" Febs j 282(9): 1703-1722.
- Scheeren, F. A., M. Naspetti, S. Diehl, R. Schotte, M. Nagasawa, E. Wijnands, R. Gimeno, F. A. Vyth-Dreese, B. Blom and H. Spits (2005). "STAT5 regulates the self-renewal capacity and differentiation of human memory B cells and controls Bcl-6 expression." Nat Immunol 6(3): 303-313.
- Schiemann, B., J. L. Gommerman, K. Vora, T. G. Cachero, S. Shulga-Morskaya, M. Dobles, E. Frew and M. L. Scott (2001). "An essential role for BAFF in the normal development of B cells through a BCMA-independent pathway." Science 293(5537): 2111-2114.
- Schmitz, R., R. M. Young, M. Ceribelli, S. Jhavar, W. Xiao, M. Zhang, G. Wright, A. L. Shaffer, D. J. Hodson, E. Buras, X. Liu, J. Powell, Y. Yang, W. Xu, H. Zhao, H. Kohlhammer, A. Rosenwald, P. Kluin, H. K. Muller-Hermelink, G. Ott, R. D. Gascoyne, J. M. Connors, L. M. Rimsza, E. Campo, E. S. Jaffe, J. Delabie, E. B. Smeland, M. D. Ogwang, S. J. Reynolds, R. I. Fisher, R. M. Braziel, R. R. Tubbs, J. R. Cook, D. D. Weisenburger, W. C. Chan, S. Pittaluga, W. Wilson, T. A. Waldmann, M. Rowe, S. M. Mbulaiteye, A. B. Rickinson and L. M. Staudt (2012). "Burkitt lymphoma pathogenesis and therapeutic targets from structural and functional genomics." Nature 490(7418): 116-120.

- Scholz, J. L., J. E. Crowley, M. M. Tomayko, N. Steinel, P. J. O'Neill, W. J. Quinn, 3rd, R. Goenka, J. P. Miller, Y. H. Cho, V. Long, C. Ward, T. S. Migone, M. J. Shlomchik and M. P. Cancro (2008). "BLyS inhibition eliminates primary B cells but leaves natural and acquired humoral immunity intact." Proc Natl Acad Sci U S A 105(40): 15517-15522.
- Scholz, J. L., J. E. Crowley, M. M. Tomayko, N. Steinel, P. J. O'Neill, W. J. Quinn, R. Goenka, J. P. Miller, Y. H. Cho, V. Long, C. Ward, T.-S. Migone, M. J. Shlomchik and M. P. Cancro (2008). "BLyS inhibition eliminates primary B cells but leaves natural and acquired humoral immunity intact." Proceedings of the National Academy of Sciences 105: 15517-15522.
- Schrander-Stumpel, C. T., L. Spruyt, L. M. Curfs, T. Defloor and J. J. Schrander (2005). "Kabuki syndrome: Clinical data in 20 patients, literature review, and further guidelines for preventive management." Am J Med Genet A 132a(3): 234-243.
- Schuettengruber, B., H. M. Bourbon, L. Di Croce and G. Cavalli (2017). "Genome Regulation by Polycomb and Trithorax: 70 Years and Counting." Cell 171(1): 34-57.
- Schuettengruber, B., A. M. Martinez, N. Iovino and G. Cavalli (2011). "Trithorax group proteins: switching genes on and keeping them active." Nat Rev Mol Cell Biol 12(12): 799-814.
- Schultz, C. L. and R. L. Coffman (1991). "Control of isotype switching by T cells and cytokines." Curr Opin Immunol 3(3): 350-354.
- Schweighoffer, E., L. Vanes, J. Nys, D. Cantrell, S. McCleary, N. Smithers and V. L. Tybulewicz (2013). "The BAFF receptor transduces survival signals by co-opting the B cell receptor signaling pathway." Immunity 38(3): 475-488.
- Sciammas, R. and M. M. Davis (2004). "Modular nature of Blimp-1 in the regulation of gene expression during B cell maturation." J Immunol 172(9): 5427-5440.
- Sciammas, R., A. L. Shaffer, J. H. Schatz, H. Zhao, L. M. Staudt and H. Singh (2006). "Graded expression of interferon regulatory factor-4 coordinates isotype switching with plasma cell differentiation." Immunity 25(2): 225-236.
- Seenundun, S., S. Rampalli, Q. C. Liu, A. Aziz, C. Palii, S. Hong, A. Blais, M. Brand, K. Ge and F. J. Dilworth (2010). "UTX mediates demethylation of H3K27me3 at muscle-specific genes during myogenesis." Embo j 29(8): 1401-1411.
- Sengoku, T. and S. Yokoyama (2011). "Structural basis for histone H3 Lys 27 demethylation by UTX/KDM6A." Genes & development 25(21): 2266-2277.
- Shaffer, A. L., K. I. Lin, T. C. Kuo, X. Yu, E. M. Hurt, A. Rosenwald, J. M. Giltnane, L. Yang, H. Zhao, K. Calame and L. M. Staudt (2002). "Blimp-1 orchestrates plasma cell differentiation by extinguishing the mature B cell gene expression program." Immunity 17(1): 51-62.
- Shaffer, A. L., M. Shapiro-Shelef, N. N. Iwakoshi, A. H. Lee, S. B. Qian, H. Zhao, X. Yu, L. Yang, B. K. Tan, A. Rosenwald, E. M. Hurt, E. Petroulakis, N. Sonenberg, J. W. Yewdell, K. Calame, L. H. Glimcher and L. M. Staudt (2004). "XBP1, downstream of Blimp-1, expands the secretory apparatus and other organelles, and increases protein synthesis in plasma cell differentiation." Immunity 21(1): 81-93.
- Shah, N. and S. Sukumar (2010). "The Hox genes and their roles in oncogenesis." Nat Rev Cancer 10(5): 361-371.
- Shapiro-Shelef, M., K. I. Lin, L. J. McHeyzer-Williams, J. Liao, M. G. McHeyzer-Williams and K. Calame (2003). "Blimp-1 is required for the formation of immunoglobulin secreting plasma cells and pre-plasma memory B cells." Immunity 19(4): 607-620.
- Shapiro-Shelef, M., K. I. Lin, D. Savitsky, J. Liao and K. Calame (2005). "Blimp-1 is required for maintenance of long-lived plasma cells in the bone marrow." J Exp Med 202(11): 1471-1476.
- Shen, X., W. Kim, Y. Fujiwara, M. D. Simon, Y. Liu, M. R. Mysliwiec, G.-C. Yuan, Y. Lee and S. H. Orkin (2009). "Jumonji modulates polycomb activity and self-renewal versus differentiation of stem cells." Cell 139(7): 1303-1314.
- Shi, Y., F. Lan, C. Matson, P. Mulligan, J. R. Whetstine, P. A. Cole, R. A. Casero and Y. Shi (2004). "Histone demethylation mediated by the nuclear amine oxidase homolog LSD1." Cell 119(7): 941-953.
- Shilatifard, A. (2006). "Chromatin modifications by methylation and ubiquitination: implications in the regulation of gene expression." Annu Rev Biochem 75: 243-269.
- Shiloh, Y. (2003). "ATM and related protein kinases: safeguarding genome integrity." Nature reviews. Cancer 3(3): 155-168.

- Shpargel, K. B., T. Sengoku, S. Yokoyama and T. Magnuson (2012). "UTX and UTY demonstrate histone demethylase-independent function in mouse embryonic development." PLoS Genet 8(9): e1002964.
- Shpargel, K. B., J. Starmer, C. Wang, K. Ge and T. Magnuson (2017). "UTX-guided neural crest function underlies craniofacial features of Kabuki syndrome." Proc Natl Acad Sci U S A 114(43): E9046-e9055.
- Shpargel, K. B., J. Starmer, D. Yee, M. Pohlers and T. Magnuson (2014). "KDM6 Demethylase Independent Loss of Histone H3 Lysine 27 Trimethylation during Early Embryonic Development." PLOS Genetics 10(8): e1004507.
- Shukla, V. and R. Lu (2014). "IRF4 and IRF8: Governing the virtues of B Lymphocytes." Front Biol (Beijing) 9(4): 269-282.
- Sigvardsson, M., D. R. Clark, D. Fitzsimmons, M. Doyle, P. Akerblad, T. Breslin, S. Bilke, R. Li, C. Yeamans, G. Zhang and J. Hagman (2002). "Early B-cell factor, E2A, and Pax-5 cooperate to activate the early B cell-specific mb-1 promoter." Molecular and cellular biology 22(24): 8539-8551.
- Simonetti, G., A. Carette, K. Silva, H. Wang, N. S. De Silva, N. Heise, C. W. Siebel, M. J. Shlomchik and U. Klein (2013). "IRF4 controls the positioning of mature B cells in the lymphoid microenvironments by regulating NOTCH2 expression and activity." J Exp Med 210(13): 2887-2902.
- Simpson, L. J. and J. E. Sale (2003). "Rev1 is essential for DNA damage tolerance and non-templated immunoglobulin gene mutation in a vertebrate cell line." The EMBO journal 22(7): 1654-1664.
- Sinha, S., R. K. Singh, N. Alam, A. Roy, S. Roychoudhury and C. K. Panda (2008). "Alterations in candidate genes PHF2, FANCC, PTCH1 and XPA at chromosomal 9q22.3 region: pathological significance in early- and late-onset breast carcinoma." Mol Cancer 7: 84.
- Skalet, A. H., J. A. Isler, L. B. King, H. P. Harding, D. Ron and J. G. Monroe (2005). "Rapid B cell receptor-induced unfolded protein response in nonsecretory B cells correlates with pro- versus antiapoptotic cell fate." The Journal of biological chemistry 280(48): 39762-39771.
- Sola, S., J. M. Xavier, D. M. Santos, M. M. Aranha, A. L. Morgado, K. Jepsen and C. M. Rodrigues (2011). "p53 interaction with JMJD3 results in its nuclear distribution during mouse neural stem cell differentiation." PLoS One 6(3): e18421.
- Song, H. and J. Cerny (2003). "Functional heterogeneity of marginal zone B cells revealed by their ability to generate both early antibody-forming cells and germinal centers with hypermutation and memory in response to a T-dependent antigen." The Journal of experimental medicine 198(12): 1923-1935.
- Sonoda, K. H. and J. Stein-Streilein (2002). "CD1d on antigen-transporting APC and splenic marginal zone B cells promotes NKT cell-dependent tolerance." Eur J Immunol 32(3): 848-857.
- Souabni, A., C. Cobaleda, M. Schebesta and M. Busslinger (2002). "Pax5 promotes B lymphopoiesis and blocks T cell development by repressing Notch1." Immunity 17(6): 781-793.
- Sparmann, A. and M. van Lohuizen (2006). "Polycomb silencers control cell fate, development and cancer." Nat Rev Cancer 6(11): 846-856.
- Srinivasan, L., Y. Sasaki, D. P. Calado, B. Zhang, J. H. Paik, R. A. DePinho, J. L. Kutok, J. F. Kearney, K. L. Otipoby and K. Rajewsky (2009). "PI3 kinase signals BCR-dependent mature B cell survival." Cell 139(3): 573-586.
- Stall, A. M., S. Adams, L. A. Herzenberg and A. B. Kantor (1992). "Characteristics and development of the murine B-1b (Ly-1 B sister) cell population." Annals of the New York Academy of Sciences 651: 33-43.
- Starnes, L. M., D. Su, L. M. Pikkupeura, B. T. Weinert, M. A. Santos, A. Mund, R. Soria, Y. W. Cho, I. Pozdnyakova, M. Kubec Hojfeldt, A. Vala, W. Yang, B. Lopez-Mendez, J. E. Lee, W. Peng, J. Yuan, K. Ge, G. Montoya, A. Nussenzweig, C. Choudhary and J. A. Daniel (2016). "A PTIP-PA1 subcomplex promotes transcription for IgH class switching independently from the associated MLL3/MLL4 methyltransferase complex." Genes Dev 30(2): 149-163.
- Stavnezer-Nordgren, J. and S. Sirlin (1986). "Specificity of immunoglobulin heavy chain switch correlates with activity of germline heavy chain genes prior to switching." Embo j 5(1): 95-102.
- Stender, Joshua D., G. Pascual, W. Liu, Minna U. Kaikkonen, K. Do, Nathanael J. Spann, M. Boutros, N. Perrimon, Michael G. Rosenfeld and Christopher K. Glass (2012). "Control of

Proinflammatory Gene Programs by Regulated Trimethylation and Demethylation of Histone H4K20." Molecular Cell 48(1): 28-38.
- Strahl, B. D. and C. D. Allis (2000). "The language of covalent histone modifications." Nature 403(6765): 41-45.
- Strobl-Mazzulla, P. H., T. Sauka-Spengler and M. Bronner-Fraser (2010). "Histone Demethylase JmjD2A Regulates Neural Crest Specification." Developmental Cell 19(3): 460-468.
- Struhl, G. and M. Akam (1985). "Altered distributions of Ultrabithorax transcripts in extra sex combs mutant embryos of Drosophila." Embo j 4(12): 3259-3264.
- Su, I. H., A. Basavaraj, A. N. Krutchinsky, O. Hobert, A. Ullrich, B. T. Chait and A. Tarakhovsky (2003). "Ezh2 controls B cell development through histone H3 methylation and Igh rearrangement." Nat Immunol 4(2): 124-131.
- Su, I. H., M. W. Dobenecker, E. Dickinson, M. Oser, A. Basavaraj, R. Marqueron, A. Viale, D. Reinberg, C. Wulfing and A. Tarakhovsky (2005). "Polycomb group protein ezh2 controls actin polymerization and cell signaling." Cell 121(3): 425-436.
- Su, S. T., H. Y. Ying, Y. K. Chiu, F. R. Lin, M. Y. Chen and K. I. Lin (2009). "Involvement of histone demethylase LSD1 in Blimp-1-mediated gene repression during plasma cell differentiation." Mol Cell Biol 29(6): 1421-1431.
- Sun, X. H. (2004). "Multitasking of helix-loop-helix proteins in lymphopoiesis." Adv Immunol 84: 43-77.
- Suzuki, K., M. Maruya, S. Kawamoto, K. Sitnik, H. Kitamura, W. W. Agace and S. Fagarasan (2010). "The sensing of environmental stimuli by follicular dendritic cells promotes immunoglobulin A generation in the gut." Immunity 33(1): 71-83.
- Suzuki, S., S. Enosawa, T. Kakefuda, T. Shinomiya, M. Amari, S. Naoe, Y. Hoshino and K. Chiba (1996). "A novel immunosuppressant, FTY720, with a unique mechanism of action, induces long-term graft acceptance in rat and dog allotransplantation." Transplantation 61(2): 200-205.
- Swaminathan, S., C. Duy and M. Müschen (2014). "BACH2-BCL6 balance regulates selection at the pre-B cell receptor checkpoint." Trends in immunology 35(3): 131-137.
- Ta, V. T., H. Nagaoka, N. Catalan, A. Durandy, A. Fischer, K. Imai, S. Nonoyama, J. Tashiro, M. Ikegawa, S. Ito, K. Kinoshita, M. Muramatsu and T. Honjo (2003). "AID mutant analyses indicate requirement for class-switch-specific cofactors." Nature immunology 4(9): 843-848.
- Takahashi, K. and S. Yamanaka (2006). "Induction of pluripotent stem cells from mouse embryonic and adult fibroblast cultures by defined factors." Cell 126(4): 663-676.
- Takeuchi, T., Y. Watanabe, T. Takano-Shimizu and S. Kondo (2006). "Roles of jumonji and jumonji family genes in chromatin regulation and development." Dev Dyn 235(9): 2449-2459.
- Takeuchi, T., Y. Yamazaki, Y. Katoh-Fukui, R. Tsuchiya, S. Kondo, J. Motoyama and T. Higashinakagawa (1995). "Gene trap capture of a novel mouse gene, jumonji, required for neural tube formation." Genes Dev 9(10): 1211-1222.
- Tang, Z., W.-Y. Chen, M. Shimada, Uyen T. T. Nguyen, J. Kim, X.-J. Sun, T. Sengoku, Robert K. McGinty, Joseph P. Fernandez, Tom W. Muir and Robert G. Roeder (2013). "SET1 and p300 Act Synergistically, through Coupled Histone Modifications, in Transcriptional Activation by p53." Cell 154(2): 297-310.
- Tanigaki, K., H. Han, N. Yamamoto, K. Tashiro, M. Ikegawa, K. Kuroda, A. Suzuki, T. Nakano and T. Honjo (2002). "Notch-RBP-J signaling is involved in cell fate determination of marginal zone B cells." Nat Immunol 3(5): 443-450.
- Tateishi, K., Y. Okada, E. M. Kallin and Y. Zhang (2009). "Role of Jhdm2a in regulating metabolic gene expression and obesity resistance." Nature 458(7239): 757-761.
- Taverna, S. D., H. Li, A. J. Ruthenburg, C. D. Allis and D. J. Patel (2007). "How chromatin-binding modules interpret histone modifications: lessons from professional pocket pickers." Nat Struct Mol Biol 14(11): 1025-1040.
- Teng, G., P. Hakimpour, P. Landgraf, A. Rice, T. Tuschl, R. Casellas and F. N. Papavasiliou (2008). "MicroRNA-155 is a negative regulator of activation-induced cytidine deaminase." Immunity 28(5): 621-629.
- Testa, G., J. Schaft, F. van der Hoeven, S. Glaser, K. Anastassiadis, Y. Zhang, T. Hermann, W. Stremmel and A. F. Stewart (2004). "A reliable lacZ expression reporter cassette for multipurpose, knockout-first alleles." Genesis 38(3): 151-158.

- Thieme, S., T. Gyarfas, C. Richter, G. Ozhan, J. Fu, D. Alexopoulou, M. H. Muders, I. Michalk, C. Jakob, A. Dahl, B. Klink, J. Bandola, M. Bachmann, E. Schrock, F. Buchholz, A. F. Stewart, G. Weidinger, K. Anastassiadis and S. Brenner (2013). "The histone demethylase UTX regulates stem cell migration and hematopoiesis." Blood 121(13): 2462-2473.
- Thome, M. (2004). "CARMA1, BCL-10 and MALT1 in lymphocyte development and activation." Nat Rev Immunol 4(5): 348-359.
- Tie, F., R. Banerjee, P. A. Conrad, P. C. Scacheri and P. J. Harte (2012). "Histone demethylase UTX and chromatin remodeler BRM bind directly to CBP and modulate acetylation of histone H3 lysine 27." Mol Cell Biol 32(12): 2323-2334.
- Tokoyoda, K., A. E. Hauser, T. Nakayama and A. Radbruch (2010). "Organization of immunological memory by bone marrow stroma." Nat Rev Immunol 10(3): 193-200.
- Tonegawa, S. (1983). "Somatic generation of antibody diversity." Nature 302(5909): 575-581.
- Trapnell, C., L. Pachter and S. L. Salzberg (2009). "TopHat: discovering splice junctions with RNA-Seq." Bioinformatics 25(9): 1105-1111.
- Tretter, T., A. E. Ross, D. I. Dordai and S. Desiderio (2003). "Mimicry of pre-B cell receptor signaling by activation of the tyrosine kinase Blk." The Journal of experimental medicine 198(12): 1863-1873.
- Tsuji, M., K. Suzuki, K. Kinoshita and S. Fagarasan (2008). "Dynamic interactions between bacteria and immune cells leading to intestinal IgA synthesis." Seminars in Immunology 20(1): 59-66.
- Tsukada, Y., J. Fang, H. Erdjument-Bromage, M. E. Warren, C. H. Borchers, P. Tempst and Y. Zhang (2006). "Histone demethylation by a family of JmjC domain-containing proteins." Nature 439(7078): 811-816.
- Tunyaplin, C., A. L. Shaffer, C. D. Angelin-Duclos, X. Yu, L. M. Staudt and K. L. Calame (2004). "Direct repression of prdm1 by Bcl-6 inhibits plasmacytic differentiation." J Immunol 173(2): 1158-1165.
- Vallabhapurapu, S. and M. Karin (2009). "Regulation and function of NF-kappaB transcription factors in the immune system." Annu Rev Immunol 27: 693-733.
- Vallabhapurapu, S., A. Matsuzawa, W. Zhang, P. H. Tseng, J. J. Keats, H. Wang, D. A. Vignali, P. L. Bergsagel and M. Karin (2008). "Nonredundant and complementary functions of TRAF2 and TRAF3 in a ubiquitination cascade that activates NIK-dependent alternative NF-kappaB signaling." Nat Immunol 9(12): 1364-1370.
- van den Heuvel, S. and N. J. Dyson (2008). "Conserved functions of the pRB and E2F families." Nat Rev Mol Cell Biol 9(9): 713-724.
- Van der Meulen, J., V. Sanghvi, K. Mavrakis, K. Durinck, F. Fang, F. Matthijssens, P. Rondou, M. Rosen, T. Pieters, P. Vandenberghe, E. Delabesse, T. Lammens, B. De Moerloose, B. Menten, N. Van Roy, B. Verhasselt, B. Poppe, Y. Benoit, T. Taghon, A. M. Melnick, F. Speleman, H. G. Wendel and P. Van Vlierberghe (2015). "The H3K27me3 demethylase UTX is a gender-specific tumor suppressor in T-cell acute lymphoblastic leukemia." Blood 125(1): 13-21.
- Van der Meulen, J., F. Speleman and P. Van Vlierberghe (2014). "The H3K27me3 demethylase UTX in normal development and disease." Epigenetics 9(5): 658-668.
- van Gent, D. C., J. F. McBlane, D. A. Ramsden, M. J. Sadofsky, J. E. Hesse and M. Gellert (1995). "Initiation of V(D)J recombination in a cell-free system." Cell 81(6): 925-934.
- van Haaften, G., G. L. Dalgliesh, H. Davies, L. Chen, G. Bignell, C. Greenman, S. Edkins, C. Hardy, S. O'Meara, J. Teague, A. Butler, J. Hinton, C. Latimer, J. Andrews, S. Barthorpe, D. Beare, G. Buck, P. J. Campbell, J. Cole, S. Forbes, M. Jia, D. Jones, C. Y. Kok, C. Leroy, M.-L. Lin, D. J. McBride, M. Maddison, S. Maquire, K. McLay, A. Menzies, T. Mironenko, L. Mulderrig, L. Mudie, E. Pleasance, R. Shepherd, R. Smith, L. Stebbings, P. Stephens, G. Tang, P. S. Tarpey, R. Turner, K. Turrell, J. Varian, S. West, S. Widaa, P. Wray, V. P. Collins, K. Ichimura, S. Law, J. Wong, S. T. Yuen, S. Y. Leung, G. Tonon, R. A. DePinho, Y.-T. Tai, K. C. Anderson, R. J. Kahnoski, A. Massie, S. K. Khoo, B. T. Teh, M. R. Stratton and P. A. Futreal (2009). "Somatic mutations of the histone H3K27 demethylase gene UTX in human cancer." Nature genetics 41: 521-523.
- Vandamme, J., G. Lettier, S. Sidoli, E. Di Schiavi, O. Nørregaard Jensen and A. E. Salcini (2012). "The C. elegans H3K27 Demethylase UTX-1 Is Essential for Normal Development, Independent of Its Enzymatic Activity." PLOS Genetics 8(5): e1002647.

- Váraljai, R., A. B. M. M. K. Islam, M. L. Beshiri, J. Rehman, N. Lopez-Bigas and E. V. Benevolenskaya (2015). "Increased mitochondrial function downstream from KDM5A histone demethylase rescues differentiation in pRB-deficient cells." Genes & development 29(17): 1817-1834.
- Varano, G., S. Raffel, M. Sormani, F. Zanardi, S. Lonardi, C. Zasada, L. Perucho, V. Petrocelli, A. Haake, A. K. Lee, M. Bugatti, U. Paul, E. Van Anken, L. Pasqualucci, R. Rabadan, R. Siebert, S. Kempa, M. Ponzoni, F. Facchetti, K. Rajewsky and S. Casola (2017). "The B-cell receptor controls fitness of MYC-driven lymphoma cells via GSK3beta inhibition." Nature 546(7657): 302-306.
- Vasanwala, F. H., S. Kusam, L. M. Toney and A. L. Dent (2002). "Repression of AP-1 function: a mechanism for the regulation of Blimp-1 expression and B lymphocyte differentiation by the B cell lymphoma-6 protooncogene." J Immunol 169(4): 1922-1929.
- Velichutina, I., R. Shaknovich, H. Geng, N. A. Johnson, R. D. Gascoyne, A. M. Melnick and O. Elemento (2010). "EZH2-mediated epigenetic silencing in germinal center B cells contributes to proliferation and lymphomagenesis." Blood 116(24): 5247-5255.
- Vences-Catalan, F. and L. Santos-Argumedo (2011). "CD38 through the life of a murine B lymphocyte." IUBMB Life 63(10): 840-846.
- Victora, G. D. and M. C. Nussenzweig (2012). "Germinal centers." Annu Rev Immunol 30: 429-457.
- Victora, G. D., T. A. Schwickert, D. R. Fooksman, A. O. Kamphorst, M. Meyer-Hermann, M. L. Dustin and M. C. Nussenzweig (2010). "Germinal center dynamics revealed by multiphoton microscopy with a photoactivatable fluorescent reporter." Cell 143(4): 592-605.
- Vinuesa, C. G., S. G. Tangye, B. Moser and C. R. Mackay (2005). "Follicular B helper T cells in antibody responses and autoimmunity." Nat Rev Immunol 5(11): 853-865.
- von Andrian, U. H. and B. Engelhardt (2003). "α4 Integrins as Therapeutic Targets in Autoimmune Disease." New England Journal of Medicine 348(1): 68-72.
- Vuong, B. Q., M. Lee, S. Kabir, C. Irimia, S. Macchiarulo, G. S. McKnight and J. Chaudhuri (2009). "Specific recruitment of protein kinase A to the immunoglobulin locus regulates class-switch recombination." Nature immunology 10(4): 420-426.
- Wagner, N., J. Lohler, E. J. Kunkel, K. Ley, E. Leung, G. Krissansen, K. Rajewsky and W. Muller (1996). "Critical role for beta7 integrins in formation of the gut-associated lymphoid tissue." Nature 382(6589): 366-370.
- Walker, E., W. Y. Chang, J. Hunkapiller, G. Cagney, K. Garcha, J. Torchia, N. J. Krogan, J. F. Reiter and W. L. Stanford (2010). "Polycomb-like 2 associates with PRC2 and regulates transcriptional networks during mouse embryonic stem cell self-renewal and differentiation." Cell stem cell 6(2): 153-166.
- Walport, L. J., R. J. Hopkinson, M. Vollmar, S. K. Madden, C. Gileadi, U. Oppermann, C. J. Schofield and C. Johansson (2014). "Human UTY(KDM6C) is a male-specific N-methyl lysyl demethylase." J Biol Chem 289(26): 18302-18313.
- Wang, C., J.-E. Lee, Y.-W. Cho, Y. Xiao, Q. Jin, C. Liu and K. Ge (2012). "UTX regulates mesoderm differentiation of embryonic stem cells independent of H3K27 demethylase activity." Proceedings of the National Academy of Sciences 109(38): 15324-15329.
- Wang, F.-S., W.-S. Lian, M. S. Lee, W.-T. Weng, Y.-H. Huang, Y.-S. Chen, Y.-C. Sun, S.-L. Wu, P.-C. Chuang and J.-Y. Ko (2017). "Histone demethylase UTX counteracts glucocorticoid deregulation of osteogenesis by modulating histone-dependent and -independent pathways." Journal of Molecular Medicine 95(5): 499-512.
- Wang, G. G., C. D. Allis and P. Chi (2007). "Chromatin remodeling and cancer, Part II: ATP-dependent chromatin remodeling." Trends Mol Med 13(9): 373-380.
- Wang, J., A. G. Muntean, L. Wu and J. L. Hess (2012). "A subset of mixed lineage leukemia proteins has plant homeodomain (PHD)-mediated E3 ligase activity." J Biol Chem 287(52): 43410-43416.
- Wang, J. K., M. C. Tsai, G. Poulin, A. S. Adler, S. Chen, H. Liu, Y. Shi and H. Y. Chang (2010). "The histone demethylase UTX enables RB-dependent cell fate control." Genes Dev 24(4): 327-332.
- Wang, J. M., J. R. Chao, W. Chen, M. L. Kuo, J. J. Yen and H. F. Yang-Yen (1999). "The antiapoptotic gene mcl-1 is up-regulated by the phosphatidylinositol 3-kinase/Akt signaling

pathway through a transcription factor complex containing CREB." Mol Cell Biol 19(9): 6195-6206.
- Wang, N. S., L. J. McHeyzer-Williams, S. L. Okitsu, T. P. Burris, S. L. Reiner and M. G. McHeyzer-Williams (2012). "Divergent transcriptional programming of class-specific B cell memory by T-bet and RORalpha." Nat Immunol 13(6): 604-611.
- Wang, P., C. Lin, E. R. Smith, H. Guo, B. W. Sanderson, M. Wu, M. Gogol, T. Alexander, C. Seidel, L. M. Wiedemann, K. Ge, R. Krumlauf and A. Shilatifard (2009). "Global analysis of H3K4 methylation defines MLL family member targets and points to a role for MLL1-mediated H3K4 methylation in the regulation of transcriptional initiation by RNA polymerase II." Mol Cell Biol 29(22): 6074-6085.
- Wang, S. P., Z. Tang, C. W. Chen, M. Shimada, R. P. Koche, L. H. Wang, T. Nakadai, A. Chramiec, A. V. Krivtsov, S. A. Armstrong and R. G. Roeder (2017). "A UTX-MLL4-p300 Transcriptional Regulatory Network Coordinately Shapes Active Enhancer Landscapes for Eliciting Transcription." Mol Cell 67(2): 308-321.e306.
- Wang, T., K. Chen, X. Zeng, J. Yang, Y. Wu, X. Shi, B. Qin, L. Zeng, M. A. Esteban, G. Pan and D. Pei (2011). "The histone demethylases Jhdm1a/1b enhance somatic cell reprogramming in a vitamin-C-dependent manner." Cell Stem Cell 9(6): 575-587.
- Weiss, U. and K. Rajewsky (1990). "The repertoire of somatic antibody mutants accumulating in the memory compartment after primary immunization is restricted through affinity maturation and mirrors that expressed in the secondary response." J Exp Med 172(6): 1681-1689.
- Welstead, G. G., M. P. Creyghton, S. Bilodeau, A. W. Cheng, S. Markoulaki, R. A. Young and R. Jaenisch (2012). "X-linked H3K27me3 demethylase Utx is required for embryonic development in a sex-specific manner." Proceedings of the National Academy of Sciences of the United States of America 109(32): 13004-13009.
- Wilkinson, F., H. Pratt and M. L. Atchison (2010). "PcG recruitment by the YY1 REPO domain can be mediated by Yaf2." J Cell Biochem 109(3): 478-486.
- Williams, K., J. Christensen, J. Rappsilber, A. L. Nielsen, J. V. Johansen and K. Helin (2014). "The Histone Lysine Demethylase JMJD3/KDM6B Is Recruited to p53 Bound Promoters and Enhancer Elements in a p53 Dependent Manner." PLOS ONE 9(5): e96545.
- Wilson, V. and F. L. Conlon (2002). "The T-box family." Genome Biol 3(6): Reviews3008.
- Wohner, M., H. Tagoh, I. Bilic, M. Jaritz, D. K. Poliakova, M. Fischer and M. Busslinger (2016). "Molecular functions of the transcription factors E2A and E2-2 in controlling germinal center B cell and plasma cell development." J Exp Med 213(7): 1201-1221.
- Wong, C. W. and M. L. Privalsky (1998). "Components of the SMRT corepressor complex exhibit distinctive interactions with the POZ domain oncoproteins PLZF, PLZF-RARalpha, and BCL-6." The Journal of biological chemistry 273(42): 27695-27702.
- Woodland, R. T., C. J. Fox, M. R. Schmidt, P. S. Hammerman, J. T. Opferman, S. J. Korsmeyer, D. M. Hilbert and C. B. Thompson (2008). "Multiple signaling pathways promote B lymphocyte stimulator dependent B-cell growth and survival." Blood 111(2): 750-760.
- Wu, Q., Y. Tian, J. Zhang, X. Tong, H. Huang, S. Li, H. Zhao, Y. Tang, C. Yuan, K. Wang, Z. Fang, L. Gao, X. Hu, F. Li, Z. Qin, S. Yao, T. Chen, H. Chen, G. Zhang, W. Liu, Y. Sun, L. Chen, K.-K. Wong, K. Ge, L. Chen and H. Ji (2018). "In vivo CRISPR screening unveils histone demethylase UTX as an important epigenetic regulator in lung tumorigenesis." Proceedings of the National Academy of Sciences 115(17): E3978-E3986.
- Wu, X., Jens V. Johansen and K. Helin (2013). "Fbxl10/Kdm2b Recruits Polycomb Repressive Complex 1 to CpG Islands and Regulates H2A Ubiquitylation." Molecular Cell 49(6): 1134-1146.
- Wu, Z., S. T. Lee, Y. Qiao, Z. Li, P. L. Lee, Y. J. Lee, X. Jiang, J. Tan, M. Aau, C. Z. H. Lim and Q. Yu (2011). "Polycomb protein EZH2 regulates cancer cell fate decision in response to DNA damage." Cell death and differentiation 18(11): 1771-1779.
- Xu, C. R., L. Schaffer, S. R. Head and A. J. Feeney (2008). "Reciprocal patterns of methylation of H3K36 and H3K27 on proximal vs. distal IgVH genes are modulated by IL-7 and Pax5." Proc Natl Acad Sci U S A 105(25): 8685-8690.
- Xu, H., V. K. Chaudhri, Z. Wu, K. Biliouris, K. Dienger-Stambaugh, Y. Rochman and H. Singh (2015). "Regulation of bifurcating B cell trajectories by mutual antagonism between transcription factors IRF4 and IRF8." Nat Immunol 16(12): 1274-1281.

- Yang, L., L. S. Song, X. F. Liu, Q. Xia, L. G. Bai, L. Gao, G. Q. Gao, Y. Wang, Z. Y. Wei, C. L. Bai and G. P. Li (2016). "The Maternal Effect Genes UTX and JMJD3 Play Contrasting Roles in Mus musculus Preimplantation Embryo Development." Sci Rep 6: 26711.
- Yang, X., R. K. Karuturi, F. Sun, M. Aau, K. Yu, R. Shao, L. D. Miller, P. B. Tan and Q. Yu (2009). "CDKN1C (p57) is a direct target of EZH2 and suppressed by multiple epigenetic mechanisms in breast cancer cells." PLoS One 4(4): e5011.
- Yapp, C., A. J. Carr, A. Price, U. Oppermann and S. J. Snelling (2016). "H3K27me3 demethylases regulate in vitro chondrogenesis and chondrocyte activity in osteoarthritis." Arthritis Res Ther 18(1): 158.
- Ye, B. H., G. Cattoretti, Q. Shen, J. Zhang, N. Hawe, R. de Waard, C. Leung, M. Nouri-Shirazi, A. Orazi, R. S. Chaganti, P. Rothman, A. M. Stall, P. P. Pandolfi and R. Dalla-Favera (1997). "The BCL-6 proto-oncogene controls germinal-centre formation and Th2-type inflammation." Nat Genet 16(2): 161-170.
- Ye, L., Z. Fan, B. Yu, J. Chang, K. Al Hezaimi, X. Zhou, N.-H. Park and C.-Y. Wang (2012). "Histone demethylases KDM4B and KDM6B promotes osteogenic differentiation of human MSCs." Cell stem cell 11(1): 50-61.
- Yokoyama, A., F. Ficara, M. J. Murphy, C. Meisel, C. Hatanaka, I. Kitabayashi and M. L. Cleary (2013). "MLL Becomes Functional through Intra-Molecular Interaction Not by Proteolytic Processing." PLOS ONE 8(9): e73649.
- Yoshida, H., T. Matsui, A. Yamamoto, T. Okada and K. Mori (2001). "XBP1 mRNA is induced by ATF6 and spliced by IRE1 in response to ER stress to produce a highly active transcription factor." Cell 107(7): 881-891.
- Yoshida, H., T. Okada, K. Haze, H. Yanagi, T. Yura, M. Negishi and K. Mori (2000). "ATF6 activated by proteolysis binds in the presence of NF-Y (CBF) directly to the cis-acting element responsible for the mammalian unfolded protein response." Molecular and cellular biology 20(18): 6755-6767.
- Yoshida, T., S. Y. Ng, J. C. Zuniga-Pflucker and K. Georgopoulos (2006). "Early hematopoietic lineage restrictions directed by Ikaros." Nature immunology 7(4): 382-391.
- Young, R. M. and L. M. Staudt (2013). "Targeting pathological B cell receptor signalling in lymphoid malignancies." Nat Rev Drug Discov 12(3): 229-243.
- Yu, B. D., J. L. Hess, S. E. Horning, G. A. Brown and S. J. Korsmeyer (1995). "Altered Hox expression and segmental identity in Mll-mutant mice." Nature 378(6556): 505-508.
- Yu, J., C. Angelin-Duclos, J. Greenwood, J. Liao and K. Calame (2000). "Transcriptional repression by blimp-1 (PRDI-BF1) involves recruitment of histone deacetylase." Mol Cell Biol 20(7): 2592-2603.
- Zandi, S., R. Mansson, P. Tsapogas, J. Zetterblad, D. Bryder and M. Sigvardsson (2008). "EBF1 Is Essential for B-Lineage Priming and Establishment of a Transcription Factor Network in Common Lymphoid Progenitors." The Journal of Immunology 181(5): 3364-3372.
- Zeisig, B. B., T. Milne, M. P. Garcia-Cuellar, S. Schreiner, M. E. Martin, U. Fuchs, A. Borkhardt, S. K. Chanda, J. Walker, R. Soden, J. L. Hess and R. K. Slany (2004). "Hoxa9 and Meis1 are key targets for MLL-ENL-mediated cellular immortalization." Mol Cell Biol 24(2): 617-628.
- Zeng, J., Z. Ge, L. Wang, Q. Li, N. Wang, M. Bjorkholm, J. Jia and D. Xu (2010). "The histone demethylase RBP2 Is overexpressed in gastric cancer and its inhibition triggers senescence of cancer cells." Gastroenterology 138(3): 981-992.
- Zhang, J., D. Dominguez-Sola, S. Hussein, J.-E. Lee, A. B. Holmes, M. Bansal, S. Vlasevska, T. Mo, H. Tang, K. Basso, K. Ge, R. Dalla-Favera and L. Pasqualucci (2015). "Disruption of KMT2D perturbs germinal center B cell development and promotes lymphomagenesis." Nature medicine 21: 1190-1198.
- Zhang, J., S. Vlasevska, V. A. Wells, S. Nataraj, A. B. Holmes, R. Duval, S. N. Meyer, T. Mo, K. Basso, P. K. Brindle, S. Hussein, R. Dalla-Favera and L. Pasqualucci (2017). "The CREBBP Acetyltransferase Is a Haploinsufficient Tumor Suppressor in B-cell Lymphoma." Cancer Discov 7(3): 322-337.
- Zhang, Y., T. Liu, C. A. Meyer, J. Eeckhoute, D. S. Johnson, B. E. Bernstein, C. Nusbaum, R. M. Myers, M. Brown, W. Li and X. S. Liu (2008). "Model-based Analysis of ChIP-Seq (MACS)." Genome Biology 9(9): R137.

- Zhang, Y. and D. Reinberg (2001). "Transcription regulation by histone methylation: interplay between different covalent modifications of the core histone tails." Genes Dev 15(18): 2343-2360.
- Zhao, W., Q. Li, S. Ayers, Y. Gu, Z. Shi, Q. Zhu, Y. Chen, H. Y. Wang and R. F. Wang (2013). "Jmjd3 inhibits reprogramming by upregulating expression of INK4a/Arf and targeting PHF20 for ubiquitination." Cell 152(5): 1037-1050.
- Zhu, Y., D. van Essen and S. Saccani (2012). "Cell-type-specific control of enhancer activity by H3K9 trimethylation." Mol Cell 46(4): 408-423.

Appendix

During my PhD in the laboratory of Stefano Casola, I had the priceless opportunity to co-author a project aimed at investigating the role of the B cell antigen receptor BCR in a mouse model of aggressive, MYC-driven, Burkitt-like B cell lymphomas.

Experiments based on the conditional ablation of the B cell antigen receptor (BCR) in mouse models have revealed the crucial importance of the BCR for the survival of mature B cells (Lam, Kuhn et al. 1997). Similarly, BCR-knock-down experiments performed in human B lymphoma cell lines have highlighted the importance of sustained antigen receptor expression for the growth of the malignant B cells (Schmitz, Young et al. 2012). Consequently, the BCR pathway has become an important target in the therapy of B-cell malignancies (Young and Staudt 2013). Our group has recently elucidated the effects of inducible genetic ablation of the BCR on the growth of aggressive c-MYC-driven mouse primary B cell lymphomas. We observed that while BCR deficient (BCR^-) tumor cells grew exponentially when kept in isolation, they rapidly disappeared in the presence of their BCR proficient (BCR^+) counterparts, both *in vitro* and *in vivo*. Hence, whereas BCR expression is dispensable for tumor growth, it is essential for optimal fitness of c-MYC transformed B cells (Varano, Raffel et al. 2017).

In the first two years of my PhD I collaborated with Dr. Gabriele Varano and performed experiments to complete this project. I was also actively involved in the revision of the paper that was eventually published on Nature in June 2017. In the frame of this study I characterized the sensitivity of λ-MYC lymphomas to PI3K delta inhibition, showing that BCR proficient tumors are sensitive to the drug CAL-101, that targets PI3Kδ. I also contributed to the isolation and the analysis of spontaneously arising BCR-less lymphoma (BCR-independent) variants that resisted their BCR^+ counterparts in competition assays and validated gain-of-function mutations in the *Nras* and *Kras* genes recurrently selected by these resistant variants.

Working on this project was an amazing experience for me because it increased both my technical skills and my scientific knowledge. I also collaborated with many experts from around the world and I was for the first time involved in the publication of a scientific paper.

In summary, during my PhD I had the chance to study B cells from many points of view, from their physiological development and functions in the immune system to their aberrant transformation during lymphomagenesis.

LETTER

doi:10.1038/nature22353

The B-cell receptor controls fitness of MYC-driven lymphoma cells via GSK3β inhibition

Gabriele Varano[1*], Simon Raffel[2*], Martina Sormani[1], Federica Zanardi[1], Silvia Lonardi[3], Christin Zasada[4], Laura Perucho[1], Valentina Petrocelli[1], Andrea Haake[5], Albert K. Lee[6], Mattia Bugatti[3], Ulrike Paul[5], Eelco Van Anken[7], Laura Pasqualucci[8], Raul Rabadan[6], Reiner Siebert[5,9], Stefan Kempa[4], Maurilio Ponzoni[10], Fabio Facchetti[3], Klaus Rajewsky[4] & Stefano Casola[1]

Acknowledgements

I would like to thank all the people that helped and supported me during these amazing four years of PhD and without whom this work wouldn't have been possible. First, I would like to thank my supervisor Stefano Casola for the opportunity to run this challenging and very interesting project, for our never-ending discussions, his scientific criticism and for always taking into account my thoughts and my ideas. The time spent in his laboratory was priceless and contributed both to my professional and personal growth.

A big "thank you" goes to all current and past SCA's members, for their help, scientific discussion and everyday life in the lab. I was very lucky to share these years with you and I want to thank you for all the beautiful memories we made together.

I am particularly grateful to Gabriele, for choosing me to continue his project. This was the first opportunity for me to study B cell-lymphomas and to be involved in the publication of a scientific paper on a high-impact journal. I would like to thank you, Gabriele, for teaching me how to be meticulous and precise while working in the lab and how to scientifically interpret my results. Thanks for the nice time spent together, that always makes me wish we had more.

An important thank goes to Valentina. Your passion and strong motivation in scientific research were inspiring. Thank you for encouraging me to be more confident without losing curiosity and willingness to learn. Thank you for our friendship, for all the joyful and difficult moments.

A huge "thank you" to Federica Zanardi. Our friendship grew through the years and it still does every day. It is supporting, honest and respectful, it's been like a long journey where I enjoyed every single moment.

To Federica La Mastra, who started her PhD with me four years ago. We've been through a lot together, and we survived all the changes, walking side by side.

To Laura, for all the light you brought to my every-day life in the lab, for sharing not just the desk with me but also science, experiences, feelings and a lot of fun.

To Federica Greco, for the trust you gave me in these years, of which I hope to be worthy, and for the time spent together in the calm and in the storm.

To Daniel, for your friendliness and helpfulness, I am truly happy to have met you. To Marianna, for bringing magic to our group.

To Federica Alberghini and Elisabetta Di Simone, for the years spent together and the priceless memories.

A special thank goes to:

Valentina Petrocelli, for sharing this project with me, for her scientific support, and for our successful teamwork during these years;

Federica Zanardi, for all the bioinformatic analyses, for her criticism in our useful scientific discussions and for her help in revising the present thesis;
Federica Mainoldi, for the ELISA assays;
Federica Pisati, for the support she gave me in performing immunofluorescent and immunohistochemical assays;

I also thank:
Our collaborator Dr. Jacob Hanna at the Weizmann Istitute, for sharing *Utx*$^{fl/fl}$ mice;
My co-supervisors Dr. Diego Pasini and Prof. Marc Schmidt-Supprian for useful help and scientific discussions;
My examiners Prof. Giuseppe Testa and Prof. Meinrad Busslinger for reading my thesis and for their evaluation and corrections.

I would like to thank the people from the IFOM-IEO Campus facilities, who constantly support our research with their expertise:
Mouse facility (Alberto Gobbi, Manuela Capillo and animal house staff)
Flow Cytometry facility, past and present members (Simona Ronzoni, Maria Grazia Totaro, Serena Magni, Sara Martone)
Imaging facility (Dario Parazzoli, Ilaria Costa, Francesca Casagrande, Emanuele Martini)
DNA sequencing facility (Sara Volorio, Filomena Ficarazzi)
Cell culture facility (Ilaria Rancati, Stefania Lavore, Laura Carmignani, Giuseppe Ossolengo)
Histology facility (Federica Pisati)
Genomic Unit (Mirko Riboni, Simone Minardi)
Bioinformatic Unit (Federica Zanardi, Fabio Iannelli)
IFOM services (Kitchen, Maintenance, Warehouse, IT)

I am also very thankful to Francesca Fiore and Veronica Viscardi from SEMM office, for their help during these years and especially in the last complicated months of thesis writing.
An important thank to the Associazione Italiana Ricerca sul Cancro (AIRC) for funding the last year of my PhD.
I would also like to thank my PhD colleagues for sharing joys and sorrows of this life's journey, especially Claudia, Alice and Giorgio. I want to thank all the people in Lab F, in particular past members Lara Sicouri, Valentina Buttiglione, Valentina De Lorenzi, Gian Maria Sarra-Ferraris for their help and support and all the time spent together.
My deepest gratitude to the Equipe Malattie Metaboliche Congenite of San Paolo Hospital in Milan and the Associazione Prevenzione Malattie Metaboliche Congenite. This thesis is the

result of your dedication and hard work and of your passion in supporting me as a PKU patient through every-day troubles. Meeting you was the greatest gift I could ever receive.
A special thank to all my friends, the ones that are close and the ones that manage to be by my side even if they are far away. To all the new ones I met in these years and to the ones that were there from the beginning. To Isabella, for the life-long friendship and for showing me that being physically distant doesn't mean a thing if we are together on the same page. To Claudia and Andrea, I feel very lucky to have met you and to have shared so many happy moments with you in these years, thank you for always being patient and understanding with me. To Lara, for all the laughter and the fun we have even if we are in different places.
The biggest thank goes to my mum and dad and to my grandparents for always believing in me and supporting my passion for scientific research. Thank you for being always there for me, through the brightest and the darkest moments and for always remembering me where I started from and also where I am going, whenever I feel lost. Thanks to Laura, Francesco, Lella and Gianfranco for always being by my side and caring about me, no matter the time passing by or the physical distance. To Lorenzo's family, that I consider as my own and I love as my own, thank you for making me feel as a part of it every day and for encouraging me in all my choices.
I address the last "thank you" to Lorenzo. My friend, my lover, my partner. I can't imagine how life would have been in these years without you by my side. I thank you for your patience, especially during the last months. I thank you for giving me your strength, when I felt I didn't have enough. I thank you for always being extremely honest with me. I thank you for always pushing me to do my best and for being happy for my successes. I thank you for all the beautiful moments we shared. You showed me that true love is built every day, one brick after the other. Thank you because we went through many changes during the last years, both on the professional and personal side, but we always found a way to go together in the same direction.